

2-D NON-LINEAR SEISMIC ANALYSIS
OF ONE-STOREY ECCENTRIC
PRECAST CONCRETE BUILDINGS

by

Surinder Singh Parmar

M.A.Sc., PANAJAB UNIVERSITY CHANDIGARH, INDIA, 1984

A THESIS SUBMITTED IN PARTIAL FULFILLEMNT OF
THE REQUIREMENTS FOR THE DEGREE OF
MASTER OF APPLIED SCIENCE

in

THE FACULTY OF GRADUATE STUDIES
(CIVIL ENGINEERING DEPARTMENT)

We accept this thesis as conforming
to the required standard

THE UNIVERSITY OF BRITISH COLUMBIA

May 1987

©Surinder Parmar, 1987

In presenting this thesis in partial fulfilment of the requirements for an advanced degree at the University of British Columbia, I agree that the Library shall make it freely available for reference and study. I further agree that permission for extensive copying of this thesis for scholarly purposes may be granted by the head of my department or by his or her representatives. It is understood that copying or publication of this thesis for financial gain shall not be allowed without my written permission.

Department of CIVIL ENGINEERING

The University of British Columbia
1956 Main Mall
Vancouver, Canada
V6T 1Y3

Date Oct. 15, 1987

Abstract

Investigations into the behaviour of precast buildings under earthquake loading have shown that the connections are likely to be the weakest link in a pre-cast structure, and the stability of the structure under earthquake loading depends upon the strength & stability of these connections. A 2-dimensional non-linear dynamic analysis of a one storey box-type pre-cast buildings is presented. The shear walls in the buildings are modelled by linear springs, the properties of which depend upon the connections connecting the rigid panels of the shear walls.

To check the effectiveness of the NBCC code design, computer studies have been made on a box-type building statically designed for different eccentricities. The strength of the shear walls was calculated assuming that each panel was a cantilever fixed at the base with dowel bars providing the flexural steel. To make the building survive a major earthquake, we need dowel connections that can take 5mm to 6mm elongation which can be easily accomodated. Studies have also shown that under the action of an earthquake, the response of a highly unsymmetric building will not be very different from that of a symmetric building as long as the building is properly designed using the NBCC code provisions for earthquake loading. It has also been shown that the NBCC code design eccentricity equation is somewhat conservative in calculating the design eccentricity and that a small change in the stiffness of walls perpendicular to the direction of earthquake has little effect on the response of the structures.

Contents

	Page
Abstract	ii
Table of Contents	iii
List of Figures	vi
List of Tables	x
Acknowledgement	xiii
1 INTRODUCTION	1
1.1 General	1
1.2 Categories of Pre-cast Concret Construction	1
1.3 Earthquake Response of Buildings	2
1.4 Scope and Objective of Present study	5
1.5 Thesis Layout	5
2 CYCLIC TESTS ON CONNECTIONS	6
2.1 Introduction	6
2.2 Types of connections	7
2.3 Dry Connections	8

2.3.1	Bolted Connections	8
2.3.2	Welded Connections	13
2.4	Wet Connections	35
2.4.1	Platform type Horizontal Connection	35
2.4.2	Dowel Connection	38
2.5	Hysteresis Model for Vertical Connection	47
2.6	Hysteresis Model for Horizontal Connection	55
3	DYNAMIC ANALYSIS	60
3.1	Introduction	60
3.2	Idealization Technique	61
3.3	2 - D Mathematical Model	65
3.4	Wall Displacements	67
3.5	Time Step Integration	68
3.6	Panel Stiffness	71
3.6.1	Case 0 : Both the foundation springs in contact with the panel	72
3.6.2	Case 1 : Only right foundation spring in contact with the panel	72
3.6.3	Case - 1 : Only left foundation spring in contact with the panel	75
3.6.4	Case 2 : Neither foundation spring in contact with the panel	75
3.7	Wall Stiffness	75
3.8	Time-Step Solution Technique	78
3.9	Damping	81
3.10	Energy Balance	82
4	Static Design of the Buildings	85

4.1	General	85
4.2	Stiffness Method	89
4.2.1	Shortcomings of the Stiffness Method	96
4.3	Strength Method	99
4.3.1	Shortcomings of the Strength Method	103
5	Results of Dynamic Analysis	104
5.1	Effect of non-symmetry in the buildings	104
5.2	Structural Data	106
5.3	Discussion of Results	111
5.3.1	Effect of different methods of static design	111
5.3.2	Effect of different E/Q data on the dynamic analysis	121
5.3.3	Effect of geometry of the building	127
5.3.4	E/Q direction	139
5.3.5	Effect of design eccentricity	142
5.3.6	Effect of variation of stiffness of wall 3 & 4	152
6	Discussion, Conclusions and Future Studies	157
6.1	Introduction	157
6.2	Discussion of results	158
6.3	Conclusions	161
6.4	Future studies	162
	Bibliography	163
	Appendix A	167
A.1	Time Periods of the Buildings Considered in the Present Studies . .	167

List of Figures

1.1 Storage Tank Analogy for the Seismic Response of Buildings by Clough [9]	4
2.1 Wall to Floor connections, from Ref. [14]	9
2.2 Floor to Floor connection, from Ref. [14]	10
2.3 Wall to Wall Horizontal connection, from Ref. [14]	10
2.4 Limited Slip Bolted connections, from Ref. [24]	11
2.5 Load-Deformation Response of Limited Slip Bolted (LSB) Joints, from Ref. [24]	12
2.6 Typical Headed Stud Connection showing two common stud configurations and the ease with which minor imperfections and misalignments may be accomodated, from Ref. [23]	14
2.7 Details of Specimens reported by Spencer & Neille [31]	15
2.8 Hysteretic Behaviours of Welded Headed Stud Connections reported by Spencer & Neille [31]	15
2.9 Alternate Embedment	19
2.10 Details of Connections reported by Aswad [2]	20
2.11 Cyclic Behaviour of Connections Anchored With Steel Bars, by Spencer [34]	24
2.12 Models Developed by Spencer [34]	28
2.13 Cyclic Tests on Thin Panel Embedded Rebar Connections reported by Kallros [17]	30

2.14 Split Pipe Connection by Saxena [29]	34
2.15 Typical platform-type horizontal connection	36
2.16 Coefficients of friction from tests on horizontal joints by Hanson [12]	36
2.17 Shear-displacement hysteretic loops from horizontal tests by Han- son [12]	36
2.18 3/32 Scale Model Interior Horizontal Joint used by Harris & Abbound [13]	37
2.19 Comparison of Coefficients of Friction by Harris & Abbound [13]	37
2.20 Specimens Tested by Dimitrov & Georgiev [10]	39
2.21 Load-Deflection Curves of Specimens in Fig. [2.20] by Dimitrov & Georgiev [10]	39
2.22 Test Specimen - Phase 1, by Hawkins & Lin [15]	41
2.23 Load-displacement curve, # 10 straight bar, Bamboo-type defor- mations, Phase 1 by Hawkins & Lin [15]	41
2.24 Test Specimens - Phase 2, by Hawkins & Lin [15]	43
2.25 Load-displacement curve, # 10 straight bar, Bamboo-type defor- mations, Phase 2 by Hawkins & Lin [15]	44
2.26 Test Specimen - Phase 3, by Hawkins & Lin [15]	46
2.27 Load-displacement curve, # 6 straight bar, Bamboo-type defor- mations, Phase 1 by Hawkins & Lin [15]	46
2.28 Elasto-plastic Model	48
2.29 Degrading Connector Models, by Muller & Becker [21]	48
2.30 Trilinear Hysteresis Loops used for both Stress-Strain and Moment-Curvature Relationships for Studs, by Neille [23]	49
2.31 Shear-slip Relationships for Shear-friction element, by Schricker & Powell [30]	50

2.32	Hysteretic Model : Primary Curve, model proposed by Tong [36]	52
2.33	Hysteretic Model : Cyclic behaviour before yielding, model proposed by Tong [36]	52
2.34	Hysteretic Model : Cyclic behaviour after yielding, model proposed by Tong [36]	53
2.35	Joint Connector Characteristics proposed by Aswad [3]	56
2.36	Bar Force-Pull Out Model for Cyclic Loading, proposed by Hawkins & Lin [15]	57
2.37	Hysteretic Model for the Dowel Connection, by Tong [36]	58
3.1	Idealization of Shear Wall	64
3.2	Three Degrees of Freedom Model	66
3.3	Linear Variation of Acceleration	69
3.4	Free body diagrams of an interior panel corresponding to Case 0	73
3.5	Free body diagrams of an interior panel corresponding to Case 1 and Case -1	74
3.6	Free body diagrams of an interior panel corresponding to Case 2	76
3.7	Shear Wall System	77
3.8	Solution Strategies	80
3.9	Strain Energy from a F- Δ curve	83
4.1	One Storey Buildings Analysed in the Present Studies	86
4.2	Assumed Line of Action of Equivalent Static Force	91
5.1	Panel Connections	107
5.2	Earthquake Accelerograms used in the present studies	109
5.3	Resisting forces on the building	112
5.4	Comparison of static & dynamic analysis results of a square building designed by the strength and stiffness methods	115

5.5	Comparison of dynamic analysis results of a square building using different earthquake accelerograms for dynamic analysis	122
5.6	Comparison of static & dynamic analysis results for square and rectangular buildings using NBCC recommended equivalent static design approach with strength method of design	128
5.7	Comparison of static & dynamic analysis results for square and rectangular buildings using NBCC recommended equivalent static design approach with design eccentricity equal to the actual eccentricity of the building and using the strength method of design	135
5.8	Comparison of dynamic analysis results of a rectangular building for the earthquake in X & Y directions	140
5.9	Comparison of static & dynamic analysis results for a rectangular building designed using NBCC recommended equivalent static design approach for various design eccentricities with the strength method of design	143
5.10	Comparison of static & dynamic analysis results for a square building designed using NBCC recommended equivalent static design approach for various design eccentricities with the strength method of design	148
5.11	Comparison of dynamic analysis results of a square building statically designed using strength method of design and using different stiffnesses of walls 3 & 4 in the dynamic analysis	153

List of Tables

4.1	Forces in various walls of a square building, Fig. [4.1a], for E/Q in X-direction, using stiffness method of design	94
4.2	Forces in various walls of a square building, Fig. [4.1a], for E/Q in Y-direction, using stiffness method of design	94
4.3	Maximum Panel Forces governing the design of various walls in a Square Building, Fig. [4.1a], using stiffness method of design	95
4.4	Code recommended Design Eccentricity & Torsional Moment for Square Building with Stiffness of each wall proportional to Wall Force in Table [4.3]	95
4.5	Forces in various walls of a square building, Fig. [4.1a], for E/Q in X-direction using stiffness method of design with Stiffness of each wall proportional to Wall Force in Table [4.3]	96
4.6	Forces in various walls of a square building, Fig. [4.1a], for E/Q in Y-direction, using stiffness method of design with Stiffness of each wall proportional to Wall Force in Table [4.3]	97
4.7	Maximum Panel Forces governing the design of various walls in a Square Building, Fig. [4.1a], using stiffness method of design with Stiffness of each wall proportional to Wall Force in Table [4.3]	97
4.8	Forces in various walls of a rectangular building, Fig. [4.1b], using stiffness method of design	98

4.9	Forces in various walls of a Square Building, Fig. [4.1a], for E/Q acting in X-direction, using Strength Method of design	101
4.10	Forces in various walls of a Square Building, Fig. [4.1a], for E/Q acting in Y-direction, using Strength Method of design	102
4.11	Maximum Panel Forces governing the design of various walls in a Square Building, Fig. [4.1a], using Strength Method of design. . . .	102
5.1	List of the dynamic analyses made in this studies	105
A.1	Time Periods (in sec) of the Buildings in Figs. [4.1a] and [4.1b], de- signed by the Strength Method, for displacements in the X direction	167

DEDICATED TO MY FAMILY

Acknowledgement

I would like to express my sincere appreciation and gratitude to my advisor, Dr. R. A. Spencer, for his invaluable assistance and guidance throughout the duration of the research period and the writing of this thesis. The advice given by coadvisor Dr. D. L. Anderson during the research is gratefully acknowledged.

Finally, I would like to thank the U.B.C. Civil Engineering Department staff, my friends and my wife for their assistance, advice, and encouragement in completing this thesis.

Chapter 1

INTRODUCTION

1.1 General :

Immediately after the second world war, an immense necessity for residence facilities was felt all over the world especially in Europe where the war had left its mark in every big and small town. The classical methods of construction were not adequate to meet this construction demand. Therefore prefabricated construction was introduced in which members like beams, columns, walls etc. were fabricated in the plants and then assembled at the construction site.

Using standard precast building components for construction offers a much greater speed in construction. This decrease in the total time of construction has enabled the concrete industry to compete effectively with the steel and timber industries which have a major advantage over in-situ concrete in this field.

The use of precast members is widely prevalent everywhere in the world especially in non-seismic regions. But in seismic regions this industry is still lagging behind because of a lack of information on the performance of precast buildings and the joints used for connecting the precast elements under the earthquake loads.

1.2 Categories of Pre-cast Concret Construction :

Precast buildings are of two types, 'jointed' and 'monolithic', with widely different structural properties [9]. In monolithic construction, precast elements are joined by

well reinforced connections possessing continuity of stiffness, strength and ductility comparable to well designed cast-in place concrete. In jointed construction the precast elements are connected to each other by relatively small connections while the inter element boundaries behave as zones of reduced stiffness, strength and ductility.

While the existing code requirements on strength and ductility can be used for the design of monolithic precast structures, code requirements for jointed structures are not well established. In a jointed precast structure, joints open and close as energy is input into the structure. If sufficient energy is input to open up the joints, connections between the precast elements will yield because they are weaker than the jointed element. These connections start acting as the localized sites for energy dissipation. As this yielding is confined to small volumes only, the energy dissipation capacity of a jointed structure will be less than that of a monolithic structure detailed as conventional cast-in situ concrete. On the other hand, in a jointed structure as connections starts yielding before the monolithic structure, the structure will exhibit a non-linear force displacement relationship even though the concrete and steel stresses in the elements are within elastic limit. This non-linear response of a jointed structure should result in reduced seismic energy input into the structure. This shows that a jointed structure behaves quite differently from a monolithic structure in terms of energy input as well as energy output.

1.3 Earthquake Response of Buildings :

Earthquakes and their ability to do damage can best be described in terms of energy. When a fault ruptures, elastic strain energy is released which sets the neighbouring earth strata into motion. The earth strata act as a filter for this wave, filtering the high frequency waves. Thus at a point some distance away from the epicentre only the low frequency waves are present.

As the waves pass underneath a structure, some energy is transferred into the structure, the amount of which depends upon characteristics of the structure and the duration of ground shaking. It takes some time to build up energy in the structure i.e. we need a finite duration of ground shaking underneath the structure. The more receptive structures are those with linearly elastic stiffness properties, and with natural vibration frequencies similar to the frequencies of the strongest ground shaking. Structures with non-linear force displacement relationship do not have well defined natural frequencies. As these structures begin to respond to harmonic loads, their effective period of vibration changes, thus forcing the structure away from resonance, reducing further energy build up.

The behaviour of structures under earthquake loads has been demonstrated as a 'Storage Tank Analogy for the Absorption and Dissipation of Seismic Energy' by Clough [9]. He represents the structure by a storage tank Fig. [1.1]. The elastic strength of the structure is represented by the height of an overflow nozzle above the base. Two large pipes conduct energy into and away from the main tank. An inlet pipe is fitted with a valve which is wide open for a linear elastic structure and partially closed for a non-linear structure. For a strong ground motion of finite duration, response will build up until the structure's elastic limit is attained i.e. the storage tank is fully filled. Any additional input of energy will lead to spill over into the smaller reservoir tank. If the structure is brittle (i.e. the size of the smaller reservoir is very small), the reservoir will soon be filled and start spilling over i.e. the structure will fail. But if the structure is ductile, the smaller tank can manage to take some of the additional energy i.e. avoiding failure. When the ground shaking stops, elastic strain and kinetic energy stored in the structure are dissipated by damping and the structure comes to rest. The contents of the overflow tank represents plastic work done on the structure which usually means structural damage.

**NEGATIVE AND POSITIVE WORK RESULT FROM THE INTERACTION OF
BASE SHEAR AND GROUND VELOCITY**

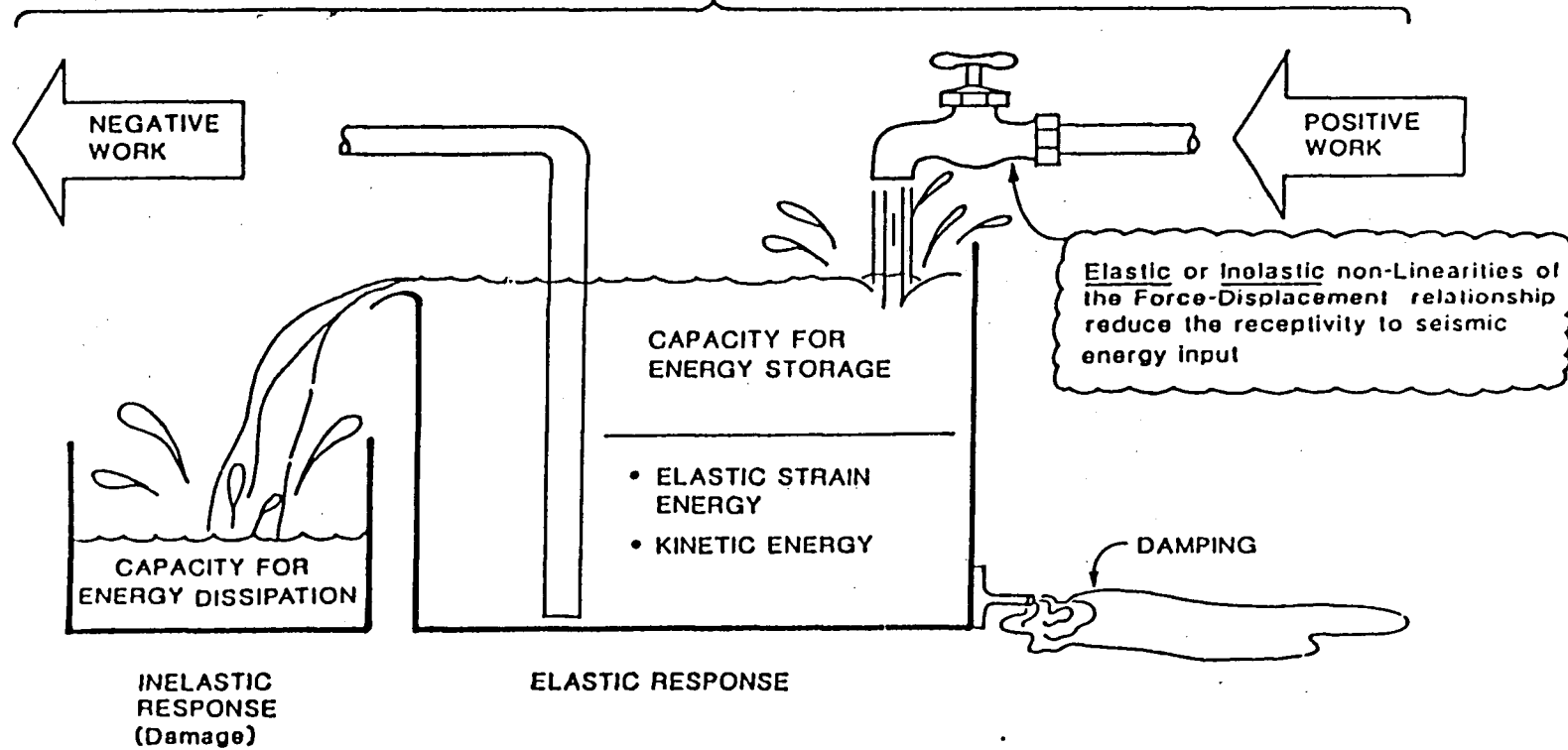


Figure 1.1: Storage Tank Analogy for the Seismic Response of Buildings by Clough [9]

1.4 Scope and Objective of Present study :

This thesis is the continuation of the work done by William Tong [36], who worked on the one dimensional earthquake response of precast jointed box type structures. In this study the two dimensional response of a one storey precast box type building is studied. The building walls are made up of standard double-tees connected together by connections. To study the effect of eccentricity, panels in one of the walls are changed while keeping the other three walls same all the times. Non-linear connection behaviour is modelled from the results of test performed on isolated precast connections under cyclic loading.

The main objectives of this study are :

1. To evaluate the validity of various static design methods for unsymmetrical buildings.
2. To evaluate the performance of unsymmetrical one storey box type precast structures designed according to building code requirements.
3. Based on analytical results, to make recommendations on any necessary changes in the building code requirements for the design of jointed structures.

1.5 Thesis Layout :

This thesis begins with a discussion of cyclic tests performed on isolated connections used for connecting the precast units. In the following chapter, detailed modelling of the one storey structure is studied. Results of the dynamic analysis of the buildings designed according to code requirements are shown in the next chapter. In the final chapter conclusions of the present study are presented.

Chapter 2

CYCLIC TESTS ON CONNECTIONS

2.1 Introduction

Connections are one of the most important parts of a precast structure because they are the weakest link in the structure. Test results on full scale structures have shown that connections start yielding even when the steel in the precast panels is in the elastic range. This is because the strength of a connection is much less than that of the surrounding panel. And once the connection starts yielding, its strength may start decreasing with the cyclic load leading to its failure. The design philosophy for the design of connections is :

- to remain elastic for small earthquakes.
- to be able to take inelastic deformations without structural collapse.

Connections can be used to dissipate energy if they show stable elasto-plastic behaviour. A word of caution here is that if connections are used as energy dissipators, extreme caution must be taken to ensure their integrity, even as they degrade, especially the connections upon which the ultimate stability of the structure depends. Thus in some connections e.g. in the diaphragm, it is desirable for connections to resist earthquake without yielding. According to Spencer [32], these relatively strong and rigid connections designed for earthquake loading can lead to certain

problems under service loads. Hence, a designer has to foresee these effects and try to eliminate them by proper detailing and design.

To reduce both erection and production costs, connections should be able to take some variation of size and mis-alignment of panel edges & faces etc. However the tolerance must not be so large as to cause aesthetically objectionable features in the completed structure, nor to cause functional problems. Joints should be detailed so as to provide adequate clearances between components of joints. Such characteristics help speed the work of erection crew by facilitating the placing of grout or welding and tightening of bolts etc.

Spencer and Tong [36] have shown that shear walls with overdesigned connections are not always the best solution for earthquake loading, because overdesigned connections mean higher probable strengths of the walls, which implies that wall to roof connections have to be stronger to take the increased load transferred to them by strong walls.

Good quality control of the steel that goes into the connections is necessary. Kallros [17] has shown that the yield and ultimate strength of two rebars he got from two different suppliers had much higher values than the recommended strength for that steel. He also found that the use of high yield strength bars for the connections will lead to brittle failure because these bars have less ductility.

2.2 Types of connections :

Precast connections are classified as

- Dry Connections
- Wet Connections

2.3 Dry Connections

These connections utilize mechanical anchors such as bolts or welded metal to transfer the load. Shear is transferred across the connection through the bearing of steel shapes; shear of the connecting elements; shear of the welds or bolts or through friction between bolted plates. Various types of dry connections available are :

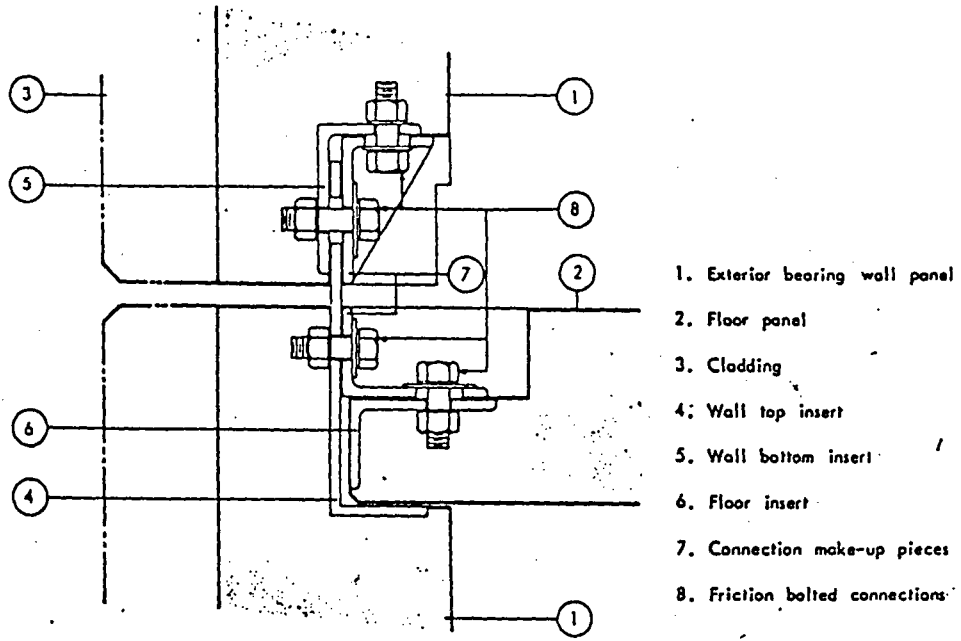
2.3.1 Bolted Connections

In these connections steel embedments are bolted together to form the connection. The advantage of these connections is that they can be quickly assembled and erected. The primary disadvantage is that close tolerances are required for placement of the connectors and its receptacle when they are embedded in concrete members.

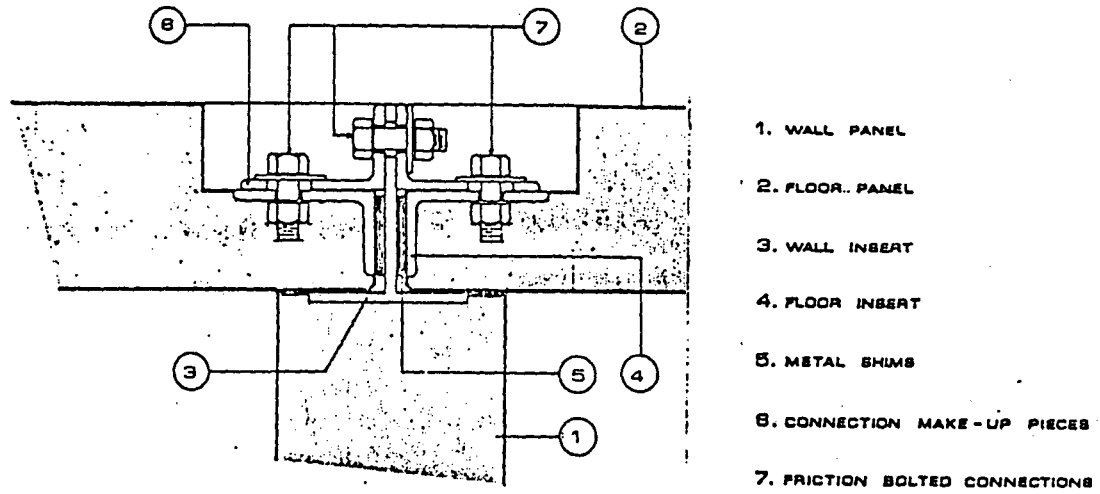
One example of bolted connections which has behaved well under the cyclic loading is *Drescon-Concordia System* [14]. Connections are generally composed of steel inserts embedded in concrete panel. These are held in place by stud-welded anchor bars which are used to develop the required strength by shear friction. During the erection when two such inserts are placed adjacent to each other, a third element (a steel make up piece) is friction bolted into the embedded inserts. The makeup pieces are pre-slotted to take up manufacturing and erection tolerances.

These connections can be used as *wall to floor* connection Fig. [2.1], *floor to floor* connection Fig. [2.2], *wall to wall horizontal connection* Fig. [2.3]. Tests made by the National Bureau of Standards in Gaithersburg, Maryland indicate that these friction bolted connections have a capacity for energy dissipation and that the capacity of the connections is not impaired for cyclic loading tests beyond the ultimate slip load.

A slightly modified form of the above connections is the Limited Slip Bolted Joint [LSB] developed by Pall & Marsh [24]. The *wall to wall vertical connection*



(a) Exterior Wall



(b) Interior Wall

Figure 2.1: Wall to Floor connections, from Ref. [14]

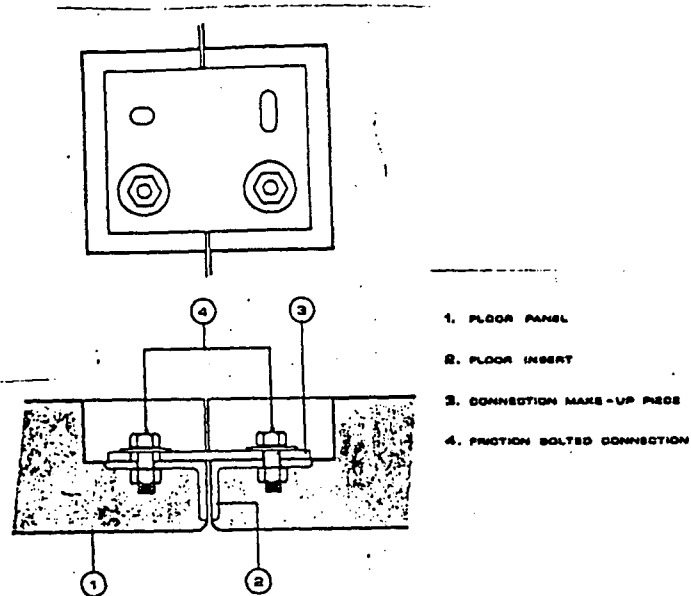


Figure 2.2: Floor to Floor connection, from Ref. [14]

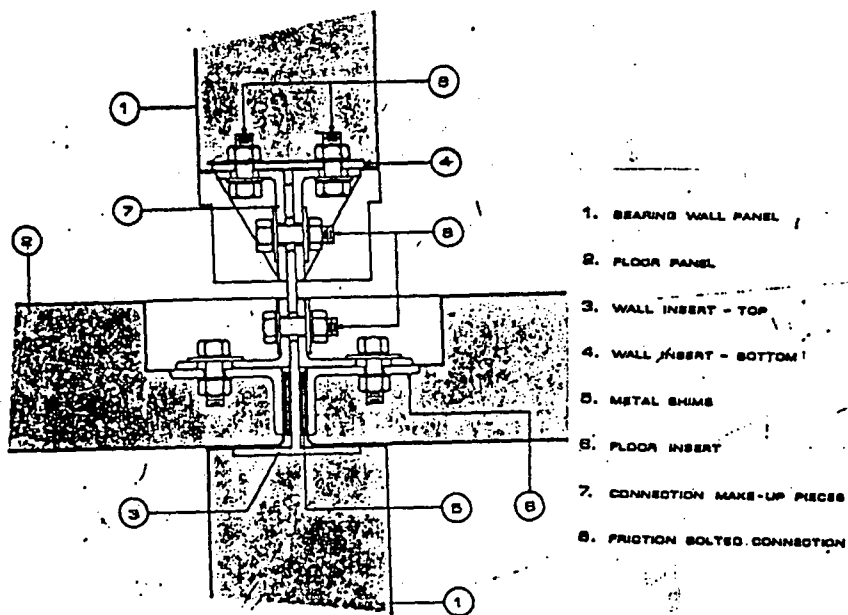
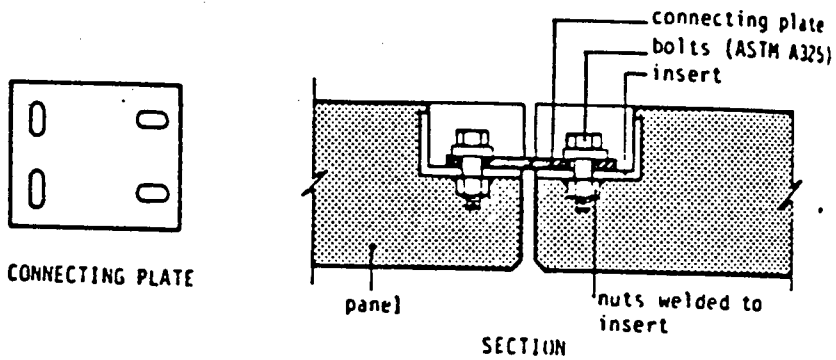
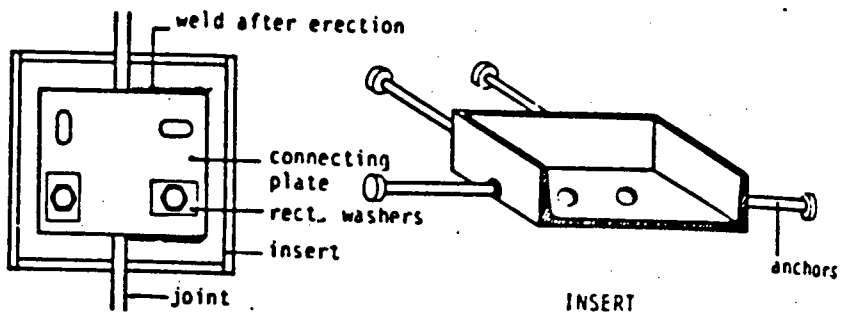
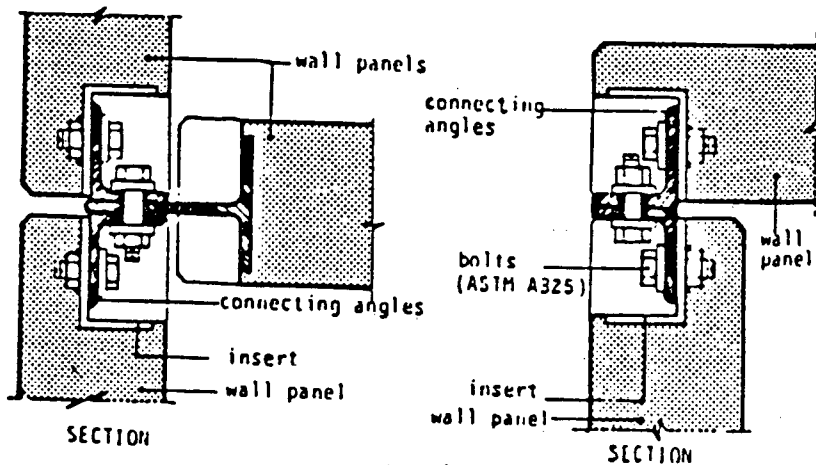


Figure 2.3: Wall to Wall Horizontal connection, from Ref. [14]



(a) Wall to Wall Joint



(b) Corner Wall to Wall Joint

Figure 2.4: Limited Slip Bolted connections, from Ref. [24]

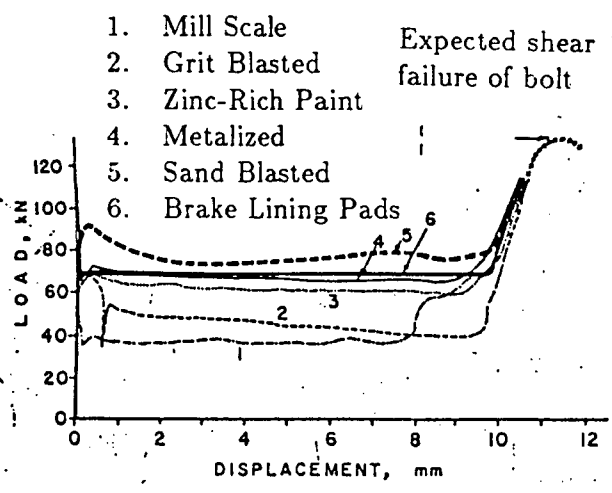
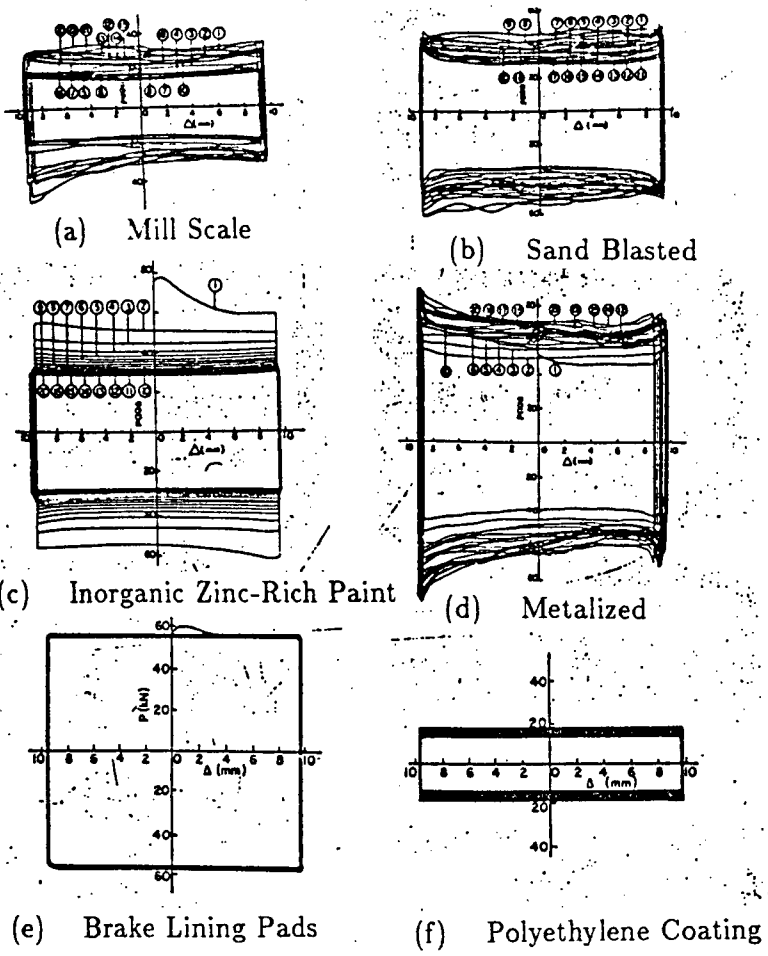


Figure 2.5: Load-Deformation Response of Limited Slip Bolted (LSB) Joints, from Ref. [24]

is shown in Fig. [2.4]. The connection plate is bolted in position during erection but is finally welded on one side to prevent the rotation of the plate when slipping occurs. These joints are designed not to slip for service loads, but are allowed to slip during severe seismic excitation and so they will not be grouted but sealed by other appropriate means.

The static and dynamic tests on LSB connections; having different slipping surface treatment were conducted by Pall & Marsh [24]. Load deformation curves and hysteresis loops; using 12.7mm (1/2 inch) diameter high strength bolts (ASTM - A325), are shown in Fig. [2.5]. The load deformation characteristics are elasto-plastic upto the point of slipping and after that these are plastic. If slipping of the bolts exceeds the hole clearance then it becomes elastic again upto the load causing failure in the bolt. The best behaviour is shown by brake lining pads inserted between steel plates with mill scale surfaces. The joint exhibited a constant repeatable slip load and nearly elasto-plastic behaviour with negligible degradation. A sand blasted steel surface was the second choice. Thus it is possible to achieve the appropriate strength and energy dissipation by an appropriate choice of joint surface and clearance of slotted holes.

2.3.2 Welded Connections

In these connections steel embedments in the precast panels are welded together with or without a steel piece used to make welding of two connections easier.

Research has been done on the cyclic behaviour of different types of welded connections. These include :

- Headed Stud Connection.
- Embedded Rebar Connection.
- Split Pipe Connection.

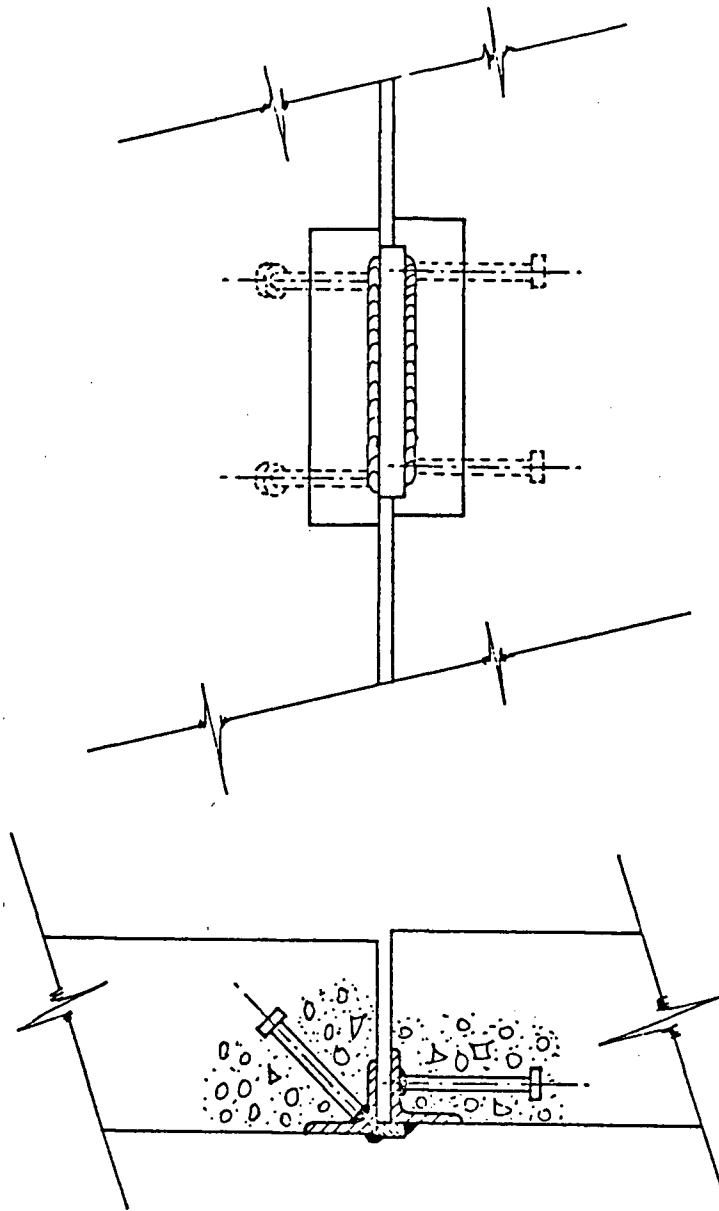
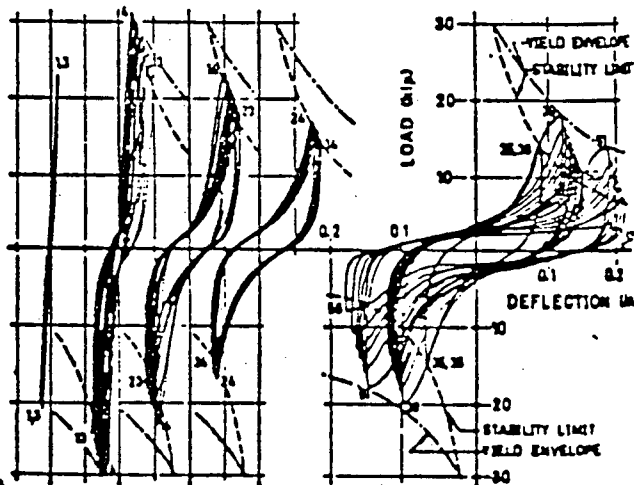


Figure 2.6: Typical Headed Stud Connection showing two common stud configurations and the ease with which minor imperfections and misalignments may be accommodated, from Ref. [23]

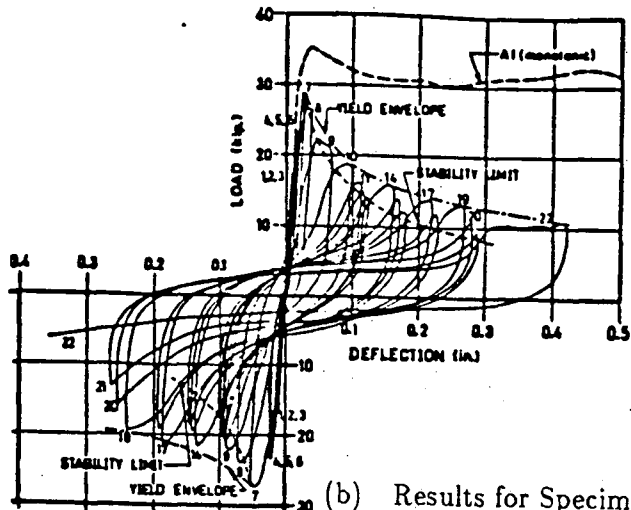
CONNECTION	DETAILS OF STUDS & PANEL REINFORCEMENT	
A1		
A2, A3		
B1		
B2		
B3		

Figure 2.7: Details of Specimens reported by Spencer & Neille [31]

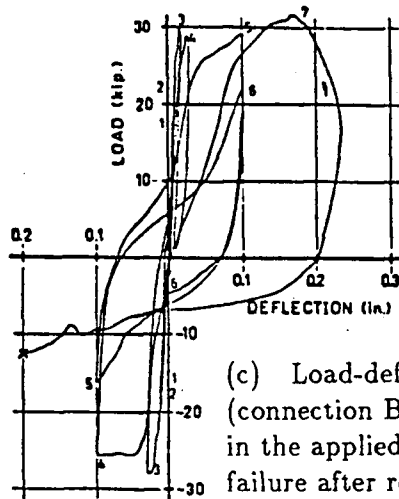


(a) Load-deflection loops (connection A2) showing stable behaviour after 35 cycles of loading. Groups of curves have been separated for greater clarity

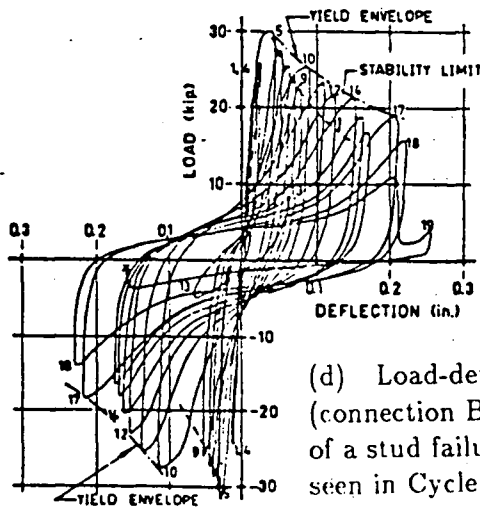
Figure 2.8: Hysteretic Behaviours of Welded Headed Stud Connections reported by Spencer & Neille [31]



(b) Results for Specimens A1 & A3



(c) Load-deflection loops (connection B1). Rapid increase in the applied deflection led to failure after relatively few cycles.



(d) Load-deflection loops (connection B2). The result of a stud failure can be seen in Cycle 19.

Figure 2.8 : Continued

Headed Stud Connection

A typical headed stud connection is shown in Fig. [2.6]. It is clear from the figure that minor imperfections and misalignments can be accommodated very easily in these connections. Spencer & Neille [31] have done work on the behaviour of headed stud connections under cyclic loading. Details of the tests are shown in Fig. [2.7]. Connection A1 was loaded monotonically to failure while the other five connections were tested for cyclic loading at frequencies in the range of .01 to .02 Hz. Load deflection curves for the connections are shown in Fig. [2.8]. The following conclusions were made by Spencer & Neille [31]. :

- The PCI procedure for calculating the ultimate design strength of these connections under static loading gives conservative results.
- The strength of the connection in the first cycle of loading up to yield will be approximately the same as the strength in monotonic loading.
- If cyclic loading is continued above the stability limit the strength of the connections will fall with increasing number of cycles and yield strength envelope will tend to approach the stability limit.
- The deflections reached before failure were seven to twenty times the theoretical elastic deflection corresponding to design ultimate strength.
- These connections, if properly designed and detailed appear to be suitable for use in earthquake-resistant box type buildings.

Neille [23] showed that three factors contributed to the capacity of these connections; friction between the faceplate and concrete; bearing of the end faceplate and concrete; and bearing and bending of studs. He showed that friction forces decreased rapidly under cyclic loading and were negligible compared to other forces in the connections. Existence of these three mechanisms through which the connection

transfers shear forces to surrounding concrete tends to contradict the shear friction analogy which is often used in the design of these connections. It was found that strength of the connection is directly dependent upon the strength of concrete in which it is cast, while the shear friction theory does not contain concrete strength as variable.

Embedded Rebar Connection

An alternate method for embedding the steel sections in precast members is to replace the headed stud with welded reinforcement as shown in Fig. [2.9]. A major advantage of these connections is the large surface area available for welding which reduces the weld stress and chances of brittle weld failure. A brief summary of the rebar connections tested for cyclic loading is given below :

Aswad [2] did some low cyclic tests on connections shown in Fig. [2.10]. The tests were done on 21' * 8' panels. Two types of connections; connections for double-tee (2" flange thickness) and connections for precast wall panel (6" thick); were tested. Load was statically applied. In the majority of cases the load was cycled three times between $\pm P_0$, where P_0 is the value smaller than the actual maximum load and the connection was brought to failure. Thus these tests do not represent the real cyclic behaviour of the connections. The load-displacement curves are shown in Fig. [2.10]. These curves do not show much deterioration in strength and stiffness because the cyclic tests remained essentially in the elastic range. The following conclusions have been stated by Aswad [2] :

- When force applied to the plate was simple shear, ultimate capacities were higher than ones listed in Ref. [1] by up to 100 % in some cases. The extra capacity was higher whenever the connection included a $\frac{3}{8}$ " thick plate which increased the bearing portion of capacity.
- Ductility of the standard plates tested was good to excellent except for D-34

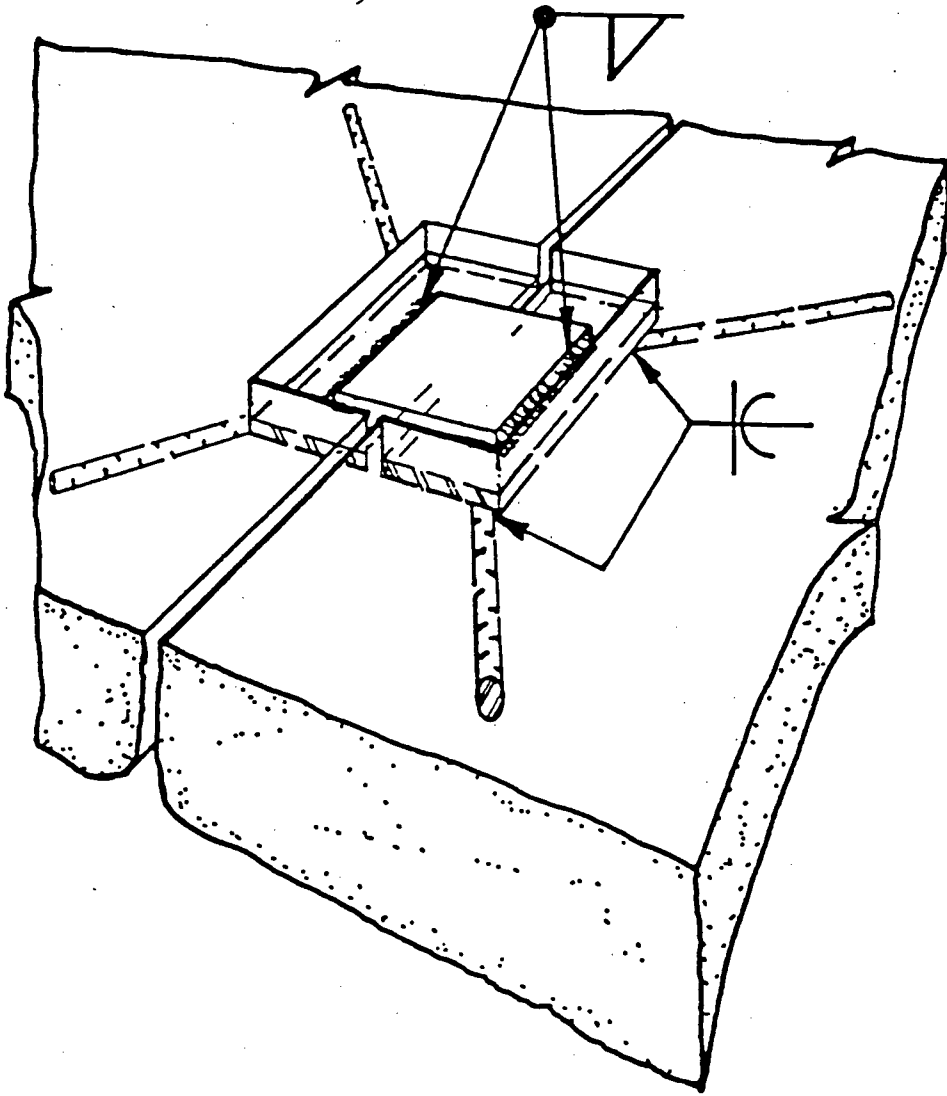
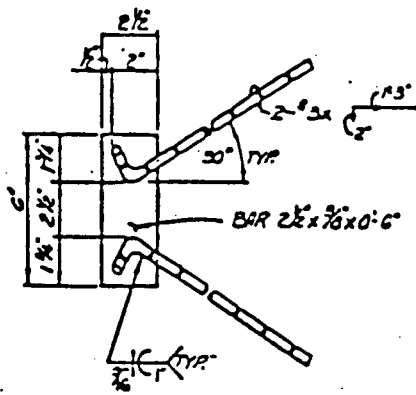
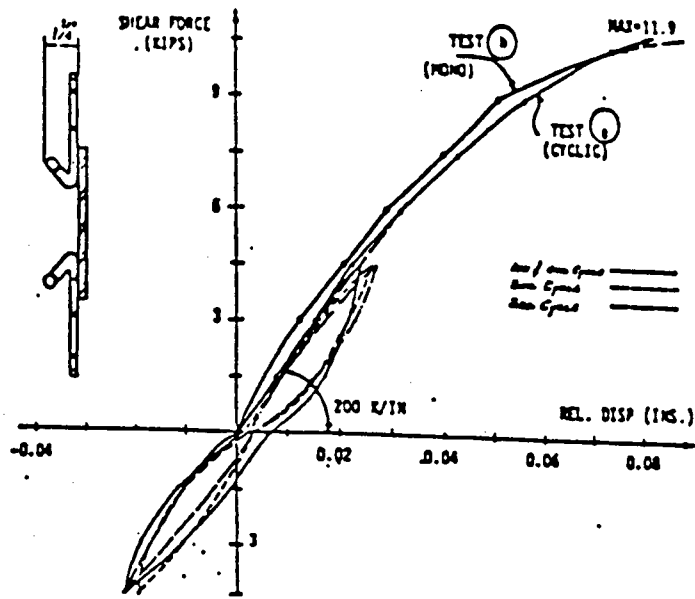


Figure 2.9: Alternate Embedment

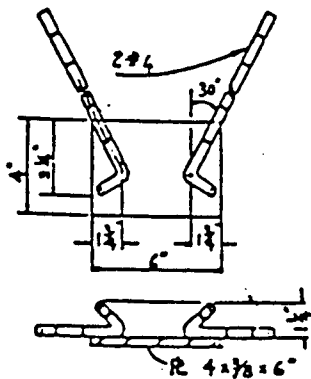


D-34

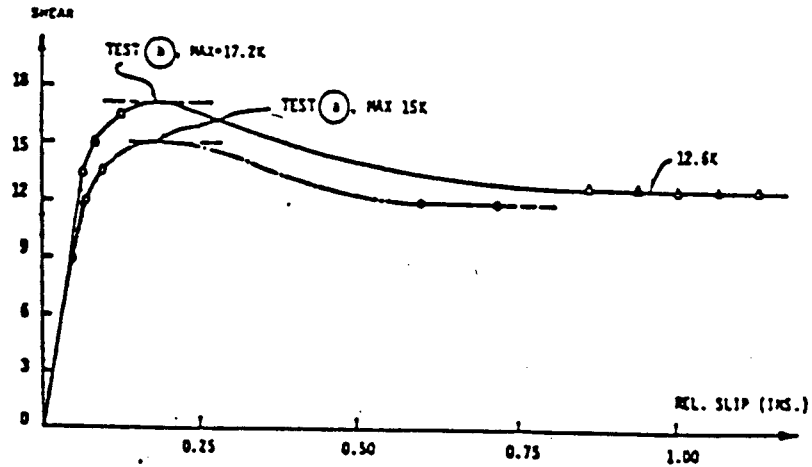


Shear Force vs. Relative Slip For D-34/D-34

(a)

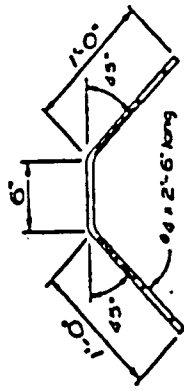


D-36

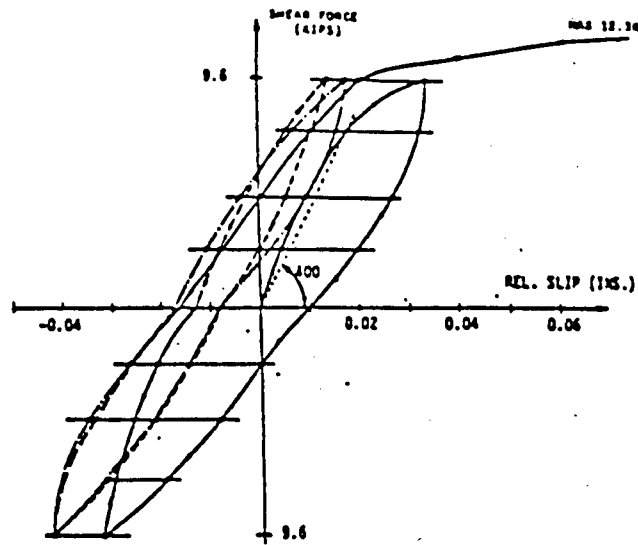


(b)

Figure 2.10: Details of Connections reported by Aswad [2]

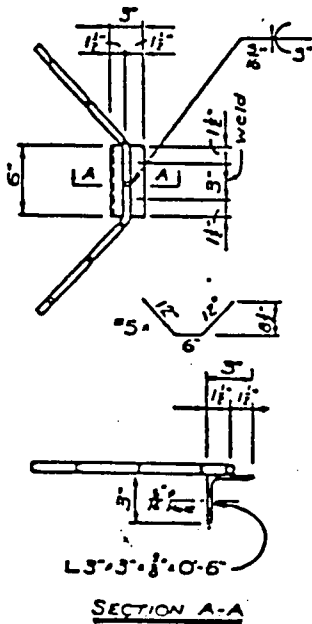


D-40 Tie

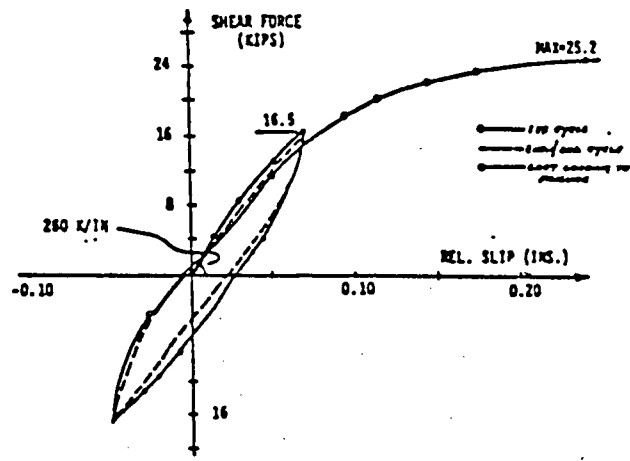


Cyclic Shear Force vs. Relative Slip for D-40/D-40 ties

(c)



P9



Cyclic Shear Force vs. Relative Slip for P-9/P-9 (connections previously loaded in Shear to 15.0 K)

Figure 2.10 : Continued

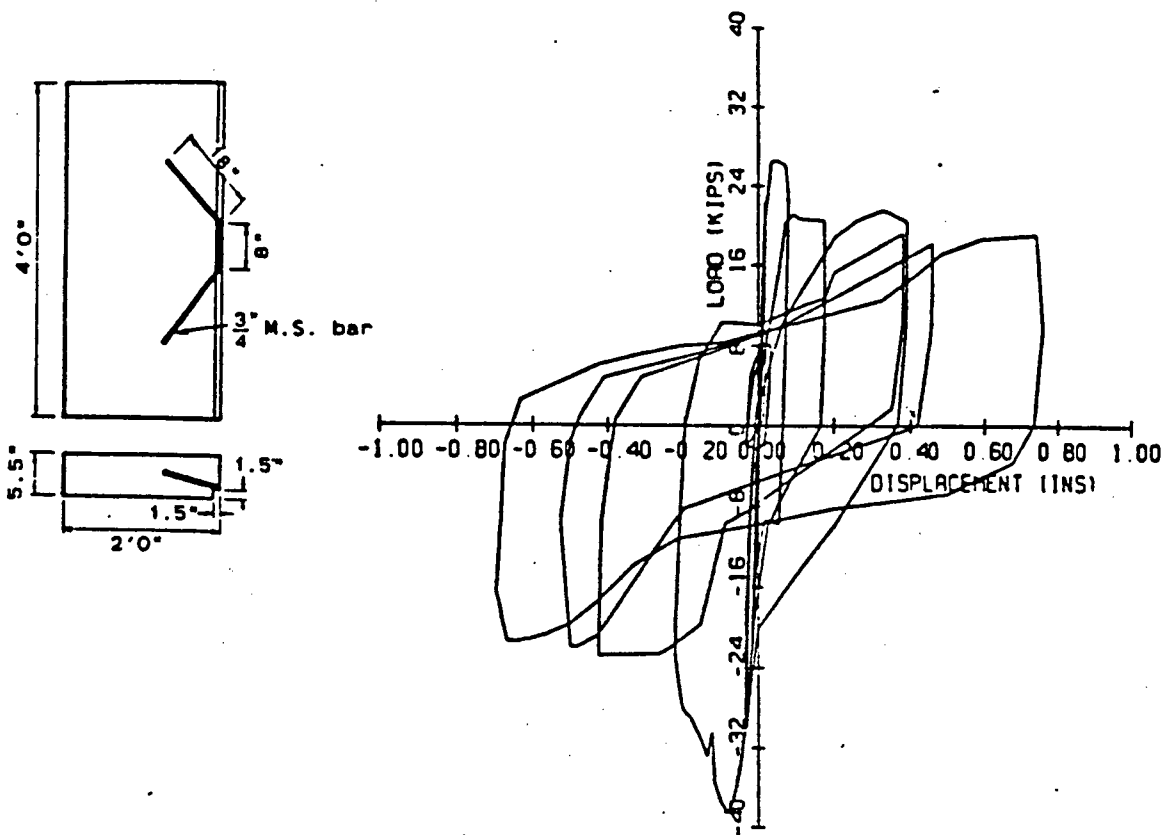
with straight rebars, although its actual capacity was superior to the recommended one.

- Rebar length was sufficient to develop ultimate capacity.
- Plates subjected to cyclic tests showed major deterioration in stiffness after three cycles.
- Pull out forces normal to the panel surface substantially decrease ultimate capacity in shear. Moderate in-plane pull-out forces acting simultaneously with shear do not noticeably affect ultimate capacity of precast connections although they reduce the connection stiffness.
- Size of field weld plates is critical in wall panel connections if premature weld failure is to be avoided.

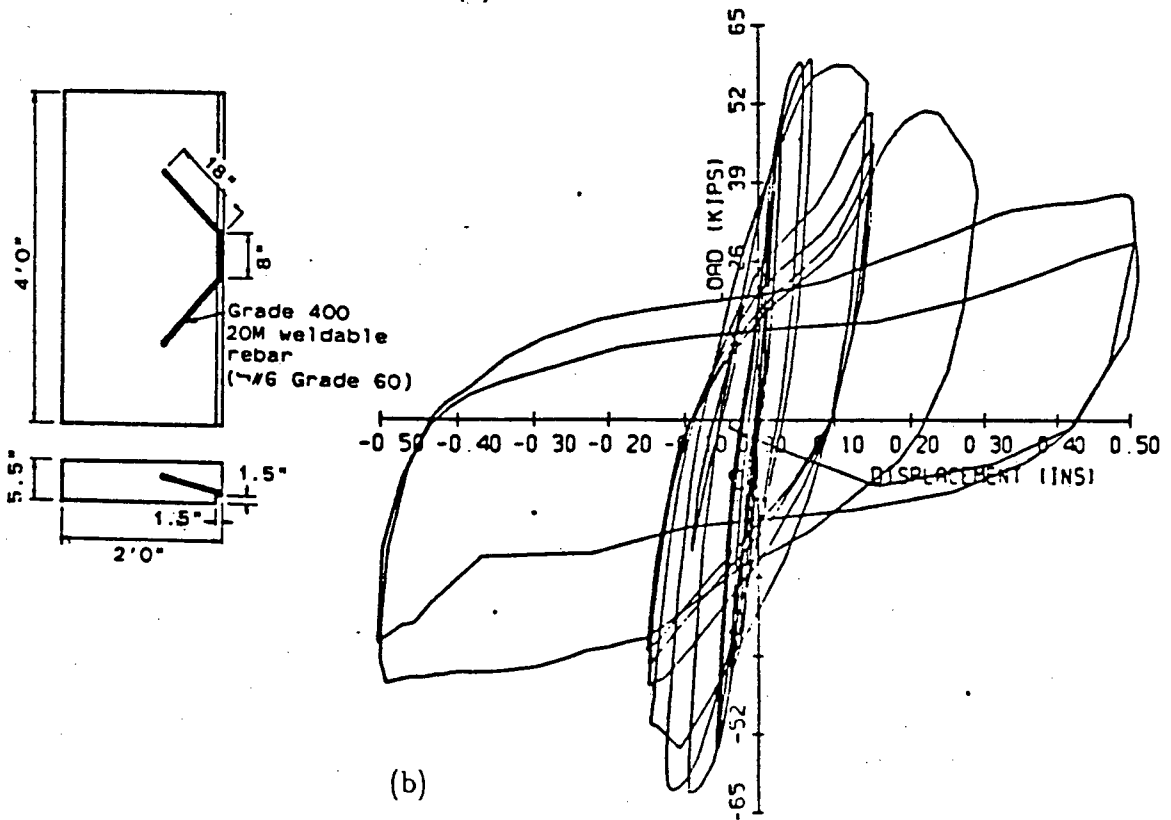
Spencer [34] has done cyclic shear load tests on connections anchored into 4' * 2' * 5.5" concrete panels. The load-displacement curves for the tests are shown in Fig. [2.11].

The following conclusions were made by Spencer [34] :

- Loading cycles in the elastic range do not reduce the strength of the connections.
- The nominal strength of the connections can be found using models shown in Fig. [2.12].
- The strength of the connections, with the rebar running into the connection at 45°, falls to about 50 % of the nominal strength under cyclic loading into inelastic range.
- The strength of connections, with rebar running at 90°, falls to less than 50 % of the nominal strength under cyclic loading into the inelastic range. These connections were not recommended for use in situations where they might be



(a)



(b)

Figure 2.11: Cyclic Behaviour of Connections Anchored With Steel Bars, by Spencer [34]

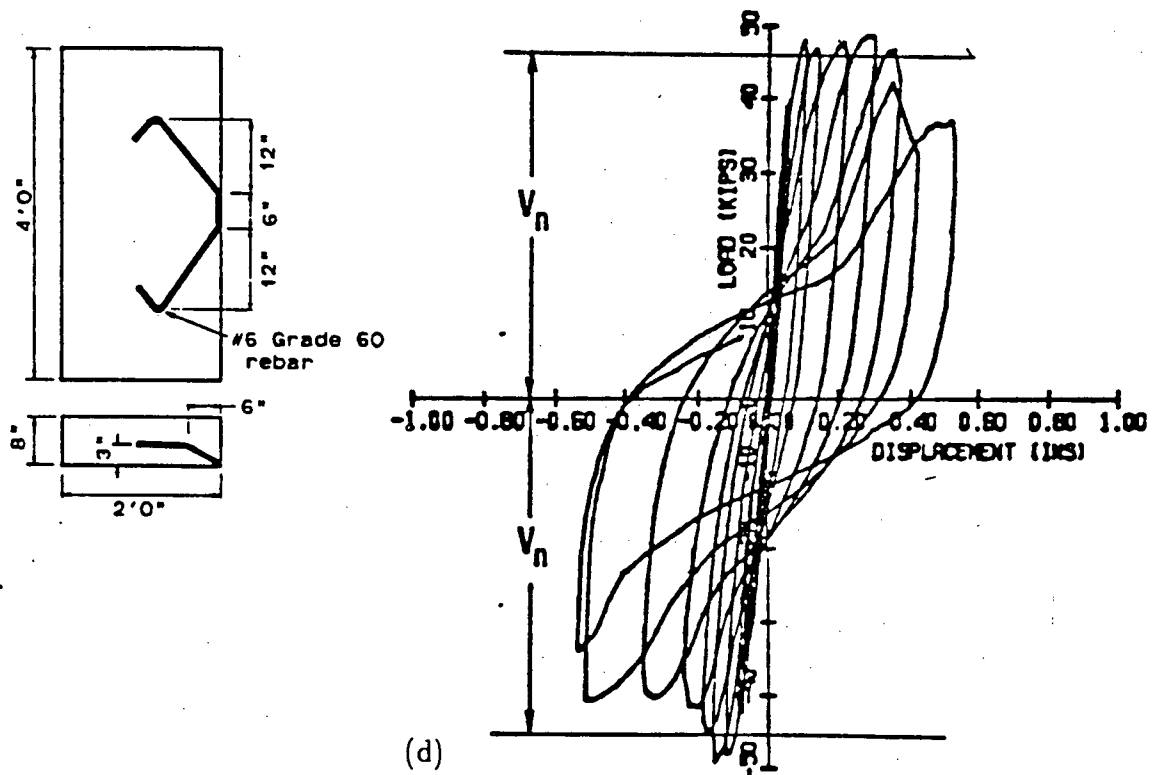
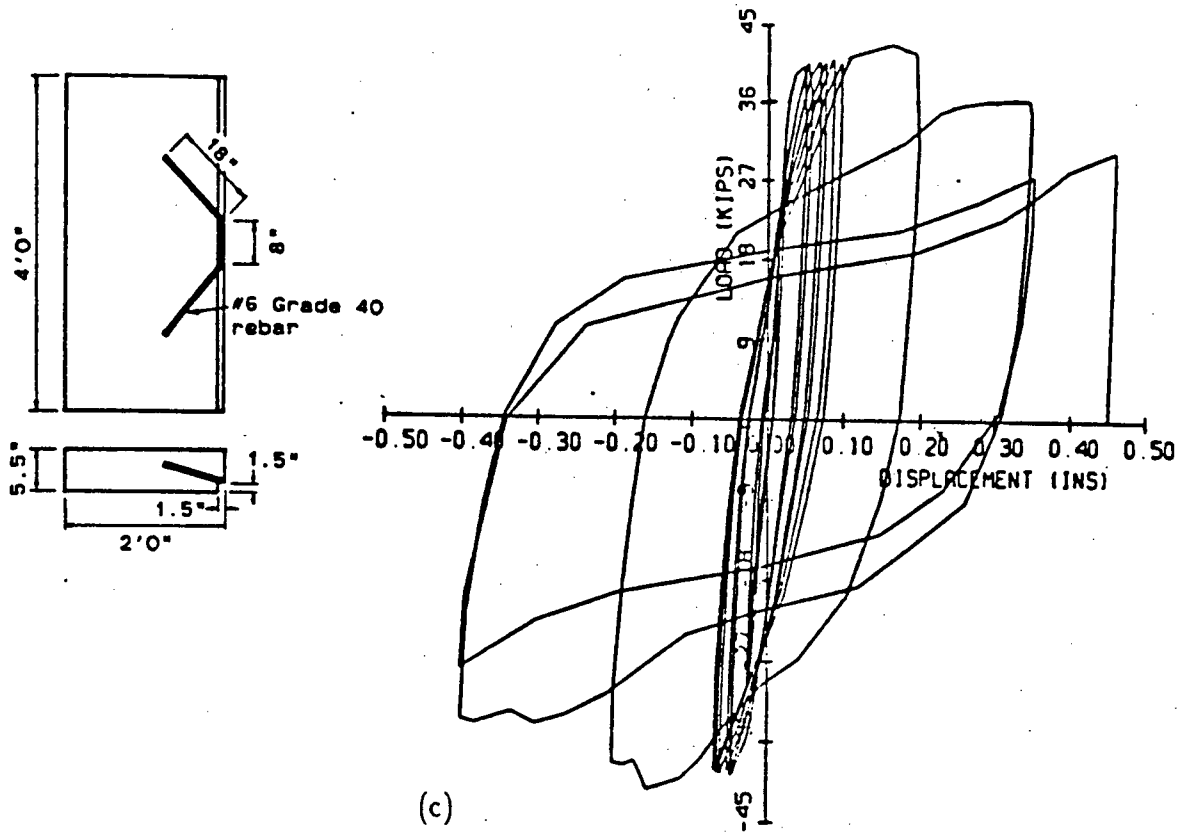


Figure 2.11 : Continued

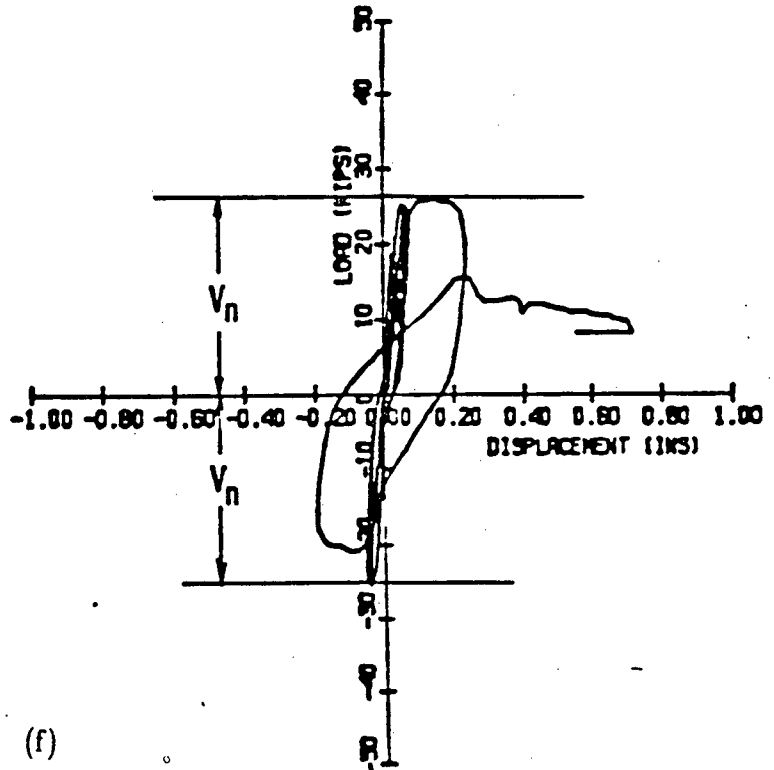
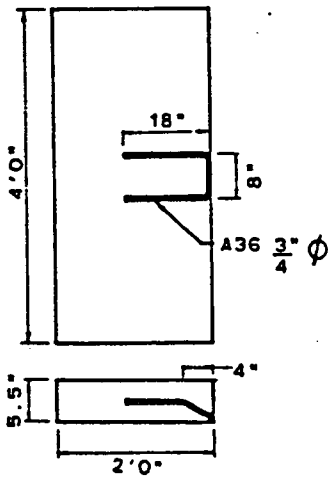
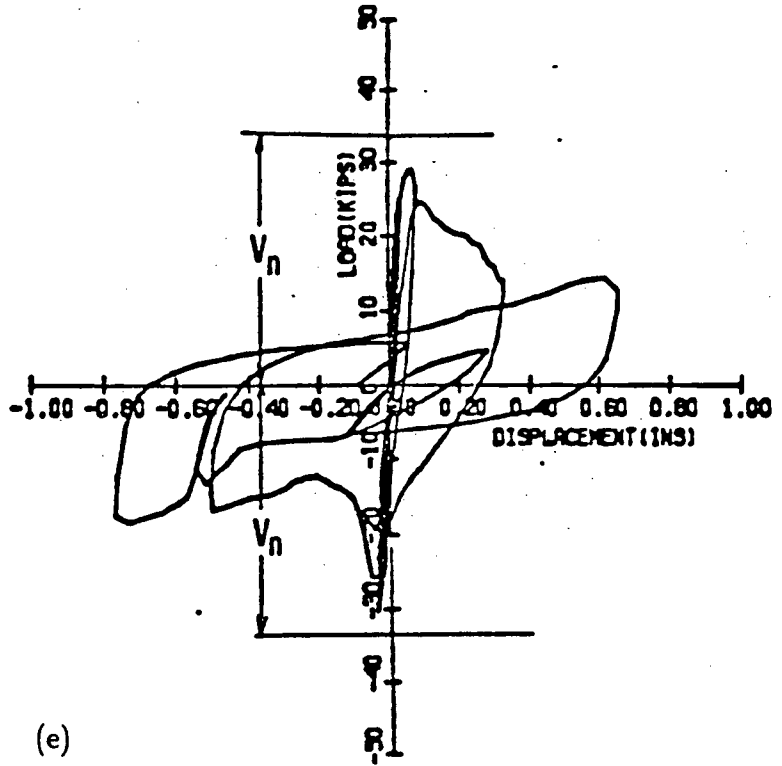
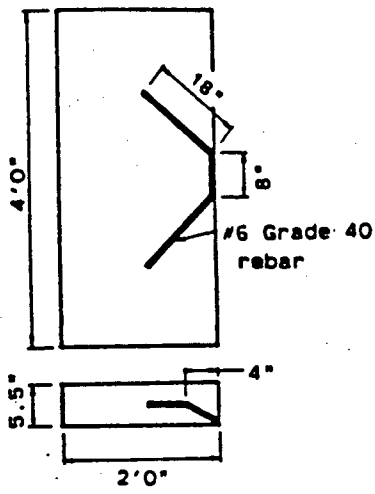
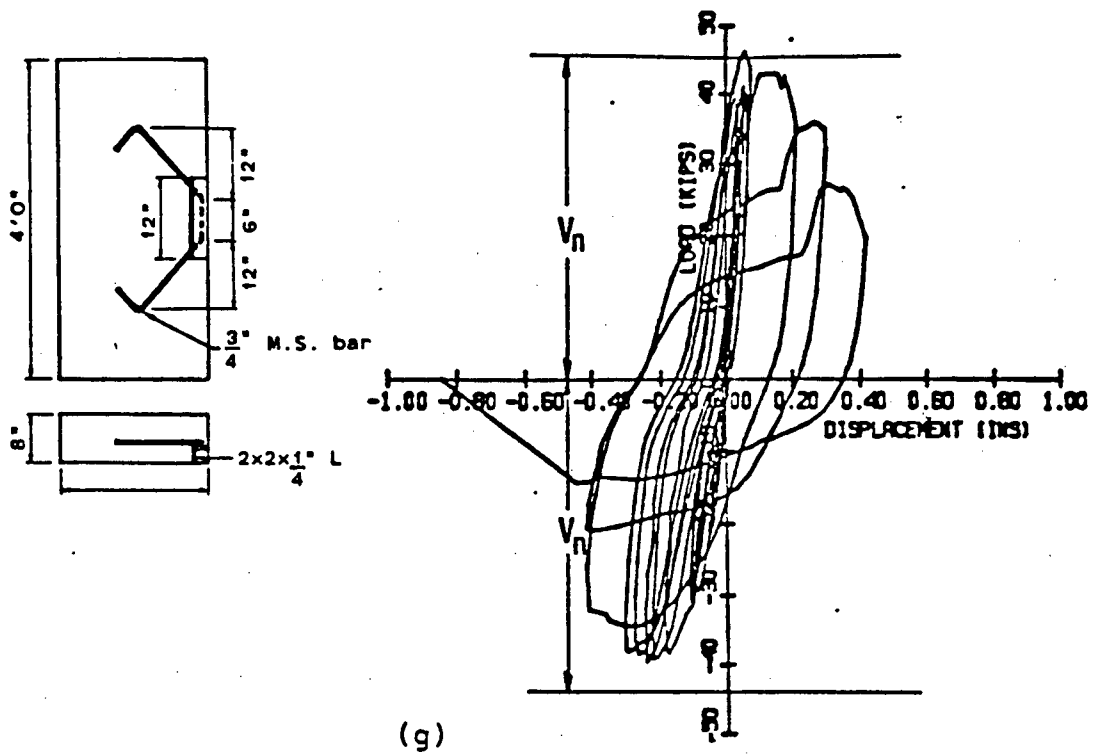
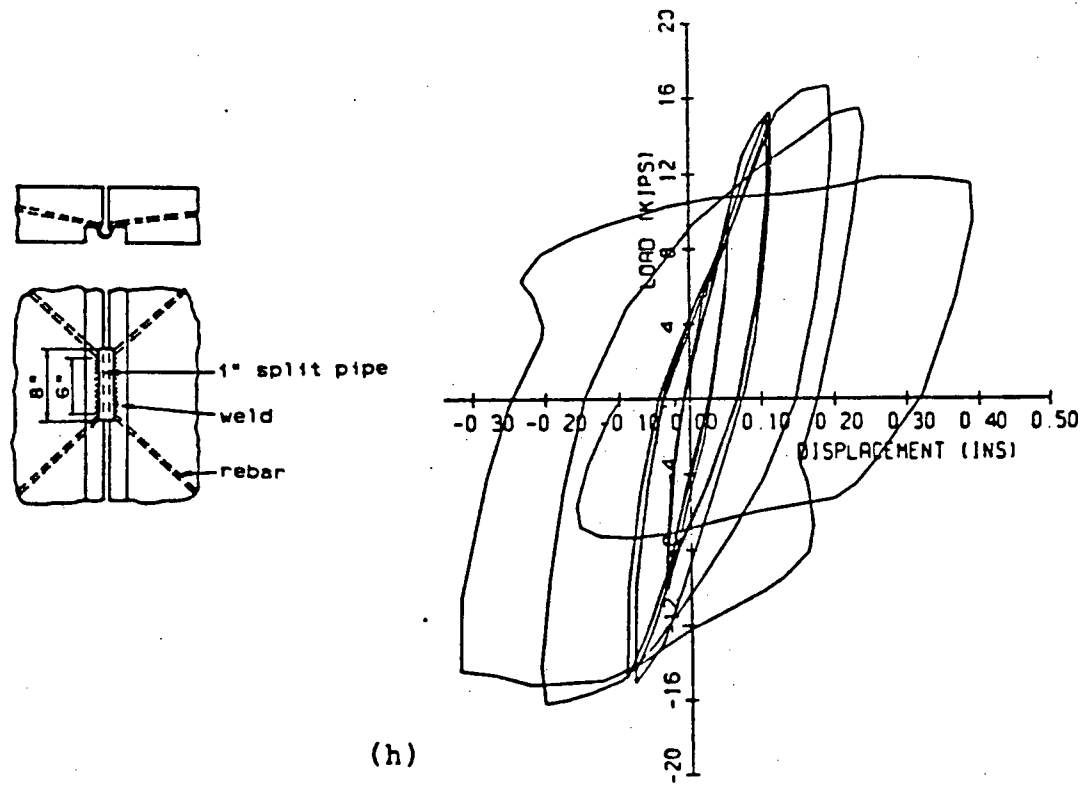


Figure 2.11 : Continued

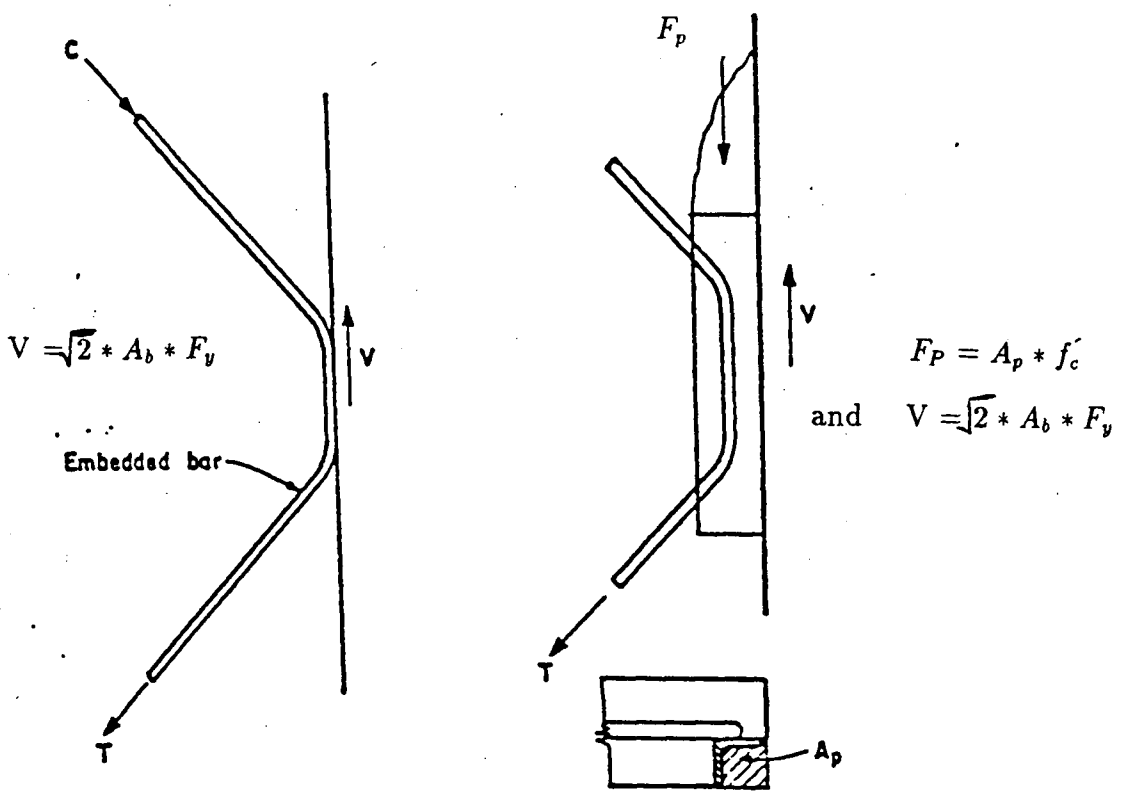


(g)



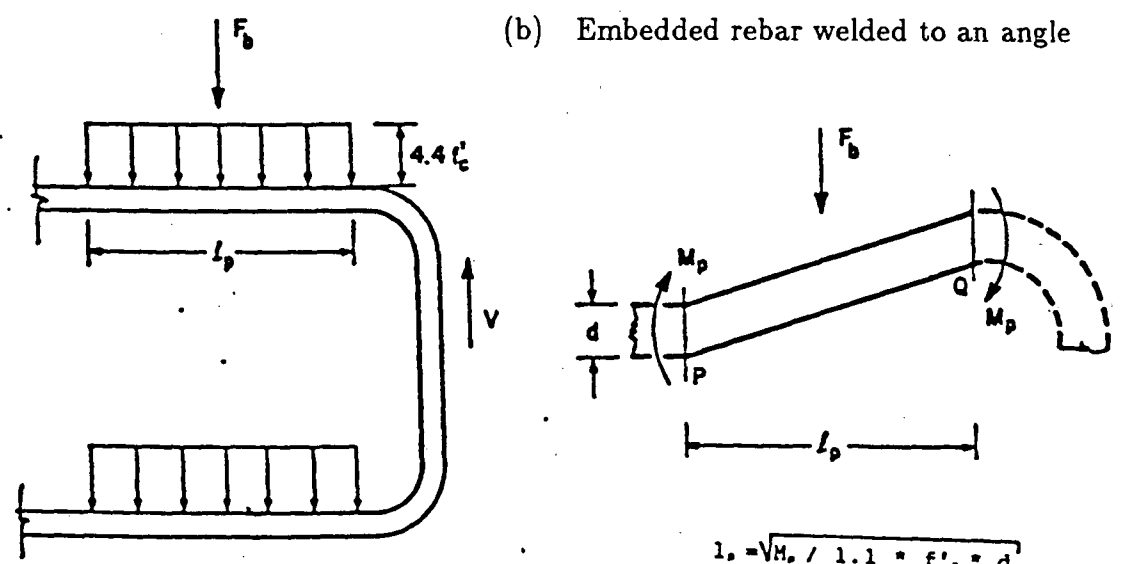
(h)

Figure 2.11 : Continued



(a) Embedded bent rebar

(b) Embedded rebar welded to an angle



$$l_p = \sqrt{M_p / 1.1 * f'_c * d}$$

$$F_b = 4.4 * f'_c * d * l_p$$

and $V = 2 * F_b$

(c) Embedded rebar at 90 degrees

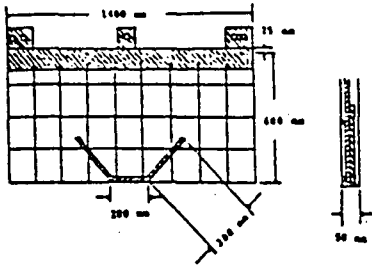
Figure 2.12: Models Developed by Spencer [34]

loaded past their elastic limit when the potential loss of strength is considered on the design.

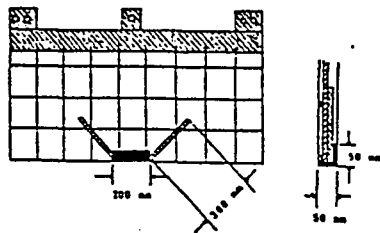
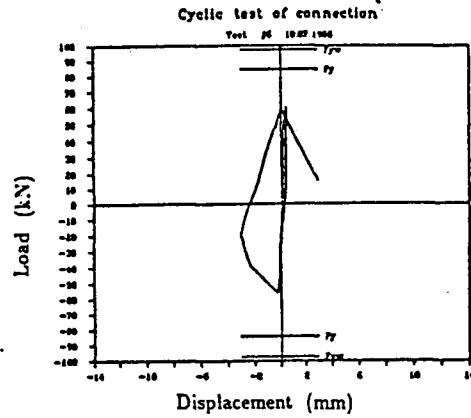
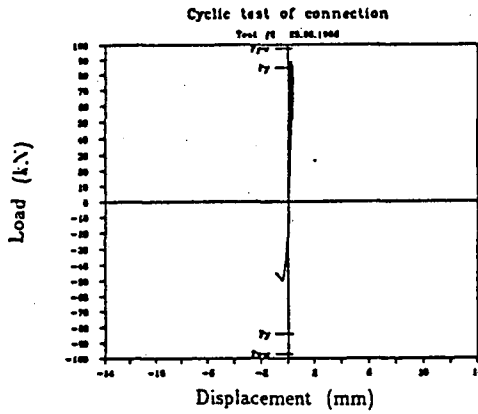
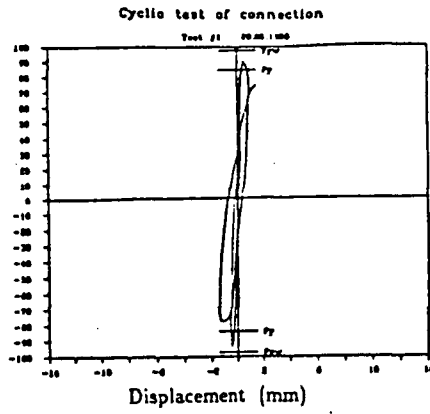
- The connection with a recess in the panel edge and straight embedded bars at 45° appears to perform best under simulated earthquake loading.
- Panel thickness and concrete quality can have a marked effect on the behaviour of connections.

Another investigation has been done by Kallros [17] on thin panel embedded rebar connections. Six different types of connections were tested. All the connections were loaded into the elastic range and loading continued until the connection failed. The failure of the connections occurred either by bar failure or by spalling of the concrete. The bar failure generally occurred at very small deflections. For the connections that failed by spalling, once the connection started cracking, the stiffness gradually decreased with increased cycles into inelastic range and width of the load-deflection curve also increased. Connections that were welded straight to reinforcing mesh did not behave well as compared to other connections. Connections with lower yield strength rebar (rebar # 1) behaved better than rebar # 2, with higher yield strength. The connections and load-deflection curves are shown in Fig. [2.13]. The following conclusions have been made by Kallros [17] :

- Good quality control of steel that goes into connections is necessary. Brittle failure of connections, which is more likely with high yield strength bars, is not desirable.
- A thicker flange will behave better during earthquake loading since there is more cover around the reinforcement. A thicker flange is also less fragile during transport.
- The design strength of connections should be taken as 50 % of expected max-



(a) Rebar # 1 at 45 degrees



(b) Rebar # 1 bent to 45 degrees and welded to an angle

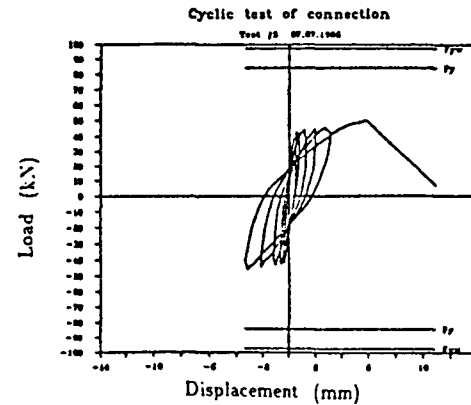
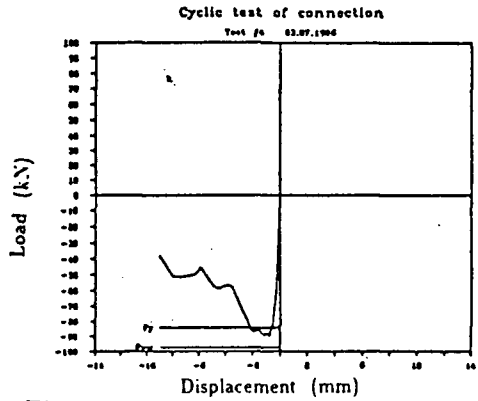
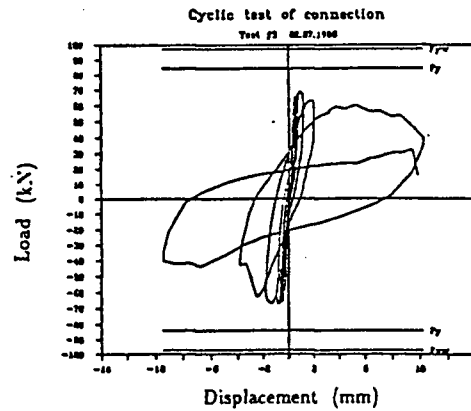
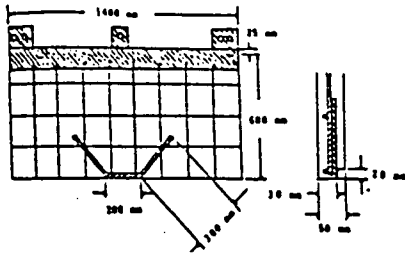
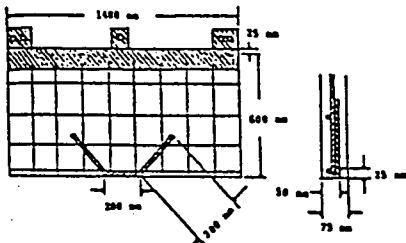
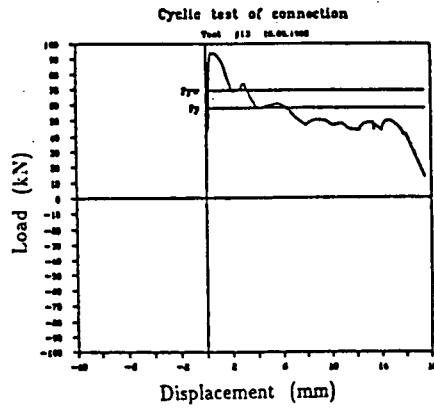
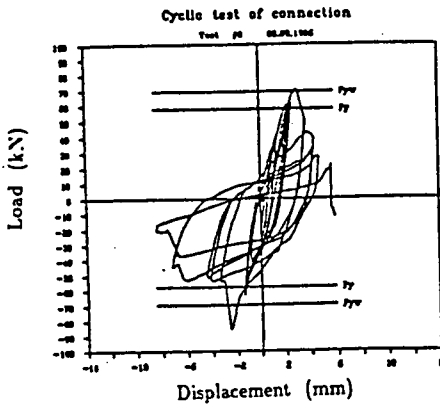
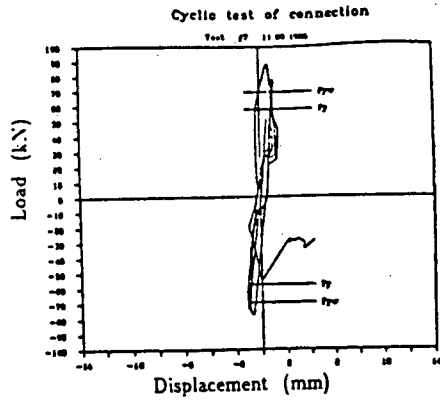


Figure 2.13: Cyclic Tests on Thin Panel Embedded Rebar Connections reported by Kallros [17]



(c) Rebar # 2 at 45 degrees with a short recess



(d) Rebar # 2 at 45 degrees with a recess in a thicker slab

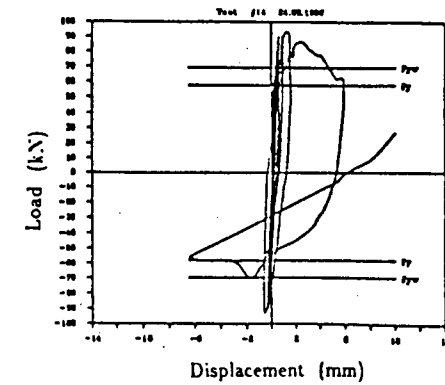
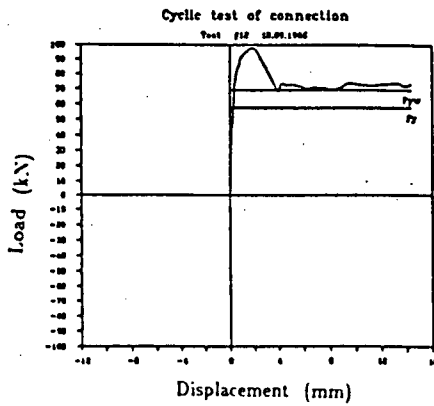
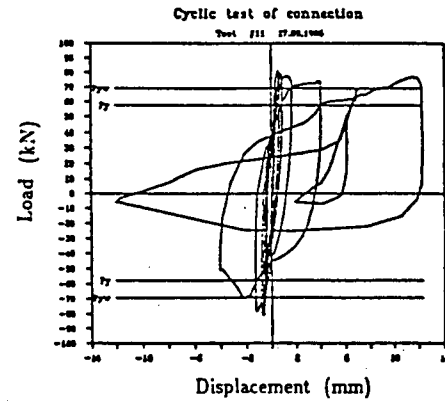
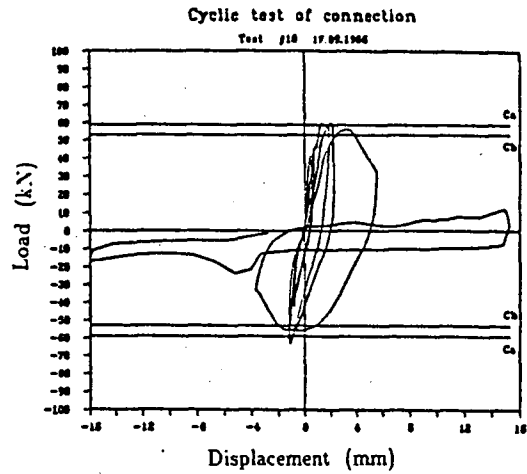
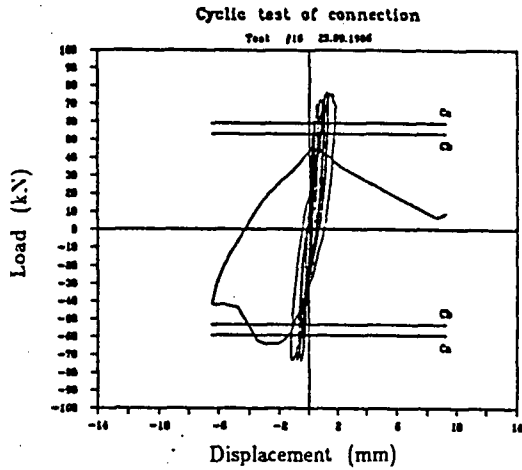
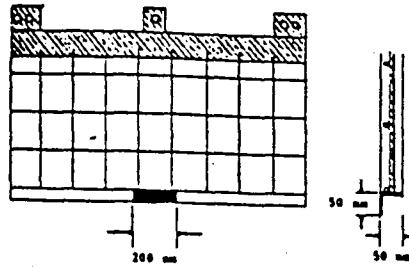


Figure 2.13 : Continued

(e) Reversed angle welded to reinforcing mesh



(f) Angle welded to reinforcing mesh

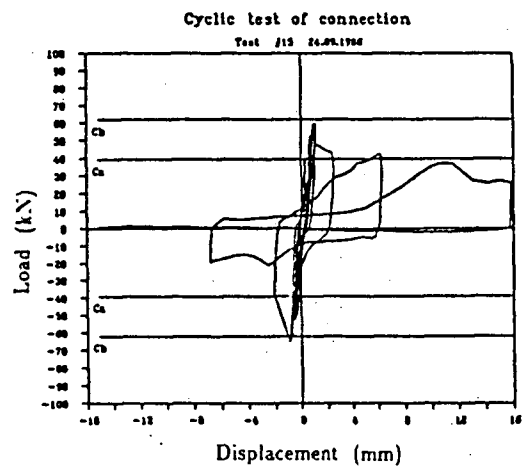
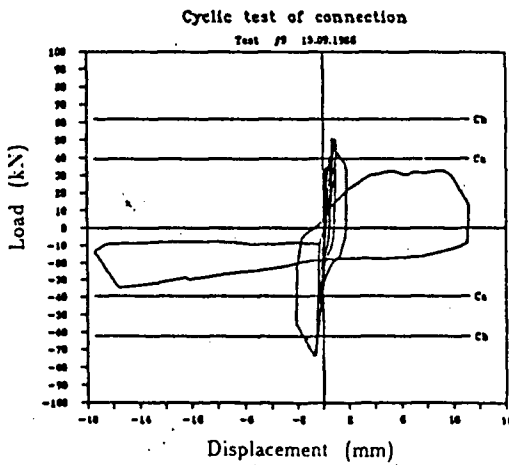
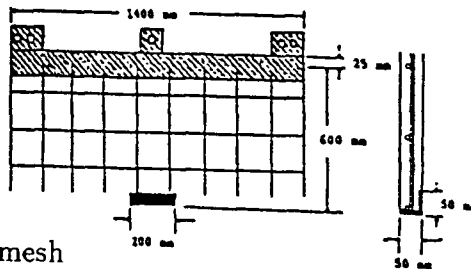


Figure 2.13 : Continued

imum capacity of the connections. Spacing between connections can be reduced in order to reduce the load on each connection.

- Loading cycles in the elastic range do not seem to reduce the capacity of the connections.
- The connections with a recess in the panel edge and embedded bars at 45° appear to perform best under simulated loading. These connections can also be easily attached to an adjacent connection.
- Connections in which an angle is welded directly to the reinforcing mesh are not recommended since they damage the reinforcing steel and cause severe cracking in flange itself.
- The models used to predict the connection strength are adequate for predicting the lower limit of the connection strength.

Split Pipe Connection

Saxena [29] replaced the rigid bar or plate normally used to connect adjacent pieces with a ductile steel connector (a steel pipe with longitudinal slit). The connection is shown in Fig. [2.14]. The following conclusions were made by Saxena [29] :

- The split pipe connection is able to accommodate the relative movement between panels due to shrinkage and temperature changes.
- The split pipe connection limits the forces that develop during dynamic loading which leaves the panels largely undamaged.
- Slight inaccuracies in the dimensions of the precast panels during casting can be easily accommodated when pipe is welded in its position.

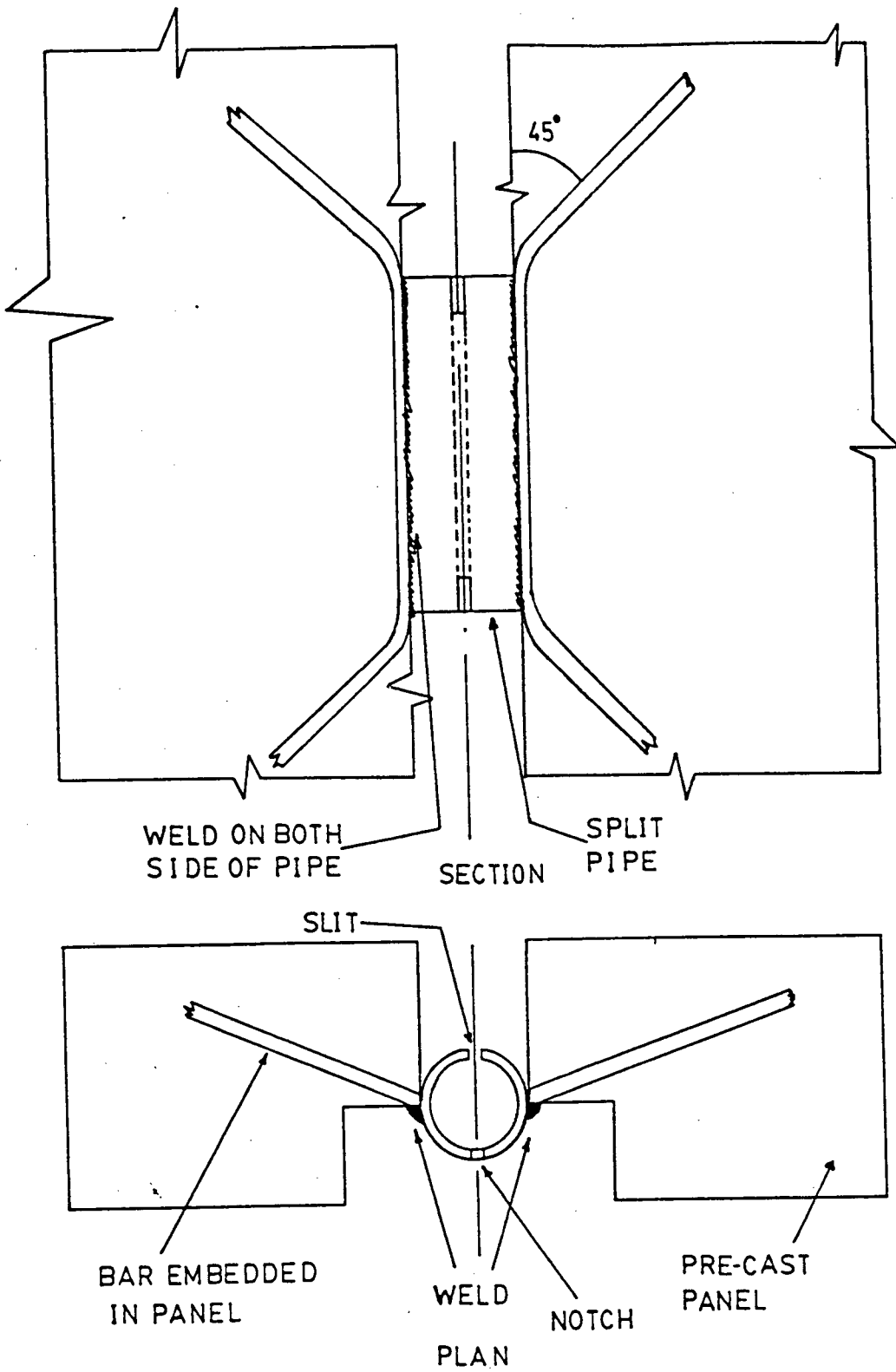


Figure 2.14: Split Pipe Connection by Saxena [29]

2.4 Wet Connections

These are cast in place connections using reinforced or unreinforced concrete to form a junction between members. The strength and performance of these connections depend upon precast and cast-in-place concrete; the amount of transverse and longitudinal steel; the tensile and compressive forces acting on the connections and the surface preparation of precast panels. Shear is transferred mainly through shear friction mechanism. Some tests have been made to test the performance of wet connections under cyclic loading. A few of these tests are summarised below :

2.4.1 Platform type Horizontal Connection

This connection is most commonly used in America as a horizontal joint between vertical panels. The cross-section of a typical platform joint is shown in Fig. [2.15].

For these connections shear transferred by friction is equal to a coefficient of friction times the compressive force acting on the joint. If the induced shear force exceeds this value then slip will occur in the joint. This shows that the coefficient of friction is important in the design of these joints. Joahl and Hanson [16] have tested these connections under monotonic loading and Hanson [12] has tested these connections under cyclic loading. These connections transfer shear through coulomb friction due to normal stress, and through shear friction due to clamping and dowel action of vertical wall reinforcement passing through the joint. It was found that the coefficient of friction effecting slip of these connections showed a very low value varying from 0.2 to 0.4 (see Fig. [2.16]). The load-displacement curve, Fig. [2.17b], was found to be elasto-plastic. When a longitudinal reinforcing bar crossed the joint, cyclic reversing loading caused spalling and damage of concrete around the bar; while the resistance of the bar to distortion caused to post-elastic-slip stiffness to develop. When longitudinal reinforcement was enclosed within a soft layer of padding, concrete spalling was avoided and the hysteresis loop shown in Fig. [2.17a]

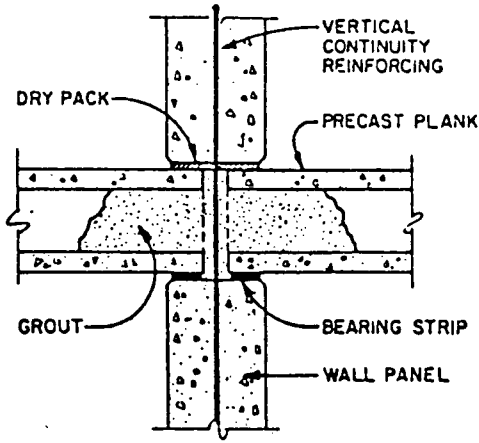


Figure 2.15: Typical platform-type horizontal connection

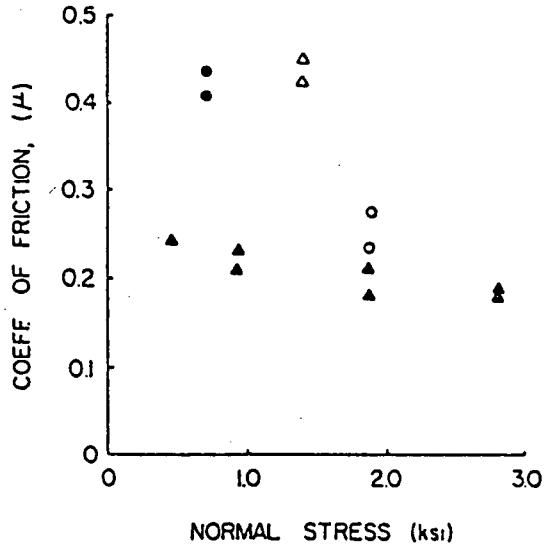


Figure 2.16: Coefficients of friction from tests on horizontal joints by Hanson [12]

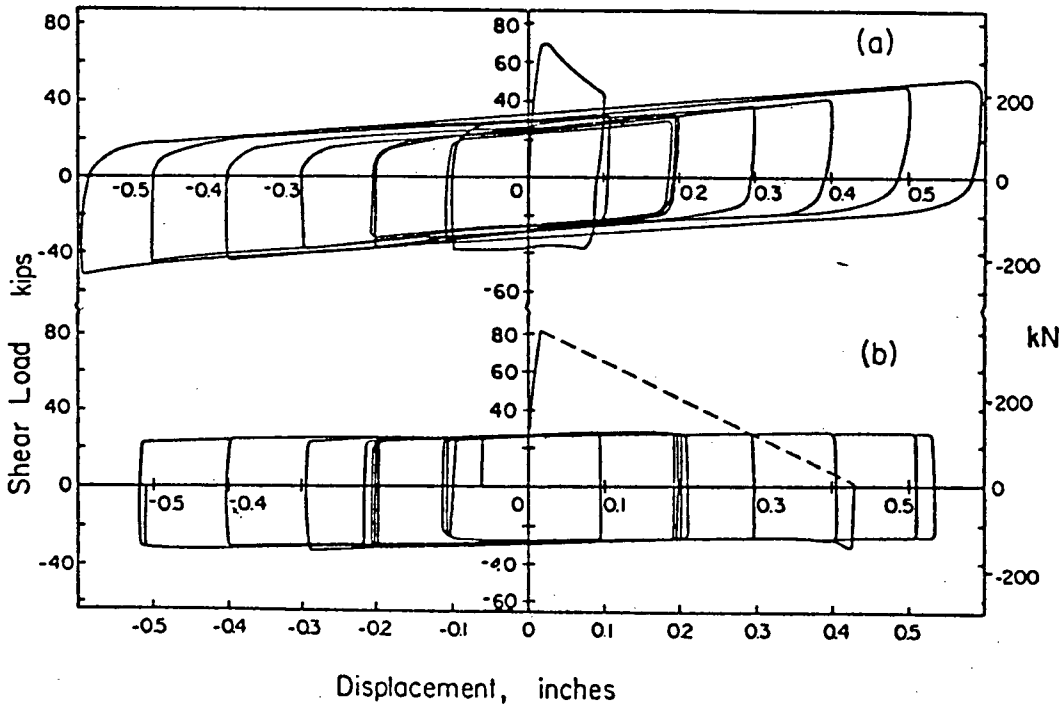


Figure 2.17: Shear-displacement hysteretic loops from horizontal tests by Hanson [12]

was obtained.

Another study on cyclic behaviour of interior American type horizontal joints has been done by Harris & Abboud [13], using $\frac{3}{32}$ scaled models of the joint shown in Fig. [2.18]. They found a much higher value of the coefficient of friction, Fig. [2.19], as compared to that from Hanson [12].

2.4.2 Dowel Connection

Dowel connections can be used as horizontal connections between wall panels and footings. The strength of these connections depends upon the area of cross section and on the embedment length and the developed bond of the dowel bars. As in the platform type connections, the co-efficient of friction is an important parameter in the design of these connections. One disadvantage of these connections is that any adjustment after the initial set of grout may destroy the dowel bond thus reducing the connection strength. Dowel connections may be keyed to increase the shear resistance through interlocking of keys Fig. [2.20]. Once keys fail, the residual shear strength depends upon the friction and strength of the dowels.

The only experimental data available on the cyclic test on dowel connection is from Dimitrov & Georgiev [10] who did tests on two full sized panels connected to a rigid base by trapezoidal dowels. The reinforcement bars passing through the dowels are welded and the cavity is closed with fine aggregates. The concrete strength in the panels was 20 MPa. The dowel reinforcement in the first specimen; (W_1 in Fig. [2.20]) consisted of two longitudinal bars each of 16 mm dia. with a design steel stress of 210 MPa and yield stress of 300 MPa. The second specimen (W_2 in Fig. [2.20]) had longitudinal reinforcement of two 22 mm dia. bars with a design steel stress of 375 MPa and a yield stress of 500 MPa. Normal forces on the panels; $2 * 270$ kN on W_1 and $2 * 275$ on W_2 ; were provided by hydraulic jacks to simulate the vertical loading on the panel. Reversed cyclic loading was applied along the top

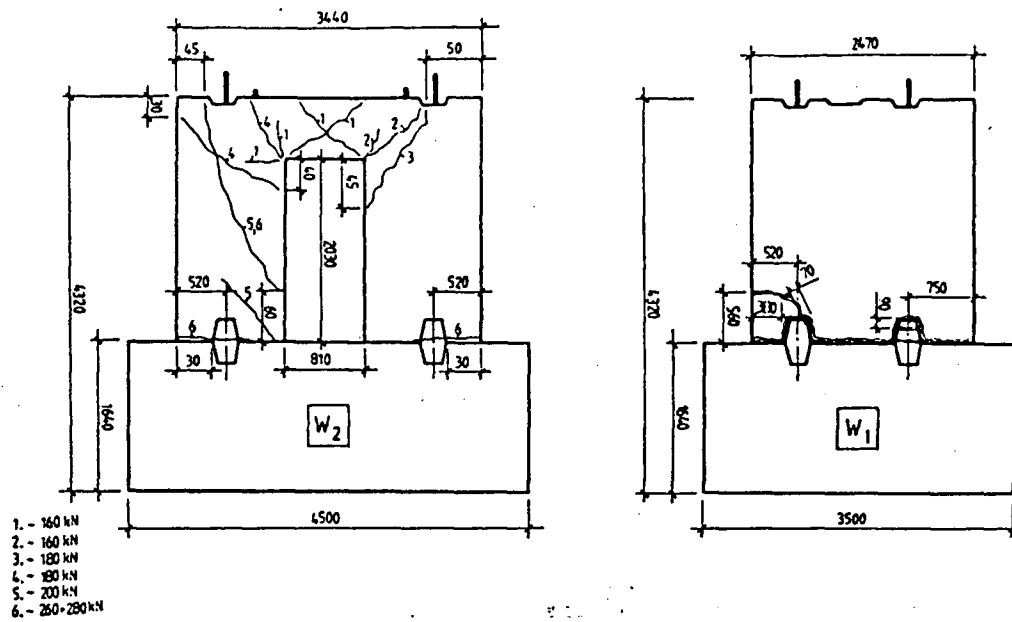


Figure 2.20: Specimens Tested by Dimitrov & Georgiev [10]

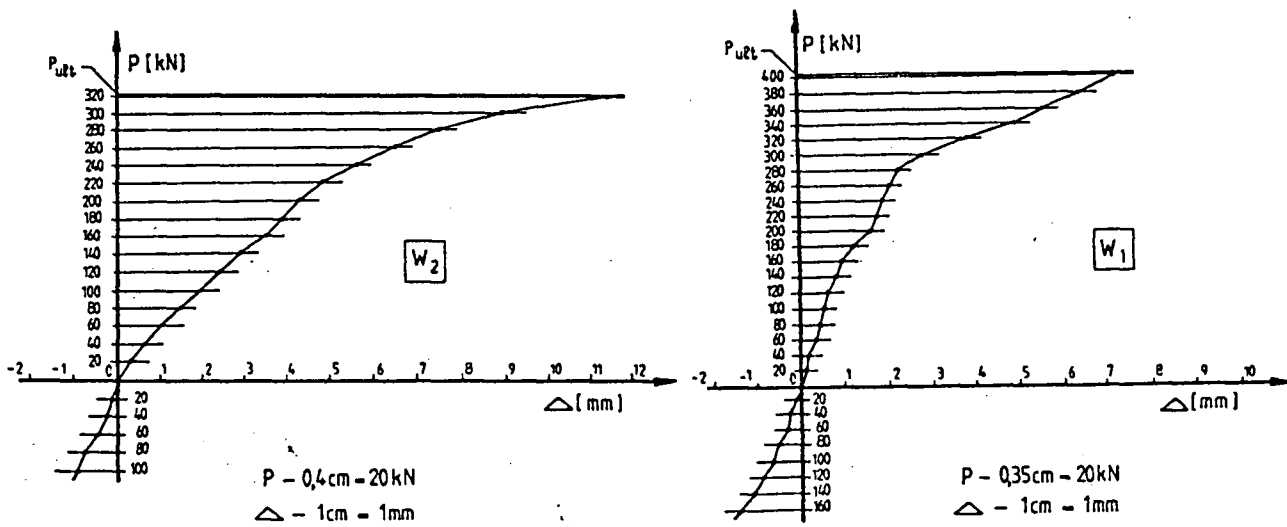


Figure 2.21: Load-Deflection Curves of Specimens in Fig. [2.20] by Dimitrov & Georgiev [10]

edge of the panel. The loading sequence followed the expression :

$$P = 0, 1H, 0, -1H, 0, 2H, \dots, 0, jH, 0, -jH, 0 -$$

in which

j is the number corresponding to loading cycle

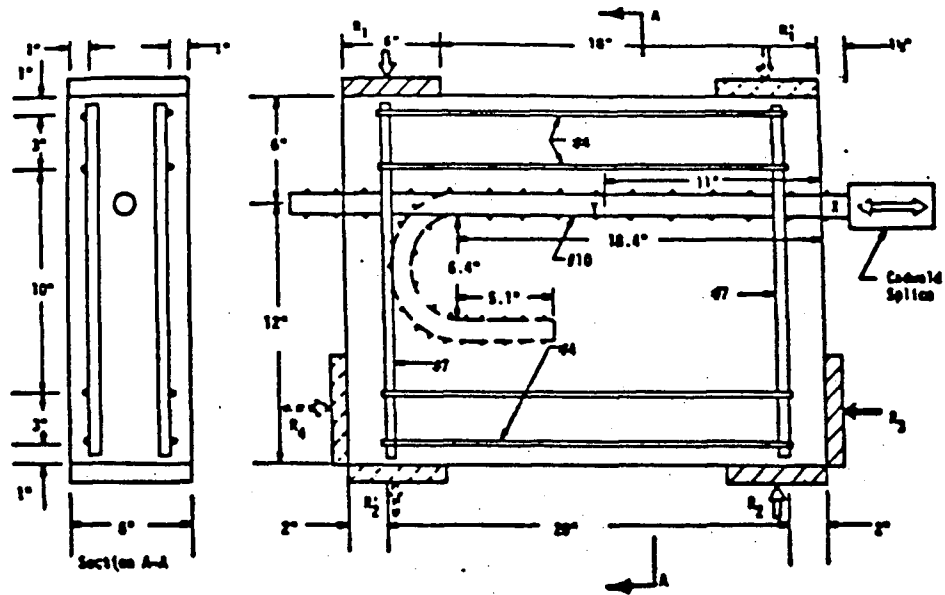
H is the load amplitude increment assumed constant at 20 kN

for each cycle.

The curves in Fig. [2.21] are obtained by connecting the peak values of the displacement at each load cycle which are obtained from the hysteresis loops of the specimens. The main objective of these tests was to check the ductility of the panel with dowel connections. From the curves in Fig. [2.21], it can be concluded that strength and stiffness of the panel does not degrade too much as the cyclic displacements go into the inelastic range.

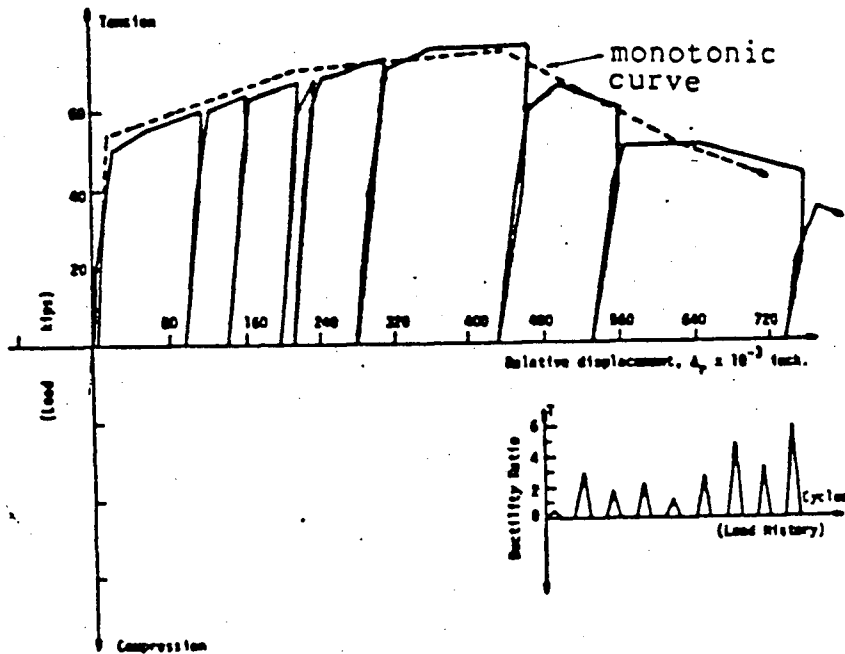
For a dowel connection if it is assumed that the connection fails due to failure of dowel bond because of the slip between dowel bar and the surrounding concrete, leading to pull out type failure; then the experimental data available on bond characteristics of reinforcing bars for seismic loading can be used in the modelling of these connections. One such study has been done by Hawkins & Lin [15]. They tested three types of test specimens Figs. [2.22, 2.24, 2.26]. Load-displacement curves are shown in Figs. [2.23, 2.25, 2.27]. The dotted line on these curves is for connections tested under monotonic loading. A brief description of conclusions reached by Hawkins & Lin [15] is given below :

- The displacements for first yielding were very similar for all specimens and equal to $40 * 10^{-3}$ inch (1.016 mm).
- The characteristics of the loading history have a marked effect on rate of bond deterioration and mode of failure.



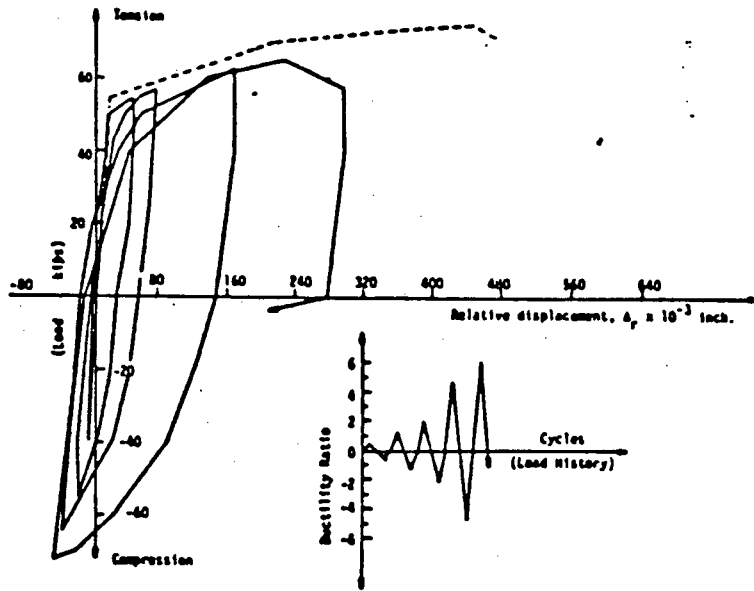
-All reinforcing bars are Grade 40.
 -Shaded areas are supports.

Figure 2.22: Test Specimen - Phase 1, by Hawkins & Lin [15]

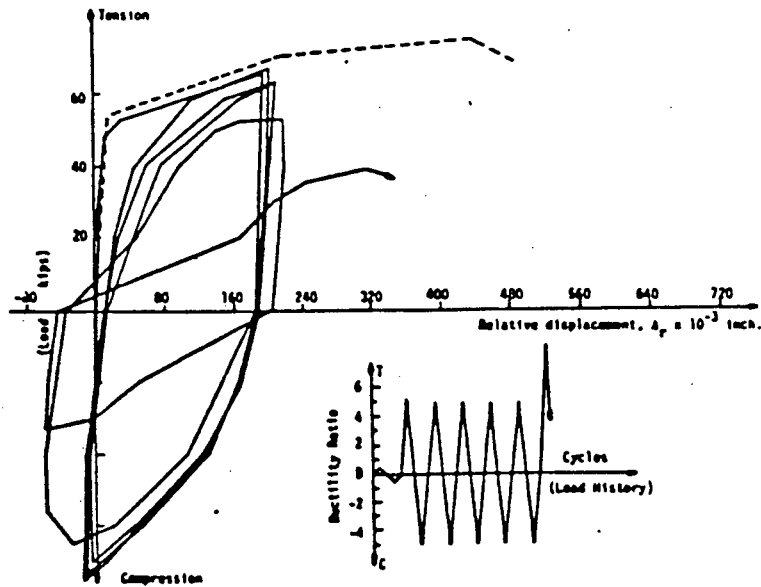


(a) $f_y = 48 \text{ Ksi}$, $f_c = 3100 \text{ psi}$

Figure 2.23: Load-displacement curve, # 10 straight bar, Bamboo-type deformations, Phase 1 by Hawkins & Lin [15]



(b) $f_y = 48$ Ksi, $f_c = 3200$ psi



(c) $f_y = 48$ Ksi, $f_c = 4200$ psi

Figure 2.23 : Continued

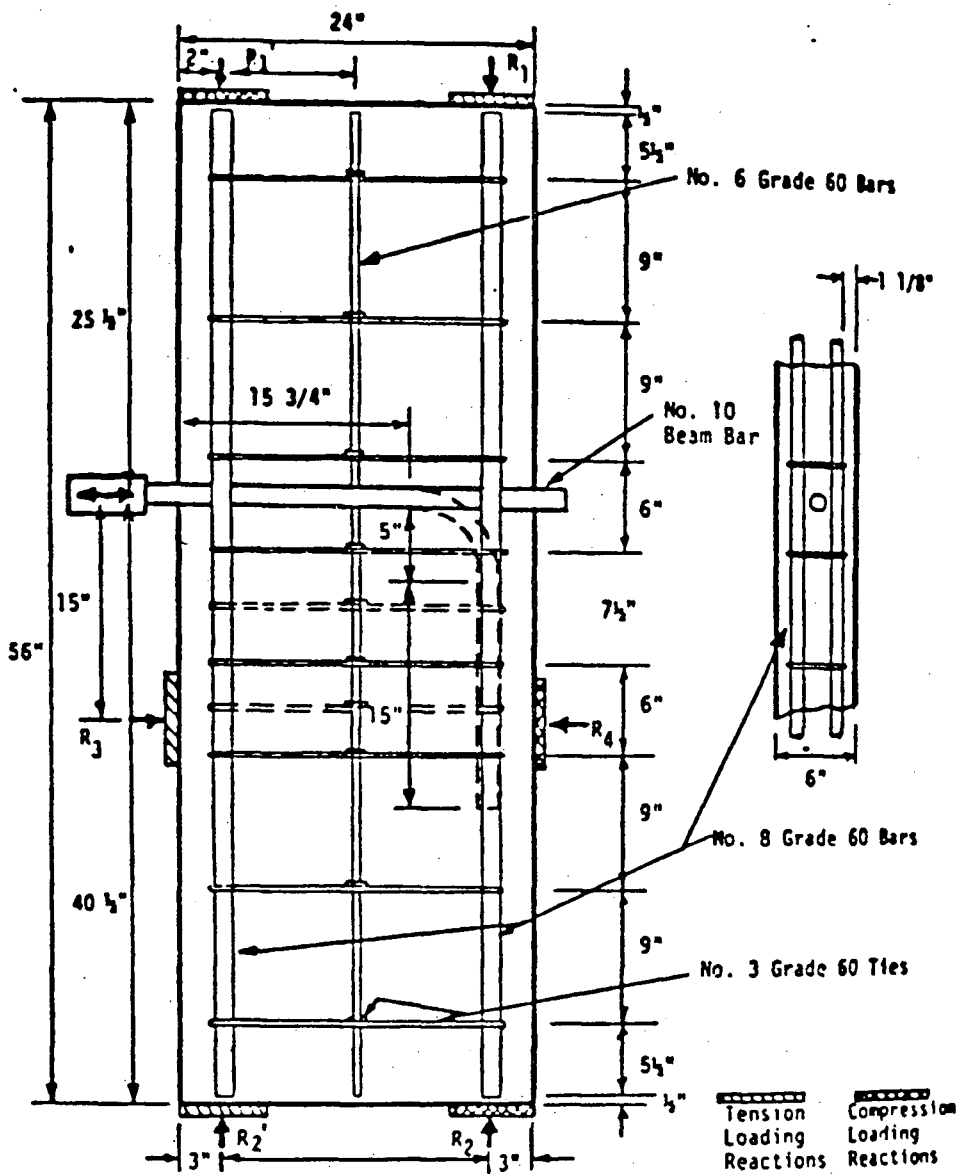
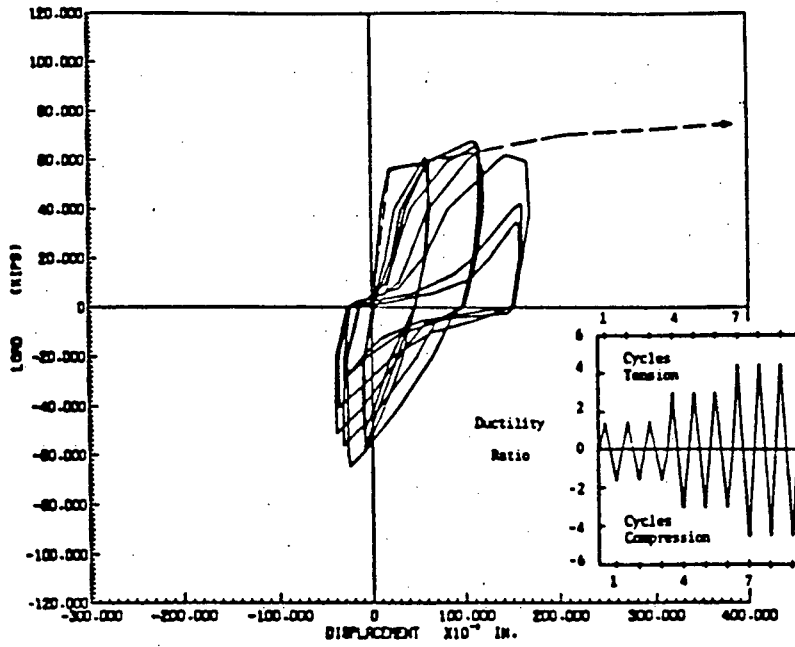
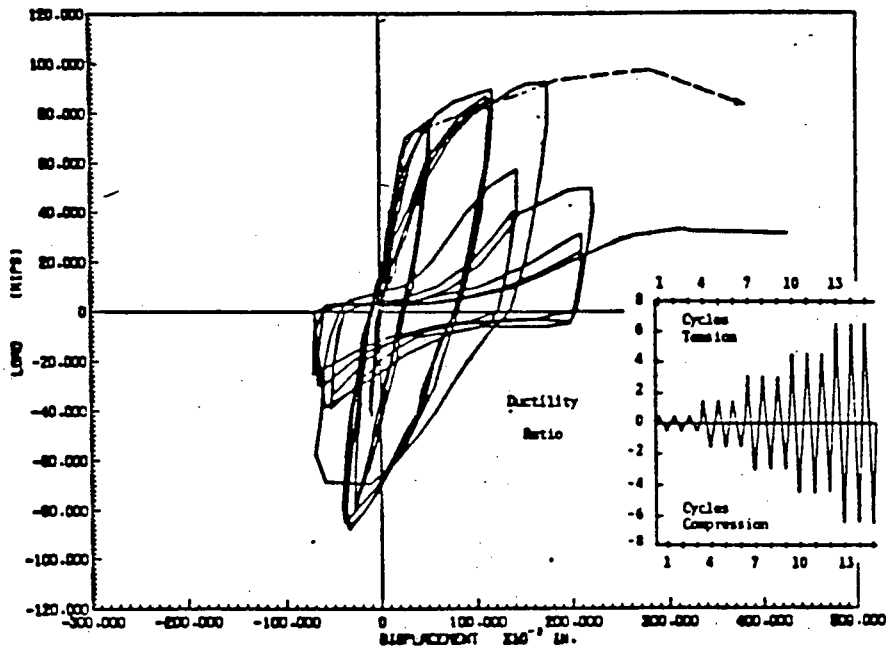


Figure 2.24: Test Specimens - Phase 2, by Hawkins & Lin [15]

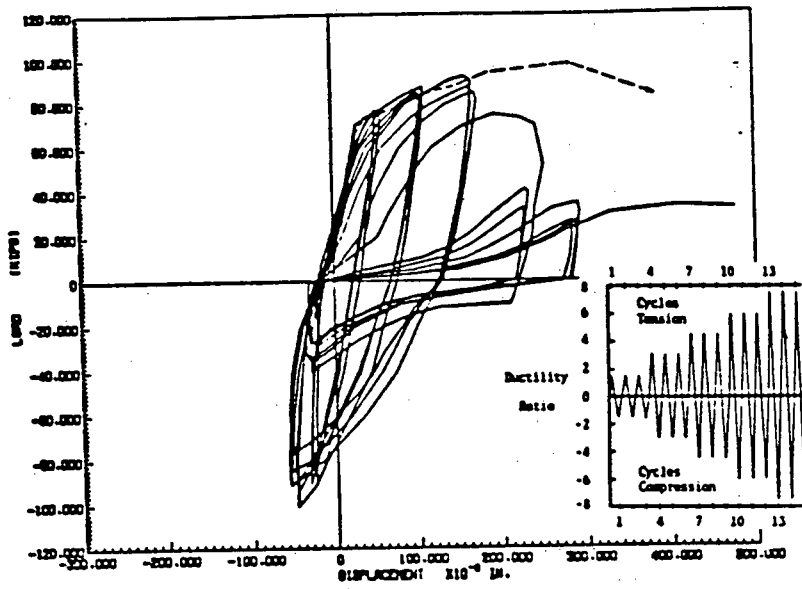


(a) $f_y = 48$ Ksi, $f_c = 2640$ psi

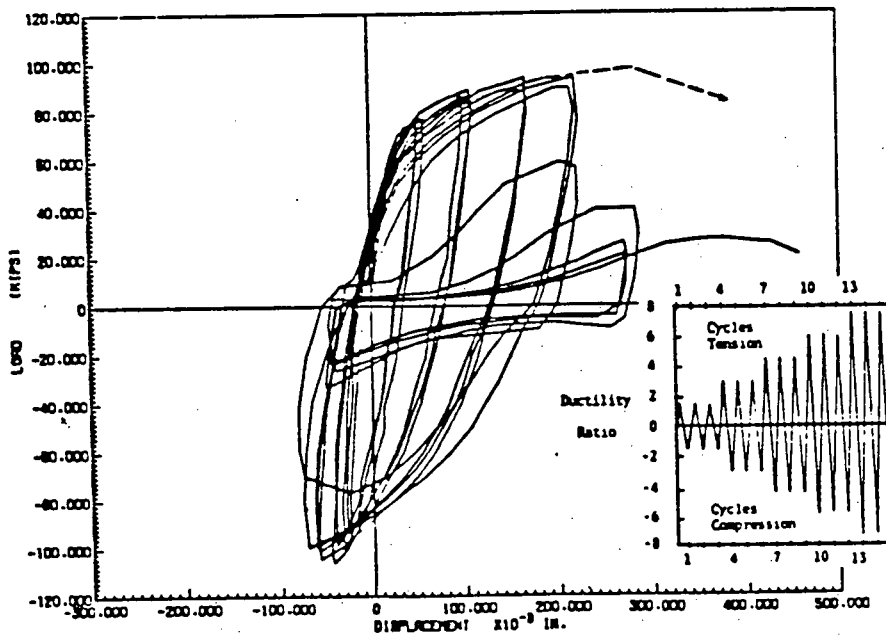


(b) $f_y = 60$ Ksi, $f_c = 3760$ psi

Figure 2.25: Load-displacement curve, # 10 straight bar, Bamboo-type deformations, Phase 2 by Hawkins & Lin [15]



(c) $f_y = 60$ Ksi, $f_c = 4100$ psi



(d) $f_y = 60$ Ksi, $f_c = 5120$ psi

Figure 2.25 : Continued

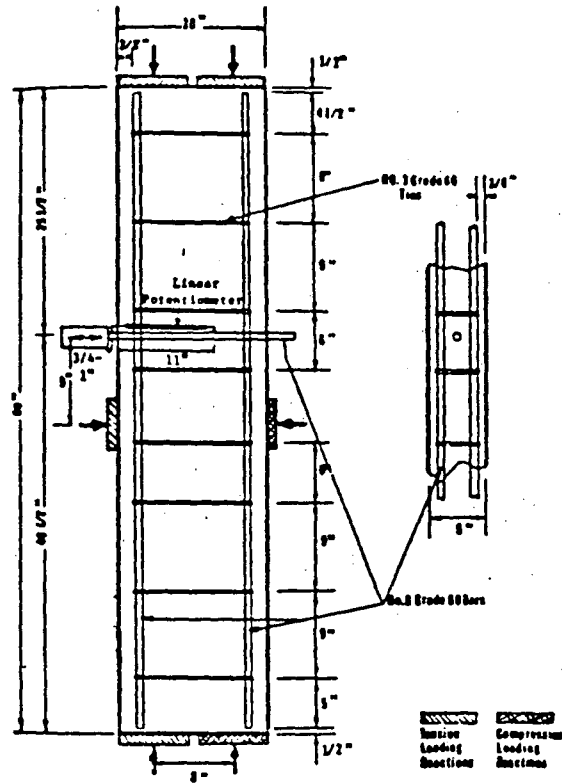
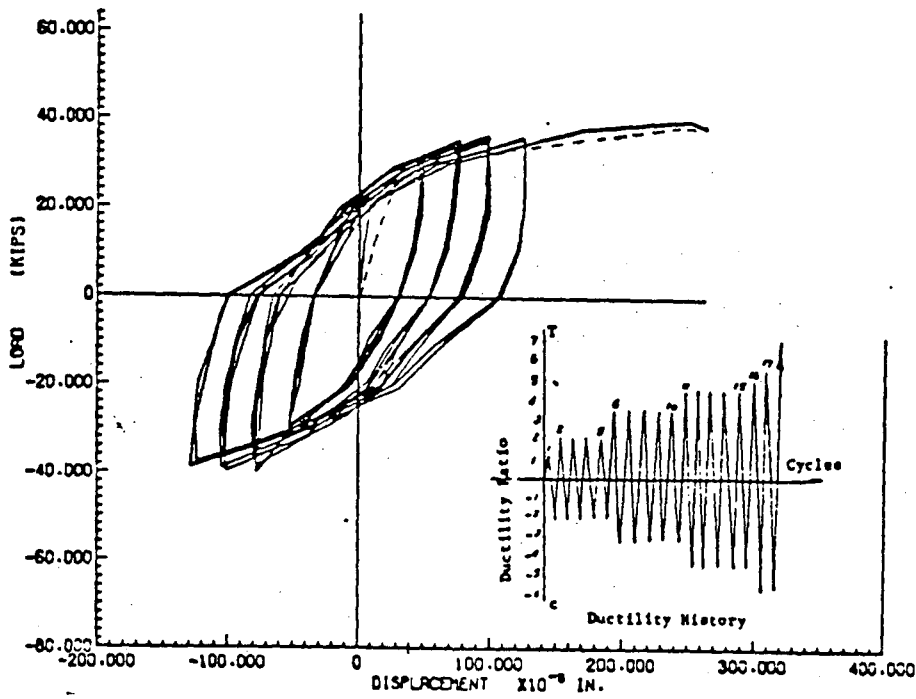


Figure 2.26: Test Specimen - Phase 3, by Hawkins & Lin [15]



(a) $f_v = 67 \text{ Ksi}$, $f_c = 3400 \text{ psi}$

Figure 2.27: Load-displacement curve, # 6 straight bar, Bamboo-type deformations, Phase 1 by Hawkins & Lin [15]

- The surface geometry of the bar had a significant effect on rate of bond deterioration. The rate increased as the ratio of lug spacing to bar diameter increased. Bars with different surface geometries and similar load displacement characteristics for monotonic loading had significantly different characteristics for reversed cyclic loading.
- For reversed cyclic loading, the response for specimens with 180° hooks was much poorer than for specimens with straight bars because once slip penetrated to the hook, the motions of the hook broke the connection. The 90° connection maintains good characteristics for tensile loading considerably longer than for compressive loading but even then its characteristics are not nearly as good as those for specimens with straight bars.
- The grade of bar had less effect than general form of its stress-strain characteristics.
- The strength of concrete had a marked effect on load displacement curves. The displacement corresponding to maximum load capacity increased in direct proportion to the concrete compressive strength.
- Additional hoop reinforcement markedly improved the load-displacement characteristics for bars terminating with 90° hooks but had little effect on the characteristics of straight bars.

2.5 Hysteresis Model for Vertical Connection

A number of mathematical models have been proposed for the connections between vertical wall panels. As there hasn't been a complete comprehensive study on a particular type of connection which would have taken into account all the variables involved all these hysteresis models are approximate to same degree. A brief discussion on these models is given below.

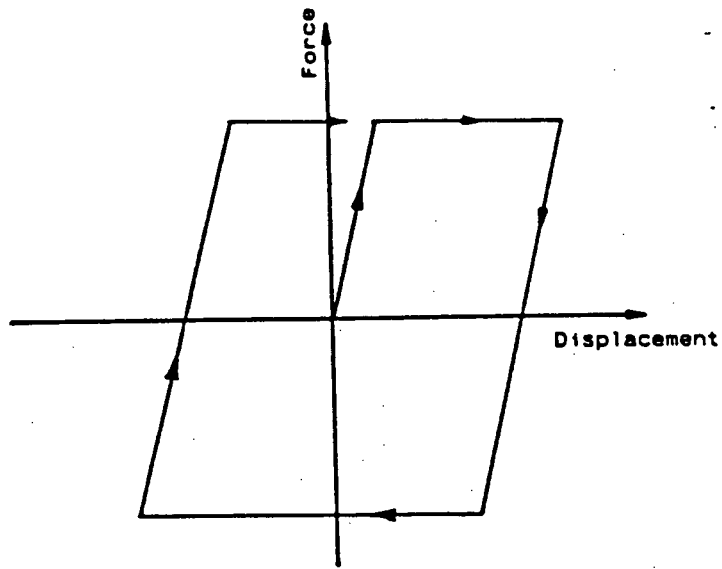


Figure 2.28: Elasto-plastic Model

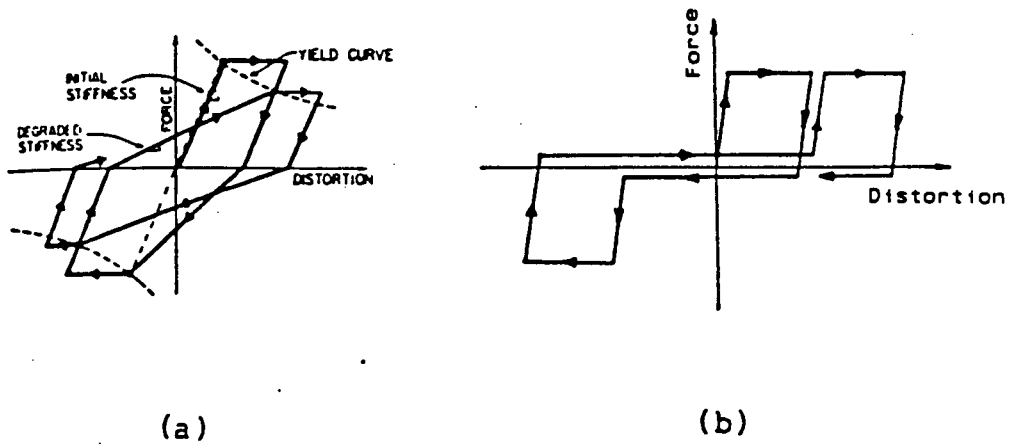


Figure 2.29: Degrading Connector Models, by Muller & Becker [21]

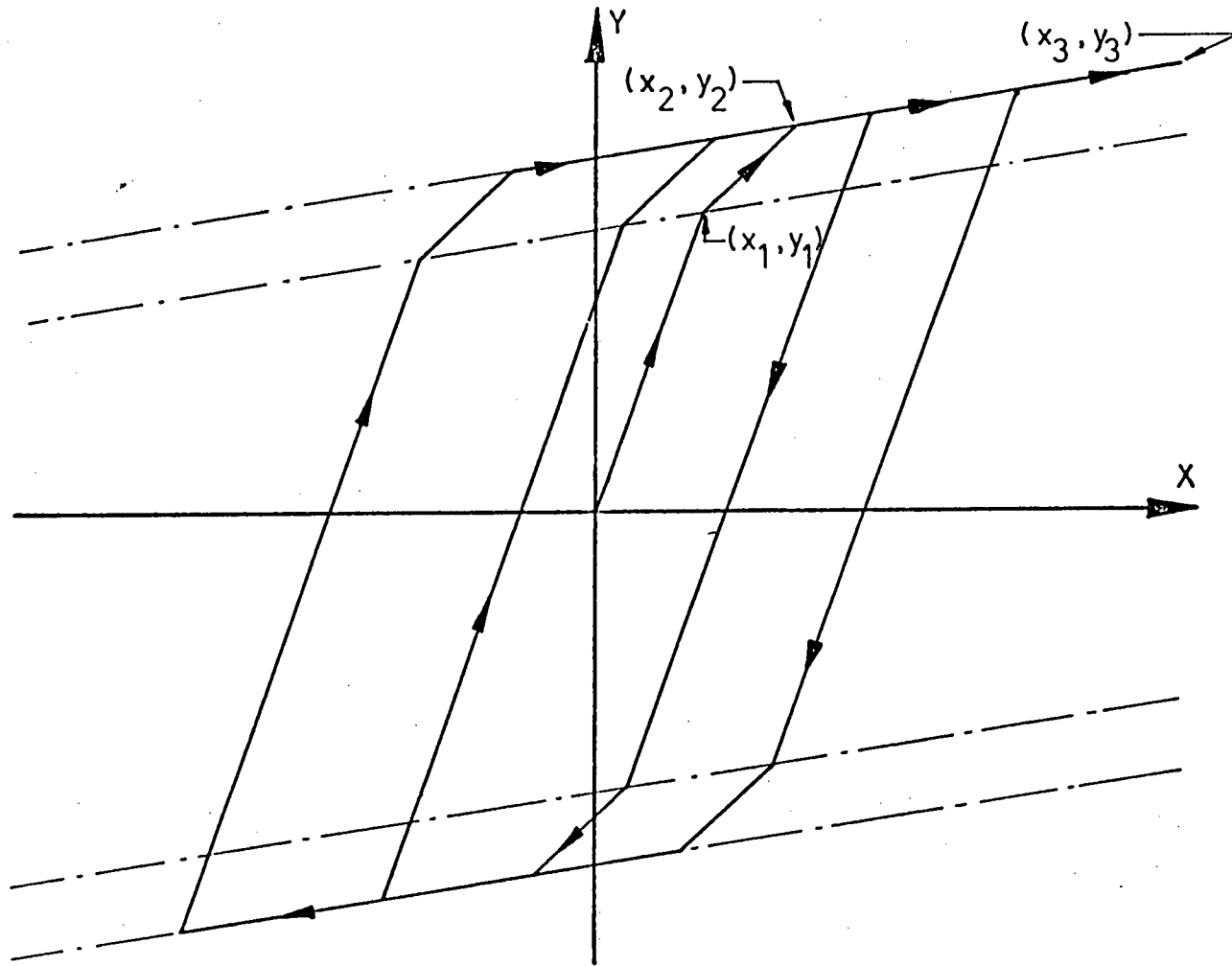
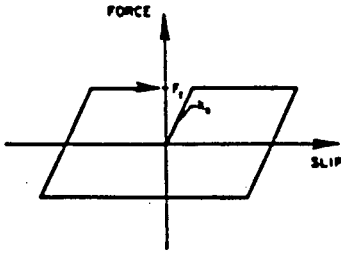
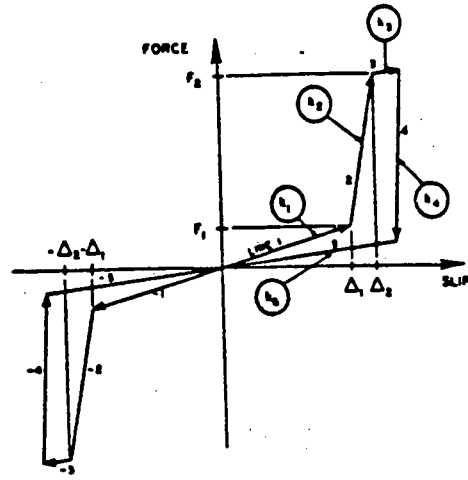


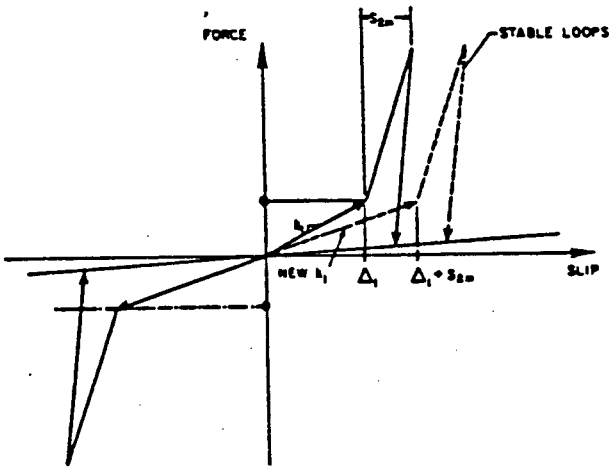
Figure 2.30: Trilinear Hysteresis Loops used for both Stress-Strain and Moment-Curvature Relationships for Studs, by Neille [23]



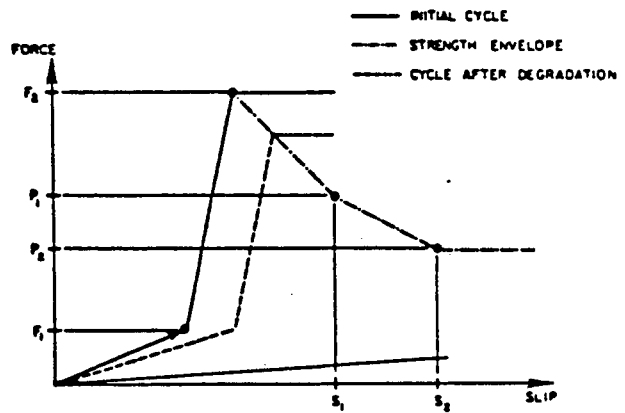
(a) Simple Friction



(b) Shear Friction



(c) Stabilized Hysteresis Loops After Stiffness Degradation



(d) Strength Envelop

Figure 2.31: Shear-slip Relationships for Shear-friction element, by Schriker & Powell [30]

The simplest of the hysteresis models used for precast connections is the elasto-plastic model Fig. [2.28]. This model has been used by Ashwad [3] to model his rebar type vertical connection. A similar model has been used by Pall & Marsh [24] to model the LSB joint. Looking at the hysteresis loops obtained by Pall & Marsh Fig. [2.5], one finds that elasto-plastic model is valid for the LSB joint, but for a rebar type connection the validity of this model is still questionable because of its inability to model degrading strength and stiffness of the connection.

Neille [23] has used a trilinear load-deformation model, Fig. [2.30], for welded headed stud connections. The test results for load decrement vs. associated maximum deflection in one cycle were represented by a parabola which has been incorporated in the model to model the strength and stiffness degradation in the connection. Muller & Becker [21] used the degrading model in Fig. [2.29a] to represent the test data obtained by Neille [23]. They proposed another model, Fig. [2.29b] to represent a highly degrading connector.

Schricker V. & Powell G. [30] have developed a number of elements to model several types of joint behaviour for the inelastic analysis of pre-cast buildings. Each element is assigned a simple force-displacement relationship Fig. [2.31]. Complex relationships for the behaviour of various joints were obtained by placing two or more elements in parallel in a single joint.

Tong [36] has used a simple degrading model with strain hardening to model the rebar connection. The model given by Tong can be used to model vertical connections between wall panels (no vertical connections have been included in the buildings studied in this thesis but the computer program has the capability to model these connections). A brief description of this model is given below.

The model consists of a primary curve Fig. [2.32] defined by four linear segments (each segment is assigned an arbitrary number). The initial stiffness of the connection is k_1 which remains constant until the elastic limit point (f_e , d_e) is

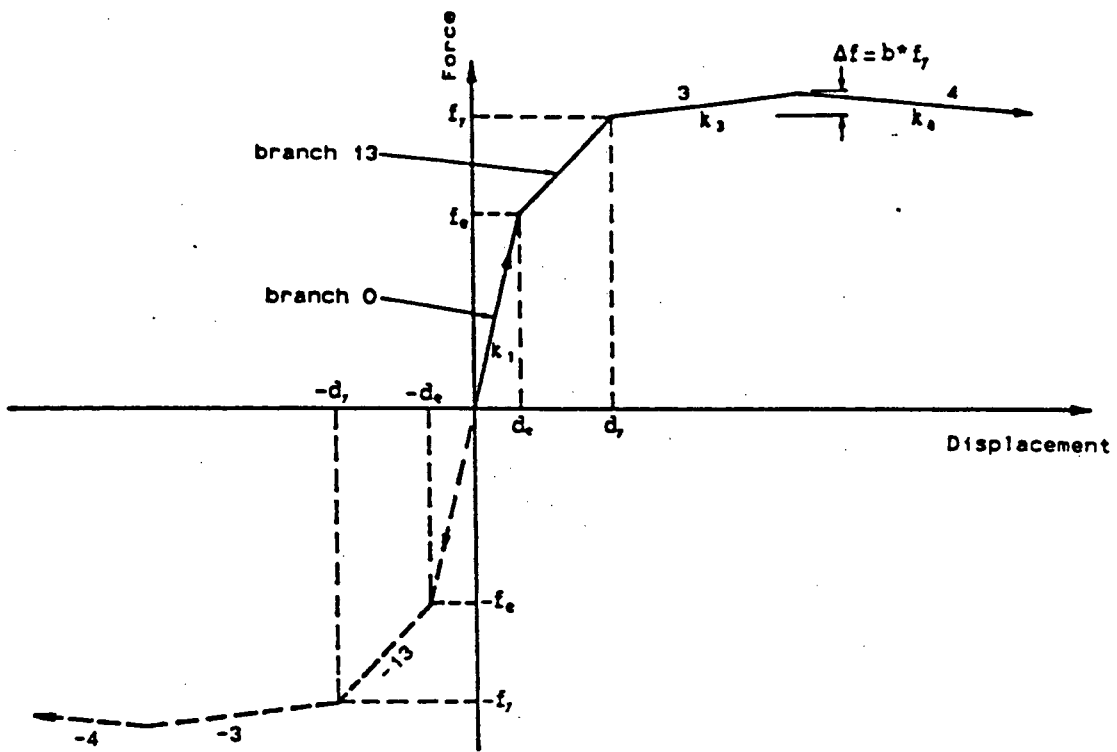


Figure 2.32: Hysteretic Model : Primary Curve, model proposed by Tong [36]

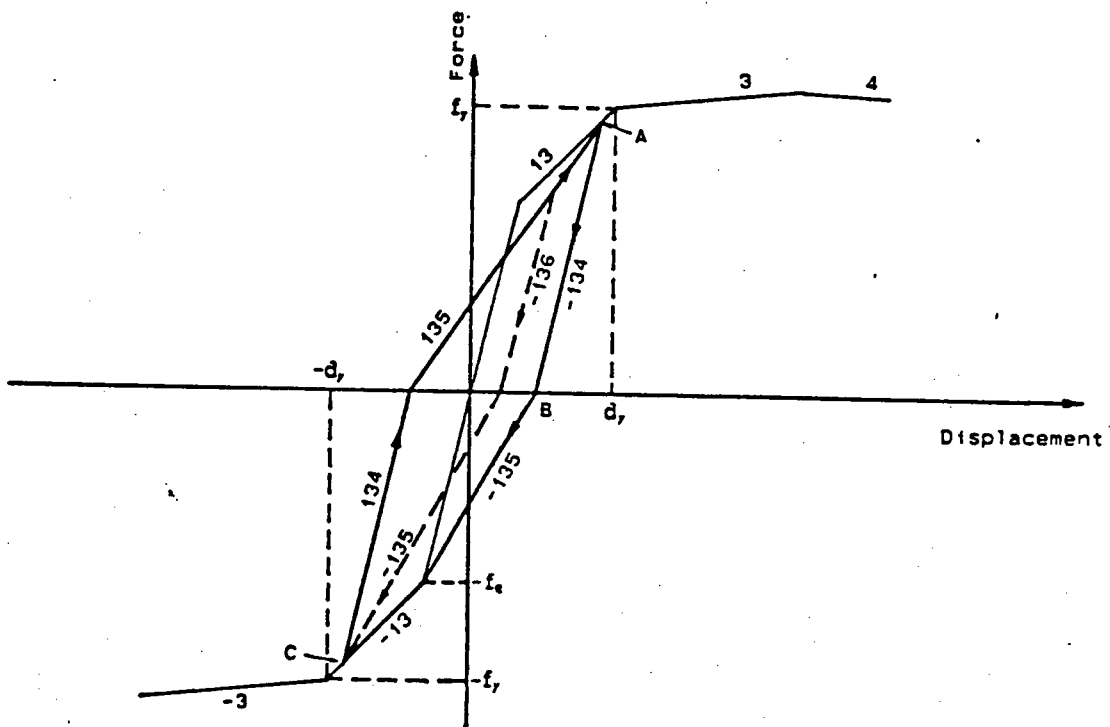


Figure 2.33: Hysteretic Model : Cyclic behaviour before yielding, model proposed by Tong [36]

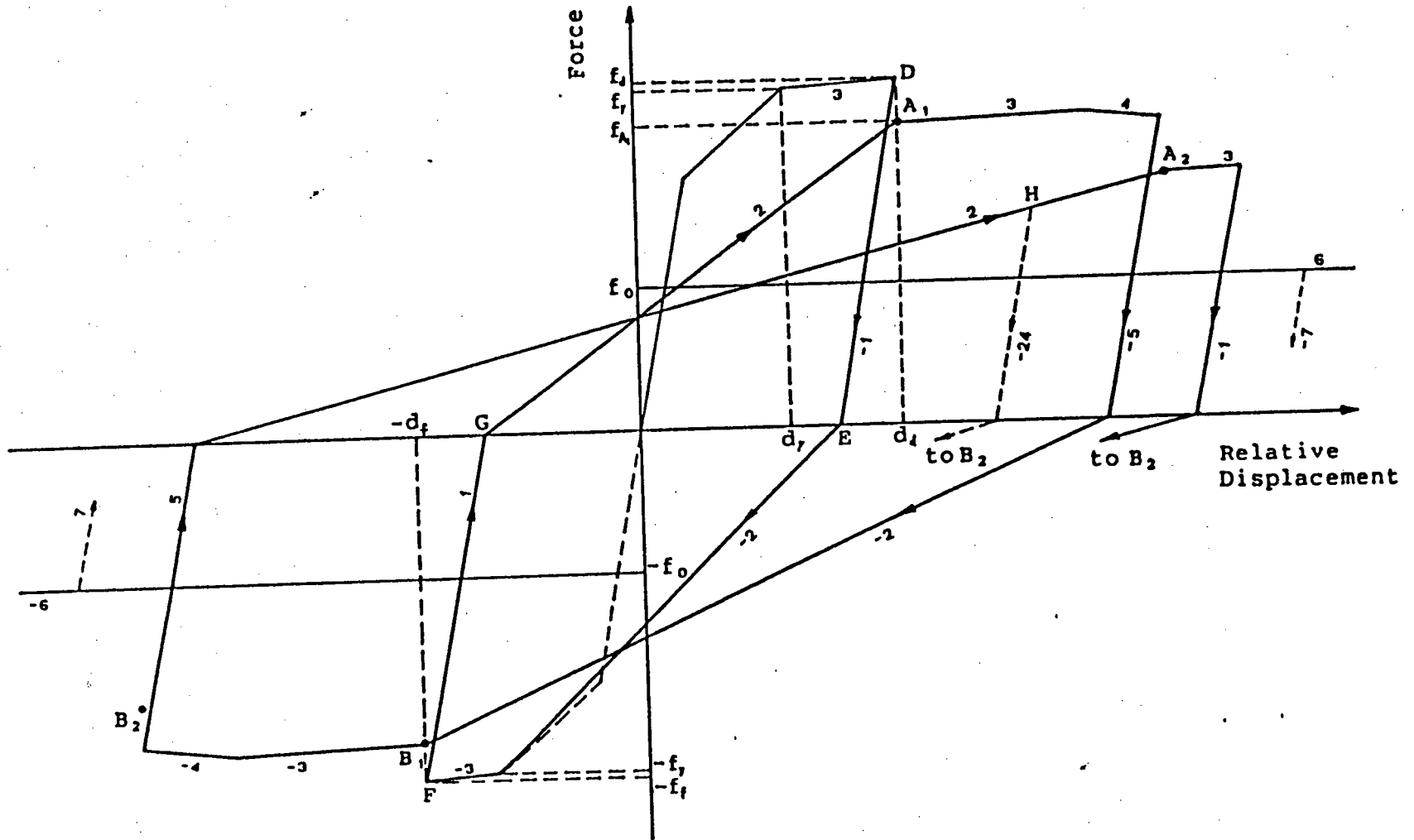


Figure 2.34: Hysteretic Model : Cyclic behaviour after yielding, model proposed by Tong [36]

reached. The ascending branch representing strain hardening starts after the yield point (f_y, d_y) is reached. The ascending branch stiffness is k_3 defined as

$$k_3 = a * k_1 \quad 0 \leq a < 1$$

Max. rise of the ascending branch is given by

$$\Delta f = b * k_3 \quad 0 \leq b < 1$$

Descending branch stiffness is defined by

$$k_4 = -c * k_3 \quad 0 \leq c < 1$$

where a, b, & c are constants.

The hysteresis model cyclic behaviour before and after yielding are shown in Fig. [2.33] & Fig. [2.34] respectively. There is no strength degradation for cyclic behaviour before yielding. Once the yielding has taken place, the strength degradation was defined during load reversals from ascending and descending branches. Everytime unloading takes place from these branches, a reduced yield limit is defined for the next cycle by multiplying the load at reversal by a factor ϕ which is given by

$$\phi = R^n$$

$$\text{where } R = 0.5 \left[\frac{d_y}{|d|} + \frac{|f|}{f_y} \right]$$

Two other constants β & α are defined, which when multiplied by slope of ascending and descending branches, give the slopes of new ascending and descending branches.

$$\beta = R^r \quad 0 \leq r < 1$$

$$\alpha = \frac{1}{R^s} \quad 0 \leq s < 1$$

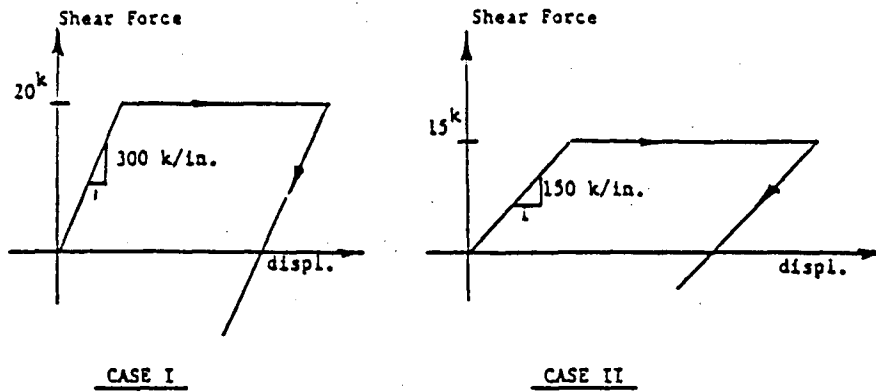
. where n, r & s are constants.

2.6 Hysteresis Model for Horizontal Connection

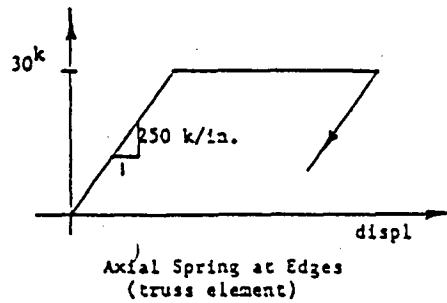
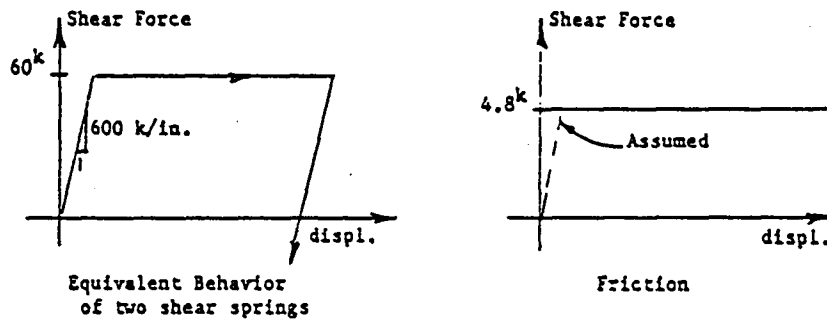
A number of models have been proposed for horizontal connections commonly used in industry. A brief discussion on these models is given below :

Aswad [3] used P-8 and P-3, (Fig. [2.9]) in combination as a horizontal joint and he modelled this connection with an elasto-plastic model shown in Fig. [2.35]. From the experimental results for tests on platform-type horizontal connection Fig. [2.17], it seems that the elasto-plastic model without any strength or stiffness degradation can be used to model this connection. There have been few other models proposed for the horizontal connections commonly used in Europe Ref. [38,39], but all the above mentioned models have been used for wall to wall horizontal connections. A model for a dowel type horizontal connection between wall panel and foundation, has been proposed by Tong [36]. His model is for the force-displacement characteristics of the dowels. He has based his model on the indirect study done by Hawkins & Lin [15]. Hawkins & Lin proposed the model given by thick unbroken lines in Fig. [2.36] while the broken lines in the figure represent the test results from which this model is derived. The model proposed by Tong is given in Fig. [2.37] and it is a further simplification of the one in Fig. [2.36]. For the present studies the model given by Tong [36] has been used to model the horizontal connection. A brief description of the model is given below :

The bilinear model has a horizontal post-yielding branch. On unloading the curve stiffness is k_1 , the same as the initial stiffness. When the load is reversed, the unloading stiffness is obtained by considering the slope of a line connecting the load reversal point to the yield point, or, if the connection has already yielded in the new direction, the point on post yielding branch corresponding to the maximum deformation experienced. Hysteresis energy dissipation for deformations smaller than yield is not considered and no strength degradation is included. The validity of this model can be questioned, but considering the approximate nature of the



(a) Vertical Joint Connector Characteristics



(b) Horizontal Joint Connector Characteristics

Figure 2.35: Joint Connector Characteristics proposed by Aswad [3]

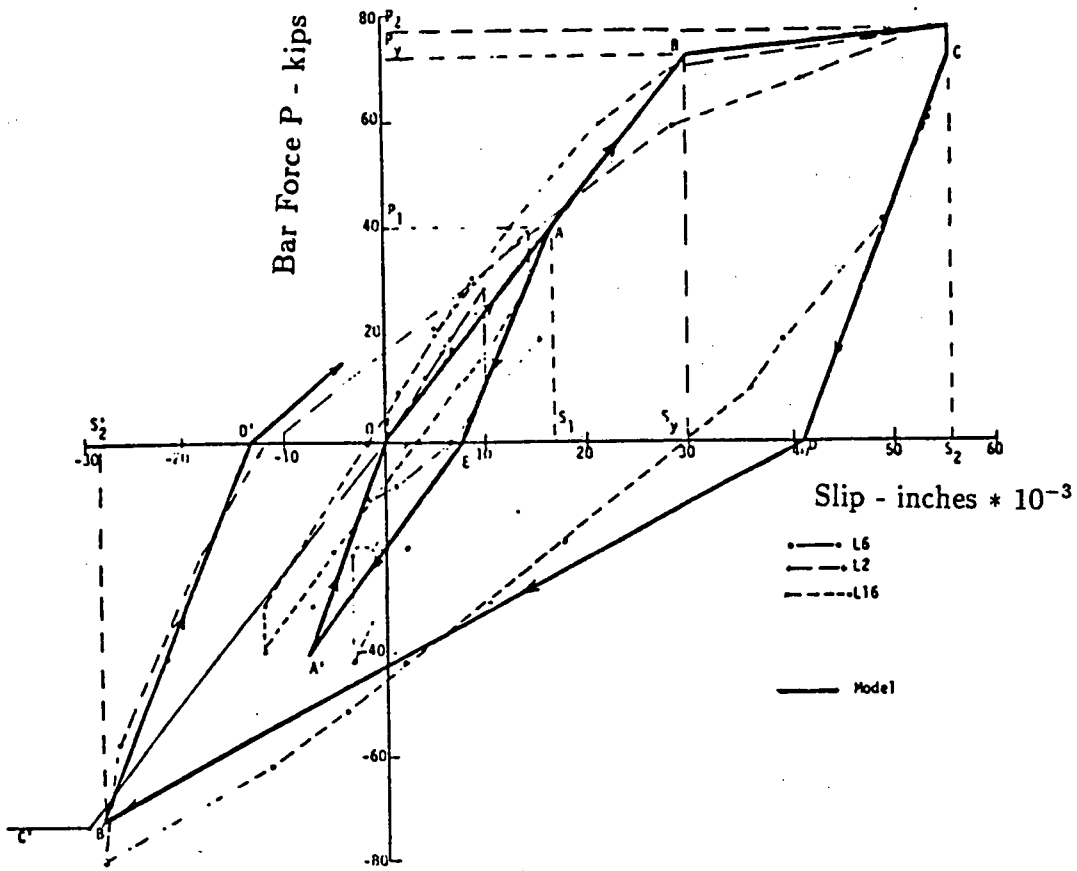


Figure 2.36: Bar Force-Pull Out Model for Cyclic Loading, proposed by Hawkins & Lin [15]

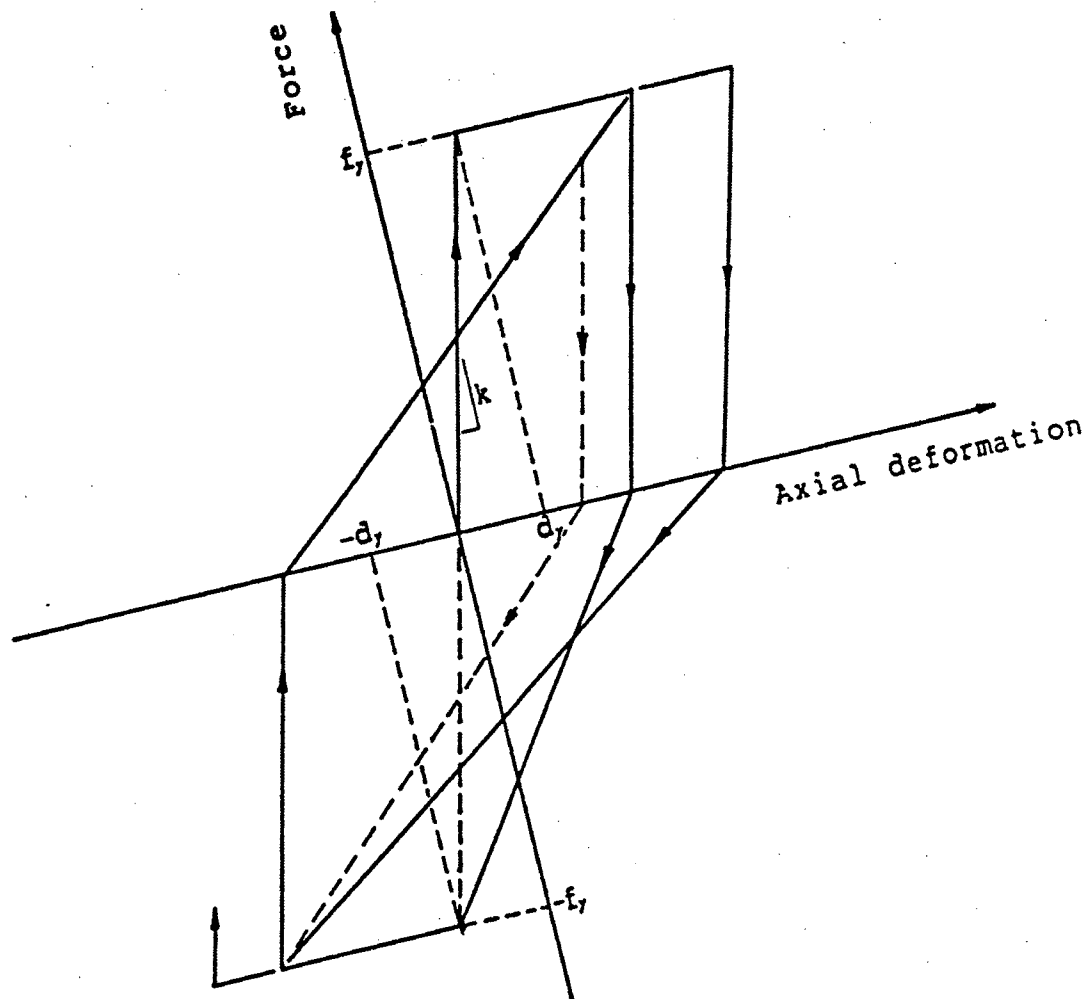


Figure 2.37: Hysteretic Model for the Dowel Connection, by Tong [36]

modelling process and conservative nature of this model as compared to one by Hawkins & Lin [15], the proposed model is adequate for present studies.

In general, for all the connections used by the precast industry, it can be said that the proposed models are approximate to varying degrees because of the lack of experimental data and analytical models available for the connections. For those connections for which some data is available, not all the variables have been taken into account, e.g. in the studies done in Ref [29,34], the effect of load normal to the connection and the effect of vertical load on the panel on the behaviour of the connection have not been taken into account.

Chapter 3

DYNAMIC ANALYSIS

3.1 Introduction :

The usual Code approach for designing buildings for earthquake loads; i.e. to calculate the equivalent static loads on the structure; does not explicitly consider the dynamic characteristics of the structure. One way to investigate the influence of the dynamic characteristics of the building on earthquake response is by using the 'response spectrum design approach'. The response spectrum used corresponds to a probability of exceedence of seismic ground motion of 10 percent in 50 years (.0021 per annum). The Supplement to NBCC - 85 [35], commentary J - 39, recommends a simplified response spectrum technique for dynamic analysis. This approach ensures that the dynamic analysis will not result in lower base shears than those prescribed by the code because the code values are already minimum values commensurate with the acceptable level of safety. Another method of dynamic analysis is to find the response of the building over the total duration of a known ground motion using either a linear or non-linear analytical model with the time-history of the earthquake as the input data. This approach is expensive and is generally used only to check the performance of the final design of complex structures.

3.2 Idealization Technique :

A number of structural idealization techniques are available to investigate the behaviour of panel structures [5]. A *Beam Modelling* technique is used for shear wall structures in which the roof or walls of the structure have no in plane rotation and the lateral rigidity of the walls is uniform. The mass is lumped at the roof and floor levels. The horizontal joints are modelled as beams. Brankov and Sachanski [4] have used this approach in the dynamic analysis of multi degree of freedom panelized structures.

Shear Medium theory has been widely used in the area of coupled shear walls and shear wall buildings. It allows not only a straight forward analysis of the overall response of the walls joined by coupling beams but has also been used successfully in shear wall buildings to reduce the number of degrees of freedom involved. In this method the coupling beams are replaced by a continuous shear medium. The basic assumptions for this theory are :

- Discrete coupling elements are evenly smeared over the joint length.
- The lateral deflections of the individual walls are equal.
- For the individual walls the classical beam theory holds i.e. plane cross sections remain plane after bending.

Muller and Becker [21] used this theory for precast walls coupled by vertical connections. For grouted connections, the replacement of coupling elements by a continuous shear medium is exact. For mechanical connections this replacement of coupling element is not exact.

In the *Frame Analogy* the structure is idealized as an equivalent frame having wide columns with rigid arms and connected by joints. The panels are modelled as beam columns with flexural, axial and shear deformations taken into account.

Constant stiffness is specified for the panels as they remain in the elastic range. This procedure is efficient in the three dimensional computer analysis of shear wall structures. Pall & Marsh [24] used this technique to model a large panel wall with Limited-slip bolts as vertical connections.

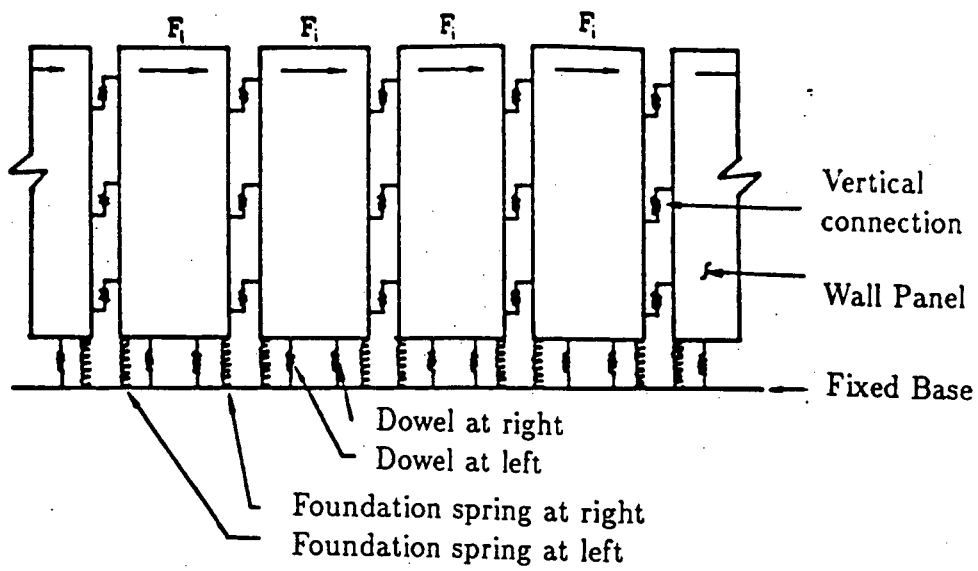
Most of the work done on the computer analysis of panelled structures has used the *Finite Element* for modelling because of this method's ability to model diverse geometries and material properties. The whole structure is discretized into small elements connected to each other only at the nodes. The response of the structure depends upon the response of the nodes. With some modifications, the existing computer programs [28] available for the earthquake analysis of the ordinary reinforced structures can be used to find the response of the panelled structures. Usually the panels are assumed to remain elastic while the connections exhibit non-linear characteristics. The size of the problem is reduced by eliminating all nodes other than that of the connections, by static condensation.

The present study is based on an idealization technique used by Tong [36]. In this technique the panels are assumed to be rigid and non-linear hysteretic models are used for the connections. The nonlinear hysteretic loop for the dowel connection is shown in Fig. [2.37]. This technique is based on the study done by Becker & Llorente [6] and Hanson [12] on the study of wall to wall pedestal type horizontal connections. They found that for a friction coefficient of 0.4 there is very little shear slip along the horizontal joint and rocking of the wall panels governs the response. Fintel, Schutz & Iqbal [11] report that the co-efficient of friction specified by design codes may vary from 0.2 - 0.8. CAN3-A23.3-M84 [8] recommends a coefficient friction of 0.5, thus for the wall panel with dowel joints as horizontal connections it can be safely assumed that rocking of the panels will govern the response and there will be no slippage in the joints.

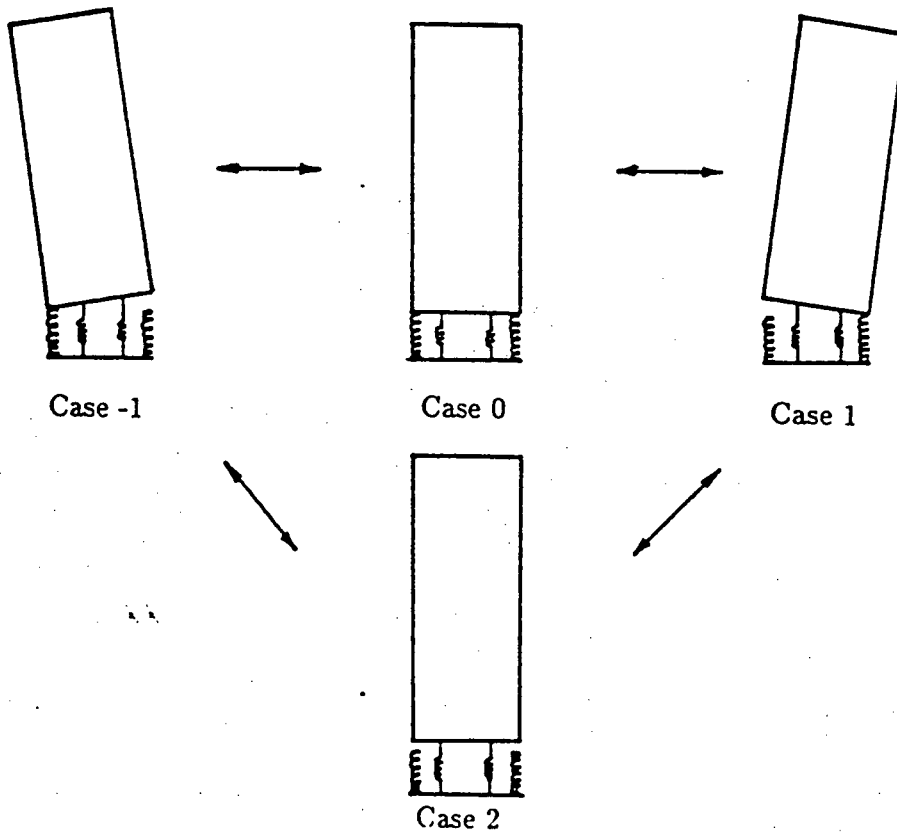
The rigid panel is assumed to rock about its base corners only. The foundation underneath the panel is replaced by two elastic springs, one at each corner of the panel. These springs are not connected to the panel i.e. the panel can lift off a foundation spring. Due to rocking of the panel, there can be three possible situations (see Fig. [3.1]) :

- Case 0 : both the foundation springs are in contact with the wall panel.
- Case 1 or -1 : only one foundation spring is in contact with the panel.
- Case 2 : neither foundation spring is in contact with the panel.

The lateral stiffness and shear force for each case for an interior panel is given in section [3.6].



(a) Idealization of Shear Wall



(b) Transition between Different Cases

Figure 3.1: Idealization of Shear Wall

3.3 2 - D Mathematical Model :

A one storey shear wall building is modelled by the mathematical model shown in Fig. [3.2]. The model has three degrees of freedom; 2 translations and a rotation at the C.G. of mass. The following notation is used in the derivation of the equation of motion for the building under earthquake loading :

- L : building dimension in the direction of ground motion
- B : building dimension perpendicular to the direction of ground motion
- M : mass of the building
- J : rotational moment of inertia about the C.G. of the building
- kw_i : lateral stiffness of wall i found as shown in Section [3.7] and i varies from 1 to 4
- \ddot{x}_g : ground acceleration acting on the structure
- C_x : damping in X-direction
- C_y : damping in Y-direction
- C_θ : rotational damping
- x : relative displacement of the building C.G. in X-direction Fig. [3.2]
- y : relative displacement of the building C.G. in Y-direction Fig. [3.2]
- θ : relative building rotation about C.G. of the building Fig. [3.2]
- \dot{x} : relative velocity of the building C.G. in X-direction Fig. [3.2]
- \dot{y} : relative velocity of the building C.G. in Y-direction Fig. [3.2]
- $\dot{\theta}$: relative rotational velocity about C.G. of the building
- \ddot{x} : relative acceleration of the building C.G. in X-direction
- \ddot{y} : relative acceleration of the building C.G. in Y-direction
- $\ddot{\theta}$: relative rotational acceleration about C.G. of the building

The equations of motion for each of freedom (for building C.G. is at center of the building) are :

$$\begin{aligned}
 M\ddot{x} + C_x\dot{x} + (kw_1 + kw_2)x + (kw_1 - kw_2)B/2\theta &= -M\ddot{x}_g \\
 M\ddot{y} + C_y\dot{y} + (kw_3 + kw_4)y + (kw_3 - kw_4)L/2\theta &= 0 \\
 J\ddot{\theta} + C_\theta\dot{\theta} + ((x + B/2\theta)kw_1 - (x - B/2\theta)kw_2)B/2 + \\
 ((y + L/2\theta)kw_3 - (y - L/2\theta)kw_4)L/2 &= 0
 \end{aligned}$$

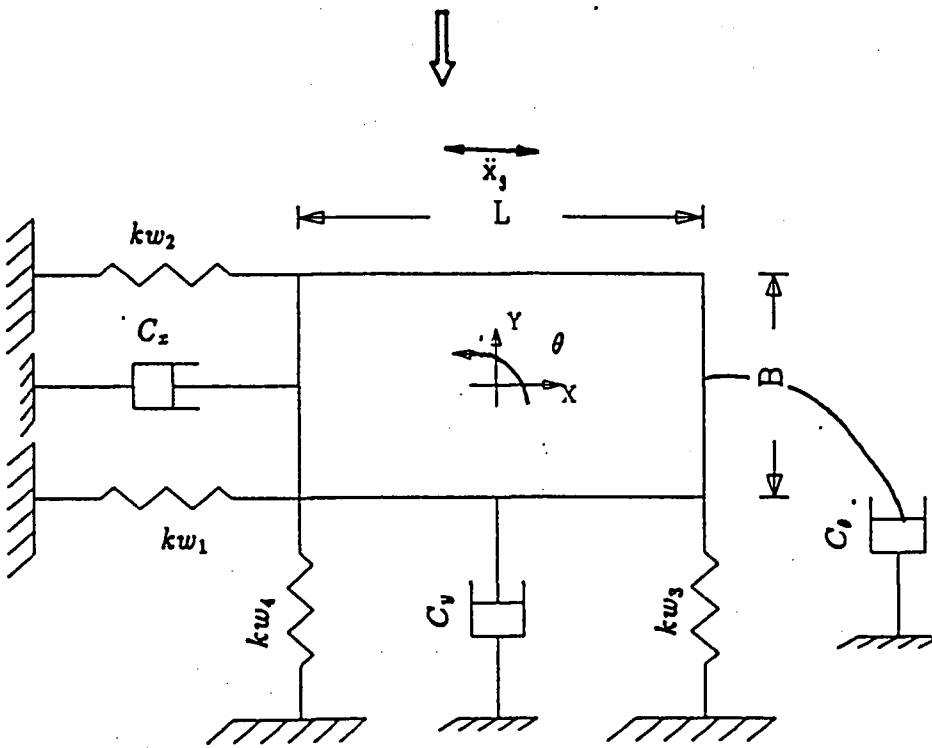
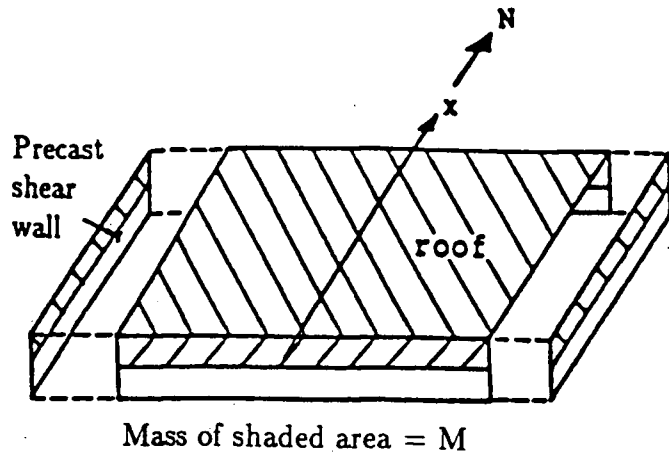


Figure 3.2: 3 Degrees of Freedom Model

In general :

$$[\mathbf{M}]\{\ddot{\mathbf{X}}\} + [\mathbf{C}]\{\dot{\mathbf{X}}\} + [\mathbf{K}]\{\mathbf{X}\} = \{\mathbf{F}\} \quad (3.1)$$

where :

$$[\mathbf{M}] = \begin{bmatrix} M & 0 & 0 \\ 0 & M & 0 \\ 0 & 0 & J \end{bmatrix}$$

$$[\mathbf{C}] = \begin{bmatrix} C_x & 0 & 0 \\ 0 & C_y & 0 \\ 0 & 0 & C_\theta \end{bmatrix}$$

$$[\mathbf{K}] = \begin{bmatrix} kw_1 + kw_2 & 0 & (kw_1 - kw_2)B/2 \\ 0 & kw_3 + kw_4 & (kw_3 - kw_4)L/2 \\ (kw_1 - kw_2)B/2 & (kw_3 - kw_4)L/2 & (kw_1 + kw_2)B^2/4 + (kw_3 + kw_4)L^2/4 \end{bmatrix}$$

$$\{\ddot{\mathbf{X}}\} = \begin{bmatrix} \ddot{x} \\ \ddot{y} \\ \ddot{\theta} \end{bmatrix}$$

$$\{\dot{\mathbf{X}}\} = \begin{bmatrix} \dot{x} \\ \dot{y} \\ \dot{\theta} \end{bmatrix}$$

$$\{\mathbf{X}\} = \begin{bmatrix} x \\ y \\ \theta \end{bmatrix}$$

$$\{\mathbf{F}\} = \begin{bmatrix} -M\ddot{x}_g \\ 0 \\ 0 \end{bmatrix}$$

3.4 Wall Displacements :

x , y & θ are the displacements at the centre of mass. If $xw_1 \dots 4$ are the displacements of Wall 1...4 . Then

$$xw_1 = x + \frac{B}{2} * \theta$$

$$xw_2 = x - \frac{B}{2} * \theta$$

$$xw_3 = y + \frac{L}{2} * \theta$$

$$xw_4 = y - \frac{L}{2} * \theta$$

3.5 Time Step Integration :

In incremental form eqn.(3.1) can be written as :

$$[M]\{\Delta\ddot{X}\} + [C]\{\Delta\dot{X}\} + [K]\{\Delta X\} = \{\Delta F\} \quad (3.2)$$

Variables with subscript 1 are for time t and

Variables with subscript 2 are for time $t + \Delta t$.

Assuming a linear variation in acceleration (see Fig. [3.3]) we get :

$$\{\ddot{X}_2\} = \{\ddot{X}_1\} + \{S\} * \Delta t \quad (3.3)$$

Integrating eqn.(3.3) :

$$\{\dot{X}_2\} = \{\dot{X}_1\} + \{\ddot{X}_1\} * \Delta t + \{S\} \frac{\Delta t^2}{2} \quad (3.4)$$

Integrating eqn.(3.4) :

$$\{X_2\} = \{X_1\} + \{\dot{X}_1\} * \Delta t + \{\ddot{X}_1\} \frac{\Delta t^2}{2} + \{S\} \frac{\Delta t^3}{6} \quad (3.5)$$

From eqn.(3.5) :

$$\{S\} = (\{X_2\} - \{X_1\}) \frac{6}{\Delta t^3} - \{\dot{X}_1\} \frac{6}{\Delta t^2} - \{\ddot{X}_1\} \frac{3}{\Delta t} \quad (3.6)$$

From eqn.(3.3) & (3.6) :

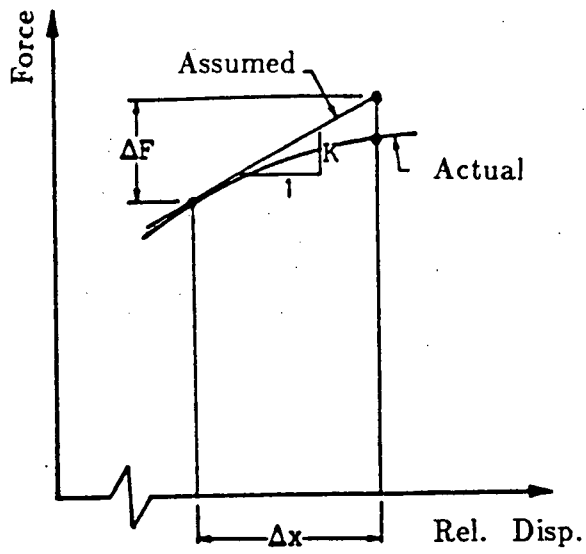
$$\begin{aligned} \{\Delta\ddot{X}\} &= \{\ddot{X}_2\} - \{\ddot{X}_1\} \\ &= (\{X_2\} - \{X_1\}) \frac{6}{\Delta t^2} - \{\dot{X}_1\} \frac{6}{\Delta t} - 3 * \{\ddot{X}_1\} \end{aligned}$$

But

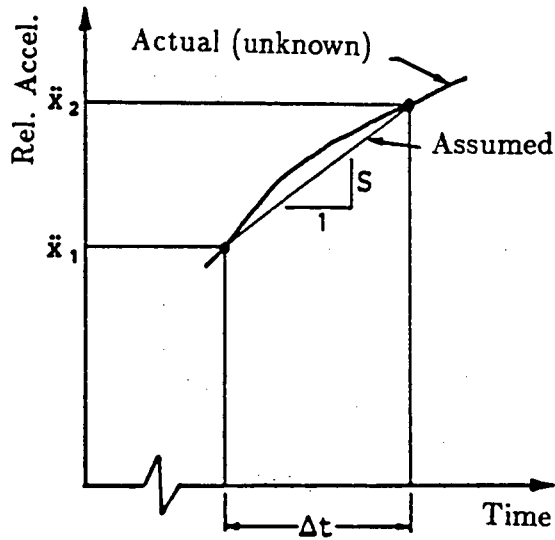
$$\{\Delta X\} = \{X_2\} - \{X_1\} \quad (3.7)$$

Thus

$$\{\Delta\ddot{X}\} = \frac{6}{\Delta t^2} \{\Delta X\} - \frac{6}{\Delta t} \{\dot{X}_1\} - 3 * \{\ddot{X}_1\} \quad (3.8)$$



(a) Assumed Constant Stiffness over ΔX



(b) Assumed Linear Variation of Acceleration

Figure 3.3: Linear Variation of Acceleration

And

$$\begin{aligned}\{\Delta \dot{X}\} &= \{\dot{X}_2\} - \{\dot{X}_1\} \\ &= \frac{3}{\Delta t} \{\Delta X\} - 3 * \{\dot{X}_1\} - \frac{\Delta t}{2} \{\ddot{X}_1\}\end{aligned}\quad (3.9)$$

Putting eqn. (3.7), (3.8), (3.9) in eqn. (3.2) we get

$$\begin{aligned}[\mathbf{M}] \left(\frac{6}{\Delta t^2} \{\Delta X\} - \frac{6}{\Delta t} \{\dot{X}_1\} - 3 * \{\ddot{X}_1\} \right) + \\ [\mathbf{C}] \left(\frac{3}{\Delta t} \{\Delta X\} - 3\{\dot{X}_1\} - \frac{\Delta t}{2} \{\ddot{X}_1\} \right) + \\ [\mathbf{K}] \{\Delta X\} = \{\Delta \mathbf{F}\}\end{aligned}\quad (3.10)$$

Rearranging various terms

$$[\mathbf{K}_{net}] \{\Delta X\} = \{\mathbf{F}_{net}\}$$

or

$$\{\Delta X\} = [\mathbf{K}_{net}]^{-1} \{\mathbf{F}_{net}\}\quad (3.11)$$

where

$$[\mathbf{K}_{net}] = [\mathbf{K}] + \frac{6}{\Delta t^2} [\mathbf{M}] + \frac{3}{\Delta t} [\mathbf{C}]\quad (3.12)$$

and

$$\begin{aligned}[\mathbf{F}_{net}] &= \{\Delta \mathbf{F}\} \\ &+ [\mathbf{M}] \left(\frac{6}{\Delta t} \{\dot{X}_1\} + 3\{\ddot{X}_1\} \right) \\ &+ [\mathbf{C}] \left(3\{\dot{X}_1\} + \frac{\Delta t}{2} \{\ddot{X}_1\} \right)\end{aligned}\quad (3.13)$$

Knowing the values of various variables at time-step t , and knowing the incremental change in the the ground acceleration from time t to $t + \Delta t$, we can find $\{\Delta X\}$ from eqns. (3.11), (3.12) & (3.13) . Then use eqn. (3.7), (3.8) & (3.9) to find the incremental change in displacement, acceleration & velocity.

3.6 Panel Stiffness

The following notations are used in the derivation of the stiffness of the panel for various possible panel positions :

- a : Width of panel
- b : Height of panel
- c : Height of panel upto roof level
- s : Separation between two panels
- e : Distance of dowel from the nearer panel face
- w : Weight of panel
- x : Horizontal wall displacement
- y_1 : Deformation of the left foundation spring
- y_2 : Deformation of the right foundation spring
- z_1 : Defomation of the left dowel springs measured from level 2
- z_2 : Defomation of the right dowel springs measured from level 2
- v : Relative shear displacement between the vertical connections
- θ : Rotation of the panel about one of the corners
- k_3 : Vertical spring stiffness
- k_4 : Left dowel spring stiffness
- k_5 : Right dowel spring stiffness
- k_9 : Foundation spring stiffness
- F_i : Horizontal force in the panel at the roof level
- f_3 : Vertical spring force
- f_4 : Left dowel spring force
- f_5 : Right dowel spring force
- f_{91} : Left foundation spring stiffness
- f_{92} : Right foundation spring stiffness
- N_v : Number of vertical connections on one face of the panel
- Level 1 : Undeformed position of foundation
- Level 2 : Deformed position of foudation under the dead load of the panel
- Level 3 : Final Deformed position of the foundation

Note : k_3 , k_4 , k_5 , are found from the hysteresis loops of the respective connections and may vary for each time-step.

3.6.1 Case 0 : Both the foundation springs in contact with the panel

The free body diagram for the panel in Case 0 is shown in Fig. [3.4]. Level 1 is the original surface of the foundation. Level 2 represents the initial deformation due to dead load of the panel, while Level 3 represents the total deformation due to the rotation of the panel. The deformations of the dowels are measured from Level 2. The stiffnesses of various springs and other structural data is given in section [5.2]. The stiffness of the panel for this case is given by the eqn.(3.14) (Ref. [36], Page 111) :

$$K_i = \left[\frac{1}{2c^2 + a|x|} \right] \left[Dk_3 + \frac{E(2k_4k_5 + k_4k_9 + k_5k_9)}{k_4 + k_5 + k_9} - \frac{aF_i}{2c} (\text{sgn } x) + G \right] \quad (3.14)$$

and .. the shear force F_i is given by :

$$F_i = \frac{2N_v c f_3 + c(a - 2e)(f_4 - f_5) + (a^2 k_9 - wb)x}{2c^2 + a|x|} \quad (3.15)$$

where

$$D = 6a(a + s) \quad (3.16)$$

$$E = (a - e)^2 \quad (3.17)$$

$$G = a^2 k_9 - wb \quad (3.18)$$

3.6.2 Case 1 : Only right foundation spring in contact with the panel

The free body diagram for the panel in Case 1 is shown in Fig. [3.5a]. The stiffness of the panel for this case is given by the eqn.(3.19) (Refer. [36], Page 114) :

$$K_i = \left[\frac{1}{2c^2 + ax} \right] \left[Dk_3 + \frac{2[E k_4 k_5 + (a - e)^2 k_4 k_9 + e^2 k_5 k_9]}{k_4 + k_5 + k_9} - aF_i - wb \right] \quad (3.19)$$

and .. the shear force F_i is given by :

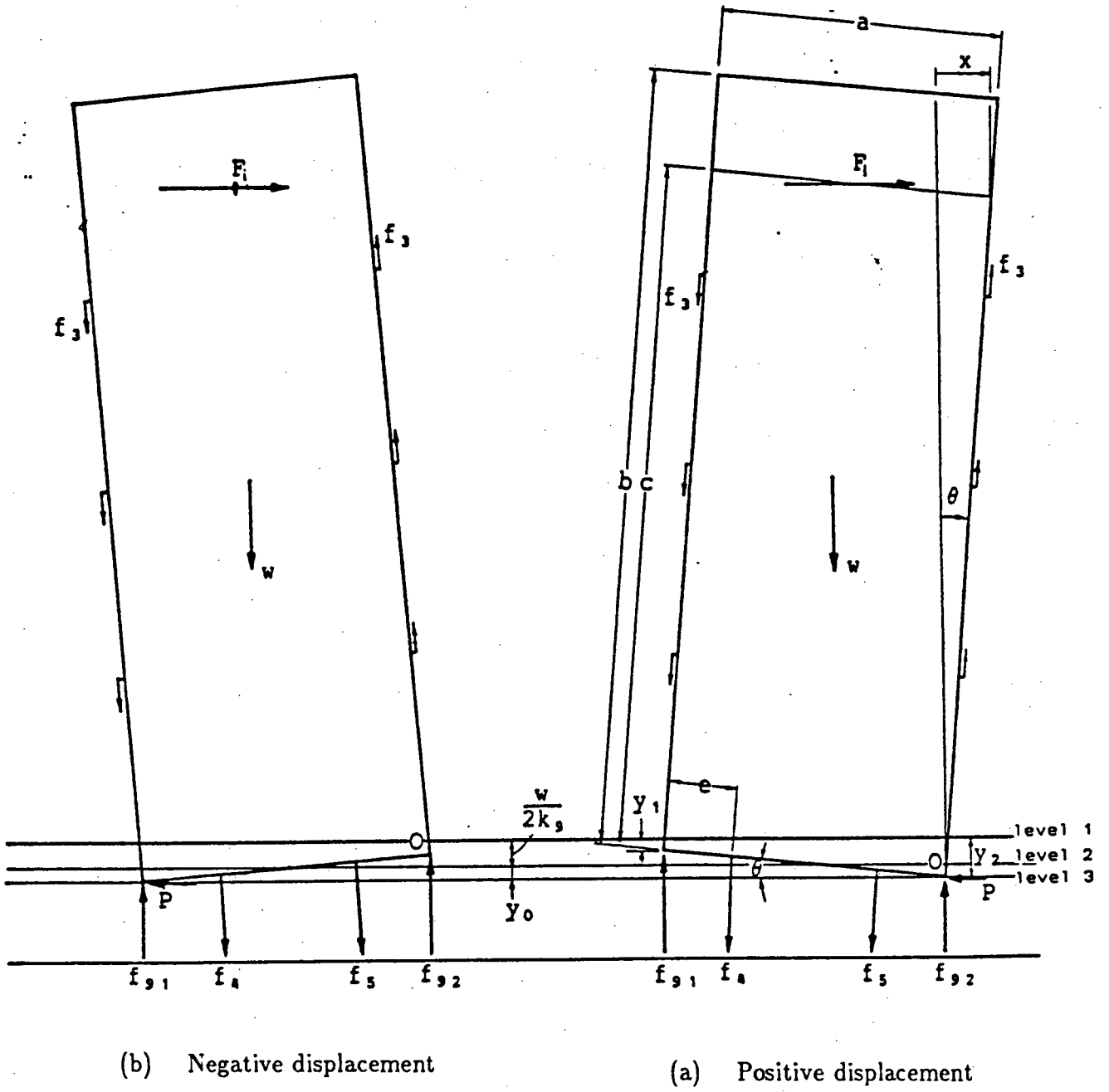


Figure 3.4: Free body diagrams of an interior panel corresponding to Case 0

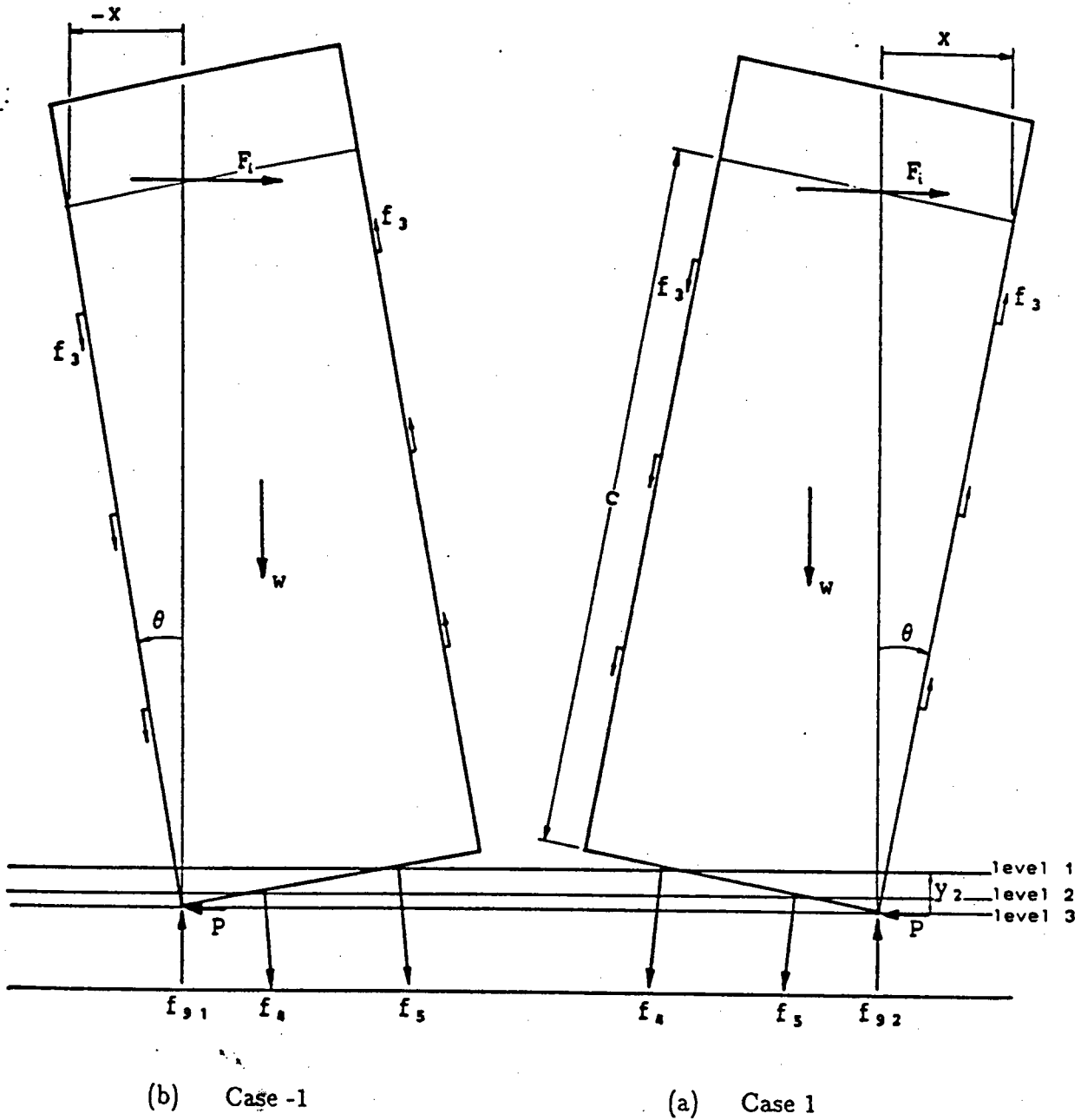


Figure 3.5: Free body diagrams of an interior panel corresponding to Case 1 and Case -1

$$F_i = \frac{2 N_v c f_3 + 2 c (a - e) f_4 + 2 c e f_5 + a c w - w b x}{2 c^2 + a x} \quad (3.20)$$

where D & E are constants given by eqn.(3.16) & (3.17).

3.6.3 Case - 1 : Only left foundation spring in contact with the panel

The free body diagram for the panel in Case -1 is shown in Fig. [3.5b]. The stiffness of the panel for this case is given by the eqn.(3.21) (Refer. [36], Page 115) :

$$K_i = \left[\frac{1}{2 c^2 - a x} \right] \left[D k_3 + \frac{2 [E k_4 k_5 + e^2 k_4 k_9 + (a - e)^2 k_5 k_9]}{k_4 + k_5 + k_9} - a F_i - w b \right] \quad (3.21)$$

and .. the shear force F_i is given by :

$$F_i = \frac{2 N_v c f_3 - 2 c e f_4 - 2 c (a - e) f_5 - a c w - w b x}{2 c^2 - a x} \quad (3.22)$$

where D & E are constants given by eqn.(3.16) & (3.17).

3.6.4 Case 2 : Neither foundation spring in contact with the panel

The free body diagram for the panel in Case 2 is shown in Fig. [3.6] The stiffness of the panel for this case is given by the eqn.(3.23) (Refer. [36], Page 115) :

$$K_i = \left[\frac{1}{2 c^2 - (a - 2 e) |x|} \right] \left[D k_3 + \frac{2 E k_4 k_5}{k_4 + k_5} - (a - 2 e) (F_i) (sgn x) - w b \right] \quad (3.23)$$

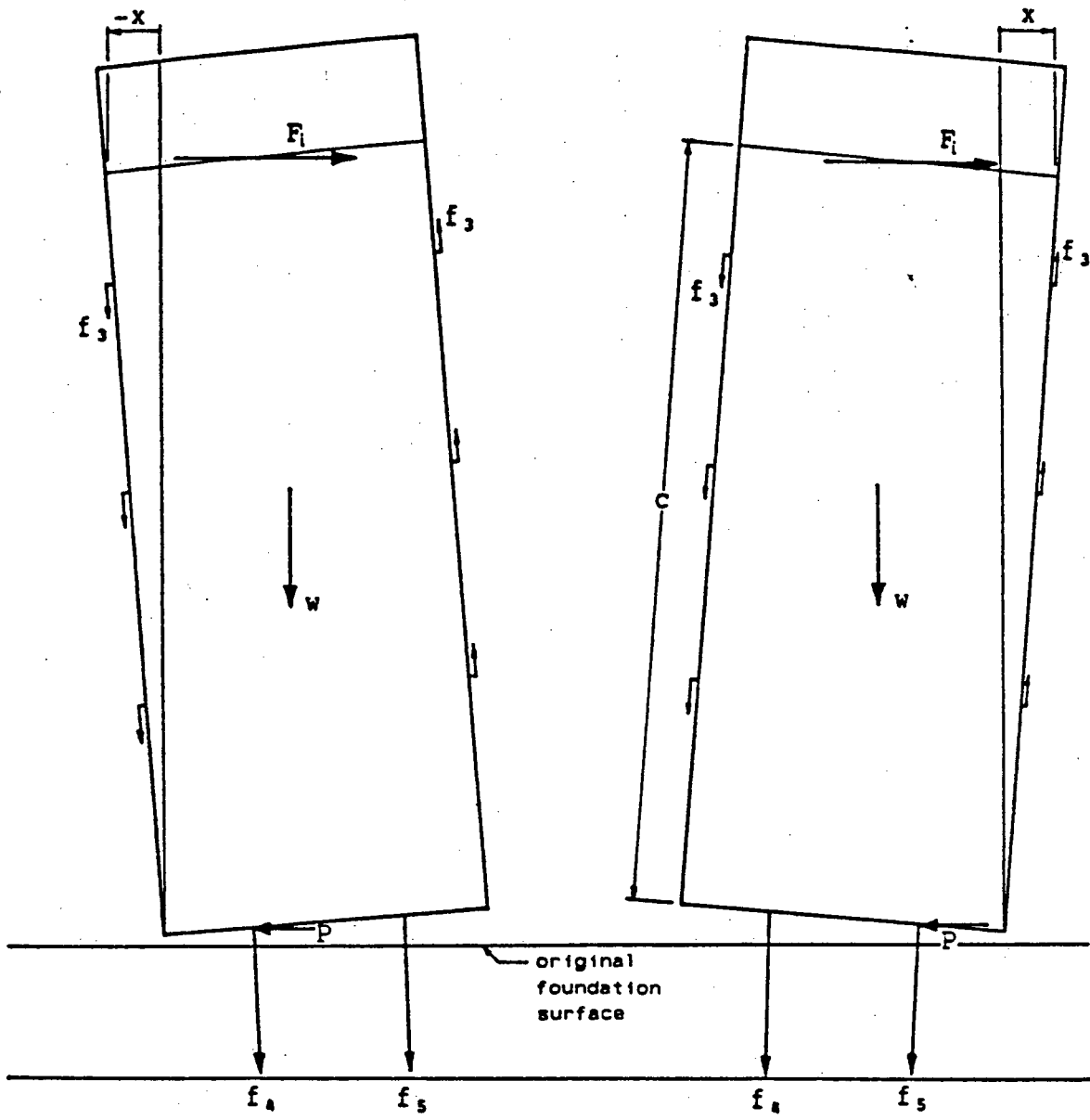
and .. the shear force F_i is given by :

$$F_i = \frac{2 N_v c f_3 + 2 c (a - 2 e) f_4 + c (a - 2 e) w - w b x}{2 c^2 - (a - 2 e) |x|} \quad (3.24)$$

where D , E & G are constants given by eqn.(3.16), (3.17) & (3.18).

3.7 Wall Stiffness

The stiffness of a wall is the sum of the stiffnesses of all the panels in the wall. A wall is made up of exterior and interior panels as shown in Fig. [3.7]. Interior panels can



(b) Negative displacement

(a) Positive displacement

Figure 3.6: Free body diagrams of an interior panel corresponding to Case 2

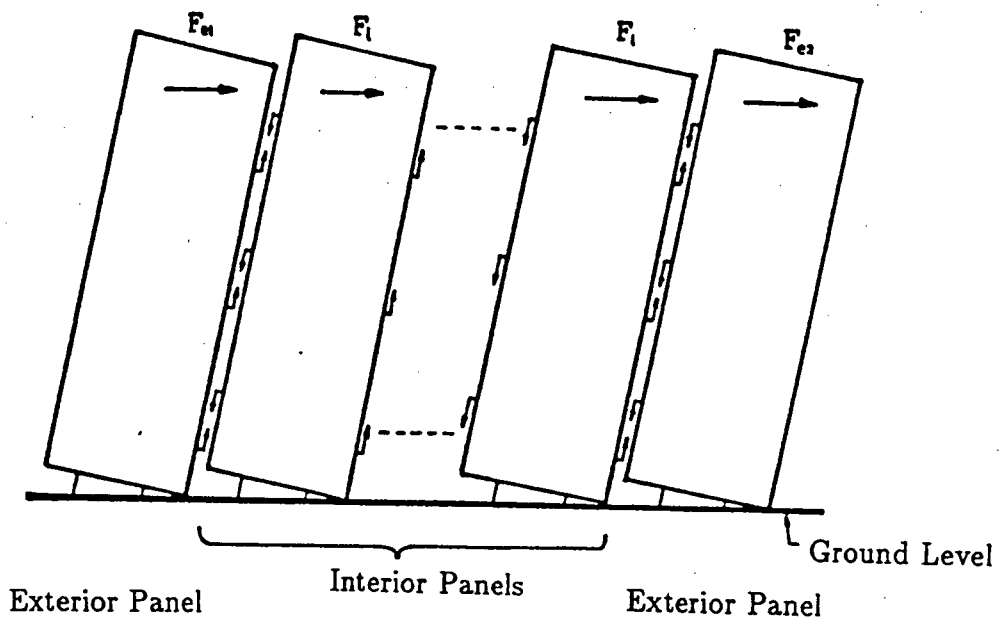


Figure 3.7: Shear Wall System

have vertical connections on both of their faces while the exterior panels can have vertical connections only on one face. The exterior panels are needed at the ends as well as at the openings in the wall. The eqns. (3.14), (3.19), (3.21) and (3.23) give the stiffness of interior panels only. The exterior panel stiffness is derived from the interior panel stiffness (Ref. [36] Appendix A). Stiffness of 'n' exterior panels is equal to the stiffness of $\frac{n}{2}$ modified interior panels . In the modified interior panel weight, dowel spring stiffness & yield strength and the foundation spring stiffness are obtained by multiplying the respective exterior panel properties by a factor of 2. Thus the stiffness of a wall with n_1 interior and n_2 exterior panels is given by :

$$K_{wall} = n_1 K_{int} + n_2 K_{ext}$$

where :

K_{int} & K_{ext} are obtained using eqns. (3.14) (3.19) (3.21) or (3.23)

using proper values of the variables

Note that if the panels do not have any vertical connections, then the exterior panel stiffness will be same as the interior panel stiffness (as is the case in the present studies).

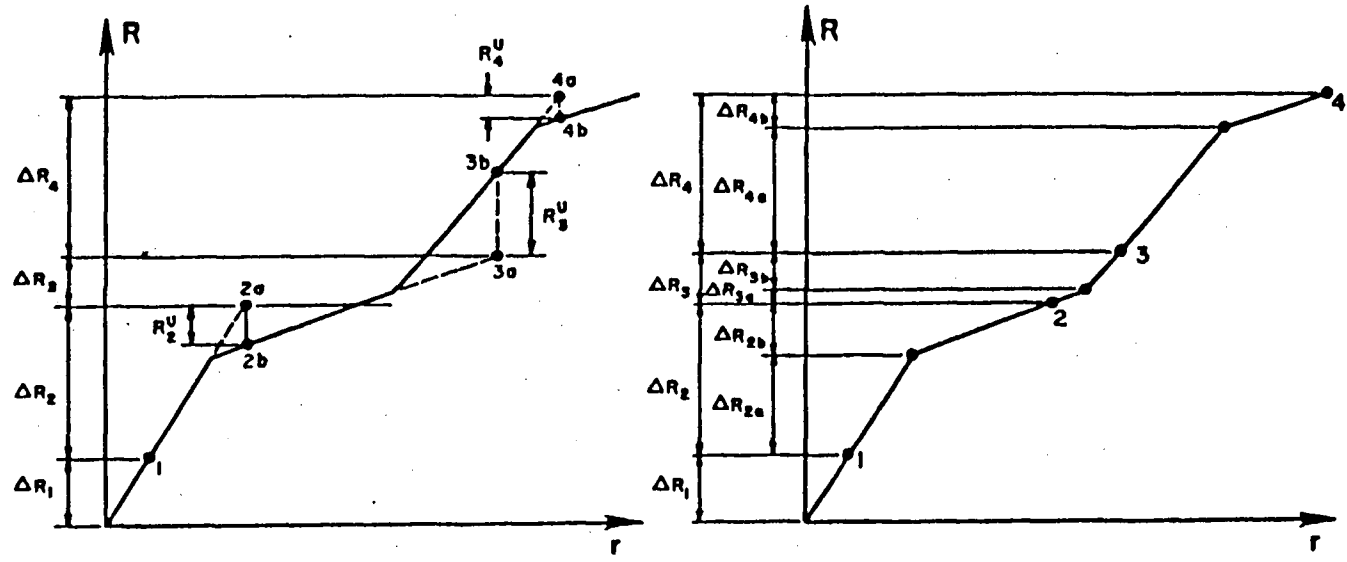
3.8 Time-Step Solution Technique

The earthquake excitation record is subdivided into small time-steps and the response of the structure is found at each time-step. This allows one to follow the exact force-deflection curve of the structure. As we know that stiffness of each wall panel varies from one stage to another as the wall displacement changes, so the force-deflection curve keeps on changing. To follow the exact force-deflection curve; we would have to use a very small time-step, and for each time-step we would have to use an iteration procedure (Newton - Raphlson or some other similar technique) so that the solution proceeds from event (i.e. stiffness change) to event

(see Fig. [3.8b]). There should be no imbalance of load at the end of any time-step and the solution should follow the exact load-deflection curve. This procedure will be very expensive.

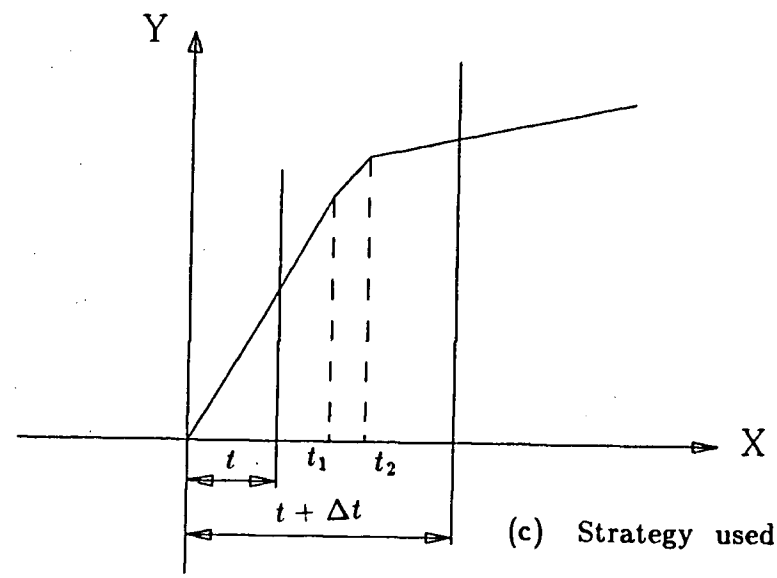
A second technique is to find the unbalanced force at the end of each time-step and add this unbalanced force R to the incremental force ΔR for the next time-step (see Fig. [3.8a]). After a few load reversals we would be far off the true load displacement curve and the energy input would not equal energy output (i.e. we loose energy balance).

The approach used here is a combination of the above two approaches. Events (i.e. stiffness changes and hence load sub-steps) are recognised for certain elements only, namely those in which large stiffness changes, and hence large equilibrium errors, can occur. These specified events occurs when the rocking of panels change from one equilibrium position to another (see Fig. [3.1b]). All other stiffness changes are ignored and any resulting errors are taken into account by applying an equilibrium correction, i.e. for each time step we follow the second approach. Then if we find that within some time step, say from time ' t ' to ' $t + \Delta t$ ', the stiffness of a panel has changed from one position of equilibrium to another, we come back to find, with a given tolerance, the time t' ; time at which the change occurred. We then find the response of the structure at time t' and use the new stiffness until the panel position changes again. If within a time-step a number of panels change their positions, then first we find the least time t'_1 at which one panel is going to change its position; find the response of the structure at this time t'_1 then use the new stiffness for that panel and find the next time t'_2 at which the next panel will change its position (see Fig. [3.8c]), and so on. In other words we try to find the times where the panel stiffnesses change, as exactly as possible.



(a) Equilibrium Correction

(b) Event to Event



(c) Strategy used in the present studies

Figure 3.8: Solution Strategies

3.9 Damping :

Damping is an inherent property of the system, and is a mechanism by which the mechanical energy of the system, kinetic and potential energy, is transferred to other forms of energy such as heat etc. The mechanics of this transformation or dissipation are quite complex. This mechanism can be accounted for by viscous damping approach described below :

Viscous Damping : In this approach the damping force is assumed to be proportional to the velocity of the system . The coefficient of damping is given by :

$$C = 2 \xi \sqrt{K_e M} \quad (3.25)$$

where K_e = Elastic stiffness of the system

M = Mass of the system

ξ = Damping ratio of the system

as % of critical damping

Experimental results have shown that damping forces in the buildings are nearly independent of the test frequency, while the viscous damping procedure has a frequency dependent damping. However there is very little literature available on damping in panelized structures. During an earthquake analysis, most of the energy is dissipated by F- Δ hysteresis loops and the energy dissipated by damping is only a small fraction of the total energy dissipated, so the assumption of viscous damping is often made regardless of the dissipative characteristics of the system because it leads to relatively simpler mathematical analysis. For the present studies, damping ratio ξ is taken as 1 %.

3.10 Energy Balance :

When the ground underneath a structure moves, energy is either input into the structure or fed back into the ground. The net energy input is given by :

$$\begin{aligned} E_{input} &= \text{Base Shear Force} * \text{Ground Displacement} \\ &= \text{Mass} * \text{Abs. Acceleration} * \text{Ground Displacement} \end{aligned}$$

For time step analysis this equation can be written as

$$\sum E_{inp} = \sum (M * \ddot{x}_t) \Delta x \quad (3.26)$$

where M = Mass of the building

\ddot{x}_t = absolute acceleration of the building

Δx = incremental displacement of the building
at time t

As the structure moves relative to the ground the stored energy is dissipated or transformed into other forms of energy. Various mechanisms through which the energy is dissipated or stored are :

(i) Energy stored as strain energy : The total cumulative strain energy stored and/or dissipated at any instant is given by area under the F- Δ curve, calculated with due regard for the signs of F and Δ . When the structure comes to rest, the net cumulative strain energy is the energy dissipated by hysteresis during the earthquake excitation.

For example in Fig. [3.9], if the slope o1 is the elastic stiffness, the energy stored at point 1 is the area o1a0 and at point 2 is o12b0 which is made up of the area o1240 which represents dissipative or heat energy, and area 2b42 which is strain energy. From point 2 to 3 as the structure unloads elastically the strain energy reduces and at point 3 the strain energy is given by the area 3c43. Now if the

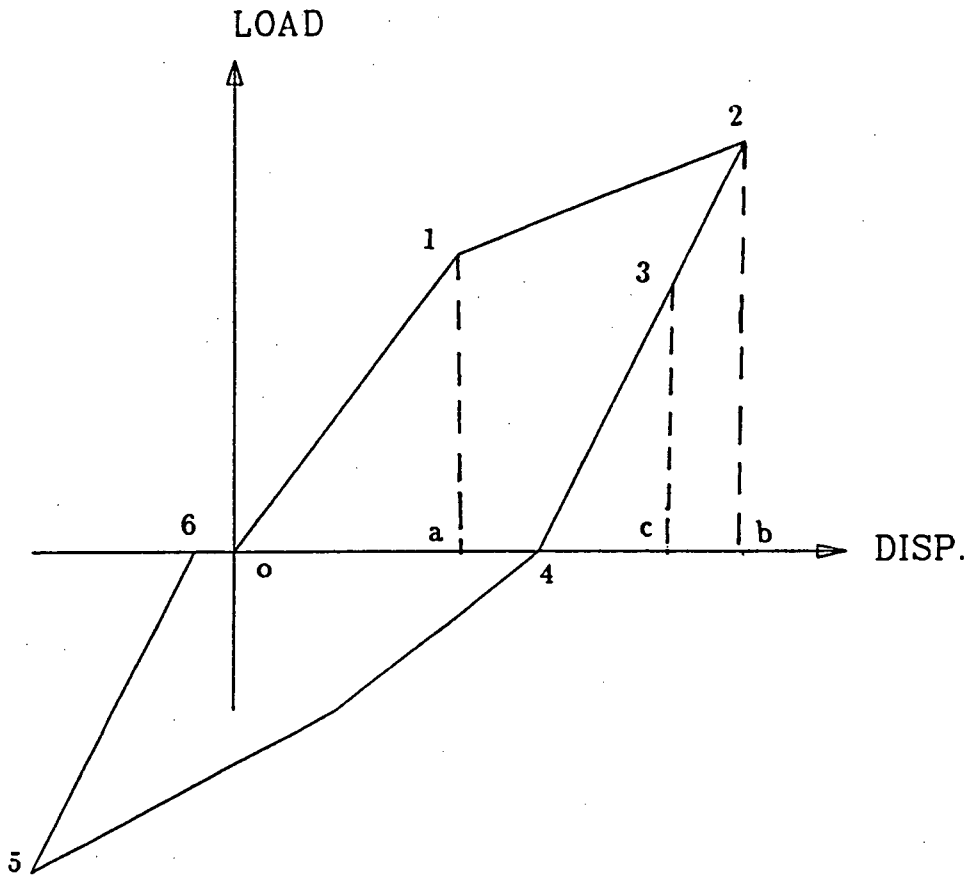


Figure 3.9: Strain Energy from a F- Δ curve

structure comes to rest at point 6, there is no strain energy and the area o123456 of the F-Δ diagram gives the total energy dissipated by hysteresis.

(ii) Energy dissipated by damping : This is the velocity proportional energy dissipated due to the damping of the system. The governing equation is :

$$E_{vis} = C * x * \dot{x} \quad (3.27)$$

where C = Coefficient of damping

x = Displacement of the structure relative to ground

\dot{x} = Velocity of the structure relative to ground

(iii) Instantaneous kinetic energy : The governing eqn. for energy stored (or dissipated) as kinetic energy is :

$$E_{K.E.} = \frac{M * \dot{x}_{abs}^2}{2} \quad (3.28)$$

where \dot{x}_{abs} is the absolute velocity of the structure

Thus the energy balance equation is given by :

$$\begin{aligned} E_{input} &= \text{Net stored strain energy} \\ &+ \sum \text{dissipated hysteresis energy} \\ &+ \sum \text{dissipated viscous energy} \\ &+ \text{kinetic energy} \end{aligned}$$

At the end of each time step energy input should be equal to energy output. During the time-step analysis, energy balance is checked at the end of each time-step. Because of the approximations in the iteration scheme, (see section [3.8]) there will be some error in the energy balance at the end of a time-step. The maximum energy balance error allowed was 5 % at any time during the dynamic analysis.

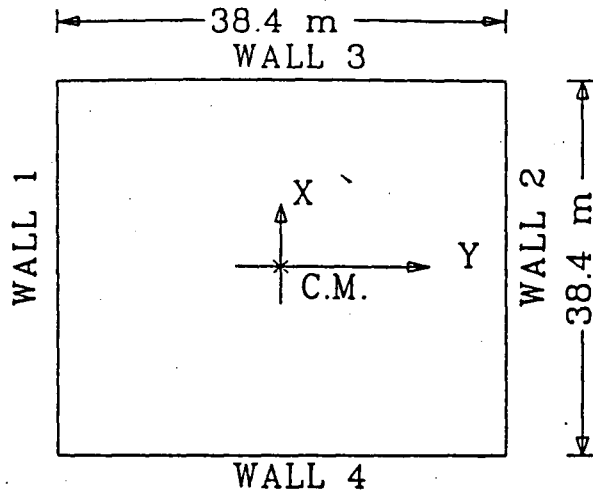
Chapter 4

Static Design of the Buildings

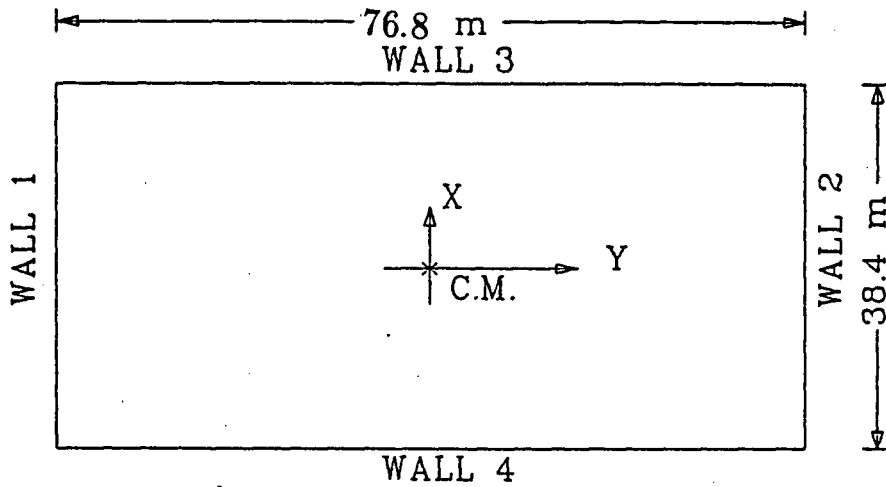
4.1 General

The loading on a structure resulting from seismic ground motion effects is quite complex. Design codes attempt to reduce this complex situation into a simpler set of equivalent static lateral forces. In a one storey building a single force is assumed to act at the roof level. The building is designed to resist this lateral force by developing forces in walls and other building components. In this chapter, two methods which are used to calculate the forces acting on the walls are discussed. The first method of design is based on the stiffness of each wall. This method is referred to as the *Stiffness Method*. This method has been used in most of the design handbooks [25] to calculate the forces in various walls. An alternate method based on the strength of the walls is also presented. This method is referred to as the *Strength Method*.

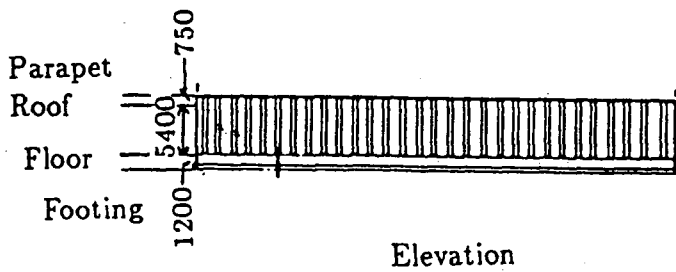
Two buildings, a square building of plan area $38.4m * 38.4m$, Fig. [4.1a], and a rectangular building of plan area $38.4m * 76.8m$, Fig. [4.1b], were designed according to the NBCC [22] recommendations, using both the strength and stiffness method techniques to calculate the forces in various walls. The roof diaphragm of each building is considered to be rigid and the mass is uniformly distributed (i.e. the centre of mass (C.M.) is at the centre of the building). Other structural data



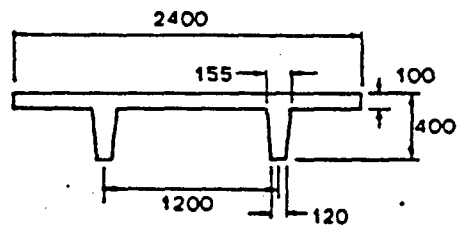
(a) Square Building



(b) Rectangular Building



Elevation



(c) Wall Panel

Figure 4.1: One Storey Buildings Analysed in the Present Studies

common to both the buildings is given below :

$$\text{Height of the building} = 5.4m$$

$$\text{Height of the parapet wall} = 0.75m$$

$$\text{Width of the panel} = 2.4m$$

$$\text{Thickness of the panel} = 100mm$$

$$\text{Weight of each panel per unit area} = 3.29 \text{ kN/m}^2$$

$$\text{Separation between panels} = 0.01m$$

For both the buildings, there are no openings in walls 2, 3 and 4. Openings in wall 1 are created by removing full panels i.e. the number of panels in wall 1 is varied from 0 to 16 to study the effects of different eccentricities. It is assumed that the number of panels in wall 1 is fixed by architectural requirements and not by strength requirements.

A brief description of the NBCC [22] recommendations for calculating the lateral force & torsional design moment acting on a building under the influence of an earthquake, section [4.1.9] in Ref. [22], is given below.

a) Minimum specified lateral seismic force

$$V = v.S.K.I.F.W \quad (4.1)$$

where v = zonal velocity ratio

S = seismic response factor for the structure

K = numerical coefficient that reflects the ductility
and other properties of the structure

I = importance factor

F = foundation factor

W = dead load, plus 25% of design snow load,
plus 60% of the storage load

b) Torsional moment in the horizontal plane of the building, about the centre of rigidity is

$$M_{tx} = (F_t + \sum_{i=x}^n F_i) e_x \quad (4.2)$$

where M_{tx} = torsional moment at level x .

F_t = portion of V concentrated at the top of the structure

F_x = lateral force applied at level x

e_x = design eccentricity at level x

Design eccentricity, e_x , is computed by one of the following equations, using whichever produces the greater stresses for a given wall:

$$e_x = 1.5e + 0.1D_n \quad (4.3)$$

$$e_x = 0.5e - 0.1D_n \quad (4.4)$$

where e = distance between the location of the resultant of all equivalent static forces applied at and above the level being considered and the centre of rigidity at the level being considered.

D_n = plan dimension of the building in the direction of computed eccentricity.

The buildings being considered are assumed to be in zone 5 of the NBCC [35]. The buildings have been designed for earthquake acting in the X direction and have been checked for the earthquake in the Y direction. The buildings have been designed according to NBCC [22] requirements for equivalent static loads using both the

stiffness and strength methods. In the following paragraphs a brief description of the two methods of design is given.

4.2 Stiffness Method

The centre of rigidity is assumed to be on the line of action of the resultants of the resisting forces acting when the building is given a lateral displacement with no rotation. In the stiffness method, the resisting force contributed by each element is assumed to be proportional to its stiffness. If it is assumed that the stiffness of each wall is proportional to its number of panels i.e. all the walls have similar panels (or panel connections), then the location of the centre of rigidity of the building can be calculated as follows :

$$e_{cr} = L/2 - N_1/(N_1 + N_2) * L$$

where e_{cr} = distance from the geometric centre of
the roof diaphragm to the centre of rigidity.

N_i = number of panels in wall i

and L = building dimension perpendicular to the
direction of the E/Q

The equivalent static force applied to the building is assumed to act through the centre of mass. If the centre of mass and the geometric centre of the building are coincident (i.e. mass is uniformly distributed in the roof diaphragm), then

$$\begin{aligned} e &= e_{cr} \\ &= L/2 - N_1/(N_1 + N_2) * L \end{aligned} \quad (4.5)$$

An example calculation of the resisting forces in the walls for the square building, Fig. [4.1a], with 16 panels in walls 2, 3 & 4 and 2 panels in wall 1, when a force is applied through the C.M., is given below :

From eqn.(4.5), eccentricity e is

$$\begin{aligned} e &= 38.4/2 - 2/(2 + 16) * 38.4 \text{ m} \\ &= 14.93 \text{ m} \end{aligned}$$

As noted above, the code requires the consideration of two design eccentricities, e_x (see eqn. (4.3) and (4.4)). The building must be designed to resist the lateral force V and the torsional moment $V * e_x$. For the design eccentricity, both the code equations; eqn.(4.3) & eqn.(4.4) are used. The resisting force system must provide a resultant lateral force (= V) acting through the C.R. and a resisting moment $M = V * e_x$. The force V is therefore assumed to be applied to the building as shown in Fig [4.2]. For each wall, the maximum resultant force found using one of the two design eccentricities is taken as the design force.

Design eccentricity e_d from eqn.(4.3) :

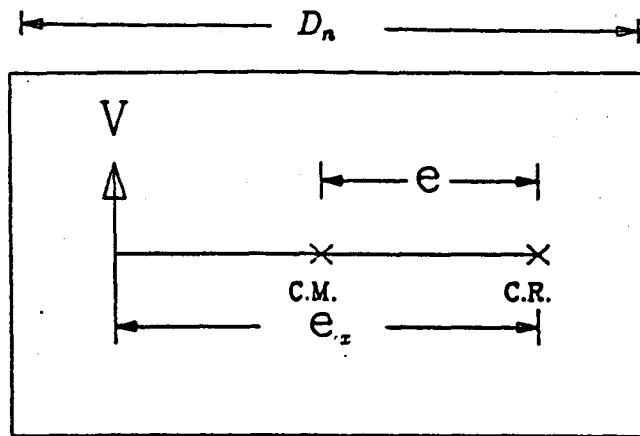
$$\begin{aligned} e_d &= 1.5 * e + 0.1 * L \text{ m} \\ &= 1.5 * 14.93 + 0.1 * 38.4 \text{ m} \\ &= 25.94 \text{ m} \end{aligned}$$

The lateral force V is calculated using eqn. [4.1]. The seismic response factor of the structure ' S ' used in the eqn. [4.1] corresponds to fundamental period of the buildings determined by the formula $0.09h_n/\sqrt{D_s}$ (section [4.1.9.1 (6)] NBCC [22])

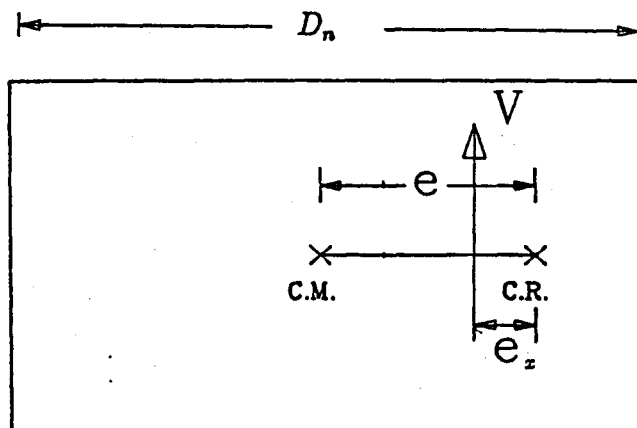
where h_n = height of the building in metres
= 5.4 m

D_s = the dimension of the building in the direction of the
= applied forces (in metres)

For the building being discussed here, the fundamental period is 0.08 sec and the corresponding seismic response factor S from NBCC [22] (Table [4.1.9.A]) is 0.44



(a) $e_x = 1.5e + 0.1D_n$



(b) $e_x = 0.5e - 0.1D_n$

Figure 4.2: Assumed Line of Action of Equivalent Static Force

(the actual fundamental periods of the statically designed buildings are shown in the Appendix [A]).

The torsional moment M , for $V = 1071$ kN is

$$\begin{aligned} M &= V * e_d \text{ kN-m} \\ &= 1071 * 25.94 \text{ kN-m} \\ &= 28124 \text{ kN-m} \end{aligned}$$

Design eccentricity e_d from eqn.(4.4) :

$$\begin{aligned} e_d &= 0.5 * e - 0.1 * L \text{ m} \\ &= 0.5 * 14.93 - 0.1 * 38.4 \text{ m} \\ &= 3.62 \text{ m} \end{aligned}$$

and corresponding torsional moment M is

$$\begin{aligned} M &= V * e_d \text{ kN-m} \\ &= 1071 * 3.62 \text{ kN-m} \\ &= 3877 \text{ kN-m} \end{aligned}$$

Now if

$$F_{vi} = \text{Force in wall } i \text{ due to lateral force } V$$

$$F_{ti} = \text{Force in wall } i \text{ due to torsional moment } M$$

Walls 1 and 2 take the lateral force V in proportion to their stiffness . Thus forces in various walls due to the lateral force V are :

$$\begin{aligned} F_{v_1} &= V * N_1 / (N_1 + N_2) \text{ kN} \\ &= 1071 * 2 / (2 + 16) \text{ kN} \end{aligned}$$

$$\begin{aligned}
&= 119 \text{ kN} \\
F_{v_2} &= V * N_2 / (N_1 + N_2) \text{ kN} \\
&= 1071 * 16 / (2 + 16) \text{ kN} \\
&= 952 \text{ kN} \\
F_{v_3} &= 0 \text{ kN} \\
F_{v_4} &= 0 \text{ kN}
\end{aligned}$$

Force on wall i due to torsional moment M is given by :

$$F_{t_i} = M \frac{r_i * d_i}{\sum_{i=1}^4 (r_i * d_i^2)} \text{ kN}$$

where :

$$\begin{aligned}
r_i &= \text{Stiffness of wall i} \\
d_i &= \text{Distance of wall i from C.R. of the building}
\end{aligned}$$

i.e. all the walls contribute in resisting the torsional moment. The forces acting on various walls for the earthquake acting in the X-direction are given in Table [4.1]. The calculations are repeated for the earthquake acting in the other direction. The design eccentricity and torsional moment for the earthquake acting in the Y direction are given below and the forces in various walls are given in Table [4.2].

$$\begin{aligned}
V &= \text{Specified lateral force on the building} \\
&= 1071 \text{ kN} \\
e &= \text{Actual eccentricity of the building} \\
&= 0.0 \text{ m (from eqn(4.5))} \\
e_d &= \text{Design eccentricity of the building} \\
&= 3.84 \text{ m (from eqn.(4.3))} \\
&= -3.84 \text{ m (from eqn.(4.4))}
\end{aligned}$$

Wall No.	No. of panels	F_v kN	F_t (kN)		Force on wall		Max. Force on wall (kN)	Panel Force (kN)
			from eqn(4.3)	from eqn(4.4)	from eqn(4.3)	from eqn(4.4)		
(1)	(2)	(3)	(4)	(5)	(6) = (3)+(4)	(7) = (3)+(5)	(8)=max. of (6) & (7)	(9) = (8)/(2)
1	2	119	133	19	252	138	252	126
2	16	952	-133	-19	819	933	933	58.5
3	16	0	-598	-83	-598	-83	598	37.3
4	16	0	598	83	598	83	598	37.3

Table 4.1: Forces in various walls of a square building, Fig. [4.1a], for E/Q in X-direction, using stiffness method of design

$$\begin{aligned}
 M &= \text{Torsional Moment on the building} \\
 &= 4113 \text{ kN-m (using eqn.(4.3))} \\
 &= 4113 \text{ kN-m (using eqn.(4.4))}
 \end{aligned}$$

Panel design is governed by the maximum of the panel forces (Col (9)) in

Wall No.	No. of panels	F_v kN	F_t (kN)		Force on wall		Max. Force on wall (kN)	Panel Force (kN)
			from eqn(4.3)	from eqn(4.4)	from eqn(4.3)	from eqn(4.4)		
(1)	(2)	(3)	(4)	(5)	(6) = (3)+(4)	(7) = (3)+(5)	(8)=max. of (6) & (7)	(9) = (8)/(2)
1	2	0	20	-20	20	-20	20	10
2	16	0	-20	20	-20	20	20	1.25
3	16	536	-88	88	448	624	624	39.
4	16	536	+88	-88	624	448	624	39.

Table 4.2: Forces in various walls of a square building, Fig. [4.1a], for E/Q in Y-direction, using stiffness method of design

Tables [4.1] & [4.2]. It was assumed that the stiffness of each wall was proportional to its number of panels but the maximum force for each wall (Col 4 in Table [4.3]) is not proportional to the number of panels in that wall. The force on each panel in wall 1 (the weaker wall) is much higher than that for each panel in the other

Wall No.	No. of panels	Maximum Wall Force kN	Maximum Panel Force kN
(1)	(2)	(3) = Max. of Col (8) in Tables 4.1 & 4.2	(4) = Max. of Col (9) in Tables 4.1 & 4.2
1	2	252	126
2	16	933	58.5
3	16	624	39
4	16	624	39

Table 4.3: Maximum Panel Forces governing the design of various walls in a Square Building, Fig. [4.1a], using stiffness method of design

Wall No.	No. of panels	r_i	V (kN)	e (m) for the E/Q in		e_d & M for the E/Q in X dir.		e_d & M for the E/Q in Y dir.	
				X dir.	Y dir.	eqn(4.3)	eqn(4.4)	eqn(4.3)	eqn(4.4)
1	2	252	1071	11.03	0.0	$e_d =$	$e_d =$	$e_d =$	$e_d =$
2	16	933				20.39	1.68	3.84	-3.84
3	16	624							
4	16	624				M = 21837	M = 1796	M = 4113	M = -4113

Table 4.4: Code recommended Design Eccentricity & Torsional Moment for Square Building with Stiffness of each wall proportional to Wall Force in Table [4.3]

walls. In general we would expect panel stiffness to be affected by panel strength. If panel stiffness is assumed linearly proportional to the panel strength, as given in Table [4.3] and the calculations are repeated then the weaker wall (wall 1) seems to attract more force per panel than the other walls because of the higher stiffness panels required for this wall. See Tables [4.4]...[4.7] for the forces in the walls. (Note that load factors must still be applied to the panel forces when the panels are design).

Wall No.	No. of panels	F_v kN	F_t (kN)		Force on wall		Max. Force on wall (kN)	Panel Force (kN)
			from eqn(4.3)	from eqn(4.4)	from eqn(4.3)	from eqn(4.4)		
(1)	(2)	(3)	(4)	(5)	(6) = (3)+(4)	(7) = (3)+(5)	(8)=max. of (6) & (7)	(9) = (8)/(2)
1	2	228	221	18	449	246	449	224.5
2	16	843	-221	-18	622	825	825	51.6
3	16	0	-348	-29	-348	-29	348	21.8
4	16	0	348	29	348	29	348	21.8

Table 4.5: Forces in various walls of a square building, Fig. [4.1a], for E/Q in X-direction using stiffness method of design with Stiffness of each wall proportional to Wall Force in Table [4.3]

4.2.1 Shortcomings of the Stiffness Method

For the example shown above, if it is assumed that all the panels have the same stiffness regardless of their strength then the walls can be designed by providing the panel strengths found from the panel forces in Table [4.3]. But for a highly eccentric building, the required panel strength for the weaker wall (wall 1) might become so high as to make the panel design impractical. This is shown in the following example of a highly eccentric rectangular building.

The rectangular building, Fig. [4.1b] has 32 panels in walls 3 & 4, 16 panels in wall 2

Wall No.	No. of panels	F_v kN	F_t (kN)		Force on wall		Max. Force on wall (kN)	Panel Force (kN)
			from eqn(4.3)	from eqn(4.4)	from eqn(4.3)	from eqn(4.4)		
(1)	(2)	(3)	(4)	(5)	(6) = (3)+(4)	(7) = (3)+(5)	(8)=max. of (6) & (7)	(9) = (8)/(2)
1	2	0	42	-42	42	-42	42	21
2	16	0	-42	42	-42	42	42	2.6
3	16	536	-66	66	470	602	602	37.6
4	16	536	+66	-66	602	470	602	37.6

Table 4.6: Forces in various walls of a square building, Fig. [4.1a], for E/Q in Y-direction, using stiffness method of design with Stiffness of each wall proportional to Wall Force in Table [4.3]

Wall No.	No. of panels	Maximum Wall Force kN	Maximum Panel Force kN
(1)	(2)	(3) = Max. of Col (8) in Tables 4.5 & 4.6	(4) = Max. of Col (9) in Tables 4.5 & 4.6
1	2	449	224.5
2	16	825	51.6
3	16	602	37.6
4	16	602	37.6

Table 4.7: Maximum Panel Forces governing the design of various walls in a Square Building, Fig. [4.1a], using stiffness method of design with Stiffness of each wall proportional to Wall Force in Table [4.3]

and 2 panels in wall 1.

V = Specified lateral force on the building

$$= 2058 \text{ kN}$$

e = Actual eccentricity of the building

$$= 29.87 \text{ m (from eqn(4.5))}$$

e_d = Design eccentricity of the building

$$= 52.5 \text{ m (from eqn.(4.3))}$$

$$= 7.25 \text{ m (from eqn.(4.4))}$$

M = Torsional Moment on the building

$$= 108025 \text{ kN-m (using eqn.(4.3))}$$

$$= 14930 \text{ kN-m (using eqn.(4.4))}$$

Forces in various walls for the rectangular building are given in Table [4.8].

Wall No.	No. of panels	F_v kN	F_t (kN)		Force on wall		Max. Force on wall (kN)	Panel Force (kN)
			from eqn(4.3)	from eqn(4.4)	from eqn(4.3)	from eqn(4.4)		
(1)	(2)	(3)	(4)	(5)	(6) = (3)+(4)	(7) = (3)+(5)	(8)=max. of (6) & (7)	(9) = (8)/(2)
1	2	229	432	60	661	289	661	330.5
2	16	1829	-432	-60	1397	1769	1769	110.6
3	32	0	-1948	-269	-1948	-269	1948	60.8
4	32	0	1948	269	1948	269	1948	60.8

Table 4.8: Forces in various walls of a rectangular building, Fig. [4.1b], using stiffness method of design

The panel force (Table [4.8], Col (9)) for wall 1 is 330.5 kN. It would be difficult to design panels to resist this force. The panel force for walls 3 and 4 is much less than that for the other walls and if it is assumed that the panels in walls 3 and

4 have lower stiffnesses than those in walls 1 and 2, the situation becomes worse because in that case the stronger walls attract more force than given in Table [4.8], thus ending up with much higher strength requirement for the panels in wall 1. This would make the design even more difficult.

4.3 Strength Method

This method is based on the idea that when a building is resisting a severe earthquake the design should be based on the assumption that all the walls would yield. The location of the centre of rigidity of the building (C.R.) is therefore calculated from the yield strength of the walls.

$$e_r = L/2 - F_1/(F_1 + F_2) * L$$

where F_i = yield strength of wall i

and e_r = distance of the C.R. from the geometric centre
of the building

If walls 1 and 2 have similar panels, then the strength of these walls will be proportional to their number of panels. If it is assumed that mass is uniformly distributed, then the eccentricity e is

$$e = L/2 - N_1/(N_1 + N_2) * L$$

i.e. same as in the stiffness method, eqn. (4.5).

The square building, Fig. [4.1a] in section [4.2] has been redesigned using the strength method for calculating the forces in the walls. The calculations for the forces in various walls are given below :

From eqn.(4.5), eccentricity e is

$$\begin{aligned} e &= 38.4/2 - 2/(2 + 16) * 38.4 \text{ m} \\ &= 14.93 \text{ m} \end{aligned}$$

In this method, the centre of rigidity (C.R.) of the building is calculated from the strength of walls 1 and 2 thus the resultant force resisting motion in the direction of the E/Q, acts through the C.R. Therefore moment of forces in walls 1 and 2 about the C.R. is zero. The design moment must therefore be resisted entirely by walls 3 & 4. As before, the NBCC [22] equations (4.3) and (4.4) are used to calculate the design eccentricity. But as walls 1 and 2 do not contribute anything to the resistance of this torsional moment; eqn.(4.3) is the only equation that needs to be used in the calculation of the applied torsional moment because this moment is always greater than that from eqn.(4.4). Design eccentricity e_d from eqn.(4.3)

$$\begin{aligned}
 e_d &= 1.5 * e + 0.1 * L \quad \text{m} \\
 &= 1.5 * 14.93 + 0.1 * 38.4 \quad \text{m} \\
 &= 25.94 \quad \text{m}
 \end{aligned}$$

Design moment M is

$$\begin{aligned}
 M &= V * e_d \quad \text{kN-m} \\
 &= 1071 * 25.94 \quad \text{kN-m} \\
 &= 28124 \quad \text{kN-m}
 \end{aligned}$$

Walls 1 & 2 resist lateral force V while Walls 3 & 4 resist moment M .

Thus forces in various walls due to the lateral force V are :

$$\begin{aligned}
 F_{v_1} &= V * N_1 / (N_1 + N_2) \\
 &= 1071 * 2 / (2 + 16) \text{ kN} \\
 &= 119 \text{ kN} \\
 F_{v_2} &= V * N_2 / (N_1 + N_2) \\
 &= 1071 * 16 / (2 + 16) \text{ kN}
 \end{aligned}$$

$$= 952 \text{ kN}$$

$$F_{v_3} = 0 \text{ kN}$$

$$F_{v_4} = 0 \text{ kN}$$

Force on wall i due to torsional moment M is given by :

$$F_{t_1} = 0 \text{ kN}$$

$$F_{t_2} = 0 \text{ kN}$$

$$F_{t_3} = M/L$$

$$= -28124/38.4 \text{ kN}$$

$$= -732.8 \text{ kN}$$

$$F_{t_4} = -F_{t_3}$$

$$= +732.8 \text{ kN}$$

Forces in various walls, for E/Q acting in X-direction are given in Table [4.9]. All

Wall No.	No. of Panels	F_v (kN)	F_t (kN)	Max. Force on wall (kN)	Panel Force (kN)
(1)	(2)	(3)	(4)	(5) = (3)+(4)	(6) = (5)/(2)
1	2	119	0	119	59.5
2	16	952	0	952	59.5
3	16	0	-733	-733	45.8
4	16	0	733	733	45.8

Table 4.9: Forces in various walls of a Square Building, Fig. [4.1a], for E/Q acting in X-direction, using Strength Method of design

walls have to be checked for the E/Q acting in the other direction i.e in the direction of wall 3 or 4 (see Table [4.10]). The largest force in each panel will govern the design (Table [4.11]).

Wall No.	No. of Panels	F_v (kN)	F_t (kN)	Max. Force on wall (kN)	Panel Force (kN)
(1)	(2)	(3)	(4)	(5) = (3)+(4)	(6) = (5)/(2)
1	2	0	107	107	6.69
2	16	0	-107	-107	6.69
3	16	536	0	536	33.5
4	16	536	0	536	33.5

Table 4.10: Forces in various walls of a Square Building, Fig. [4.1a], for E/Q acting in Y-direction, using Strength Method of design

Wall No.	No. of panels	Maximum Wall Force kN	Maximum Panel Force kN
(1)	(2)	(3) = Max. of Col (8) in Tables 4.8 & 4.9	(4) = Max. of Col (9) in Tables 4.8 & 4.9
1	2	119	59.5
2	16	952	59.5
3	16	733	45.8
4	16	733	45.8

Table 4.11: Maximum Panel Forces governing the design of various walls in a Square Building, Fig. [4.1a], using Strength Method of design.

4.3.1 Shortcomings of the Strength Method

As explained in the above paragraph, with this method it was assumed that the walls in the direction of the earthquake do not take part in resisting the torsional moment. To resist the torsional moment, walls which are not parallel to the direction of the earthquake are needed. For the example given in section [4.2], the strength method cannot be used if there are no panels in walls 3 and 4; because then there are no walls to take the torsional moment.

Another shortcoming of this method may be the increased ductility demand in the weaker wall because the strength of the weaker wall designed by this method is less than that designed by the stiffness method. This may lead to an increase in the eccentricity if the walls tend to decrease in strength over several cycles above the yield level.

Chapter 5

Results of Dynamic Analysis

5.1 Effect of non-symmetry in the buildings

If the center of mass and center of resistance of a building do not coincide, a rotational couple will act on the building during an earthquake. It is not easy to develop a design method using equivalent static lateral forces that properly considers their effects. To study the adequacy or inadequacy of the code design, a number of dynamic analyses were made for different variables such as earthquake data, building geometry etc. (see Table [5.1]).

In each of the these cases, the panels in walls 2, 3 & 4 were not changed while the panels in wall 1 were varied from 0 to 16 i.e. moving from a highly unsymmetrical building with no panels in wall 1 to a symmetrical building with wall 1 & wall 2 having the same number of panels. All the panels were designed as cantilevers with dowel bars at the base acting as flexural steel. To reduce the time required for dynamic analysis, the panels were the same in every wall. All dowels in a given wall were the same, but different walls could have different dowels. In the static design, the dowels used were not limited to standard dowel sizes available in the industry, but it was assumed that any dowel area which would give adequate resisting force could be used, i.e. no wall had any surplus strength beyond that required in the design. For example say the required factored panel strength is 128.5 kN which can be provided by using two dowel connections each of area 888 mm^2 . If we used

Building	Design Method	E/Q	E/Q Direction	Static Design Eccentricity	Stiffness
Square	Stiffness Strength	El Centro	X	e_d	r_3 & r_4
	Strength	El Centro	X	e	r_3 & r_4
	Strength	El Centro San Fernando Taft	X	e_d	r_3 & r_4
Rectangular	Strength	El Centro	X Y	e_d	r_3 & r_4
	Strength	El Centro	X	$0.95e_d$ $0.85e_d$ $0.75e_d$ $0.65e_d$	r_3 & r_4
	Strength	El Centro	X	e_d	$0.5 r_3$ & $0.5 r_4$ $0.2 r_3$ & $0.2 r_4$

Note :- r_3 & r_4 are the stiffnesses of walls 3 & 4 respectively, derived from the panel connections required in the static design with assumption that the stiffness of each wall is proportional to the number of panels in the wall.

Note :- Dynamic analysis has always been done using the actual eccentricity of the building.

Table 5.1: List of the dynamic analyses made in this studies

dowels that are available in market then we would have to use a dowel of area of 1000 mm^2 which would increase the panel strength as well as the wall strength beyond that required by design. As a consequence we would not be able to check the adequacy of the static design.

5.2 Structural Data

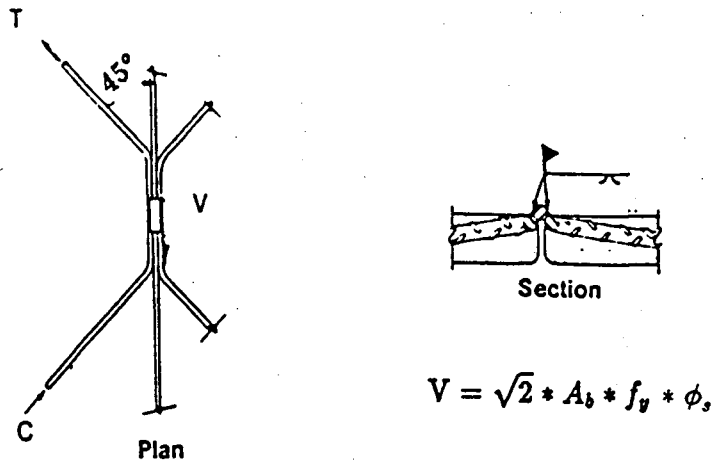
The two buildings used in these studies are shown in Fig. [4.1]. Building and panel dimensions are given in section [4.1] and the properties of the connections used in the studies are discussed below. See Appendix A for the time periods of the square and rectangular buildings designed by the strength method using NBCC design eccentricity.

Panel to Panel Connections :-

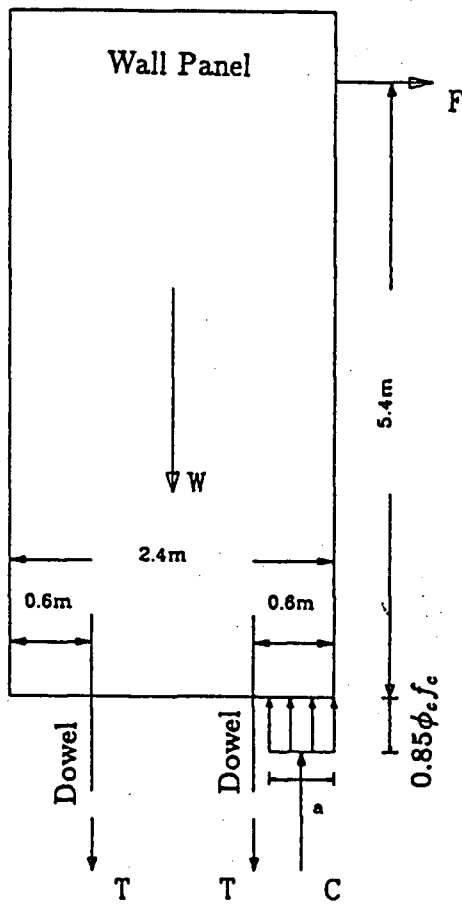
In the design of the buildings, it was assumed that there are no vertical connections between the wall panels because in the initial runs it was found that the dowel connections are more effective in taking the lateral shear force than the vertical connections. However both the computer program for the dynamic analysis and the static design program in LOTUS - 123 has the capability of including panel to panel connection data. The static design program has been written to consider connections which use embedded rebars, as shown in Fig. [5.1a].

Panel to Foundation Connections :-

These connections consist of two dowels, one embedded in each stem as shown in Fig. [5.1b]. As explained in section [5.1], dowels used in the design are not limited to those available in the market, but may have any area. Initial stiffness of the dowels was based on the study done by Hawkins & Lin [15] who found that the displacement at the loaded end of the embedded bars under axial loads was 1.066 mm



(a) Panel to Panel Connection



(b) Dowel Connection

Figure 5.1: Panel Connections

at the onset of yielding for all the cases. Thus for the present studies it is assumed that all dowel connections have 1.066 mm displacement at yield point regardless of dowel size i.e. for any dowel of area A_s :

$$\text{Yield force } F_y = 1.25 f_y * A_s \quad N$$

$$\text{Stiffness } k_{dow} = F_y / (1.066 * 10^{-3}) \quad N/m$$

where $1.25 f_y$ is the probable strength of the steel.

After yielding the load deflection curve is parallel to the deflection axis.

Foundation Springs :-

The foundation underneath the panel is modelled by two linear elastic springs. The stiffness of the foundation is found from the equation $k = (A * E_c) / L$ where A is the bearing area of the flange of the panel on the foundation, E_c is the modulus of elasticity of concrete and L is the depth of the foundation equal to 1000 mm. The approximate value of k used in the studies is $6.0 * 10^9$ N/m.

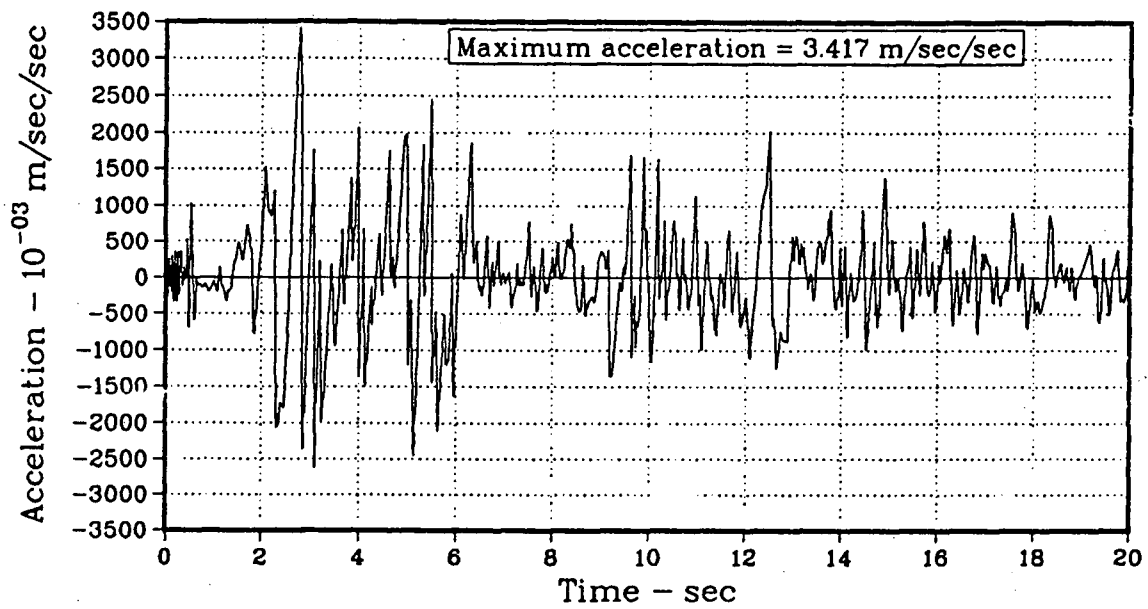
Damping :-

In all the computer runs, viscous damping of approximately 1% of critical damping has been used.

Earthquake Records :-

Three earthquakes have been used for these studies; El Centro - S00E 1940, San Fernando - S62E recorded at 2011 Zonal Ave. and Taft - N21E. Time vs. ground acceleration plots for first 20 seconds of these earthquakes are shown in Fig. [5.2a...c]. The El Centro E/Q has a peak acceleration of $3.417m/sec^2$ (0.35g) which is quite close to 0.32g, the acceleration requirement for zone 5 from Ref. [35]. Ground accelerations of the other two earthquakes were linearly scaled so as to have a peak acceleration of $3.417m/sec^2$.

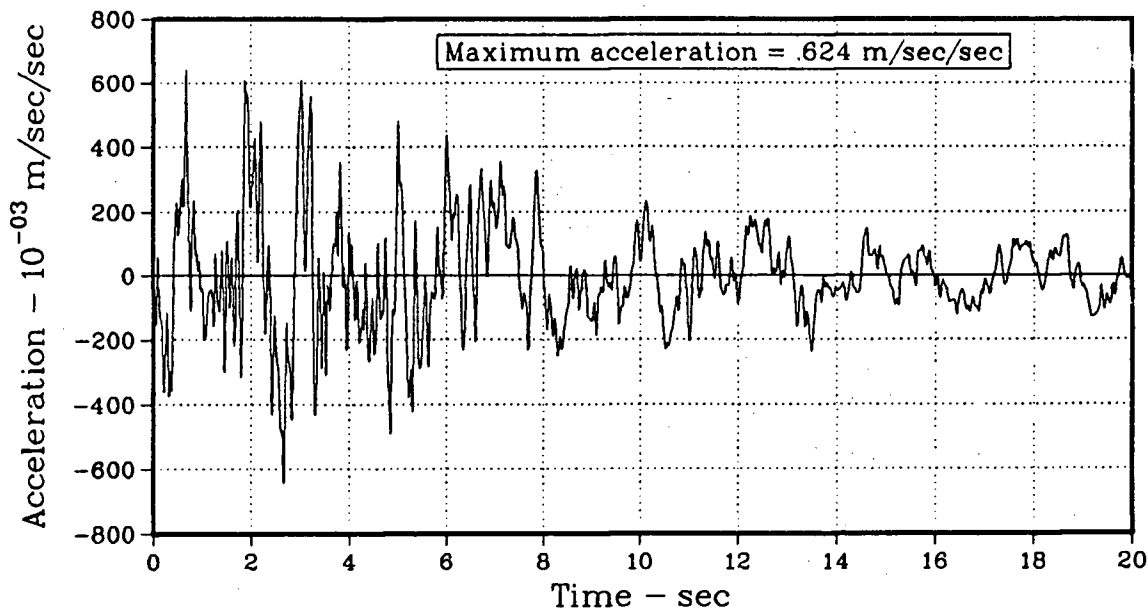
GROUND ACCELERATION for ELCENTRO - 1940 E/Q



(a) Accelerogram for the El Centro E/Q

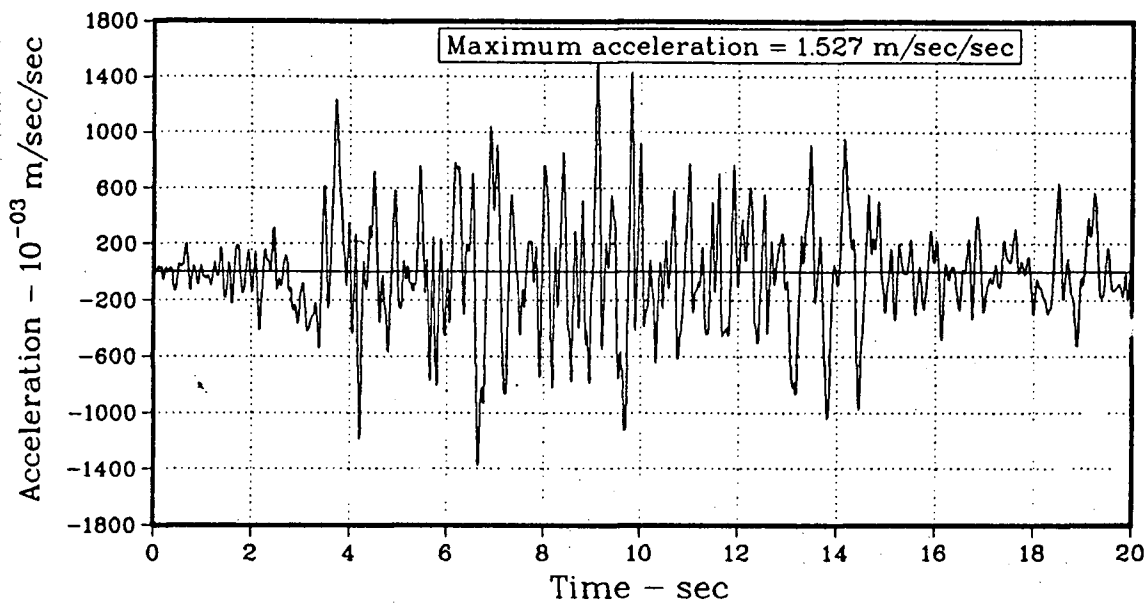
Figure 5.2: Earthquake Accelerograms used in the present studies

GROUND ACCELERATION for SANFERNANDO - S62E E/Q



(b) Accelerogram for the San Fernando E/Q

GROUND ACCELERATION for TAFT E/Q



(c) Accelerogram for the Taft E/Q

Fig. 5.2: Continued

Both El Centro & Taft have ratios of acceleration to velocity (a/v - units m/sec) approximately equal to 1, while San Fernando has a/v equal to 0.48.

5.3 Discussion of Results

The results have been divided into the following subsections to discuss the effects of various parameters involved. (Note that dynamic analysis has always been done using the actual eccentricity of the building).

- Effect of different methods of static design.
- Effect of different E/Q data in the dynamic analysis.
- Effect of the geomtry of the building.
- E/Q direction
- Effect of change in the design eccentricity of the buildings in the static design (to calculate the torsional moment) with dynamic analysis done using actual eccentricity of the buildings.
- Effect of the variation of stiffnesses of walls 3 & 4.

5.3.1 Effect of different methods of static design

As explained earlier in section [4.1], two methods, a strength method and a stiffness method, have been used in the static design of the buildings shown in Fig. [4.1]. To enable one to measure the effect of the two methods of design, Strength ratios (SR) and Moment ratios (MR) are defined which relate the actual design strength of the walls to certain forces required from the static design. These ratios are defined to be, with reference to Fig. [5.3] :

$$\text{Strength Ratio SR} = \frac{\text{Strength of the walls in the X-direction}}{\text{Code recommended lateral force (factored)}}$$

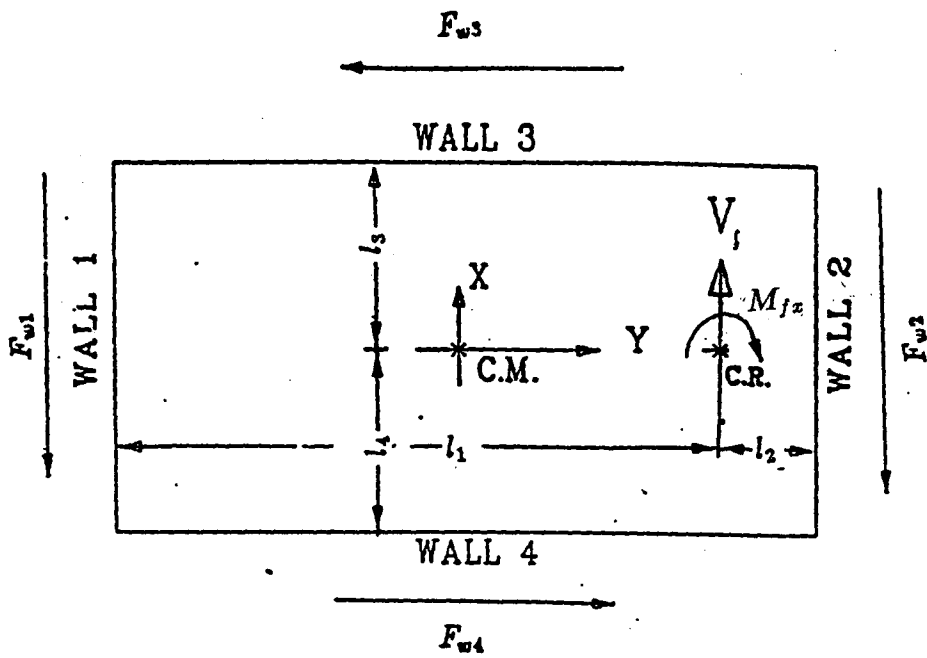


Figure 5.3: Resisting forces on the building

$$= \frac{F_{w1} + F_{w2}}{V_f}$$

$$\begin{aligned} \text{Moment Ratio MR} &= \frac{\text{Moment Strength of walls for the E/Q in X-dir.}}{\text{Larger moment used for the design in the X-dir. (factored)}} \\ &= \frac{F_{w1} * l_1 - F_{w2} * l_2 + F_{w3} * l_3 + F_{w4} * l_4}{M_{fx}} \end{aligned}$$

The wall strengths are calculated from considering the earthquake requirements in both the X and Y directions, and thus the strengths may be larger than required if only the X direction was considered.

Considering the SR the wall strengths F_{w1} and F_{w2} are not affected by the earthquake in the Y direction, and thus for the strength method of design SR is equal to one for all cases. For the stiffness method of design, part of the wall strength is used to resist torsion, and thus in most cases the lateral strength exceeds the lateral force and so SR is greater than 1.

The MR considers the torsional capacity of the walls at the same time as the X direction V_f is resisted, that is, it is not the pure torsional capacity of the walls. This is why the forces F_{w1} and F_{w2} are shown in the same direction in Fig. [5.3]. For most cases considered the F_{w3} and F_{w4} capacities are governed by the earthquake capacities in the Y direction and for these cases the MR will be greater than unity.

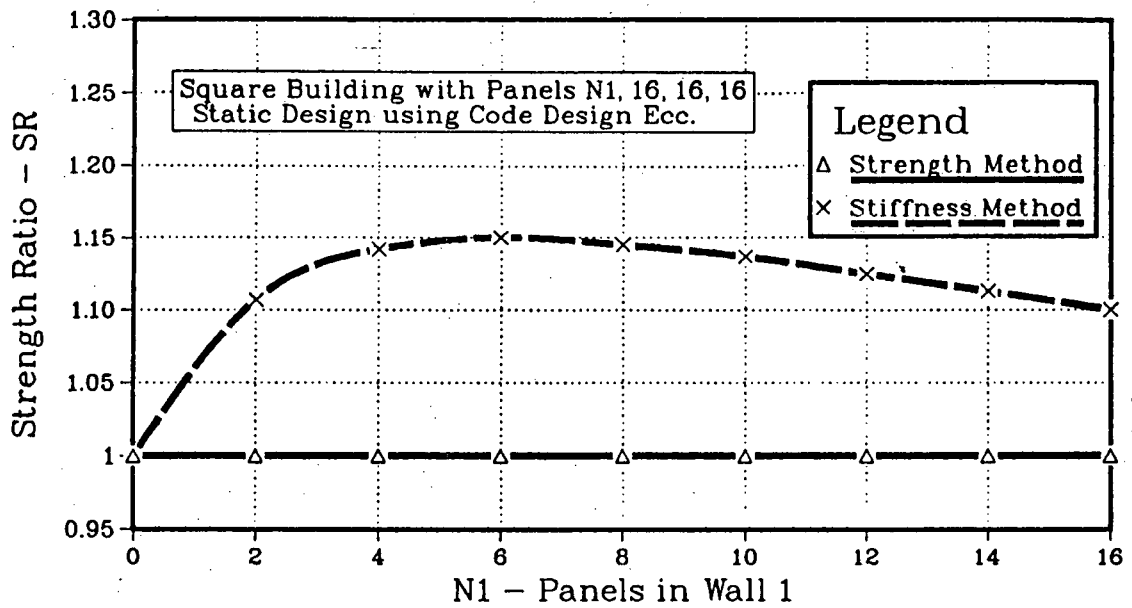
It will be shown that displacement of the C.M. tends to fall as the SR increases, and rotation θ tends to fall as the MR increases. It will also be shown that buildings designed by the stiffness method generally have higher SR and MR than the same building designed by the strength method

The strength ratio SR and moment ratio MR for the square building (Fig. [4.1a]) with varying degrees of eccentricity, are shown in Figs.[5.4a..b]. To investigate the

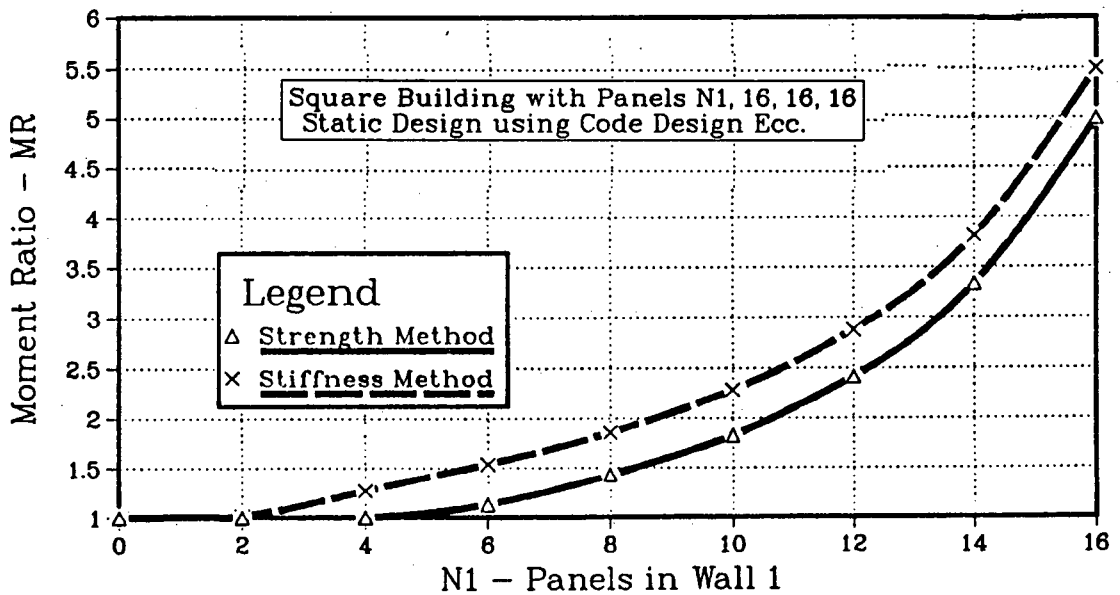
effect of different methods on the response of the buildings, the buildings were subjected to the El Centro earthquake. Comparison of various variables e.g. building displacement x at C.M., rotation θ etc. obtained from the dynamic analysis have been shown in Fig. [5.4 c...l]. The static design results show that the stiffness method is more conservative than the strength method for all the eccentricities except when the number of panels in wall 1 is 0 (i.e. N_1), for which two methods give the same results.

Dynamic analysis results confirm that the stiffness method is conservative. Fig [5.4c] shows the variation of building displacement at C.M. as N_1 (the number of panels in wall 1) is varied from 0 to 16. Both design methods give similar results for $N_1 = 0$. Then for the stiffness method, displacement decreases as N_1 is increased. The average value of this displacement at C.M. for the strength method is slightly higher than for the stiffness method as N_1 is varied from 0 to 16. The reason for this is the high strength of walls in the direction of the earthquake with the stiffness method approach (see Fig [5.4a]). The maximum difference in the building displacement at C.M. for the two methods is 25% which is obtained at $N_1 = 4$ when the wall designed by the stiffness method had extra strength of 15% in X direction as compared to that for strength method Fig [5.4a].

Variation of rotation θ for the two methods is shown in Fig. [5.4d]. Curves for both the methods are similar except that the strength method gives slightly higher results than stiffness method which is predictable because the moment ratio, Fig. [5.4b], for the former is lower. The maximum value of θ for all buildings is $0.28 * 10^{-3}$ rad. which is very small and can be easily accomodated. The decrease in rotation as N_1 increases is related to the moment ratio. As long as the moment ratio is equal to 1 there is only a small change in θ with increase in N_1 showing that static design methods give reasonable results as the eccentricity varies. And as moment ratio starts increasing, the extra strength in walls 3 & 4 causes θ to

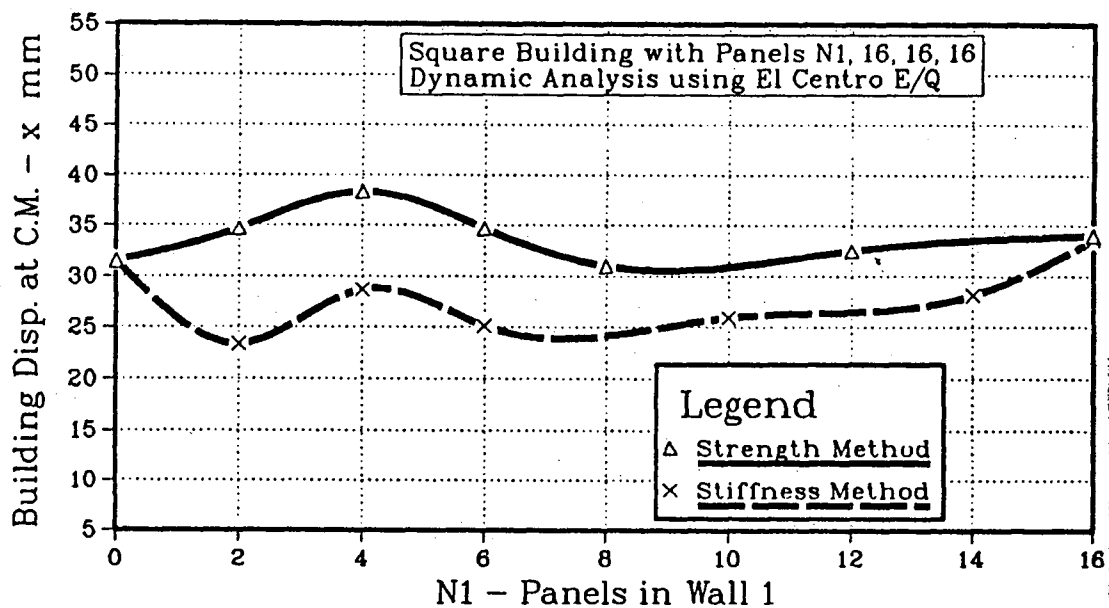


(a) Strength Ratio

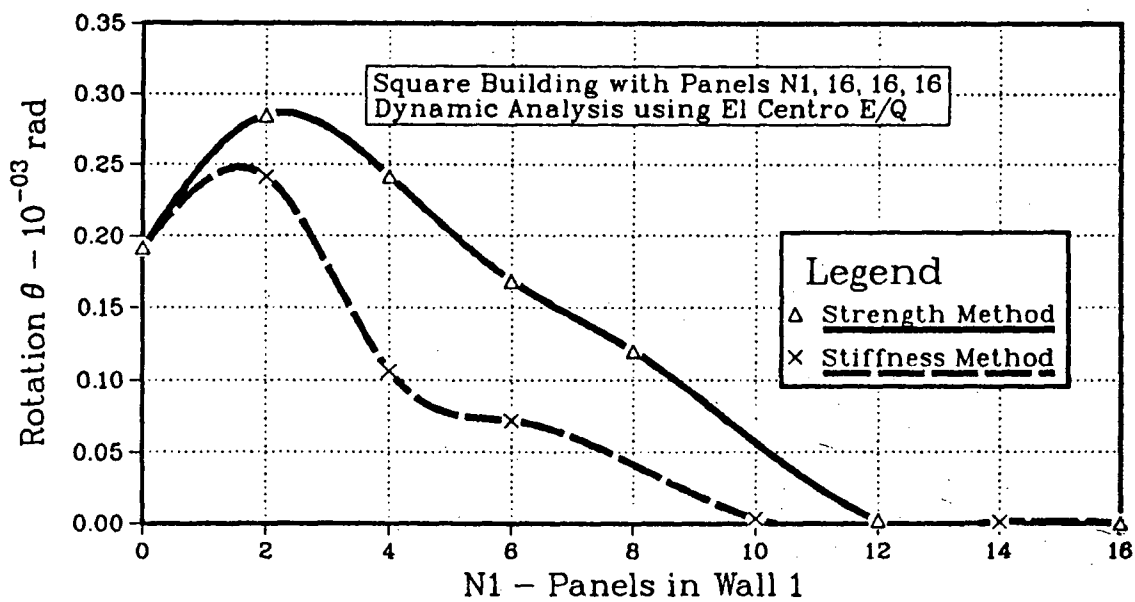


(b) Moment Ratio

Figure 5.4: Comparison of static & dynamic analysis results of a square building designed by the strength and stiffness methods

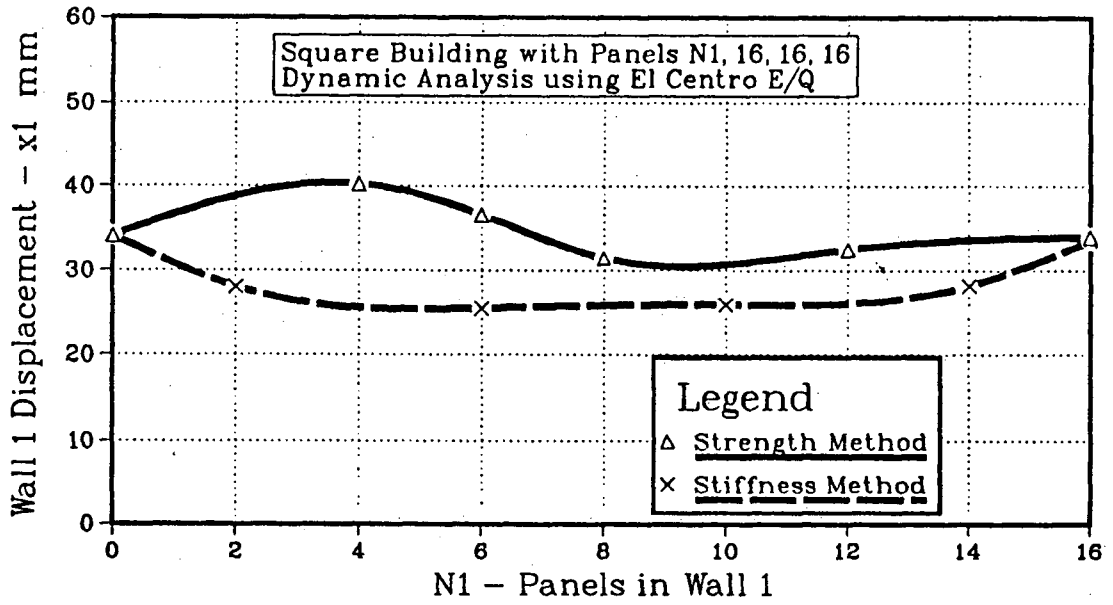


(c) Building Displacement at C.M.

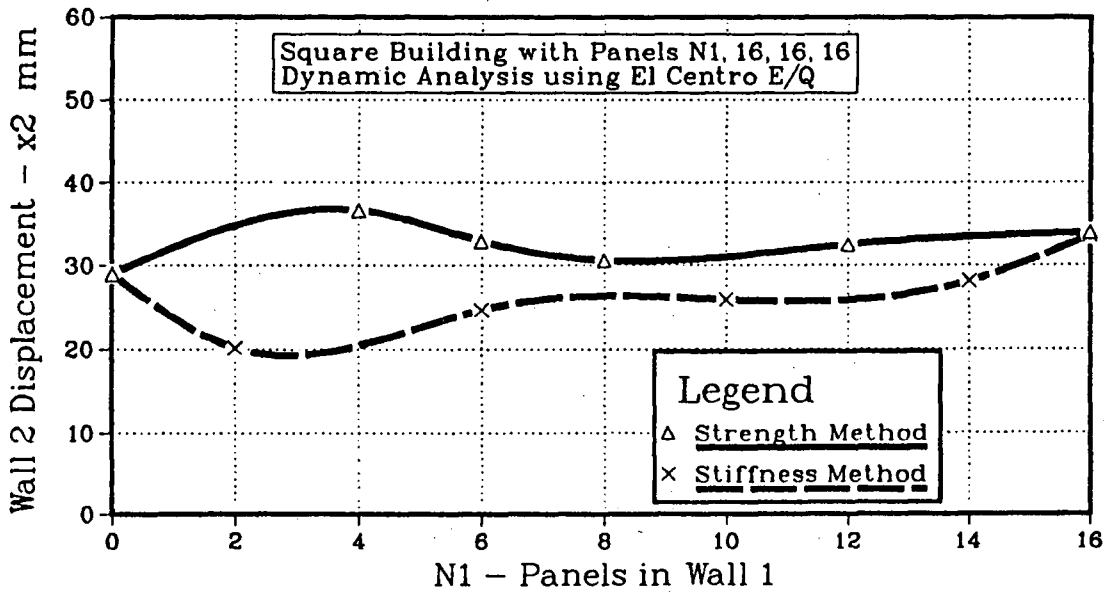


(d) Rotation θ

Fig. 5.4: Continued

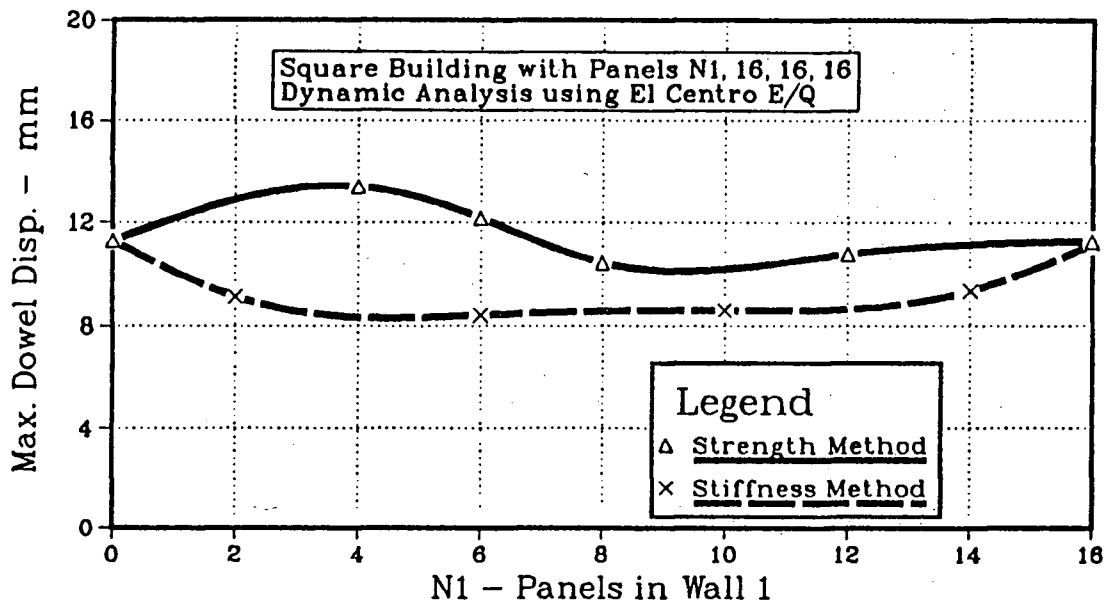


(e) Wall 1 Displacement

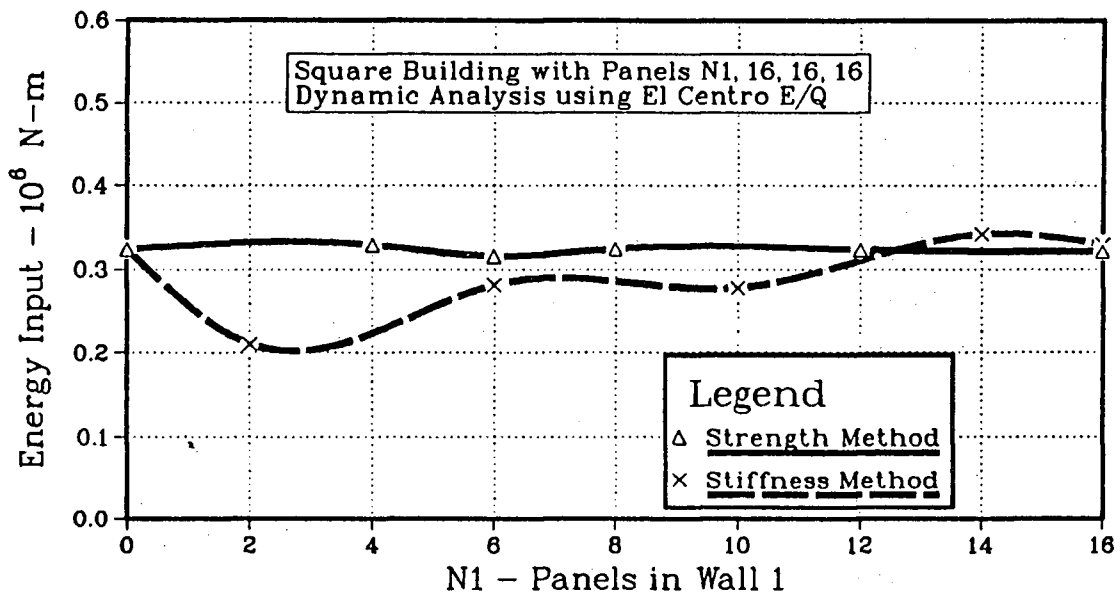


(f) Wall 2 Displacement

Fig. 5.4: Continued

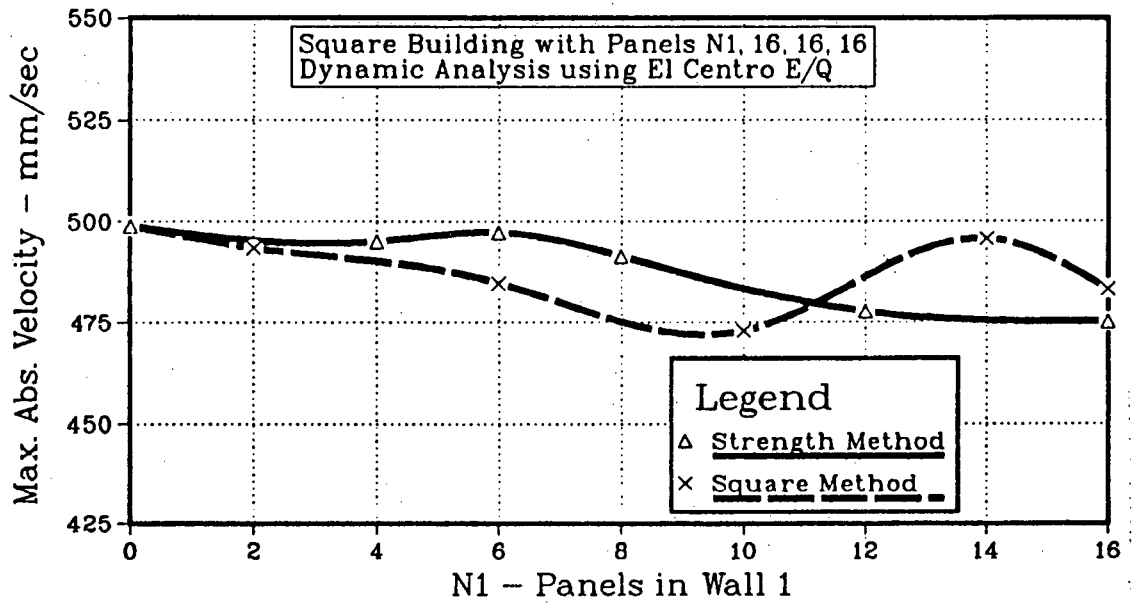


(g) Max. Dowel Displacement

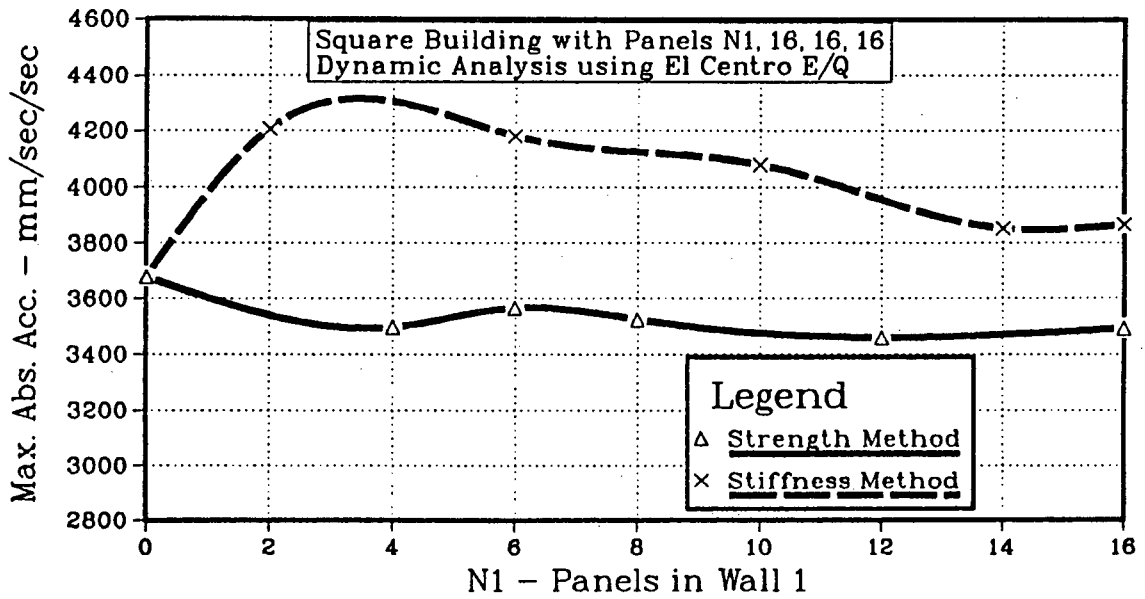


(h) Energy Input

Fig. 5.4: Continued

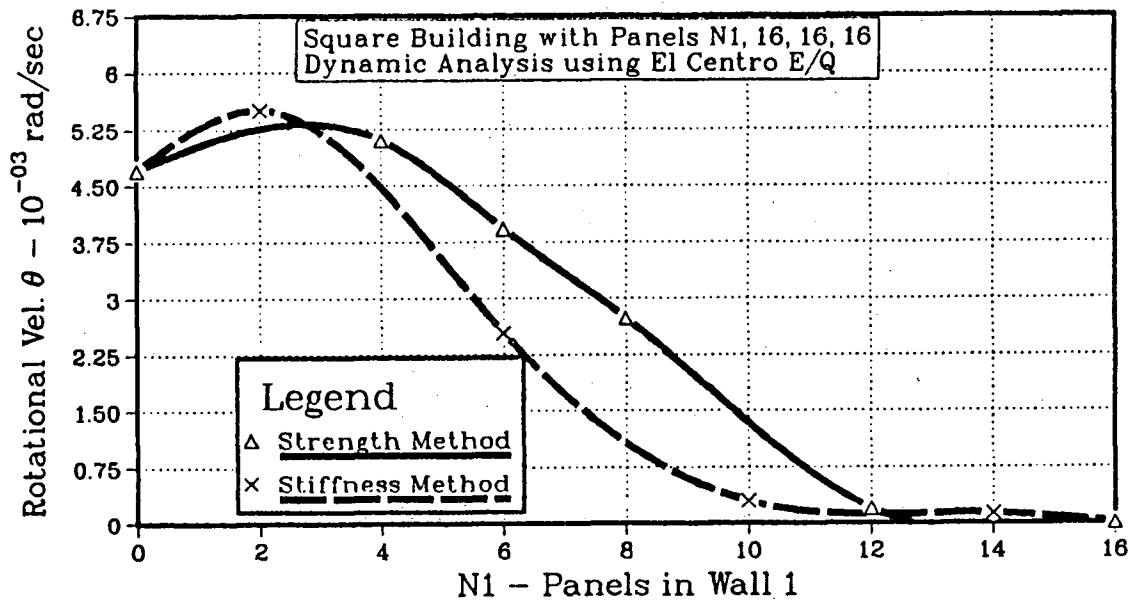


(i) Max. Absolute Velocity

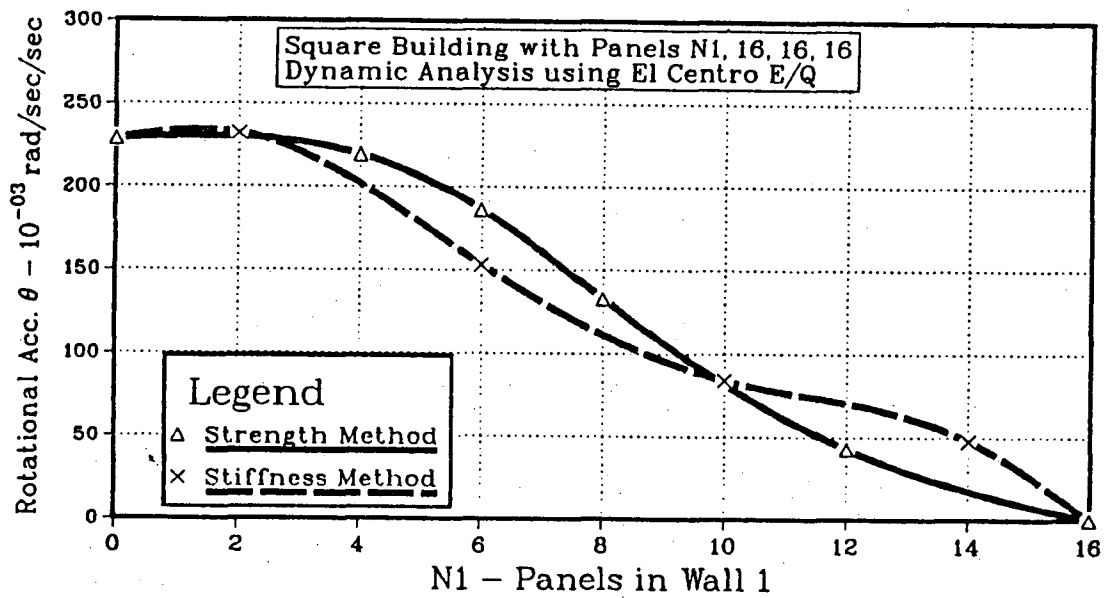


(j) Max. Absolute Acceleration

Fig. 5.4: Continued



(k) Max. Absolute Rotational Velocity



(l) Max. Absolute Rotational Acceleration

Fig. 5.4: Continued

decrease sharply.

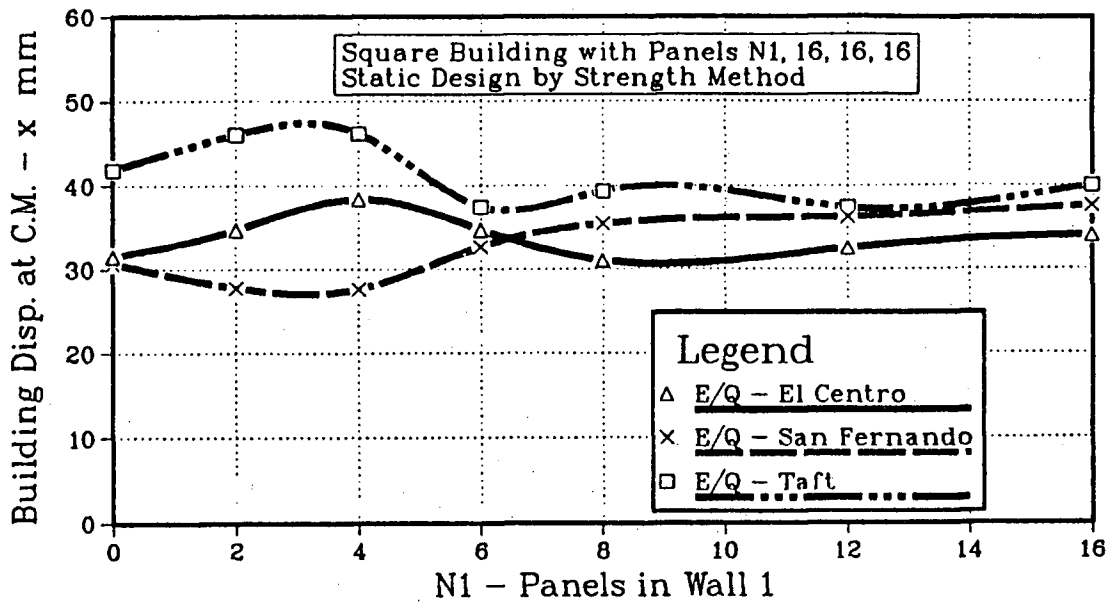
Curves for displacements of wall 1, wall 2 are similar to building displacement confirming that the rotation θ is small and has only a slight effect on the wall displacements. Maximum dowel displacement is 13mm which is well within the capability of the dowel connections. Other variables such as energy input E_{inp} , maximum velocity \dot{x} , maximum rotational velocity $\dot{\theta}$, and maximum rotational acceleration $\ddot{\theta}$ are similar for both the methods, but maximum acceleration \ddot{x} is quite different for the two methods. This can be explained by the fact that the stiffness method results in stronger walls and hence in higher forces and accelerations.

5.3.2 Effect of different E/Q data on the dynamic analysis

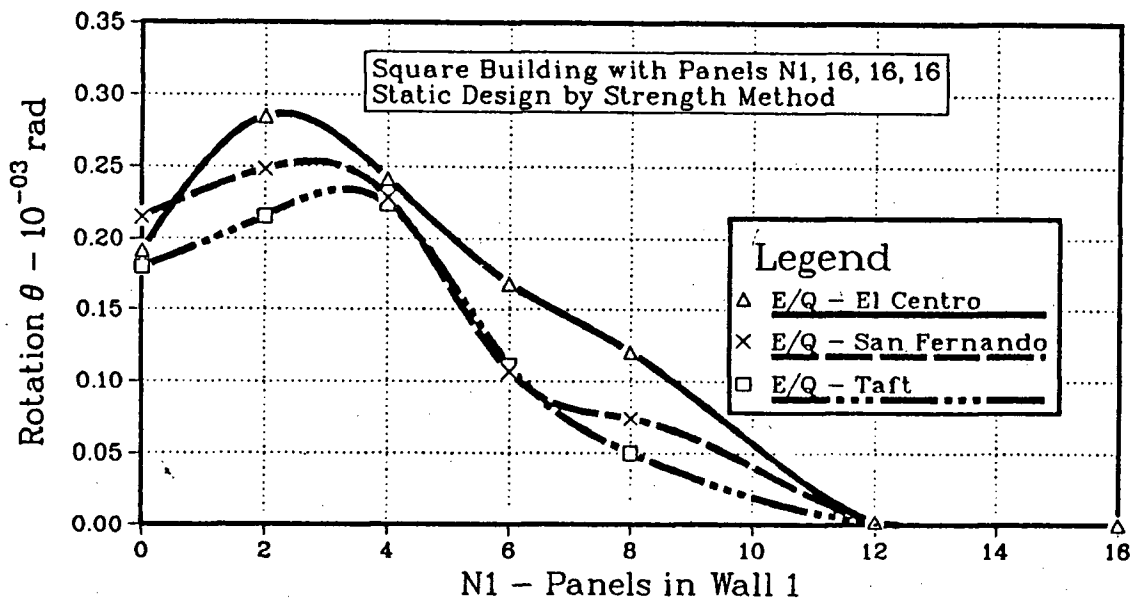
In this section dynamic analysis results for a square building Fig [4.1a], designed by the strength method, using ground acceleration data for the three earthquakes, El Centro [5.2a], San Fernando [5.2b] & Taft [5.2c], are discussed and shown in Figs. [5.5a...j].

The building displacement at the C.M. (x) is quite similar for all the three earthquakes. For each earthquake the value of x does not vary significantly as N_1 increases from 0 to 16. Curves for rotation θ for the three earthquakes are very close with the maximum value being $0.28 * 10^{-3}$ rad. which is very small. Curves for displacement of wall 1, wall 2 and maximum dowel displacement are similar to building displacement thus confirming that the small rotations have only a small effect on the wall displacement.

Curves for maximum acceleration \ddot{x} , maximum rotational velocity $\dot{\theta}$ and maximum rotational acceleration $\ddot{\theta}$ are also similar for these earthquakes. Maximum velocity \dot{x} is similar for the El Centro & the Taft earthquakes while for the San Fernando earthquake it is almost double. This is because the $\frac{a}{g}$ ratios for El Centro and Taft earthquakes are approximately equal to 1 while for the San Fernando earth-

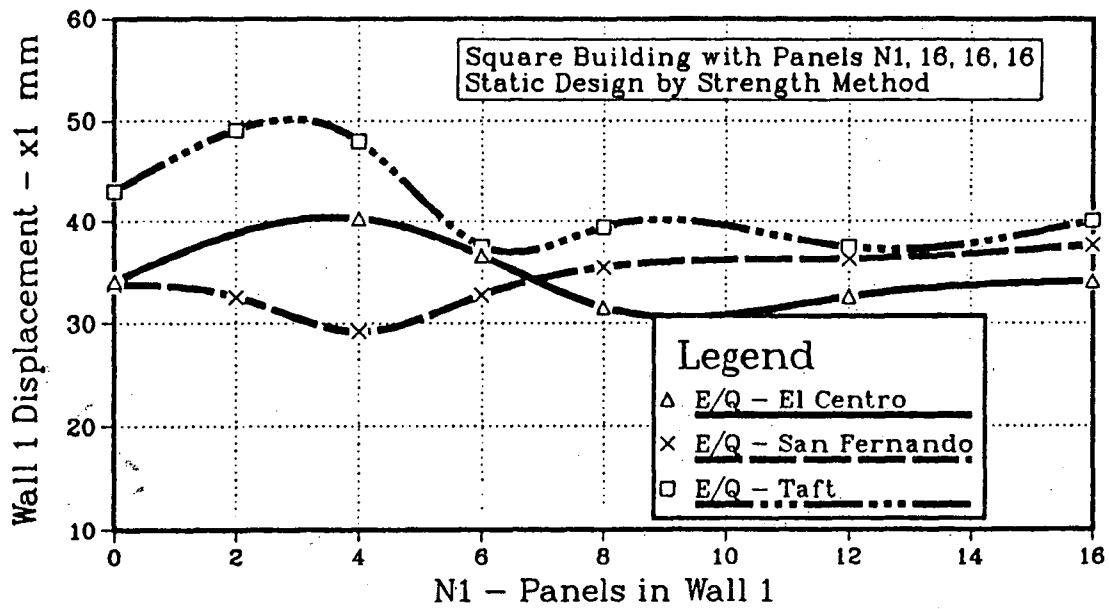


(a) Building Displacement at C.M.

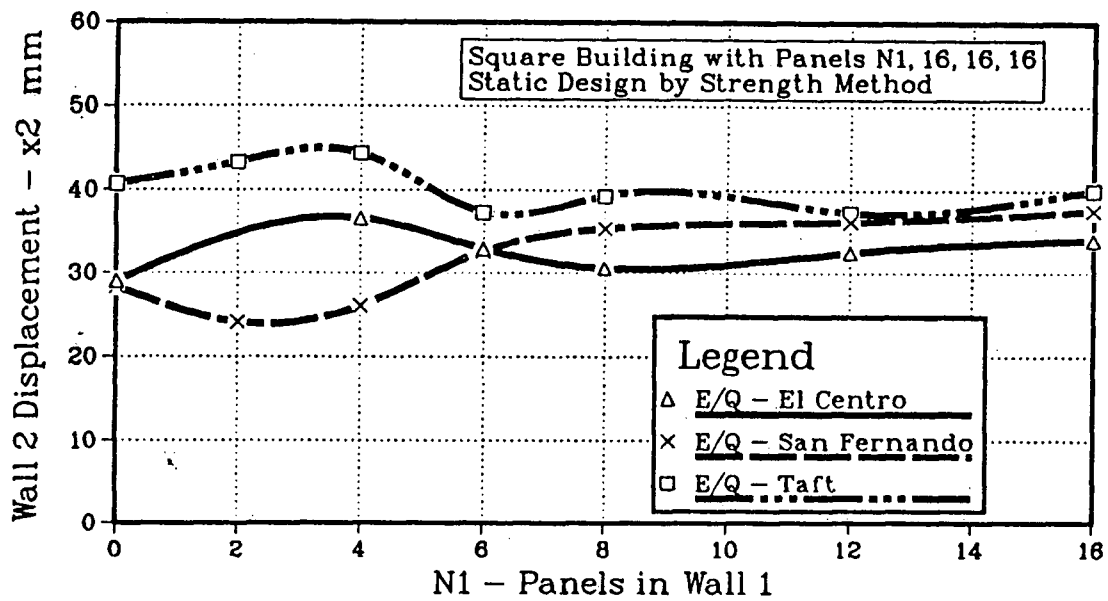


(b) Rotation θ

Figure 5.5: Comparison of dynamic analysis results of a square building using different earthquake accelerograms for dynamic analysis

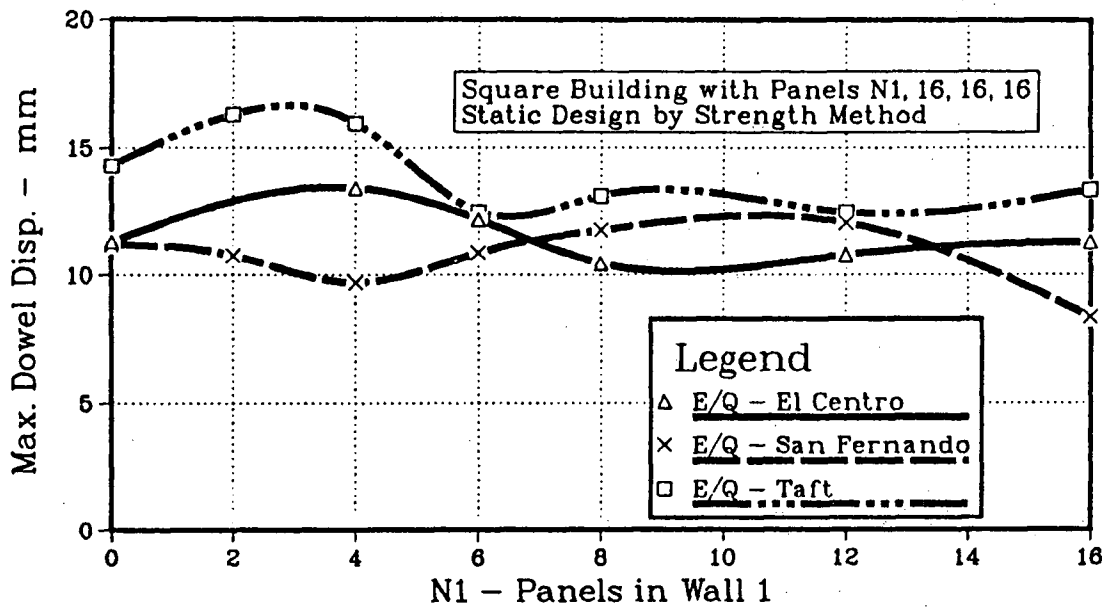


(c) Wall 1 Displacement

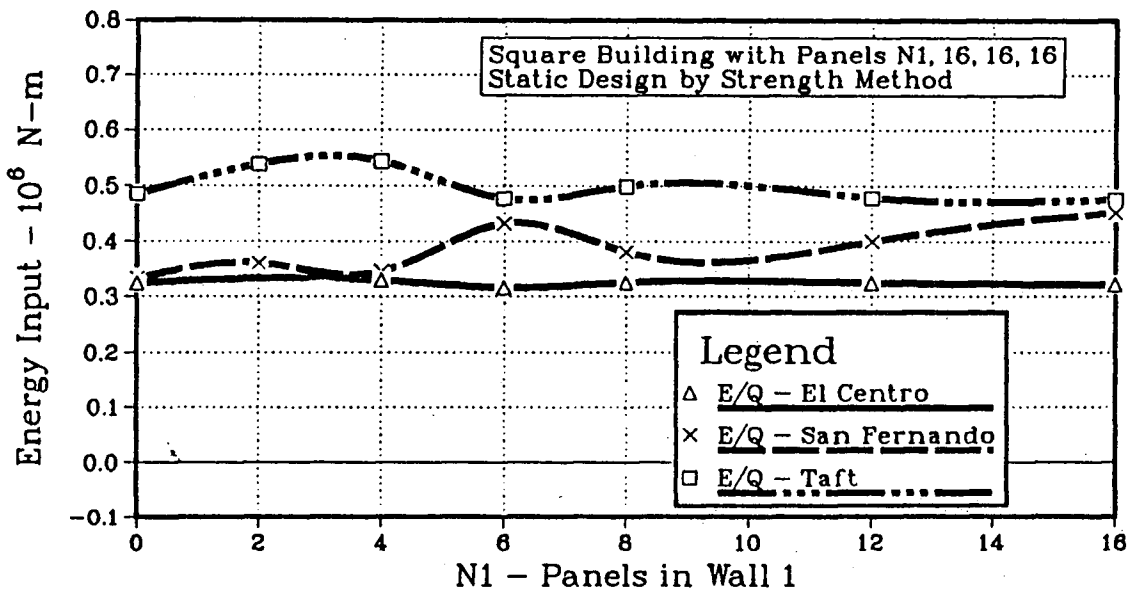


(d) Wall 2 Displacement

Fig. 5.5: Continued

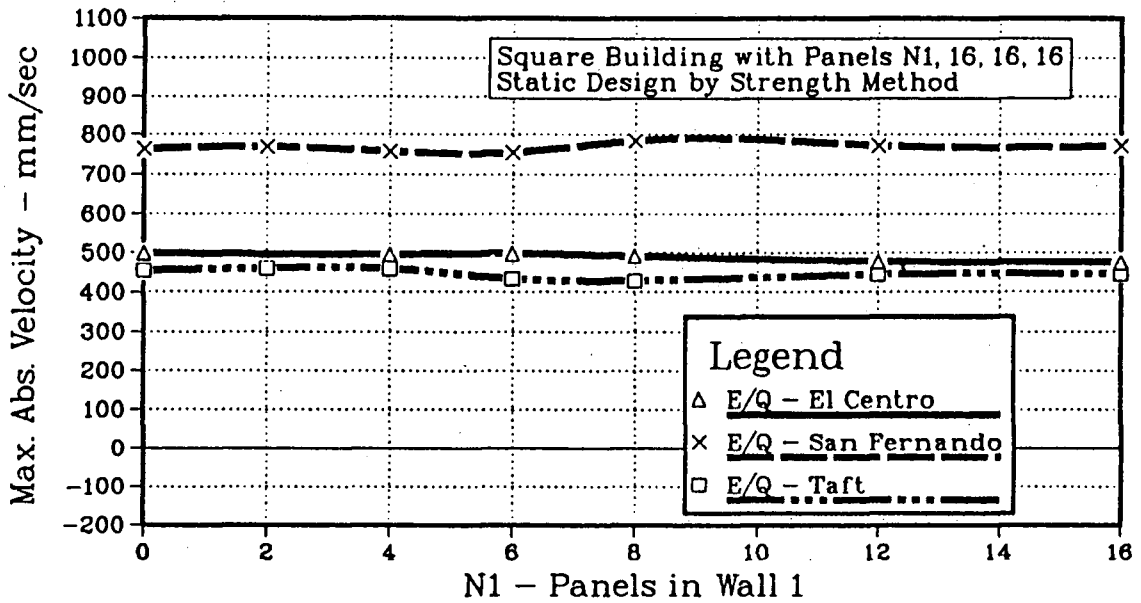


(e) Max. Dowel Displacement

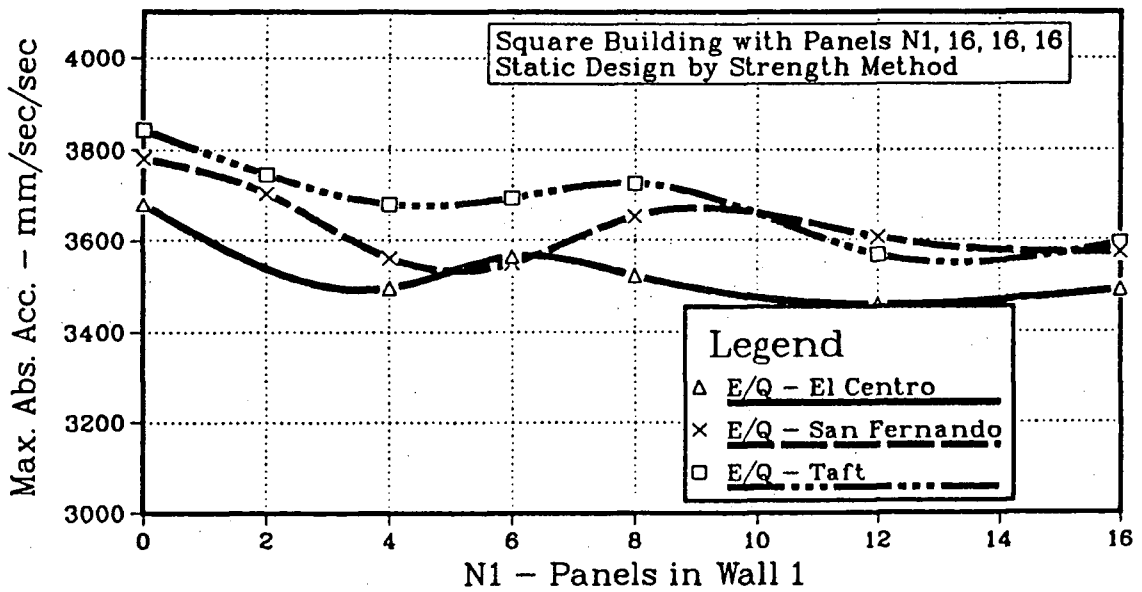


(f) Energy Input

Fig. 5.5: Continued

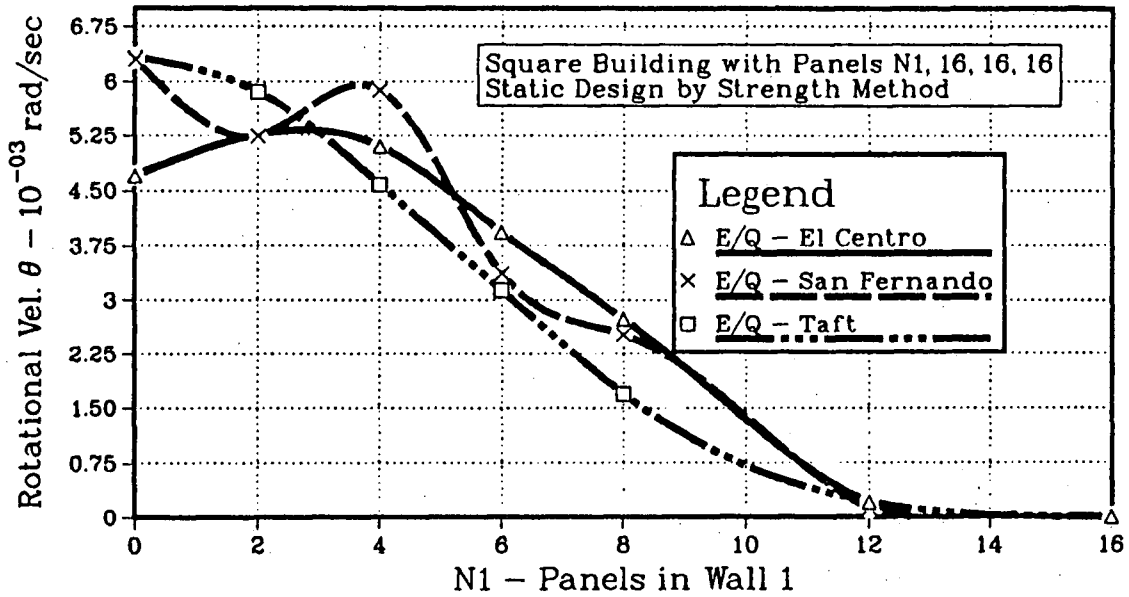


(g) Max. Absolute Velocity

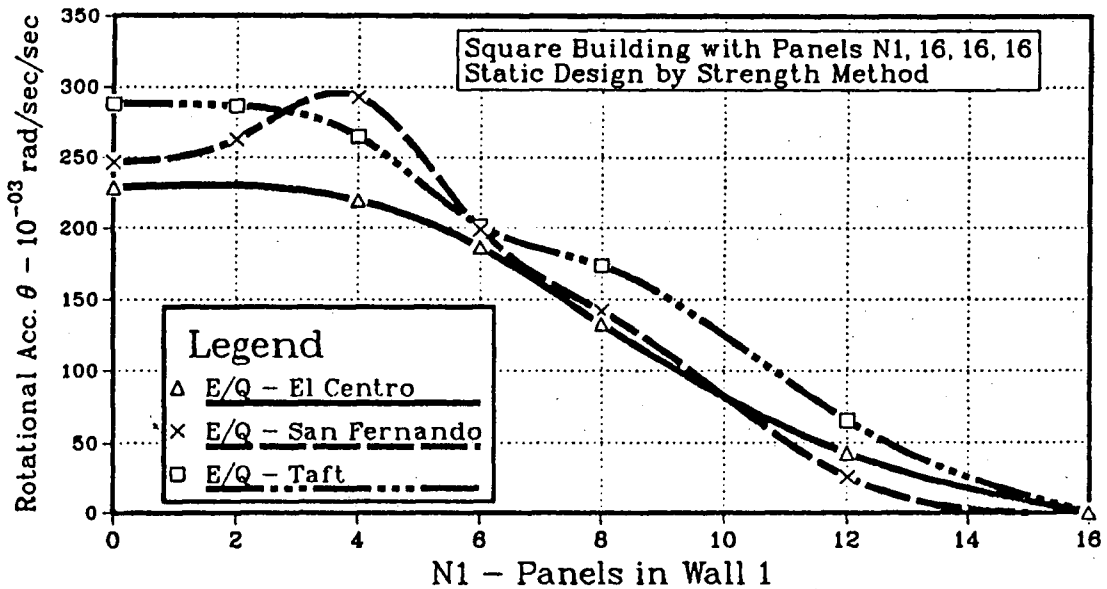


(h) Max. Absolute Acceleration

Fig. 5.5: Continued



(i) Max. Absolute Rotational Velocity



(j) Max. Absolute Rotational Acceleration

Fig. 5.5: Continued

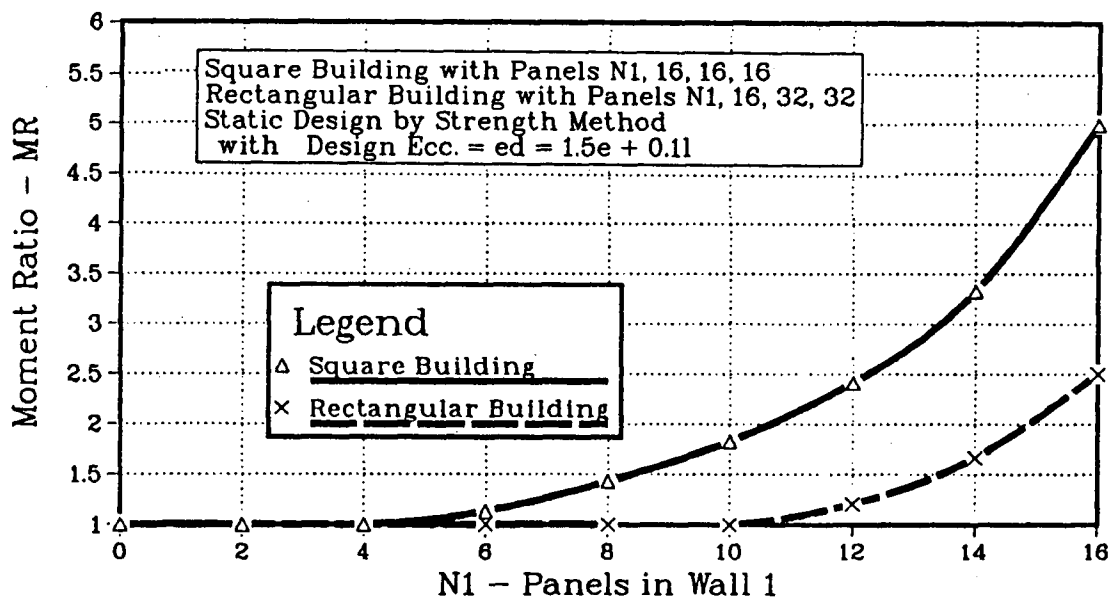
quake this ratio is 0.48. As the acceleration (a) for all the earthquakes was made same for the dynamic analyses, the velocity (v) for the San Fernando earthquake is almost doubled.

5.3.3 Effect of geometry of the building

In this section dynamic analysis results for a square building Fig. [4.1a] and a rectangular building Fig. [4.1b], statically designed by the strength method, are compared. The moment ratio (MR) is shown in Fig. [5.6a]. The El Centro earthquake acting in the X direction has been used in the dynamic analysis. Results for the two buildings are shown in Fig. [5.6b...k].

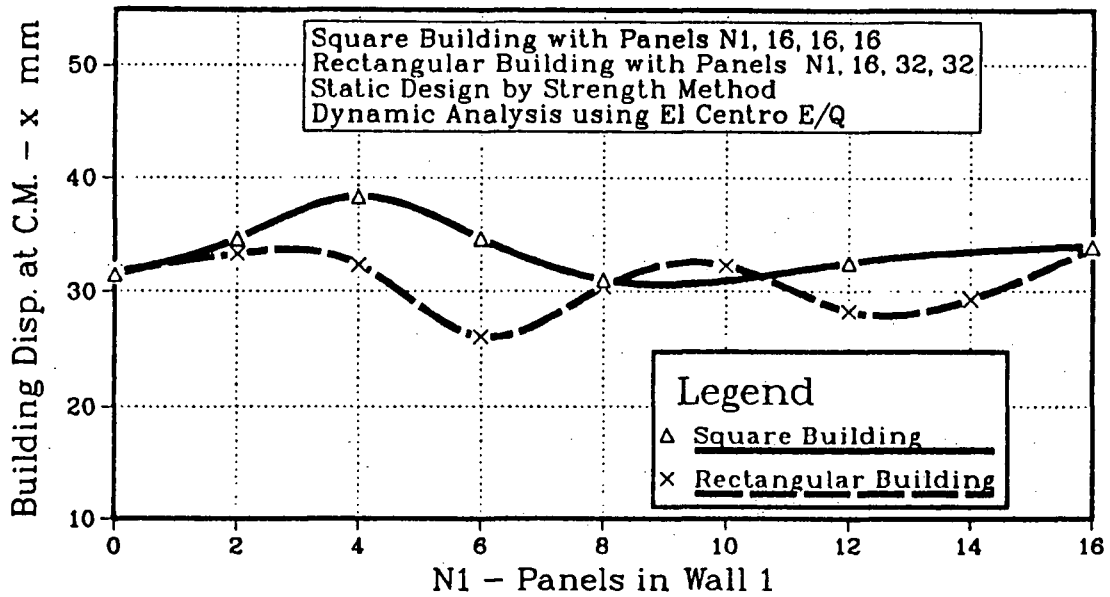
Building displacement at the C.M. (x) for the two buildings is shown in Fig. [5.6b]. The maximum difference for the two buildings is about 15%. If for each building an average value of displacement x is taken as N_1 varies from 0 to 16, then two buildings will have very close average displacement values showing that geometry of the building has very little effect on the building displacement at the C.M.

Variation of rotation θ is shown in Fig. [5.6c], which shows that the value of θ for the square building decreases very sharply for $N_1 > 2$ while θ for the rectangular building does not decrease until $N_1 > 10$, and after that it decreases sharply. This phenomenon can be explained from Fig. [5.6a], which shows that the moment ratio MR for the square building starts increasing from unity for $N_1 > 4$ while for the rectangular building MR does not increase until $N_1 > 10$. For MR values near 1 the rotation varies around $0.25 * 10^{-3}$ radians. It is interesting to note that when MR reaches 2.5, the rotation essentially vanishes. This again shows that the code equation for calculating the design moment is adequate for a wide range of eccentricities and for different geometries. Displacements of wall 1, wall 2 & maximum dowel displacements for the two buildings are quite close to each other and

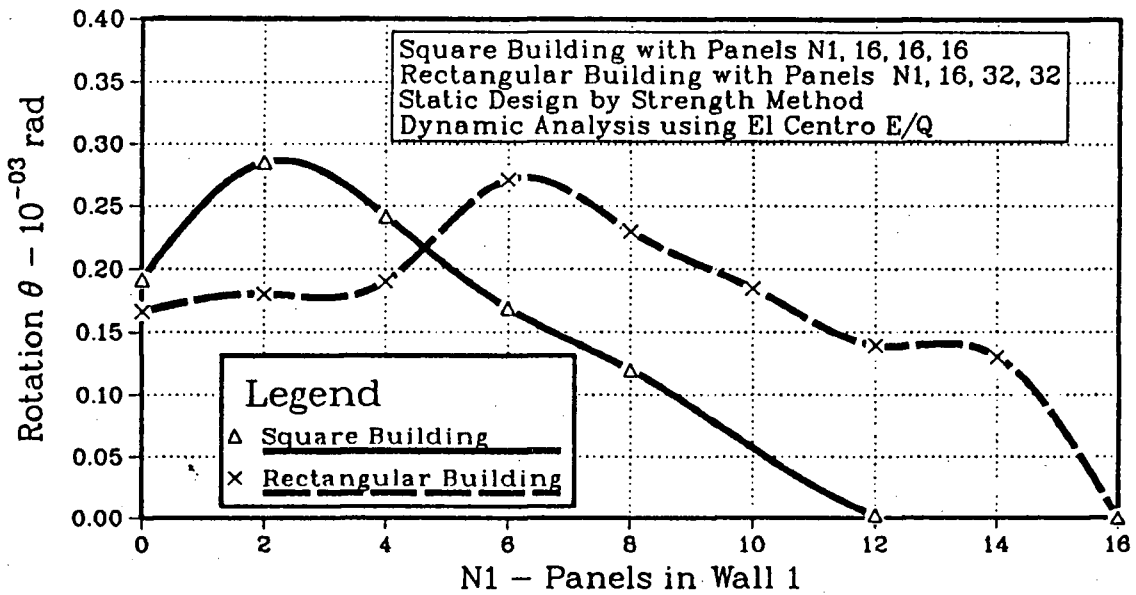


(a) Moment Ratio

Figure 5.6: Comparison of static & dynamic analysis results for square and rectangular buildings using NBCC recommended equivalent static design approach with strength method of design

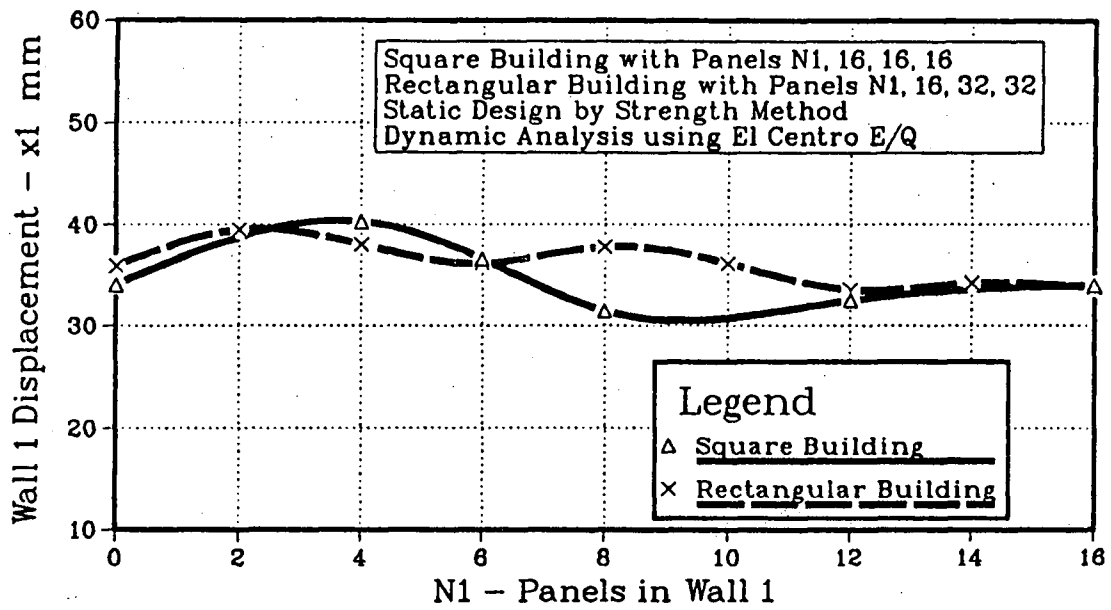


(b) Building Displacement at C.M.

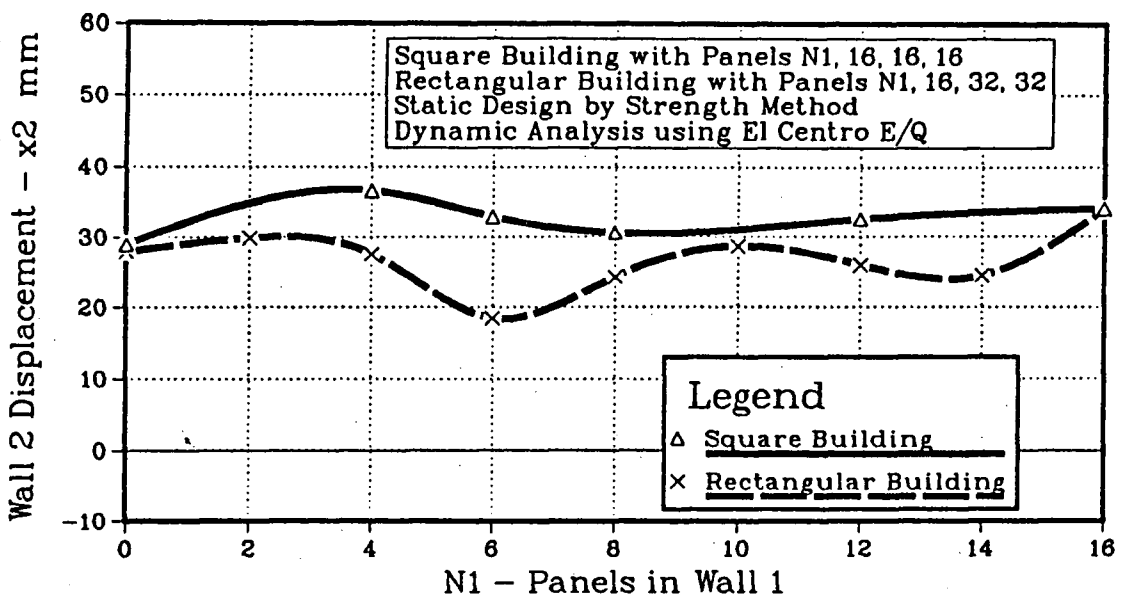


(c) Rotation θ

Fig. 5.6: Continued

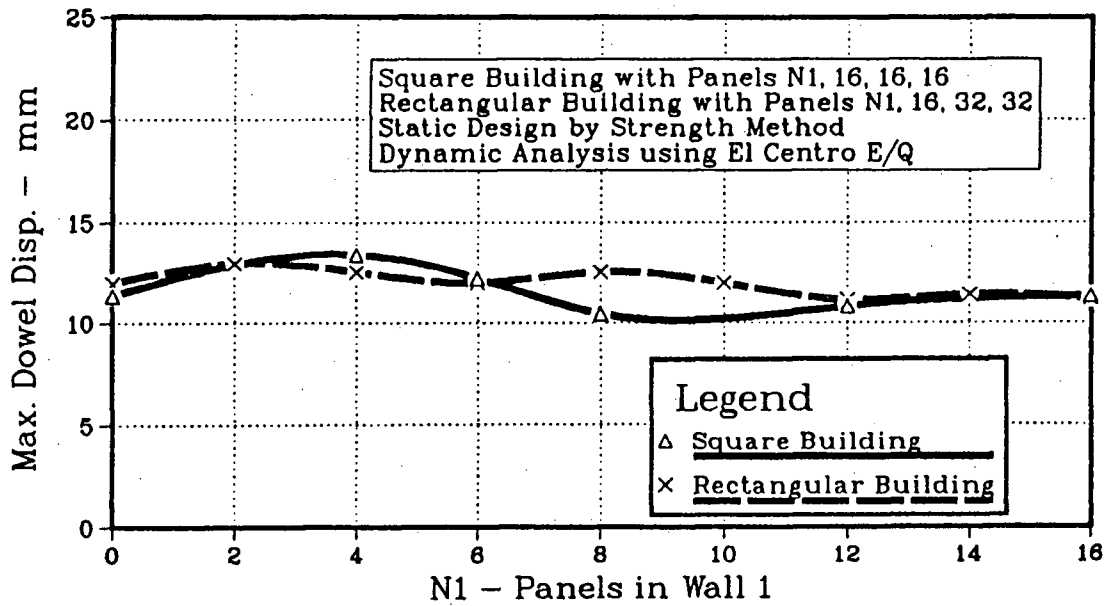


(d) Wall 1 Displacement

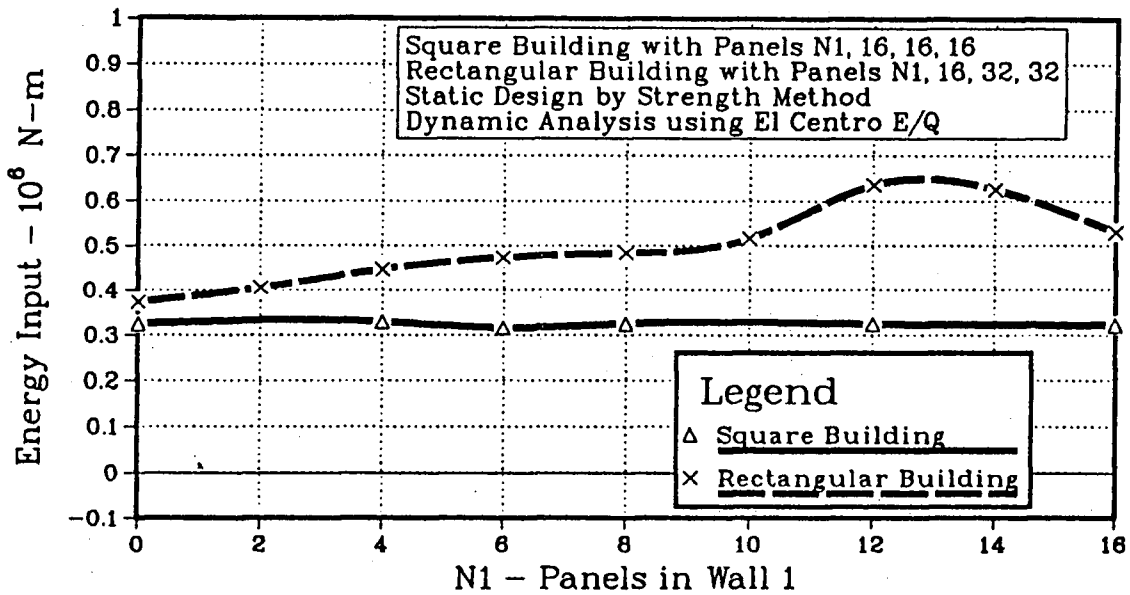


(e) Wall 2 Displacement

Fig. 5.6: Continued

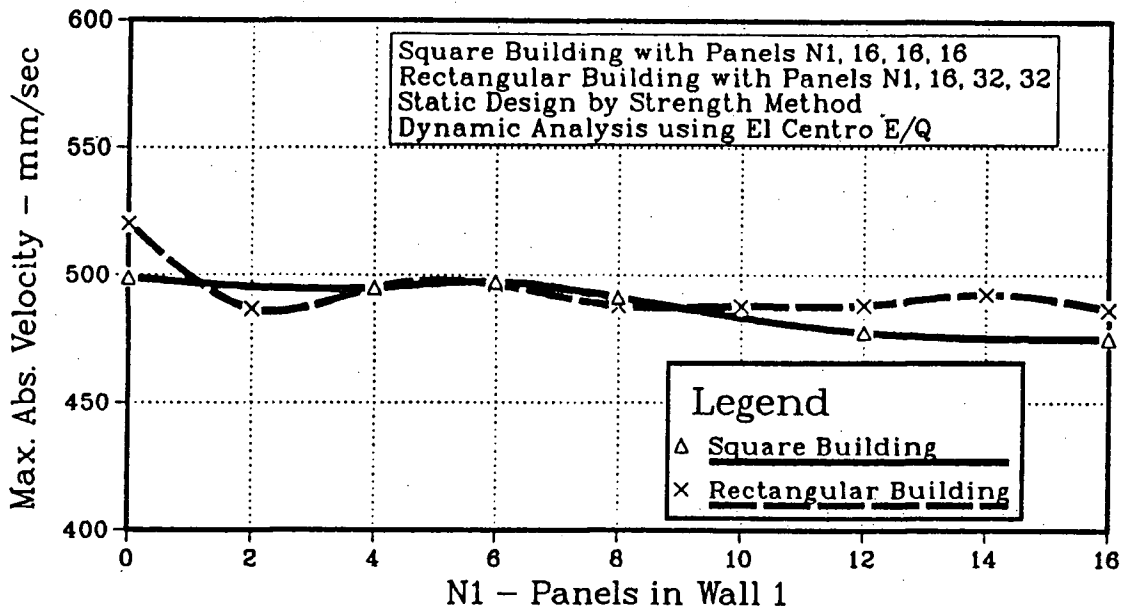


(f) Max. Dowel Displacement

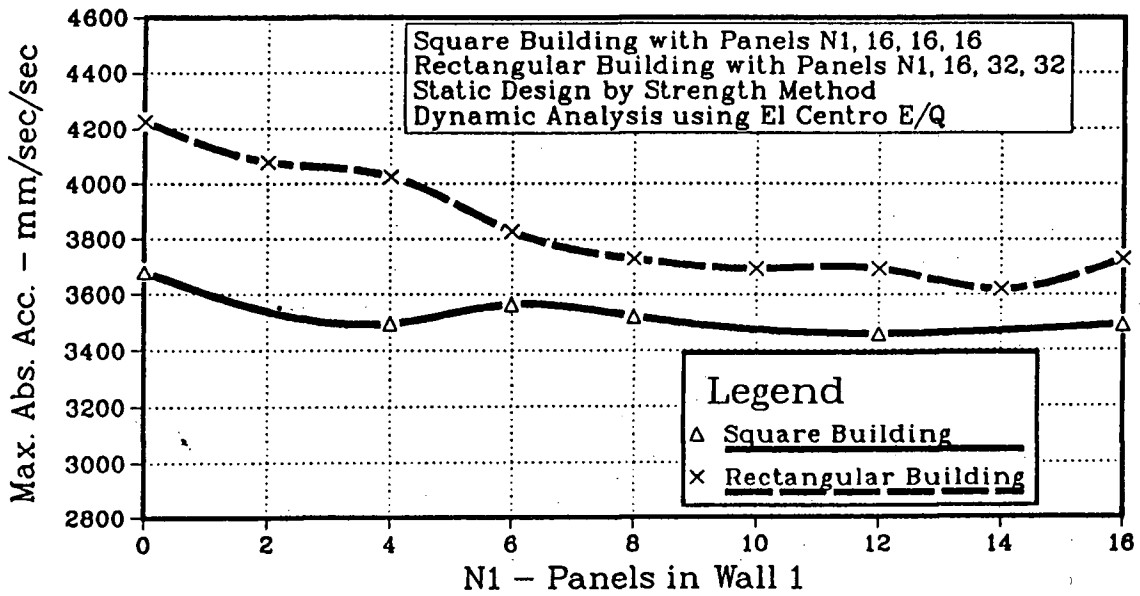


(g) Energy Input

Fig. 5.6: Continued

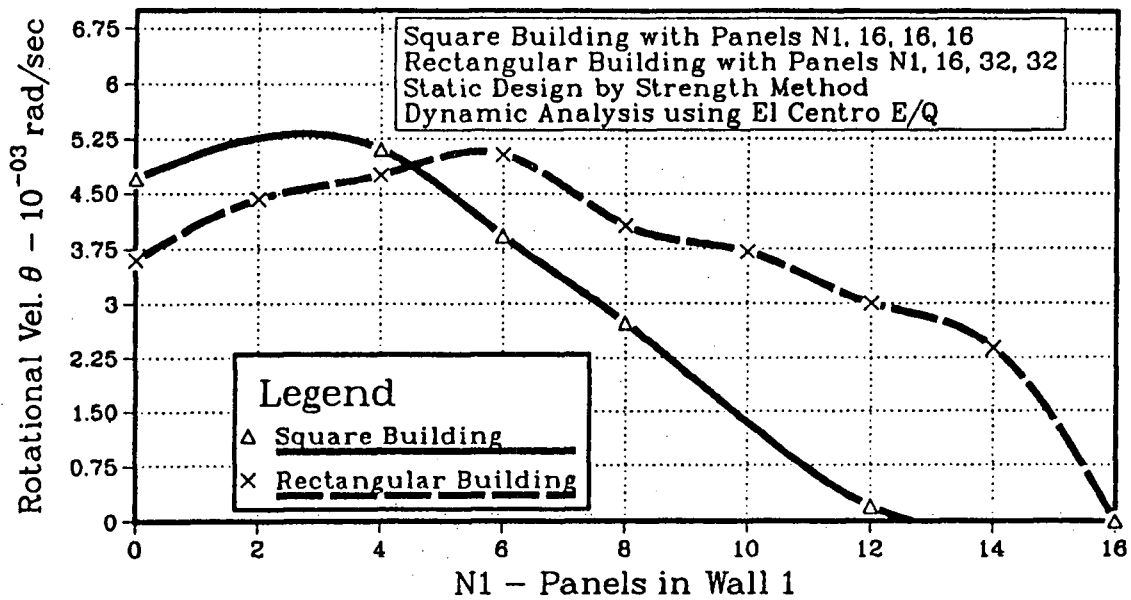


(h) Max. Absolute Velocity

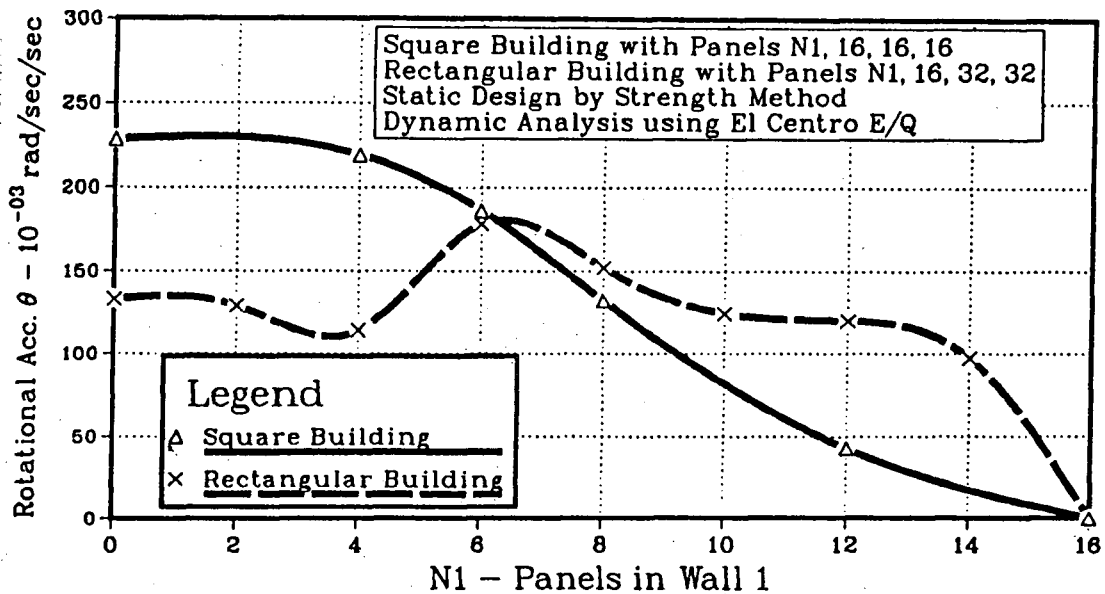


(i) Max. Absolute Acceleration

Fig. 5.6: Continued



(j) Max. Absolute Rotational Velocity



(k) Max. Absolute Rotational Acceleration

Fig. 5.6: Continued

have a shape that is similar to the shape of the curves for the building displacement at the C.M.

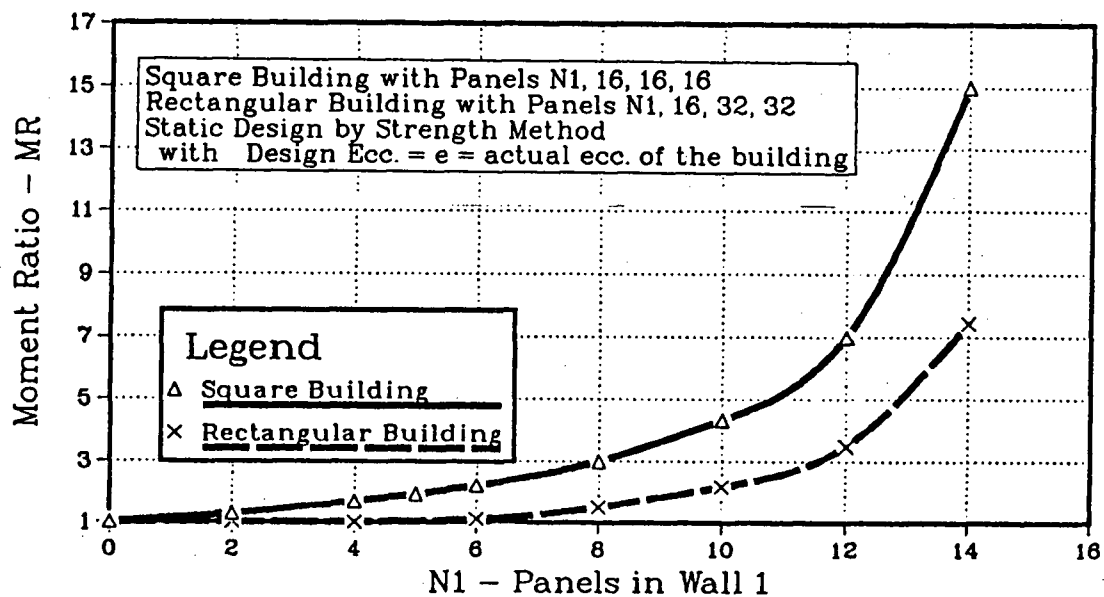
The energy input for the rectangular building is higher because it has a higher mass than the square building. Maximum velocity \dot{x} is almost constant for the two buildings while the curve for rotational velocity has a shape that is similar to that for rotation θ . For rotational acceleration the trend is similar but the curves are flatter.

Static Design with Design Ecc. = e

Fig. [5.7a...g] shows the static and dynamic analysis results for a square and a rectangular building designed using the strength method and taking the design eccentricity equal to the actual eccentricity of the building i.e. no extra eccentricity for calculating the design moment. Fig. [5.7a] shows that for the square building the moment ratio MR becomes greater than 1 for $N_1 \geq 2$ i.e. for $N_1 > 1$ the design of walls 3 & 4 is governed by the earthquake in the Y direction. (Note that the larger moment used in calculating MR is calculated using actual eccentricity e and not the code design eccentricity e_d).

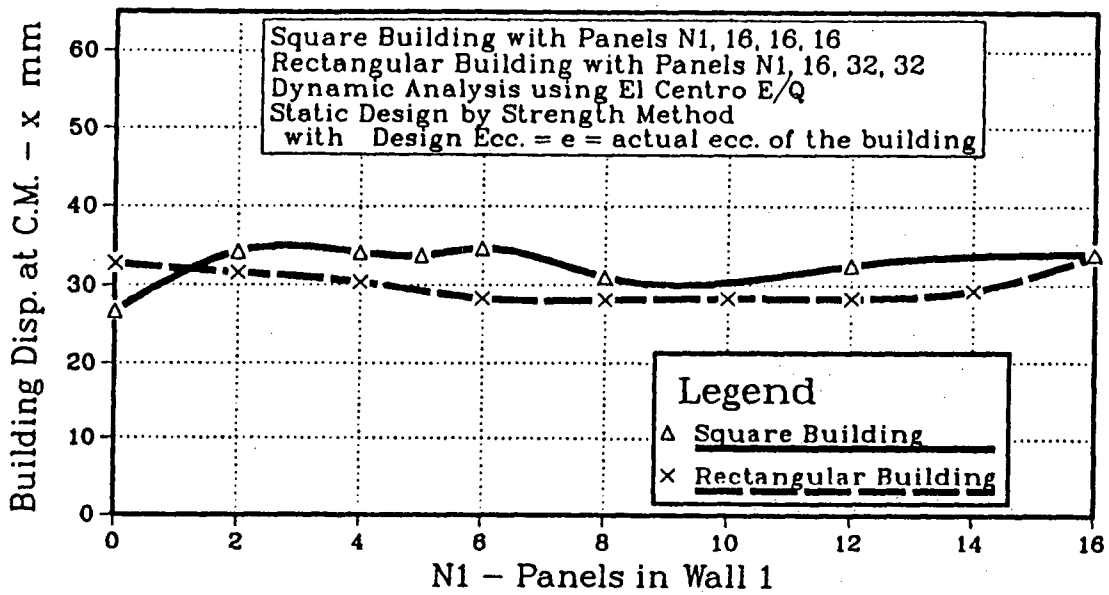
Fig. [5.7b] shows the variation of building displacement at C.M. (x) for the two buildings. The displacements are quite similar as N_1 is varied from 0 to 16. The reason for this is that the strength ratio SR of the walls in the direction of the earthquake (i.e. parallel to X direction) is the same. Maximum rotation θ for both the buildings is quite high at $N_1 = 0$. For the square building θ decreases quite rapidly to a value comparable to that obtained for the building designed for code eccentricity (Fig. [5.6c]); θ for the rectangular building is approximately $0.7 * 10^{-3}$ rad. when $MR = 1$ and then decreases rapidly as the value of MR increases.

For both the buildings the maximum value of θ is very high; which means that displacements of wall 1 and wall 2 are greatly influenced by rotation and these

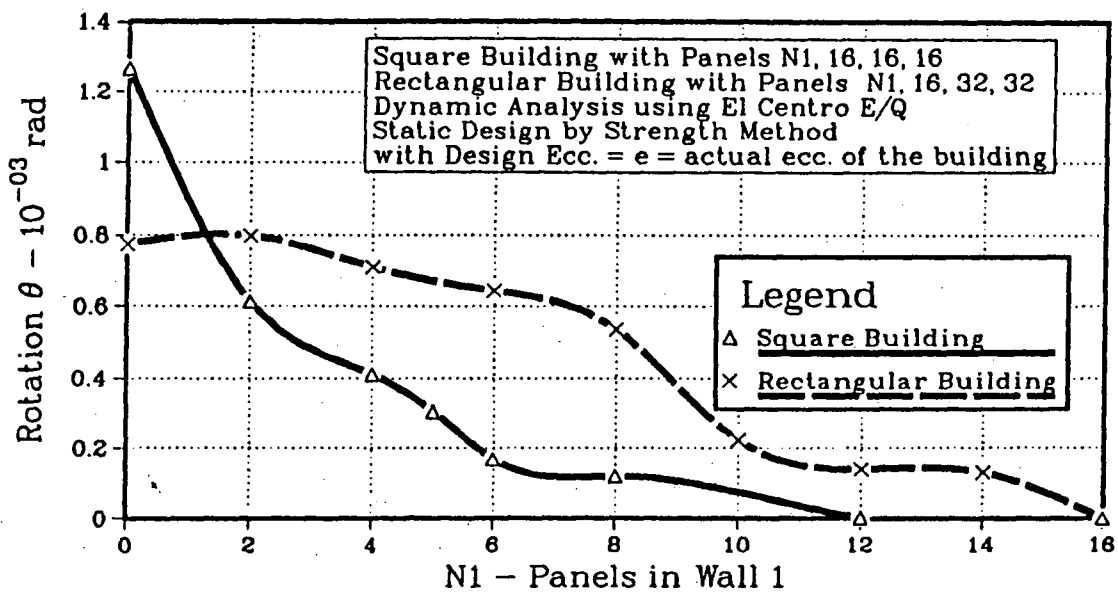


(a) Moment Ratio

Figure 5.7: Comparison of static & dynamic analysis results for square and rectangular buildings using NBCC recommended equivalent static design approach with design eccentricity equal to the actual eccentricity of the building and using the strength method of design

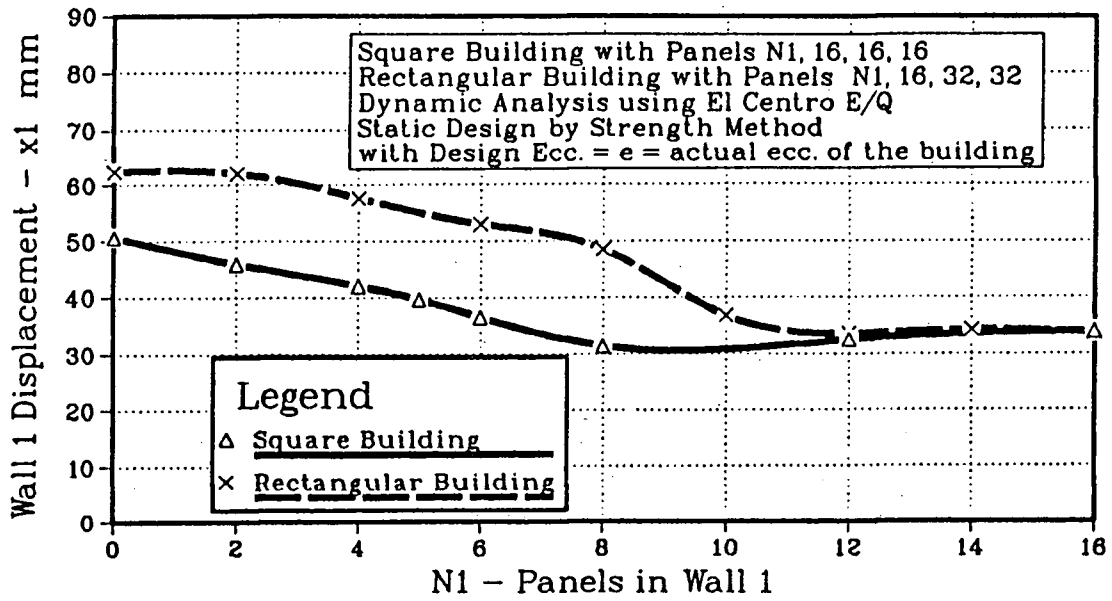


(b) Building Displacement at C.M.

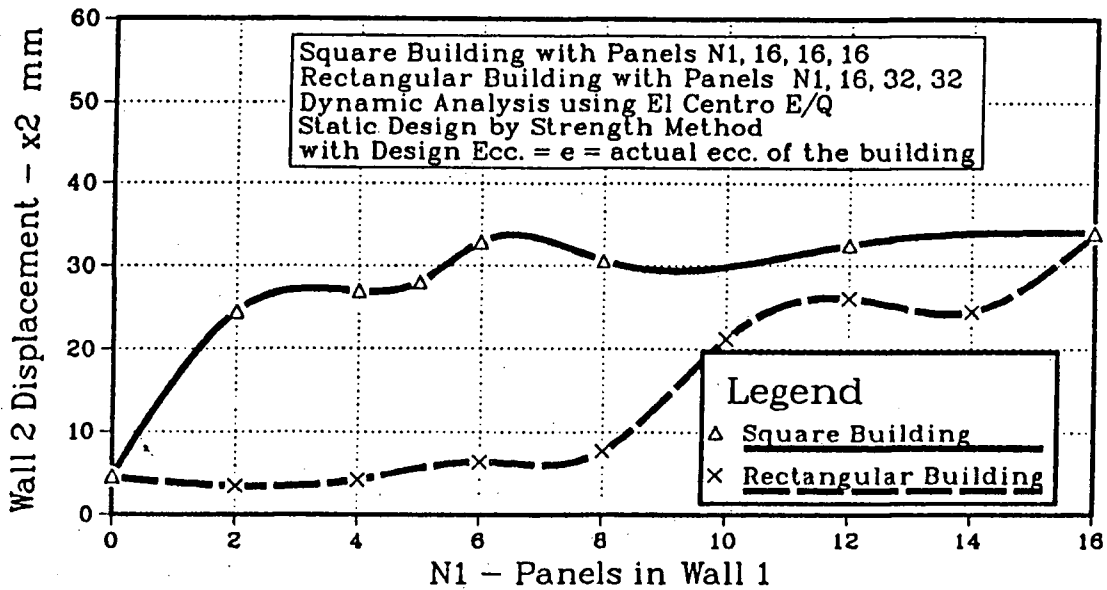


(c) Rotation θ

Fig. 5.7: Continued

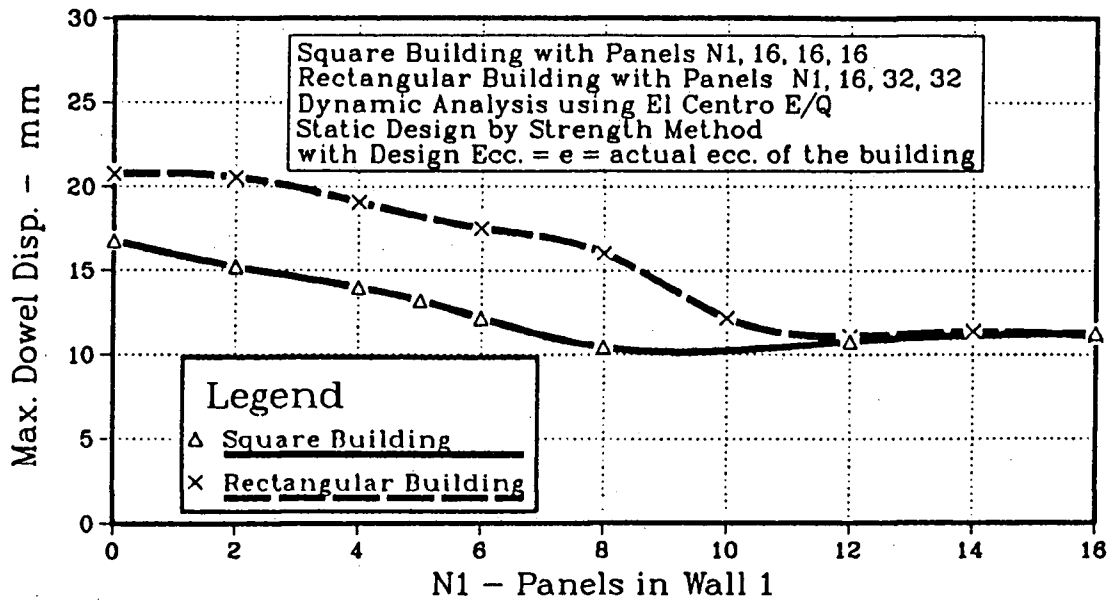


(d) Wall 1 Displacement

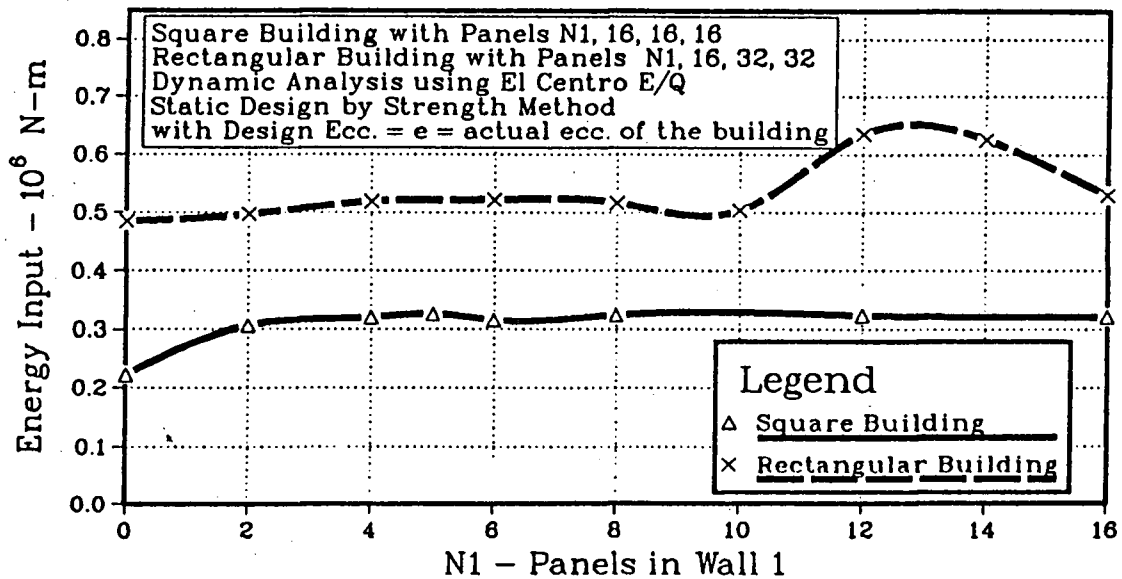


(e) Wall 2 Displacement

Fig. 5.7: Continued



(f) Max. Dowel Displacement



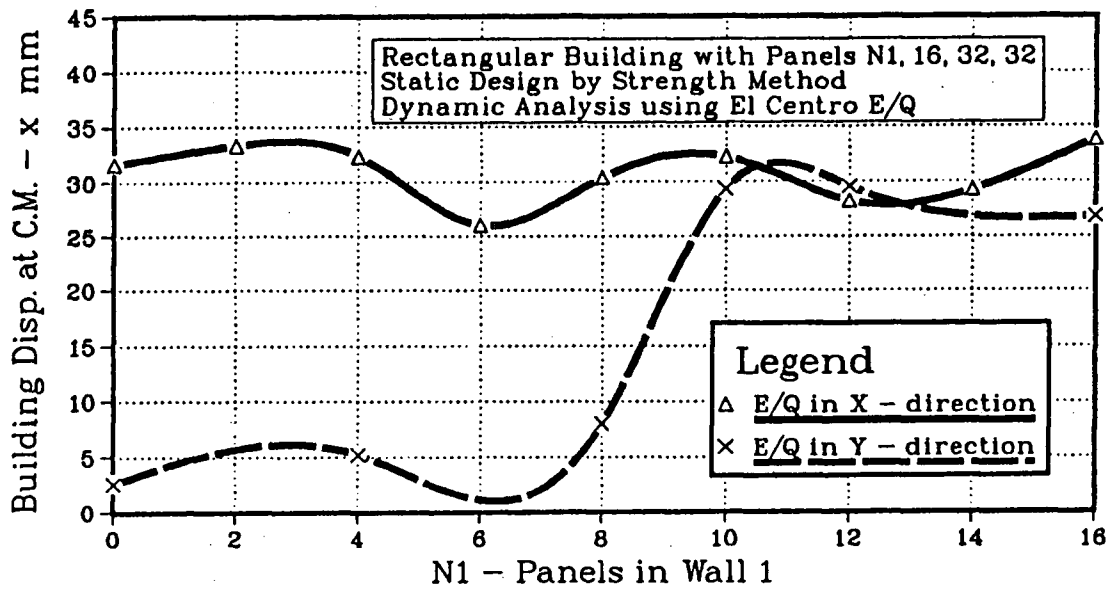
(g) Energy Input

Fig. 5.7: Continued

displacements are too large to be handled by typical pre-cast connections. Looking at the wall and dowel displacements for this case one concludes that the rectangular building, which has a higher eccentricity e because of its dimensions, is effected to a greater extend than the square building. This conclusion is in agreement with the code design equation eqn. [4.3] which shows the necessity of larger design eccentricity for the building with high eccentricity e . The dynamic analysis results confirm that the actual eccentricity of the building alone is insufficient for calculating the design moment.

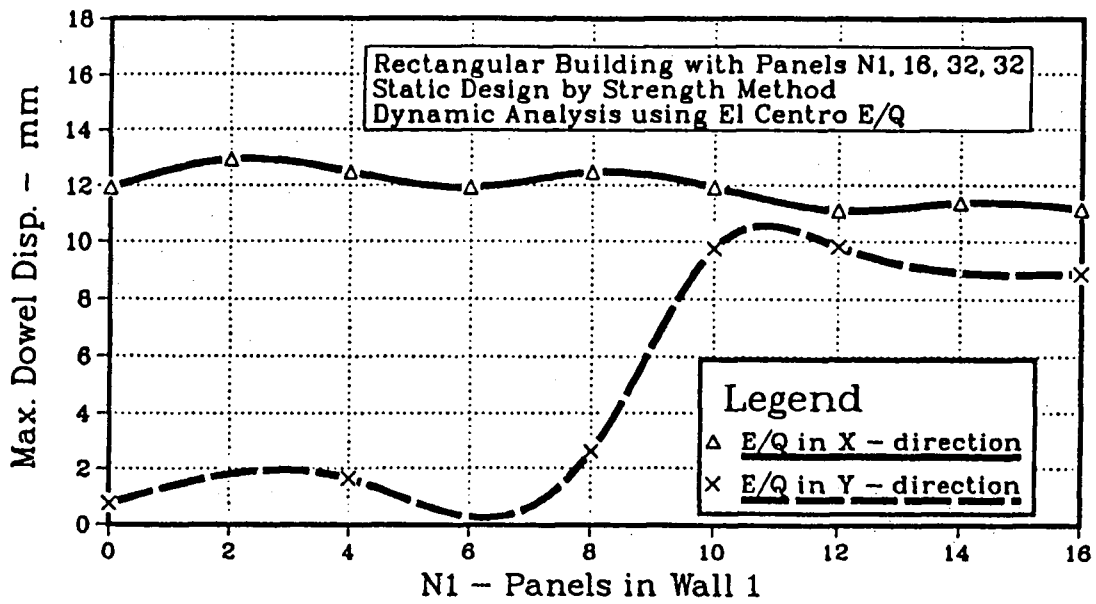
5.3.4 E/Q direction

NBCC [22] recommends that a building has to be designed to withstand the earthquake in two mutually perpendicular directions. In the preceeding paragraphs we have dicussed various results for the earthquake acting in the X direction on a building designed for earthquake in the X & Y directions. To check the adequacy of the building design to withstand the earthquake in the Y direction, a comparison of the various results obtained from dynamic analysis of the rectangular building (see Fig. [4.1b]) subjected to the El Centro earthquake acting in X & Y direction is given in Fig. [5.8a...c] (actual eccentricity in the X & Y directions used in the dynamic analysis). The results show that all the variables for the earthquake in Y direction are lower than those for the X direction. The difference is much more for lower values of N_1 . This occurs because for these values of N_1 the design of walls 3 & 4 is goverened by moment requirements in the X direction (i.e. $MR = 1$). For higher values of N_1 ($N_1 > 10$), the design of walls 3 & 4 is governed by force requirements in the Y direction (i.e. $MR > 1$ in Fig. [5.56]). The values of the results for the earthquake in both the directions become comparable, although the Y direction results for the displacements and energy input are slightly lower than the X direction results. This shows that the building design is safe for the earthquake

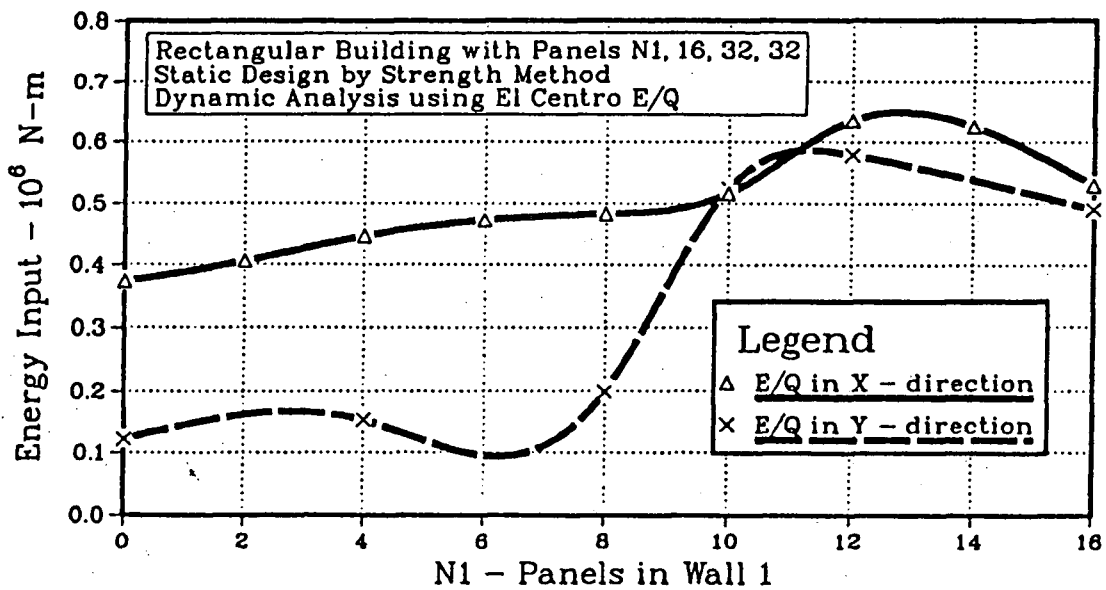


(a) Building Displacement at C.M.

Figure 5.8: Comparison of dynamic analysis results of a rectangular building for the earthquake in X & Y directions



(b) Max. Dowel Displacement



(c) Energy Input

Fig. 5.8: Continued

in the Y direction. The critical direction for dynamic response will always will be the direction where e is greater.

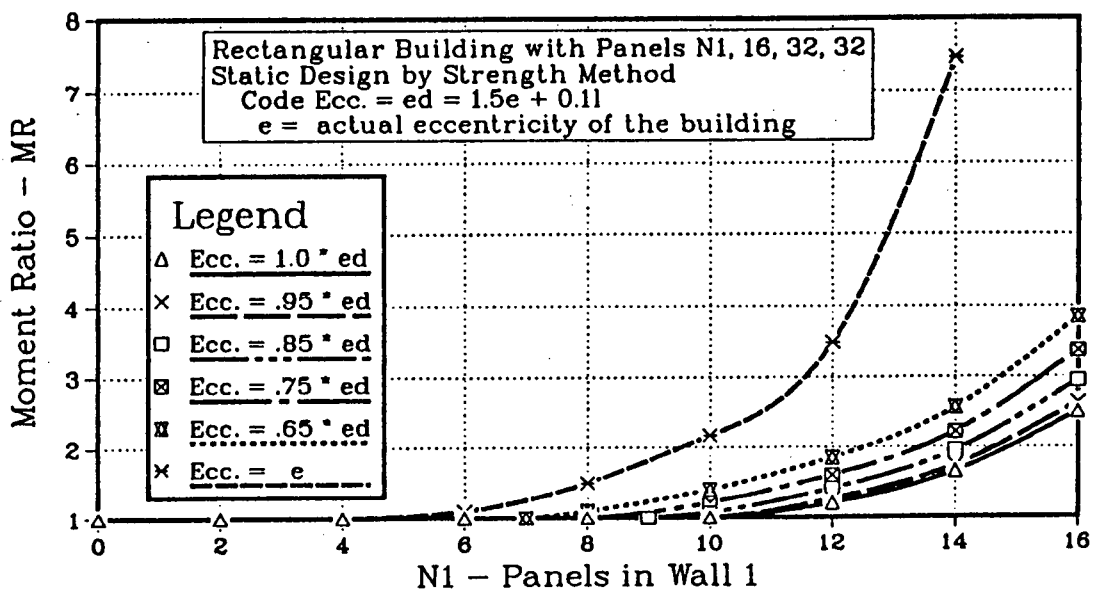
5.3.5 Effect of design eccentricity

Rectangular Building :-

The NBCC [22], in its equivalent static design approach, has given two equations, eqn.(4.3) & eqn.(4.4) to calculate the design eccentricity of the building, although as explained earlier in section [4.3], only eqn.(4.3) is needed for calculating the design eccentricity when the building is designed by the strength method. The following section presents a comparison of results obtained from the dynamic analysis, which always use the actual eccentricity of the building, for buildings using different design eccentricities in the static design. Fig.[5.9a] shows the moment ratio for different static designs. Fig. [5.9b...g] shows the variation of response with N_1 for a rectangular building. The El Centro earthquake has been used for the dynamic analysis. e_d is the code design eccentricity given by eqn. [4.3].

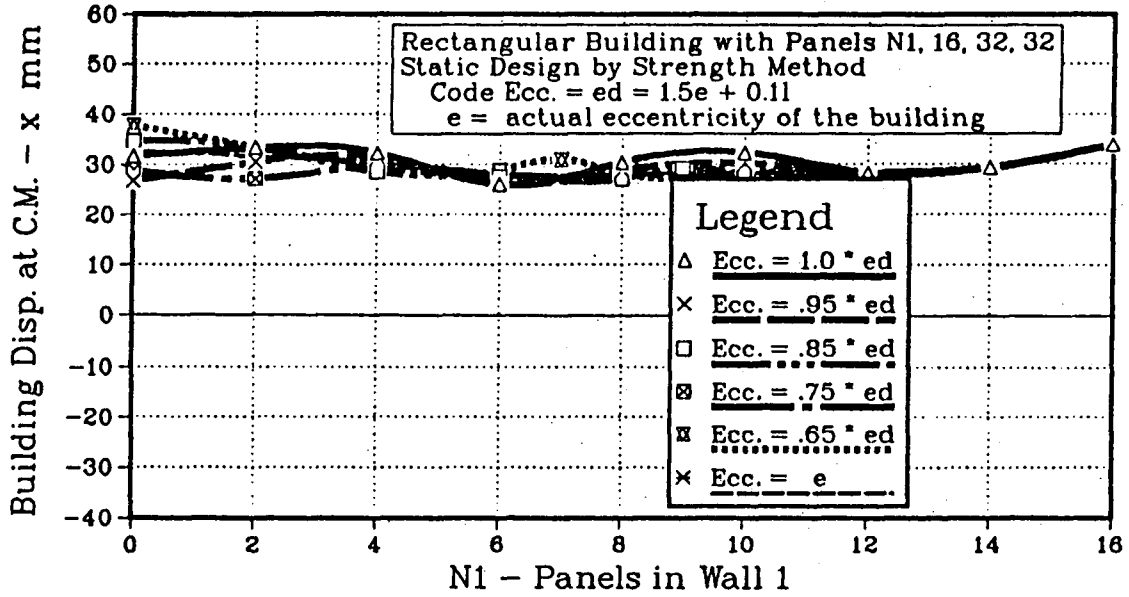
Variation of building displacement at the C.M. (x), with N_1 for various design eccentricities is given in Fig. [5.9b]. Displacement x does not vary significantly for various design eccentricities because the walls have the same strength in the direction of the earthquake for all the design eccentricities.

Rotation θ also does not vary greatly as design eccentricity is changed from $1.0e_d$ to $0.85e_d$. Then from $0.85e_d$ to $0.75e_d$ there is 100 % increase in the value of θ for low values of N_1 and as the eccentricity is further decreased from $0.75e_d$ to $0.65e_d$ there is another increase of 100 % in the value of θ . Wall 1 & wall 2 displacements also show similar trends of very small variation for design eccentricities of $1.0e_d$, $0.95e_d$ & $0.85e_d$ with displacements increasing quickly after that as the eccentricity is further reduced. From this we conclude that the code equation to calculate the design eccentricity, eqn. [4.3] is conservative and reducing e_d by a

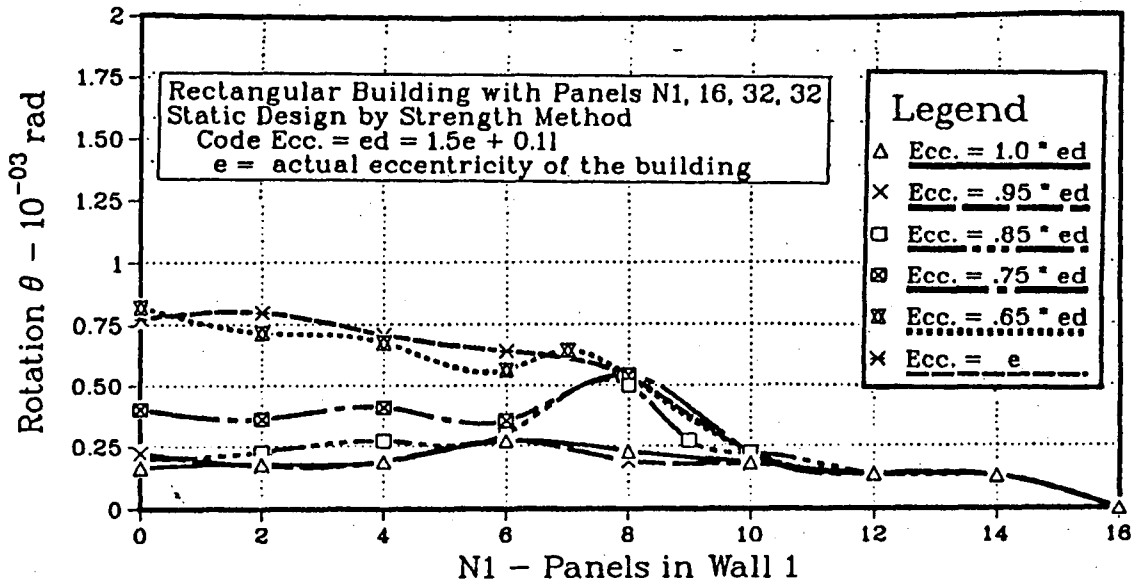


(a) Moment Ratio

Figure 5.9: Comparison of static & dynamic analysis results for a rectangular building designed using NBCC recommended equivalent static design approach for various design eccentricities with the strength method of design

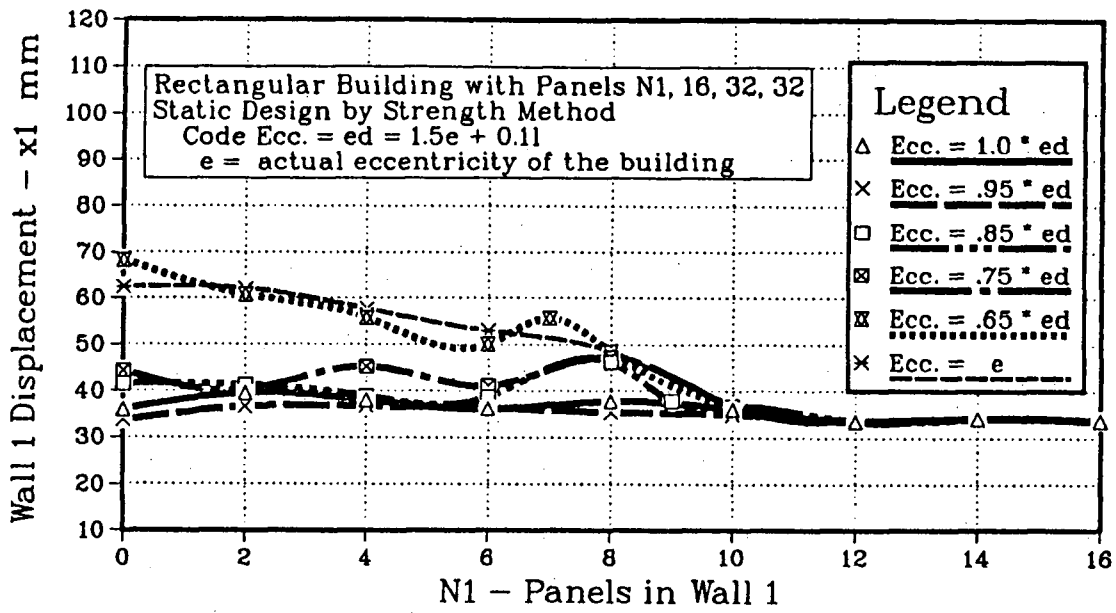


(b) Building Displacement at C.M.

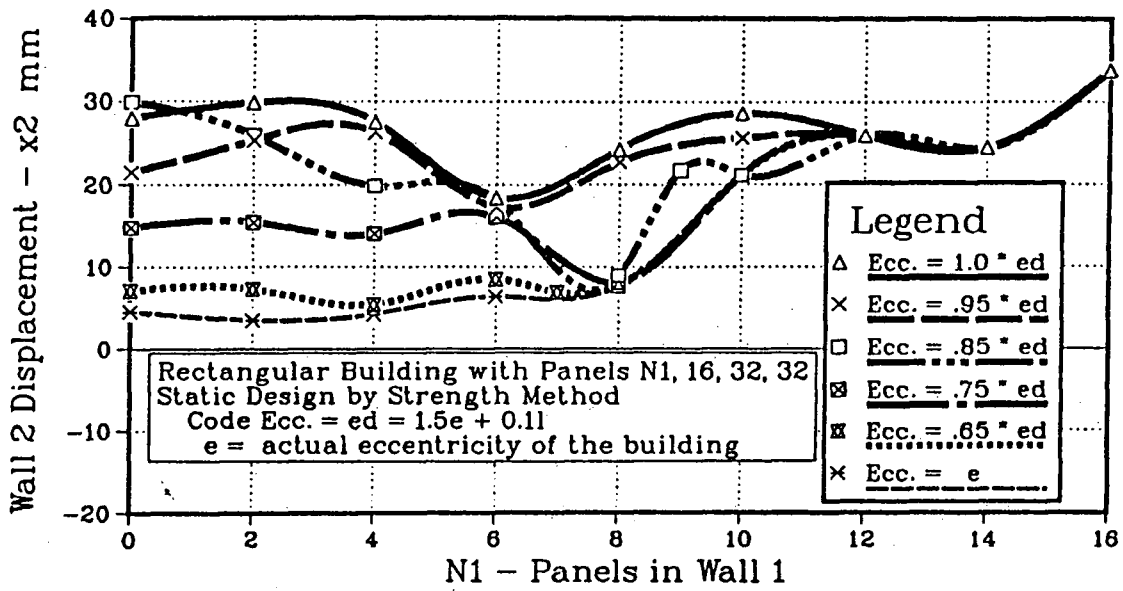


(c) Rotation θ

Fig. 5.9: Continued

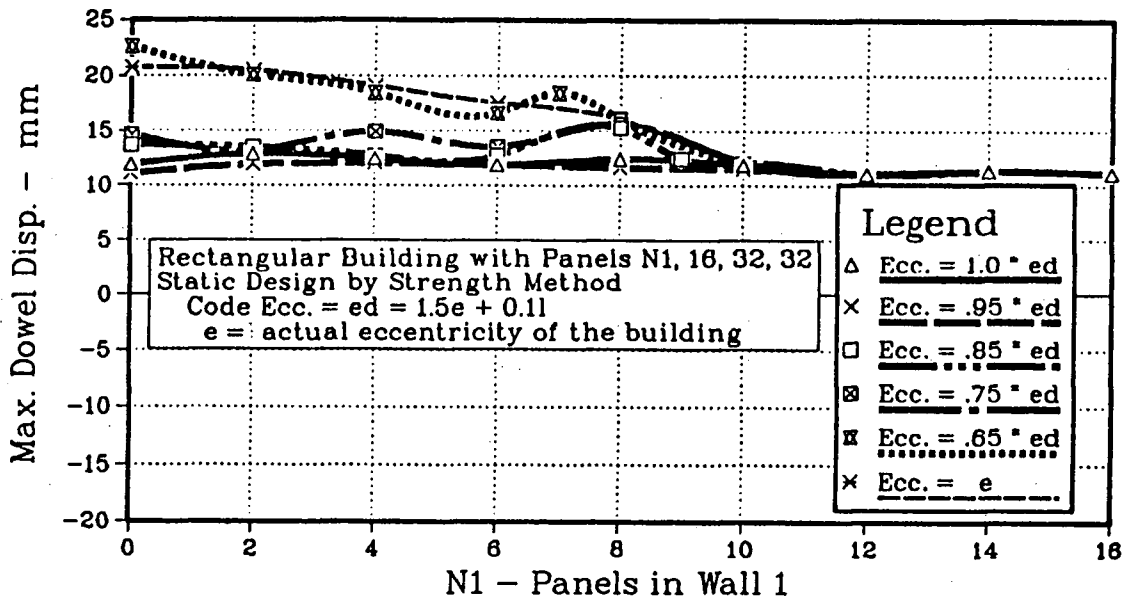


(d) Wall 1 Displacement

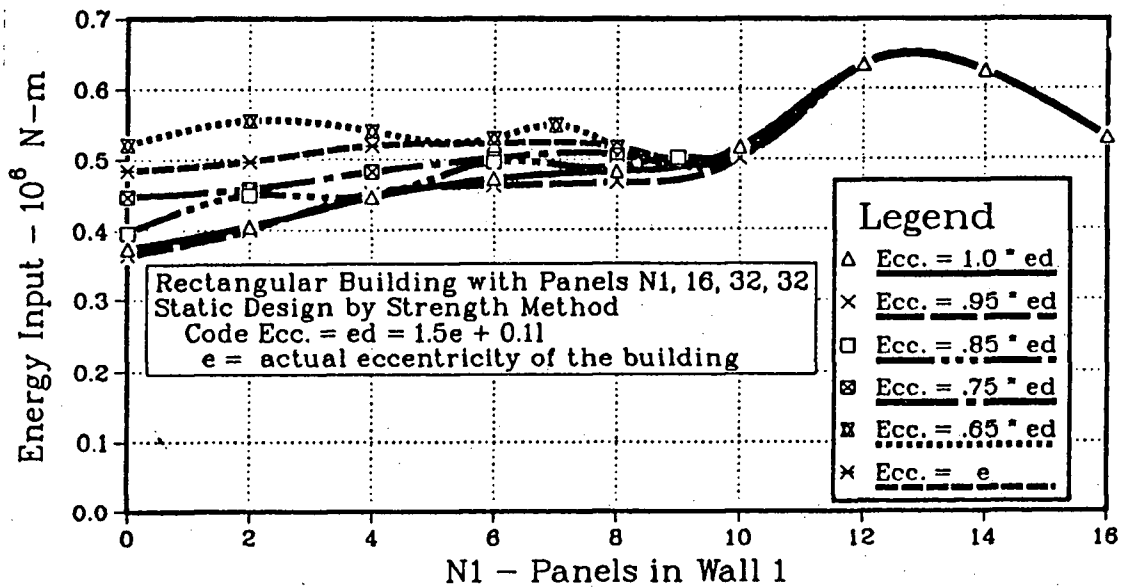


(e) Wall 2 Displacement

Fig. 5.9: Continued



(f) Max. Dowel Displacement



(g) Energy Input

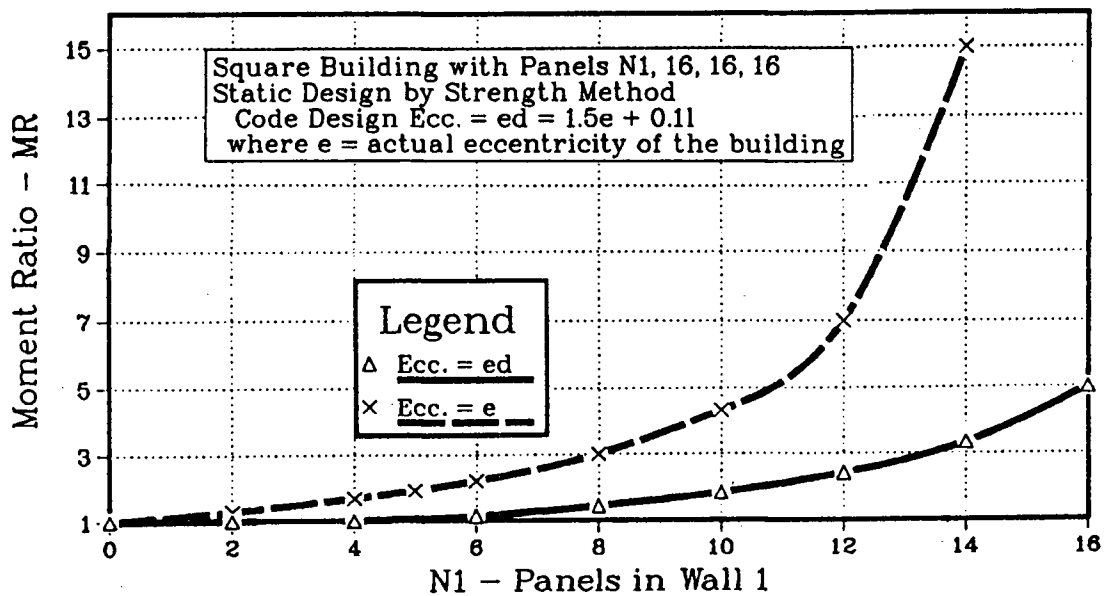
Fig. 5.9: Continued

factor of 0.85 would not significantly increase the response of the buildings analysed here.

Square Building:-

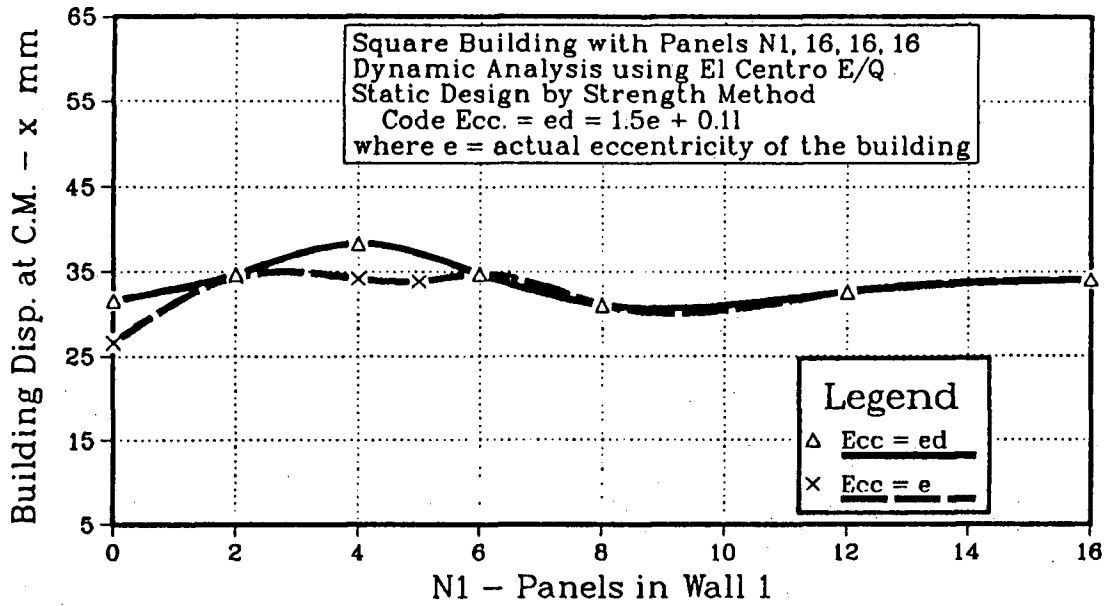
Fig.[5.10a] shows the moment ratio for a square building shown in Fig. [4.1a] statically designed using the strength method of design, with design eccentricity equal to the code recommended design eccentricity e_d and the actual eccentricity e of the building. Fig. [5.10b...g] shows the comparison of the dynamic analysis results of the building. Dynamic analysis has been done using the El Centro earthquake acting in the X direction. From Fig. [5.10a], the moment ratio MR for the square building with eccentricity equal to the actual eccentricity e , is > 1 at $N_1 \geq 2$. For this reason there is a sharp decrease in rotation θ for the building with Ecc. = e as N_1 increases from 0. For the moment ratio of 1.5 (at $N_1 = 4$ in Fig. [5.10a]) i.e. walls 3 & 4 capable of resisting a moment 50 % higher than that obtained from the design eccentricity Ecc. = e , θ reduces to values comparable to those obtained using Ecc. = e_d . The displacements of wall 1, wall 2 and maximum dowel displacements show similar trends. As the results of the wall displacements for $N_1 = 3$ are very close for the two cases, it could be said that the code design eccentricity e_d could be reduced by a factor of ($30933/38076$) 0.812 for this case (at $N_1 = 3$ the moment strength of the building with Ecc. = e_d is 38076 kN-m and with Ecc. = e it is 30933 kN-m..)

The square building reduction factor of 0.812 is quite close to the reduction factor of 0.85 obtained for the rectangular building. Thus it is safe to conclude that the NBCC [22] gives a conservative equation to find the design eccentricity and a reduction factor of 0.85 could be applied to the code design eccentricity equation, at least for buildings similar to those considered here.

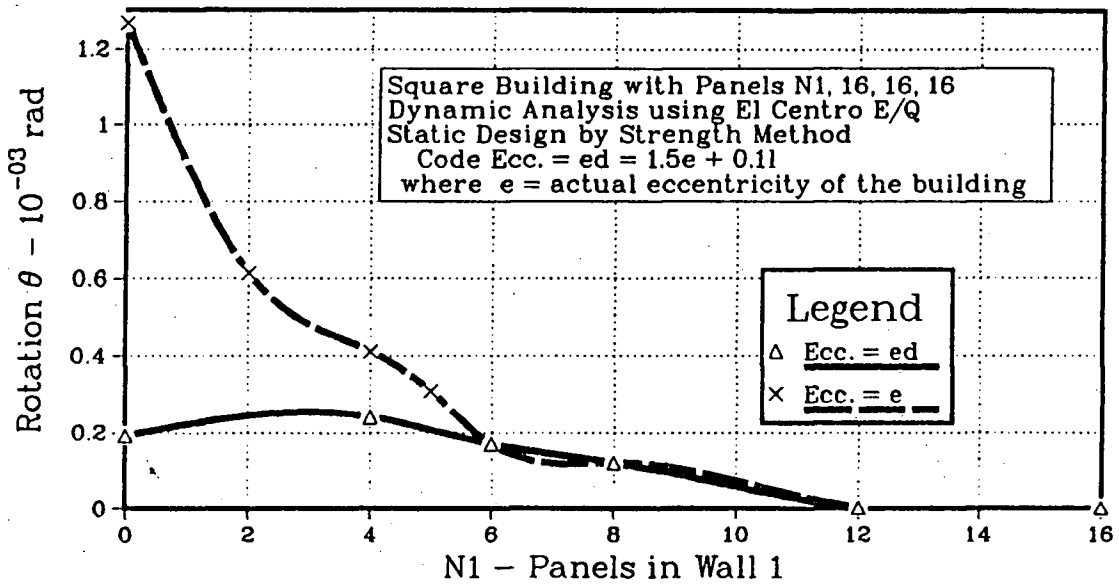


(a) Moment Ratio

Figure 5.10: Comparison of static & dynamic analysis results for a square building designed using NBCC recommended equivalent static design approach for various design eccentricities with the strength method of design

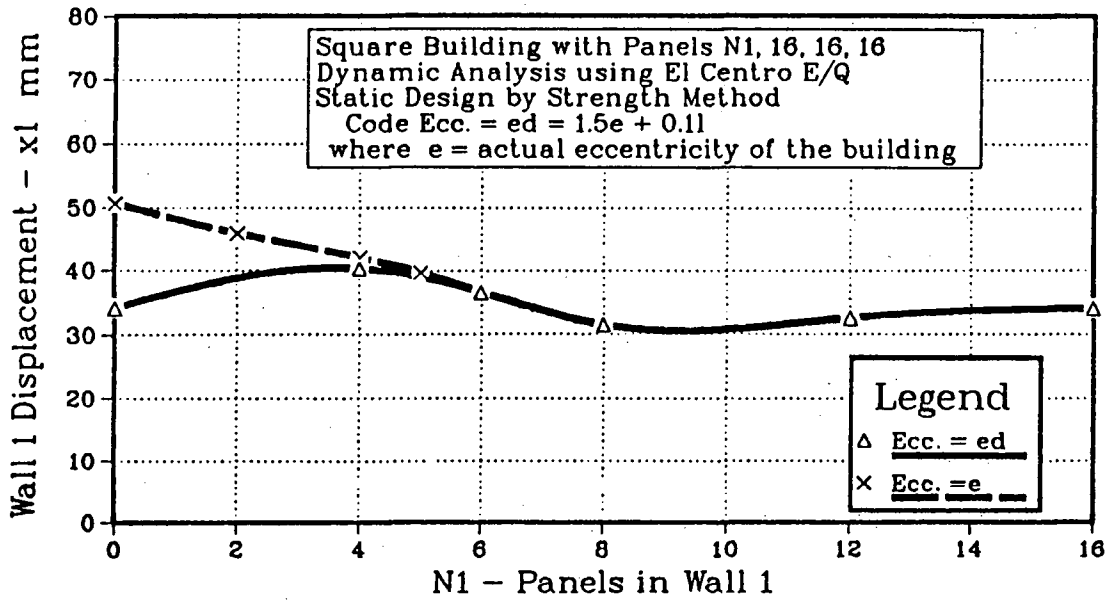


(b) Building Displacement at C.M.

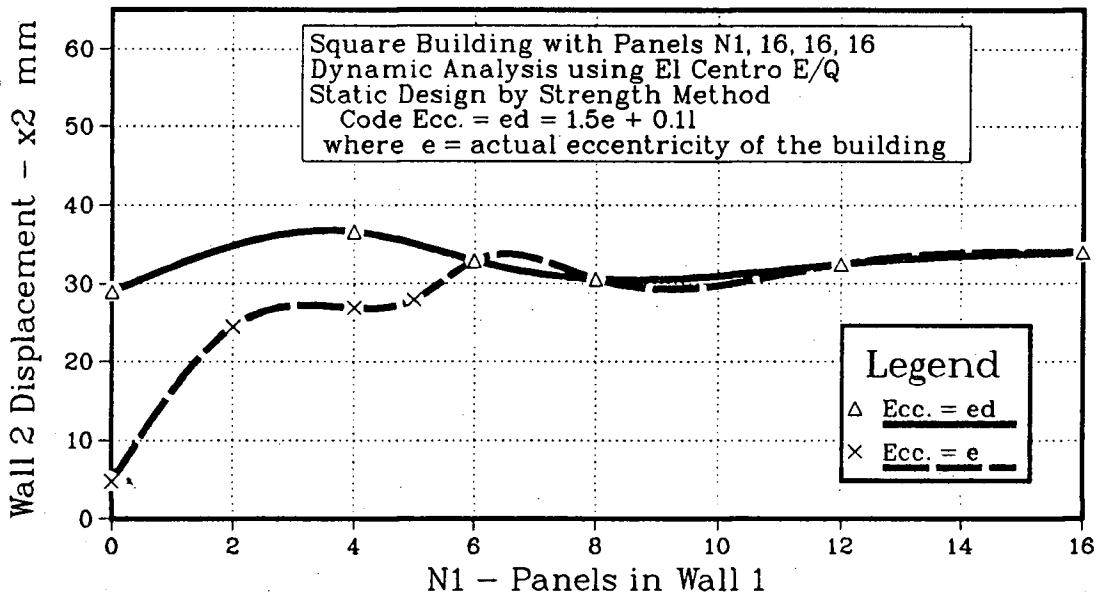


(c) Rotation θ

Fig. 5.10: Continued

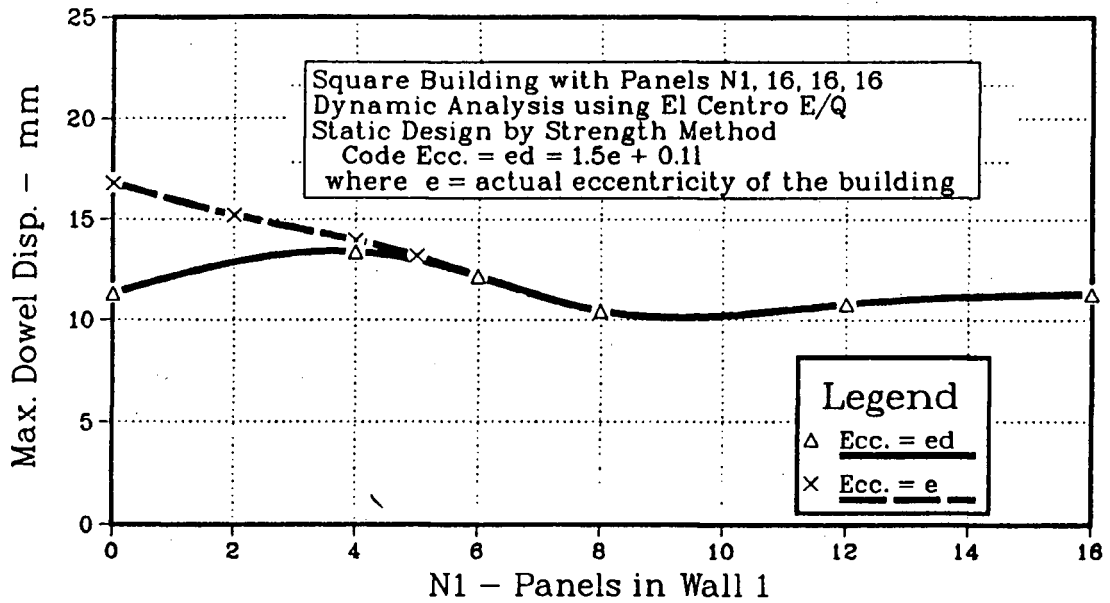


(d) Wall 1 Displacement

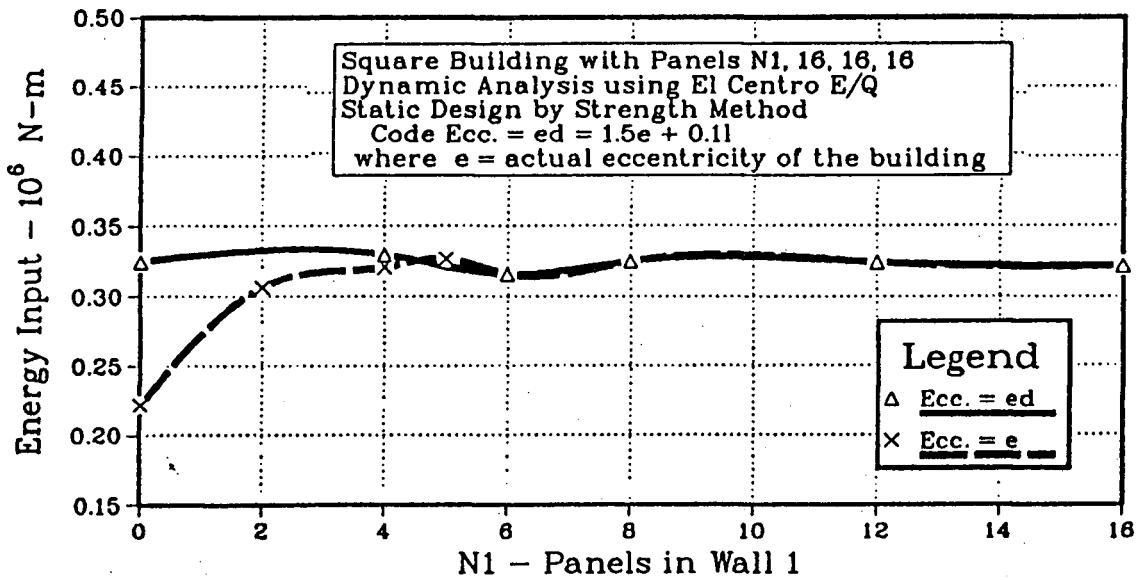


(e) Wall 2 Displacement

Fig. 5.10: Continued



(f) Max. Dowel Displacement



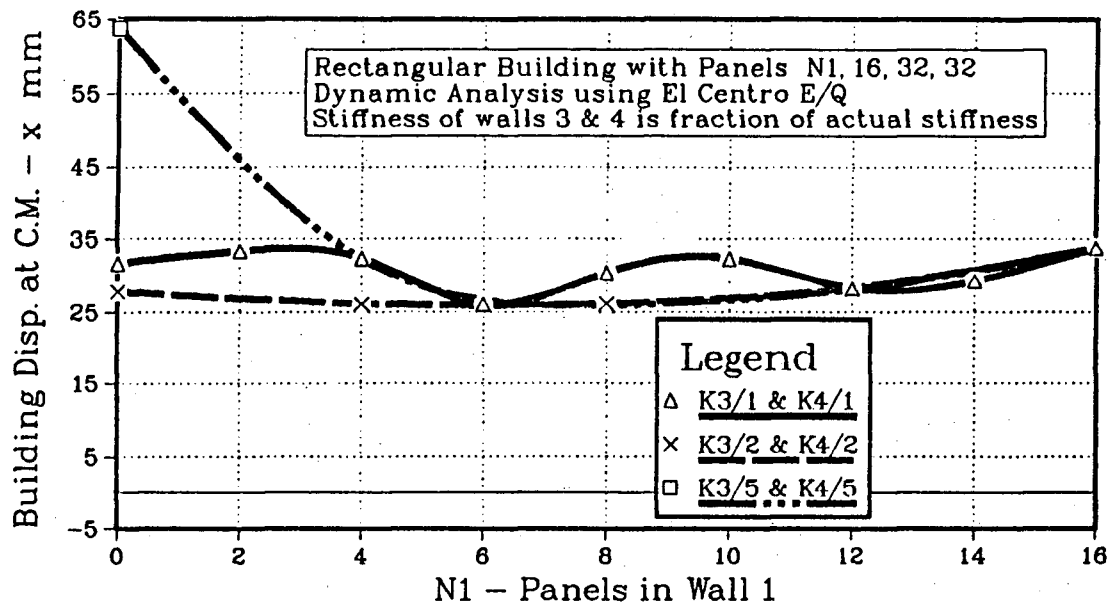
(g) Energy Input

Fig. 5.10: Continued

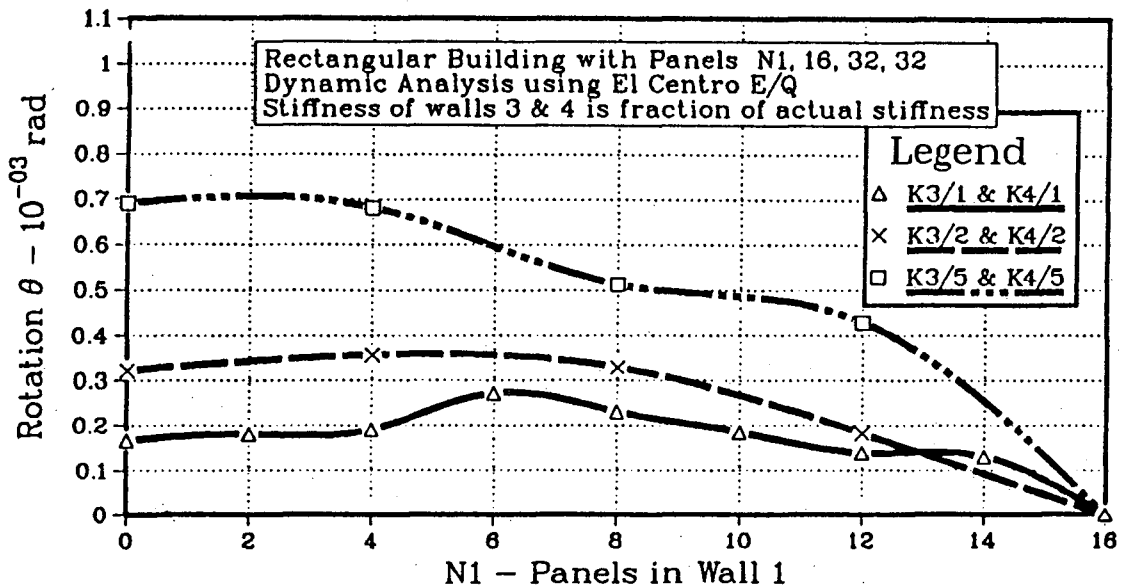
5.3.6 Effect of variation of stiffness of wall 3 & 4

As explained earlier in section [4.2] for the stiffness method of design the force in each wall is distributed according to the its stiffness. To check the effect of wall stiffness on response, the rectangular building in Fig. [4.1b] was designed by the strength method. The stiffness of walls 3 & 4 was then varied when the dynamic analysis was done for the earthquake in X direction. The stiffness of walls 3 & 4 (K_3 & K_4) was reduced by factors of 1.0, 0.5 & 0.2 while the strength was kept constant.

The results of the response of the building for the X direction earthquake are shown in Fig. [5.11a...f]. The building displacement at C.M. (see Fig. [5.11a]) does not vary significantly as the stiffness of walls 3 & 4 is reduced from K_3 to $K_3/2$. For low values of N_1 building displacement at C.M. (x) increases by about 100% as the stiffness of walls 3 & 4 is further reduced to $K_3/5$. For high values of N_1 , there is not too much change even when stiffness varies from $K_3/1$ to $K_3/5$. Rotation θ shows a change of 100% as stiffness is reduced from $K_3/1$ to $K_3/2$. θ increases by another 100% as the stiffness is reduced to $K_3/5$. For low eccentricities i.e. high N_1 , the variation is less drastic. Curves for maximum wall displacement and dowel displacement show a variation similar to building displacement at C.M. This shows that reduction in stiffnesses of walls 3 & 4 by one half has no significant effect on the response of the buildings for all values of N_1 . For low eccentricities, even a further reduction in the stiffness does not effect the response drastically. Thus we conclude that the stiffness of walls 3 & 4 does not play a major role in the response of the structure for low eccentricities. For high eccentricities, the reduction in the stiffnesses of walls 3 & 4 from $K_3/2$ to $K_3/5$ effects the response. The variation of stiffness from $K_3/1$ to $K_3/5$ is quite large whereas the corresponding variation in the response is not that large. We can assume that small variations in panel connection stiffness from one wall to another which may arise due to different strength panel

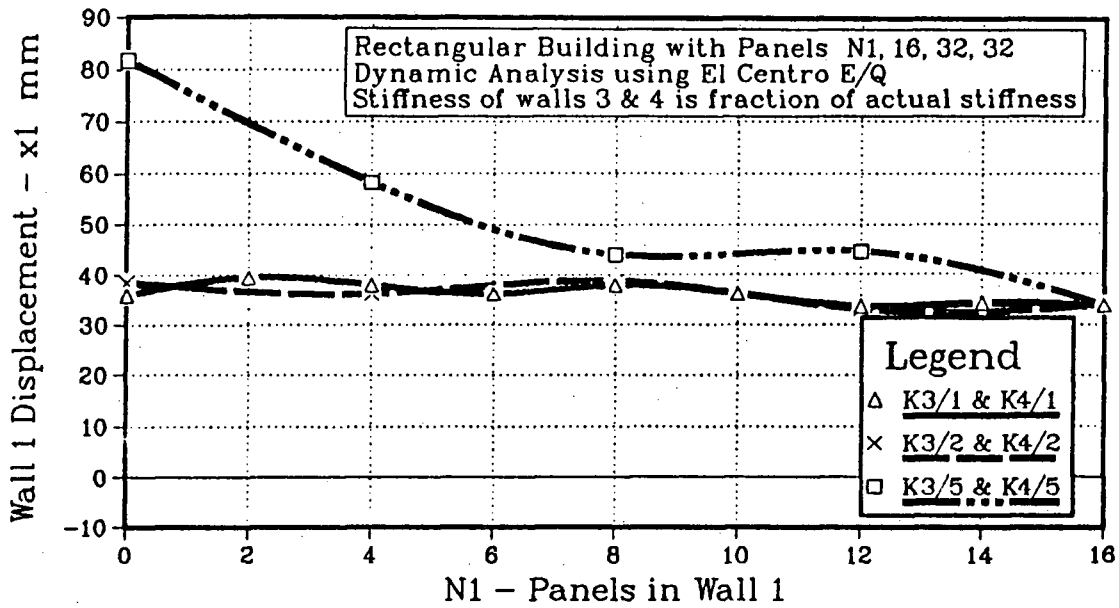


(a) Building Displacement at C.M.

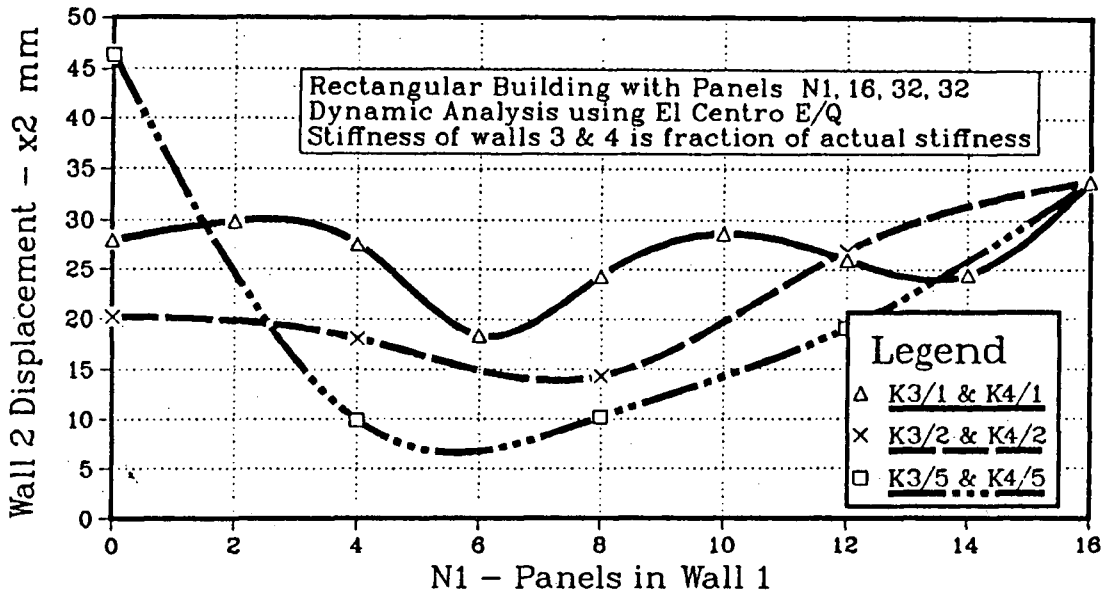


(b) Rotation θ

Figure 5.11: Comparison of dynamic analysis results of a square building statically designed using strength method of design and using different stiffnesses of walls 3 & 4 in the dynamic analysis

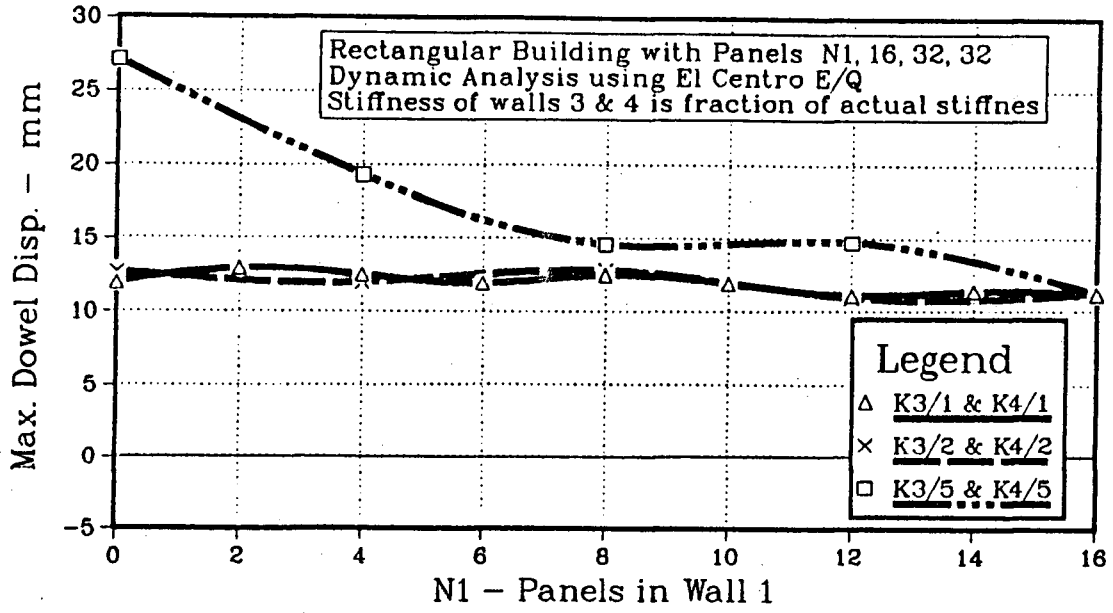


(c) Wall 1 Displacement

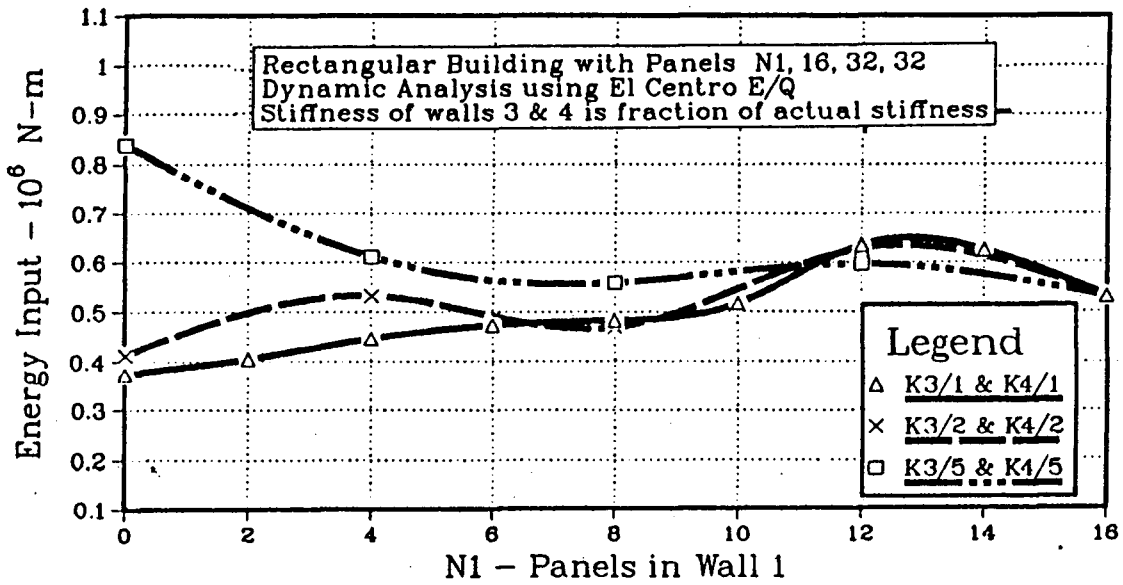


(d) Wall 2 Displacement

Fig. 5.11: Continued



(e) Max. Dowel Displacement



(f) Energy Input

Fig. 5.11: Continued

connections will not greatly effect the response.

It has been shown that small variations in the panel connection stiffness will not significantly effect the results. This variation in the stiffness could be caused by using different strength panel connections in different walls. For a building designed by the stiffness method, it is safe to assume the stiffness of each wall proportional to the number of panels in that wall instead of calculating the stiffness of each panel connection and then calculating the stiffness of the walls.

Chapter 6

Discussion, Conclusions and Future Studies

6.1 Introduction

This investigation was made to study the behaviour of eccentric precast concrete buildings designed according to the seismic provisions of the NBCC [22]. Two different approaches were taken in applying the static lateral load provisions of the NBCC [22]. These are referred to in chapter 4 as the strength method and the stiffness method of design. Results obtained from the dynamic analysis have been presented in chapter 5.

The NBCC-1985 [22] contained major changes in the provisions for seismic loads on eccentric buildings. The torsional design moment was increased to take into consideration the effects of dynamic magnification [7]. The previous recommendation for doubling the computed torsional effects when eccentricity exceeds $0.25D$ was eliminated because it was found to be unnecessarily conservative [37]. According to the NBCC [35], the peak horizontal seismic ground acceleration expected in zone 5 is $0.32g$. Thus the El Centro 1940 earthquake, which has a peak acceleration of $0.35g$, can be considered as a typical earthquake for earthquake-resistant design in zone 5.

The CPCI has also modified its recommended design method for calculating the

strength of one storey precast panel buildings [20] because the previous method did not properly consider the strength of the lateral force resisting elements. The design example given in the CPCI handbook calculates the strength of a shear wall constructed from isolated wall panels by considering the probable & design flexural strength resulting from the dowels at the base of each panel.

6.2 Discussion of results

Section [5.3] discusses the effects of changes in various parameters on eccentric buildings. The overall objective of this study was to answer the following questions :

- Are the requirements for considering torsion in the NBCC-1985 [22] appropriate for the design of buildings of the type considered here ?
- What recommendations can be made to improve the earthquake design of these buildings ?

Guidelines to help answer the first question are given in Commentary J.1 of Ref. [35], which states that :

Structures designed in conformance with NBCC provisions should be able to resist moderate earthquakes without significant damage and major earthquake without collapse. For the purpose of this section, collapse is defined as the state at which exit of the occupants from the building becomes impossible because of the failure of the primary structure.

Although the terms moderate and major earthquakes are not explicitly defined, NBCC [35] has given recommendations for the maximum acceleration with a certain probability of exceedance that can be expected in any part of the country. So for zone 5, an earthquake with peak acceleration of 0.32g can be taken as a major earthquake. In this study 3 different earthquakes with peak acceleration scaled to 0.35g have been used in the dynamic analysis (see section [5.3]).

Figs. [5.4c...l] [5.5a...j] & [5.6b...k] show the effect of various parameters such as building geometry, earthquake data, method of design etc., on the response of the buildings for various eccentricities. The maximum value of wall displacement for a building designed according to the NBCC recommendations using the strength method of design is 50 mm which is obtained for the Taft earthquake with $N_1=4$ in Fig. [5.5c]. The average value of maximum wall displacement for various eccentricities for various parameters is between 35 to 40 mm. This is larger than the NBCC [35] recommended inter storey drift limitation of 0.005 times the storey height or 27mm in the present studies. But this NBCC drift limitation has been recommended assuming monolithic behaviour of the buildings in which a large volume of materials yield; thus the inelastic deformation is comparable to elastic deformation (3 times maximum as recommended by NBCC [35]). But in a jointed pre-cast structure only a small volume of materials yield thus resulting in large inelastic deformations. At failure these can be 8 or more times the elastic deformations depending upon the connection type. So for this type of structure we can accept much higher deformations than recommended by NBCC and these should not result in collapse. Thus for the type of the structure being discussed here, a displacement of the order of 35 to 40 mm is quite reasonable.

The average value of dowel displacements (see Fig. [5.4g, 5.5e & 5.6f]) for buildings designed according to NBCC recommendations, is between 10 to 12 mm i.e. each side of the connection will be elongated by 5 to 6 mm. This elongation is well within the capability of the dowel connections.

From Fig. [5.4d] [5.5b] & [5.6c] it is clear that the rotation θ for the buildings designed according to NBCC recommendations does not vary significantly as long as the moment ratio MR for that case is equal to 1 i.e. as long as the design of the walls perpendicular to the earthquake direction, for the strength method of design, is done by the moment requirements for the earthquake in X direction.

The maximum value of θ for these cases is $0.28 * 10^{-3}$ radians which is very small. The effect of this small θ on the wall displacements is very small compared to the building displacement at the center of mass. Also the maximum values of rotational velocity $\dot{\theta}$ and rotational acceleration $\ddot{\theta}$ are very small and have only a very small effect on the overall response of the buildings. For buildings designed using the calculated building eccentricity with no magnification as the design eccentricity, the wall displacements and the rotation θ are very large as shown in Figs. [5.7b..g], for buildings with large eccentricity. This shows that building eccentricity alone is not adequate for the design of all buildings. The code design eccentricity eqn. (4.3) appears to be adequate for a wide range of eccentricities.

Section 4.1.9.1 (13) of NBCC [35] states that total shear in the horizontal plane shall be distributed to various elements of the lateral force- resistant system according to their rigidities found from a rational analysis; i.e. NBCC recommends the use of stiffness method approach explained in section [4.2] for finding the forces in the shear walls. Fig. [5.4c...1] show the response of the square building using both the stiffness method and the strength method of design. These figures show that the response of the building for the two methods of design is quite close. It has also been explained in section [4.2.1] that the stiffness method may not be too practical for the highly eccentric precast buildings (rectangular building Fig. [4.1 b]) being considered in the present studies while the proposed strength method of design is applicable for all the eccentricities. This suggests that the proposed strength method is better suited for the design of pre-cast buildings of the type being considered in the present studies. Another advantage of the strength method is that we need only one design eccentricity equation (eqn. (4.3)) instead of the two equations, eqns.(4.3) & (4.4), recommended by NBCC [22], thus reducing the mathematical computations.

6.3 Conclusions

1. Design of connections based solely on their monotonic strength is inappropriate. Connections should exhibit stable hysteresis loops without strength degradation to effectively dissipate the energy.
2. The CPCI suggested method for designing this type of building gives satisfactory results.
3. The results of the dynamic analysis indicate that eccentric one storey box type precast buildings designed according to the NBCC recommendations will survive a major earthquake.
4. The strength method for calculating the forces in the walls is more effective than the code recommended stiffness method because the stiffness method tends to result in a requirement for higher strength connections in the weaker walls. For a highly eccentric building it becomes very difficult to provide these high strength connections.
5. The NBCC recommendations for building design are suitable for highly unsymmetrical as well as symmetrical buildings of the type being considered here.
6. For buildings of the type being considered here, it appears that the design eccentricity from eqn.(4.3) could be reduced by 15% without any significant changes in the overall response of the buildings.
7. A small reduction in the stiffness of the walls perpendicular to the direction of the earthquake does not effect the response of the buildings.
8. For a building designed by the stiffness method, the stiffness of the walls can be taken as proportional to their number of panels regardless of the different

strength panel connections used in the walls without significantly affecting the dynamic response.

6.4 Future studies

A few of the areas which need to be studied further are given below :

1. Very little experimental data is available on the behaviour of the panel connections, especially dowel connections, under cyclic loading. This work would increase our understanding on the seismic performance of the connections and thus of pre-cast structures as a whole.
2. Large scale tests on pre-cast buildings could be done to allow calibration of the results of computer studies.
3. The computer program should be extended to model an elastic roof diaphragm i.e. rigid roof panels connected by elastic springs.
4. The computer program should be modified to handle multi-storey buildings with different methods of construction.

Bibliography

- [1] Anon, *Standard Plate Book*; Published by Stanley Structures, Denver, June 1977.
- [2] Ashwad A.; 'Selected Precast Connections : Low - cycle behaviour and strength'; Proc. 3rd *Canadian Conference on Earthquake Engineering*; vol 2, Montreal 1979.
- [3] Ashwad A.; 'Seismic Design and In-plane Behaviour of Single Panel Coupled Walls'; Proc. *Workshop on Design of Prefabricated Concrete Buildings for Earthquake Loads*; conducted by Applied Technology Council, Berkeley, April 1981.
- [4] Brankov G. & Sachaniski S.; 'Response of Large Panel Buildings for Earthquake Excitation in Non-elastic state'; Proc. 6th *World Conference on Earthquake Engineering*, New Delhi, India, Jan 1977.
- [5] Becker J.M., Llorente C., 'Seismic Design of Precast Concrete Panel Buildings'; Proceedings, *Workshop on Earthquake Resistant Reinforced Concrete Building Construction*, University of California, Berkeley, June 1977.
- [6] Becker J.M., Llorente C., 'Seismic Response of a Simple Precast Concrete Panel Walls'; Proceedings, *Second U.S. National Conference on Earthquake Engineering*, Stanford, California, 1979.
- [7] Bustamante J.I. & Rosenblueth E.; 'Building Code Provisions on Torsional Oscillations'; Proc. 2nd *World Conference on Earthquake Engineering*, Japan 1960, vol 2, pp 879-892.
- [8] *CAN3 - A23.3 - M84 - Design of Concrete Structures for Buildings*, Canadian Standard Association (CSA), 178 Rexdale Boulevard Rexdale Ontario, Canada.
- [9] Clough D.P.; *Design of Connections for Precast Prestressed Concrete Buildings for the effects of earthquake*; Prestressed Concrete Institute, Chicago, Illinois, March 1985.
- [10] Dimitrov M.L. & Georgier G.B.; 'Determination of Hysteresis Curves in the Connections of Large - Panel Buildings'; Proc. 8th *European Conference on Earthquake Engineering*; Lisbon 1986, vol 4.

- [11] Fintel M., Schultz D., and Iqbal M.; 'PCA Report No. 2 : Philosophy of Structural Response of Normal & Abnormal Loads'; *Design and Construction of Large Panel Structures* ; office of Policy Development & Research, Deptt. of Housing and Urban Development, Washington D.C.; Aug 1976.
- [12] Hanson N.W.; 'Seismic tests of Horizontal Joints'; *Design and Construction of Large Panel Structures, Supplement Report C*; office of Policy Development & Research, Deptt. of Housing and Urban development, Washington D.C.; Jan 1979, NTIS No. PB 79-22701.
- [13] Harris H.G. & Abboud B.E.; 'Cyclic Shear Behaviour of Horizontal Joints in Precast Concrete Large Panel Buildings'; Proc. *Workshop on Design of Prefabricated Concrete Buildings for Earthquake Loads*, April 1981, pp 403-438.
- [14] Hawkins N.W.; 'State of the art report on Seismic Resistance of Prestressed and Precast Structures, Part 2 - Precast Concrete'; *PCI Journal*, Jan-Feb 1978, vol 23, No. 1, pp 40-58.
- [15] Hawkins N.M. & Lin I.J.; 'Bond Characteristics of Reinforcing Bars for Seismic Loading'; Proc. 3rd *Canadian Conference on Earthquake Engineering*; vol 2, Montreal 1979.
- [16] Joahl L.S. & Hanson N.W.; 'Horizontal Joints Tests'; *Design and Construction of Large Panel Structures, Supplement Report B*; office of Policy Development & Research, Deptt. of Housing and Urban Development, Washington D.C.; Jan 1979, NTIS No. PB 79- 22701.
- [17] Kallros M.; *An Experimental Investigation of the Behaviour of Connections in Thin Precast Concrete Panels under Earthquake loading*; M.A.Sc. Thesis, University of British Columbia, April 1987.
- [18] Llorente C., Becker J.M. & Roessel J.M.; 'The effects of Non- linear Inelastic Connection Behaviour of Precast Panelized Shear Walls'; *Reinforced Concrete Structures Subjected to Wind & Earthquake Forces*, ACI Publication, SP - 63, American Concrete Association, Detroit, Michigan, 1980.
- [19] Martin L.D. & Korkosz W.J.; *Connections for Precast Prestressed Concrete Buildings, including earthquake resistance*; Technical Report No. 2; Prestressed Concrete Institute, Chicago, Illinois, March 1982.
- [20] *Metric Design Manual*, Canadian Prestressed Concrete Institute, Ottawa, 2nd Edition, 1986.
- [21] Muller P. & Becker J.M.; 'Seismic Characteristics of Composite Precast Walls'; Proc. 3rd *Canadian Conference on Earthquake Engineering*; vol 2, Montreal 1979.

- [22] *National Building Code of Canada 1985*, Associate committee on the National Building Code, National Research Council of Canada.
- [23] Neille D.S.; *Behaviour of Headed Stud connections for Precast Concrete Panels under Monotonic and Cycled Shear Loading*; Ph.D. Thesis, University of British Columbia, May 1977.
- [24] Pall A.S. & Marsh C.; 'Seismic Response of Large Panel Structures using Limited-Slip bolted Joints'; Proc. 3rd *Canadian Conference on Earthquake Engineering*; vol 2, Montreal 1979.
- [25] Phillips W.R. & Sheppard D.A. *Plant cast Precast and Prestressed Concrete, a design guide*.
- [26] Poller E., Tso W.K., Heidebrecht A.C.; 'Analysis of Shear Walls in Large Panel Construction'; *Canadian Journal of Civil Engineering*, vol 2, No. 3, Sept 1975.
- [27] Popov E.P.; 'Mechanical Characteristics and Bond of Reinforcing Steel under Seismic Conditions'; Workshop on *Earthquake - Resistant Reinforced Concrete Building Construction*; (ERCBC), University of California, Berkeley, July 1977, pp 658-682.
- [28] Powell G.H., *Drain - 2D Users Guide*, Report No. UCB/EERC - 73/22, Earthquake Engineering Research Centre, University of California, Berkeley, Oct 1973.
- [29] Saxena R.P.; *An Experimental Investigation of a Precast Connection*; M.A.Sc. Thesis, University of British Columbia, Sept 1983.
- [30] Schriker V. & Powell G. et. Al., *Inelastic seismic analysis of large panel buildings*; California University Berkeley, Earthquake Engineering Research Centre, Sept. 1980, NTIS No. PB 81-154338.
- [31] Spencer R.A. & Neille D.S.; 'Cyclic Tests of Welded Headed Stud connections'; *PCI Journal*; May-June 1976, vol 15, No. 1, pp 67-78.
- [32] Spencer R.A.; 'Serviceability of Precast Diaphragms & Connections designed for Earthquake Resistant Structures'; Proc. *Workshop on Design of Prefabricated Concrete Buildings for Earthquake Loads*, April 1981, pp 551-573.
- [33] Spencer R.A. & Tong W.K.T.; 'Design of a One-Storey Precast Concrete Building for earthquake loading'; Proc. 8th *World Conference on Earthquake Engineering*; San Francisco 1984, vol 5, pp 653- 660.
- [34] Spencer R.A.; 'Earthquake Resistant Connections for Low Rise Precast Concrete Buildings'; *Seminar on Precast Concrete Construction in Seismic zones*; Tokyo, October 27-31, 1986, pp 61-81.
- [35] *Supplement to the National Building Code of Canada 1985*, Associate committee on the National Building Code, National Research Council of Canada.

- [36] Tong W.K.T.; *Non-Linear Seismic Analysis of a One-Storey Precast Concrete Building*; M.A.Sc. Thesis, University of British Columbia, February 1984.
- [37] Tso W.K. & Dempsey K.M.; 'Seismic Torsional Provisions for Dynamic Eccentricity'; *Journal of Earthquake Engineering and Structural Dynamics*, vol 8, 1980, pp 275-289.
- [38] Velkov Miodrag; 'Large Panel Systems in Yugoslavia : Design, Construction and Research for Improvement of Practice & Elaboration of Codes'; *Proc. Workshop on Design of Prefabricated Concrete Buildings for Earthquake Loads*; conducted by Applied Technology Council, Berkeley, April 1981.
- [39] Zamolo Mihaela; 'Evaluation of a Large - Panel Building System for Seismic Zones - Experimental Part'; *Proc. 8th European Conference on Earthquake Engineering*; Lisbon 1986, vol 5.
- [40] Zeck U.I.; *Joints in Large Panel Precast Concrete Structures*; NTIS No. PB-252852/9GI by U.S. Deptt. of Commerce Jan 1976.

Appendix A

Time Periods of the Buildings Considered in the Present Studies

Number of Panels in Wall 1 N_1	Square Building with Panels $N_1, 16, 16, 16$	Rectangular Building with Panels $N_1, 16, 32, 32$
0	0.29	0.265
4	0.29	0.272
8	0.302	0.281
12	0.31	0.2897
16	0.311	0.293

Table A.1: Fundamental Periods (in sec) of the Buildings in Figs. [4.1a] and [4.1b], designed by the Strength Method

Note : The stiffness of the walls in the direction of the earthquake is determined from eqn. (3.19) (corresponding to Case 1).